SYNTHESIS AND REACTIVITY OF TRANSITION METAL CYAPHIDE COMPLEXES

BY

Madeleine Claire Levis

Department of Chemistry

School of Life Science

University of Sussex

A Thesis submitted for the degree of Doctor of Philosophy.

September 2020

DECLARATION

I hereby declare that this thesis has not been and will not be, submitted in whole or in part to another university for the award of any other degree.

Signature: …….

ACKNOWLEDGMENTS

I would first like to thank my supervisor Dr Ian Crossley for his advice, assistance and support throughout as well as his patience for the numerable ways I have spelt 'Phosphorus' in the many drafts of this thesis, and to EPSRC for financially supporting this work. Thank you, Crossley group past and present: Dr Sam Furfari and Dr Mathew Leech for teaching me the ropes and quirks of working in Lab14, Kyle for the constant conversations about science and the gym as well as being the person to go to for distillation and X-ray help and finally, to all the MChem and summer students, Joe, Jennifer, Josh, Vlad, Ellie and Harry for providing entertainment throughout these last four years. Thanks too, everyone else past and present of Lab14, it would not have been the same without any of you.

Thank you to my thesis committee, Prof. Geoff Cloke, Prof. John Spencer and Dr John Turner for the continued support, encouragement and advice. Thank you to Dr Iain Day, Dr Alla Abdul-Sada, Dr Mark Roe and Verity Holmes for their invaluable assistance.

Thank you to my school and university friends (you know who you are) and the many friends I have made in Brighton, particularly my housemates (Dee, Greg, Emma, Josh and Tom) for their remarkable ability to listen to my moaning, and for Josh for teaching me how to properly crash a mountain bike. Thank you to my David Lloyd gym family (There are too many of you to name) for always providing top notch entertainment, who would do jumping lunges and burpees for any other reason?

Finally, thank you to my family; Mum, Dad, Chris and the late Mumba (Cat), for the limitless support during this time in so many ways, finically, emotionally, providing comical relief (I am looking at you Dad) and the unlimited amount of encouragement.

"*The key to making progress is to recognise how to take that very first step. Then you start your journey. You hope for the best and stick with it day in day out. Even if you're tired, even if you want to walk away, you don't. Because you are a pioneer, and nobody ever said it would be easy*."

– ***Meredith Grey, Grey's Anatomy Season 10, Man on the Moon***

SUMMARY

This thesis describes the synthesis, characterisation and reactivity of a series of ruthenium cyaphide complexes featuring *trans* alkynyl, methyl and halide ligands, to understand how the *trans* ligand affects the properties of the cyaphide moiety and ultimately develop reactivity of the cyaphide moiety, seeking to engage both the phosphorus lone pair and the π-system.

A series of *trans*-alkynyl cyaphide complexes, *trans*-[Ru(C≡P)(C≡CR)(dppe)$_2$] were synthesised via the corresponding η^1-phosphaalkyne complexes, *trans*-[Ru(P≡CSiMe$_3$)(C≡CR)(dppe)$_2$]$^+$ and the compounds characterised through NMR and infra-red spectroscopy as well as X-ray diffraction. In addition, cyclic voltammetry was undertaken to further understand the electrochemical behaviour of these complexes. Preliminary exploration into the reactivity of the ligated cyaphide was undertaken with limited success. The synthesis of the first example of a *trans*-[Ru(C≡CR)(C≡N)(dppe)$_2$] complex was achieved to seek the comparison of the cyanide, cyaphide and alkyne ligands, albeit, further work is needed to optimise the synthetic procedure to yield pure product.

The synthesis of the first *trans*-alkyl cyaphide complex, *trans*-[RuMe(dppe)$_2$(C≡P)] via its corresponding η^1-phosphaalkyne complex, *trans*-[RuMe(dppe)$_2$(P≡CSiMe$_3$)]OTf was achieved. Both the η^1-phosphaalkyne and cyaphide complexes were characterised through NMR and infra-red spectroscopy, with the latter also being structurally characterised through X-ray diffraction. Comparable to the *trans*-alkynyl cyaphide complexes the initial reactivity studies to coordinate the ligated cyaphide to metal centres (Pt, Pd, Au, Ag and Rh) were unsuccessful. However, the first series of *trans*-halo cyaphide complexes, *trans*-[RuX(dppe)$_2$(C≡P)] (X = Cl, Br or I) was synthesised through the treatment of *trans*-[RuMe(dppe)$_2$(C≡P)] with ZnX$_2$ (X = Cl, Br, I) in the presence of PPh$_3$, a rare example of ruthenium demethylation using a zinc halide.

The series of *trans*-halo cyaphide complexes had long been sought after due to the ability for post-synthetic modification, thus exploration into the reactivity of the *trans*-[RuBr(dppe)$_2$(C≡P)]

was undertaken. Halide abstraction of *trans*-[RuBr(dppe)$_2$(C≡P)] led to the synthesis, isolation and characterisation of the first 5-coordinate cyaphide complex, [Ru(C≡P)(dppe)$_2$])OTF. X-ray diffraction data showed the 5-coordinate cyaphide complex to exhibit a square-based pyramidal structure with an accessible vacant coordination site *trans*- to the cyaphide moiety. The susceptibility to ligand addition at this site was investigated and exploited to synthesise a series of novel cyaphide complexes *trans*-[Ru(R)(dppe)$_2$(C≡P)]OTf, (R = C≡O, C≡N, F, SC≡N, OC≡N, P≡CSiMe$_3$, C≡P, C≡NCH$_3$ and NC$_5$H$_5$), which have previously proven inaccessible via established routes to cyaphide complexes. The reduction chemistry of [Ru(C≡P)(dppe)$_2$]OTF was also investigated, with the reactions with LiCp and sodium naphthalenide which yielded the synthesis of the CPPC bridged dimer [(Ru(dppe)$_2$)$_2$(CPPC)] and the sodium bridged dimer [Ru(dppe)$_2$(C≡P)Na]$_2$ respectively. Furthermore, the UV-vis spectra, electrochemistry and spectroelectrochemistry of a selection of the cyaphide complexes including the 5-coordiante cyaphide complex, which have been supported through DFT and TD-DFT calculations, were obtained.

Contents

LIST OF ABBREVIATIONS

°	Degrees
°C	Degrees Celsius
Å	Angstrom
Ad	Adamantyl
An	Anisole
Ar	Arene
cm^{-1}	Wavenumber
Cp	Cyclopentadienyl
Cp*	Pentamethylcyclopentadienyl
Cy	Cyclohexyl
DABCO	1,4-diazabicyclo[2.2.2]octane
DBU	1,8-Diazabicyclo[5.4.0]undec-7-ene
DCM	Dichloromethane
DFT	Density Functional Theory
DIPA	Diisopropylamine
DIPP	Diisopropylphenyl
DME	Dimethoxyethane
DMSO	Dimethylsulfoxide
dppe	1,2-bis(diphenylphosphino)ethane
dppm	1,2-(diphenylphosphino)methane
ESI-MS	Electro-Spray Ionisation Mass Spectrometry
Et	Ethyl

eV	Electronvolt
Fc	Ferrocenyl
FVP	Flash Vacuum Pyrolysis
HOMO	Highest Occupied Molecular Orbital
ILCT	Intra-Ligand Charge Transfer
^{i}Pr	Isopropyl
IR	Infrared
L	Ligand
LLCT	Ligand to Ligand Charge Transfer
LMCT	Ligand to Metal Charge Transfer
LUMO	Lowest Unoccupied Molecular Orbital
M	Molar
***m*-**	Meta
m/z	Mass/Charge Ratio
Me	Methyl
Mes*	2,4,6-Tri-tert-butyl phenyl
MLCT	Metal to Ligand Charge Transfer
^{n}Bu	n-Butyl
***o*-**	Ortho
OTf	Triflate
***p*-**	Para
Ph	Phenyl
SOMO	Singly Occupied Molecular Orbital

TBAF	Tetrabutylammonium fluoride
TBAT	Tetrabutylammonium difluorotriphenylsilicate
^{t}Bu	Tert-butyl
THF	Tetrahydrofuran

NMR Abbreviations

{^{1}H}	Proton Decoupled
br	Broad
d	Doublet
dquint	Doublet of Quintets
HMBC	Heteronuclear Multiple Bond Correlation
HSQC	Heteronuclear Single-Quantum Coherence
Hz	Hertz
K	Kelvin
m	Multiplet
NMR	Nuclear Magnetic Resonance
ppm	Parts Per Million
q	Quartet
quint	Quintet
s	Singlet
t	Triplet
^{x}J	Coupling Constant Over x Bonds
δ	Chemical Shift

Electrochemistry Abbreviations

Δ*E*	Difference in Potential
CV	Cyclic Voltammetry
$E_{½}$	Half-Wave Potential
E_{pa}	Oxidation Peak Potential
E_{pc}	Reduction Peak Potential

LIST OF COMPOUNDS SYNTHESISED AND PURSUED

1.58f$^+$	*trans*-[Ru(P≡CSiMe$_3$)(C≡CCO$_2$Et)(dppe)$_2$]$^+$
1.58g$^+$	*trans*-[Ru(P≡CSiMe$_3$)(C≡CCO$_2$Me)(dppe)$_2$]$^+$
1.59f	*trans*-[Ru(dppe)$_2$(C≡CCO$_2$Et)(C≡P)]
1.59g	*trans*-[Ru(dppe)$_2$(C≡CCO$_2$Me)(C≡P)]
2.2a$^+$	*trans*-[Ru(P≡CSiMe$_3$)(C≡C^{n}Bu)(dppe)$_2$]$^+$
2.2b$^+$	*trans*-[Ru(P≡CSiMe$_3$)(C≡C^{t}Bu)(dppe)$_2$]$^+$
2.2e$^+$	*trans*-[Ru(P≡CSiMe$_3$)(C≡CC$_6$H$_4$-*p*-CO$_2$Et)(dppe)$_2$]$^+$
2.2f$^+$	*trans*-[Ru(P≡CSiMe$_3$)(C≡CC$_6$H$_3$-3,5-(CF$_3$)$_2$)(dppe)$_2$]$^+$
2.3a	*trans*-[Ru(dppe)$_2$(C≡C^{n}Bu)(C≡P)]
2.3b	*trans*-[Ru(dppe)$_2$(C≡C^{t}Bu)(C≡P)]
2.3e	*trans*-[Ru(dppe)$_2$(C≡CC$_6$H$_4$-*p*-CO$_2$Et)(C≡P)]
2.3f	*trans*-[Ru(dppe)$_2$(C≡CCC$_6$H$_3$-3,5-(CF$_3$)$_2$)(C≡P)]
3.1$^+$	[RuMe(dppe)$_2$]$^+$
3.2$^+$	*trans*-[RuMe(P≡CSiMe$_3$)(dppe)$_2$]$^+$
3.3	*trans*-[RuMe(C≡P)(dppe)$_2$]
3.4	*trans*-[RuBr(C≡P)(dppe)$_2$]
3.5	*trans*-[RuCl(C≡P)(dppe)$_2$]
3.6	*trans*-[RuI(C≡P)(dppe)$_2$]
4.1$^+$	*trans*-[Ru(C≡P)(dppe)$_2$]$^+$
4.2$^+$	*trans*-[Ru(C≡P)(C≡O)(dppe)$_2$]$^+$
4.3	*trans*-[Ru(C≡P)(C≡N)(dppe)$_2$]
4.4	*trans*-[Ru(C≡P)(SC≡N)(dppe)$_2$]
4.5	*trans*-[Ru(C≡P)(OC≡N)(dppe)$_2$]
4.6	*trans*-[RuF(C≡P)(dppe)$_2$]

4.7$^+$	*trans*-[Ru(C≡P)(P≡CSiMe$_3$)(dppe)$_2$]$^+$
4.8	*trans*-[Ru(C≡P)$_2$(dppe)$_2$]
4.9$^+$	*trans*-[Ru(C≡P)(N≡CCH$_3$)(dppe)$_2$]$^+$
4.10$^+$	*trans*-[Ru(C≡P)(NC$_5$H$_5$)(dppe)$_2$]$^+$
4.11$^+$ - 4.18$^+$	[Ru(PMe$_3$)$_{1+x}$(dppe)$_{2-x}$(C≡P)]$^+$ (where x = 0, 2 or 4)
4.14$^+$	[Ru(C≡P)(PMe$_3$)$_5$]$^+$
4.19	[(Ru(dppe)$_2$)$_2$(CPPC)]
4.20	[Ru(dppe)$_2$(C≡P)]$_2$Na$_2$
4.21	*trans*-[Ru(C≡P)(=C=CH(SiMe$_3$))(dppe)$_2$]$^+$
4.22	*trans*-[Ru(C≡P)(C≡CSiMe$_3$)(dppe)$_2$]
4.23	*trans*-[Ru(C≡P)(C≡CH)(dppe)$_2$]
4.24	[{Ru(dppe)$_2$}$_3${μ-(C≡C)$_3$C$_6$H$_3$}(C≡P)$_2$]
4.25	[{Ru(dppe)$_2$}$_2${μ-(C≡C)$_2$C$_4$H$_2$S}(C≡P)$_2$]
4.26$^+$	*trans*-[Ru(N≡C-(C$_6$H$_3$(CO$_2$H)$_2$)(dppe)$_2$(C≡P)]$^+$

CHAPTER 1 : INTRODUCTION

1.1 LOW COORDINATE PHOSPHORUS CHEMISTRY

Phosphorus possess extensive and diverse chemistry with applications ranging from biological systems to catalysis and coordination chemistry, just to name a few, and has transcended the boundaries between organic and inorganic chemistry.[1,2] This is predominantly due to the ability of phosphorus to access a variety of coordination numbers (σ) and valences (λ) (**Figure 1-1**) which has resulted in the development of organophosphorus chemistry and its subfield phosphaorganic chemistry.[1,2] Organophosphorus chemistry is typically where phosphorus possesses a coordination number of three or four and there are one or more direct C-P σ-bonds whereas phosphaorganic chemistry is where carbon is directly replaced with phosphorus due to them being isolobal and isoelectronic to each other. When phosphacarbons have a coordination number of one or two they are also known as low coordinate phosphorus compounds and these will be the focus of the discussion throughout this introduction.[3]

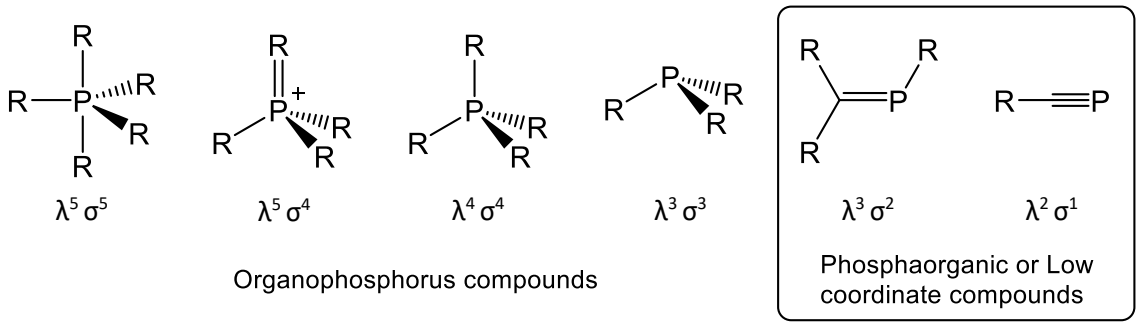

Figure 1-1: *Common structures of organophosphorus and phosphaorganic compounds*

The isolobal analogy was first discussed by Roald Hoffmann in 1982, where he drew on chemical similarities between the CH_3 fragment and d^7-ML_5 metal fragments, such as $Mn(CO)_5$ (**Figure 1-2**), with both possessing similar frontier orbitals and exhibiting very similar radical-based chemistry, with tendencies to dimerize.[4] It was defined that if two fragments have the same

electron occupancy and their frontier molecular orbitals are of similar energy and symmetry, they are isolobal to one another.[4]

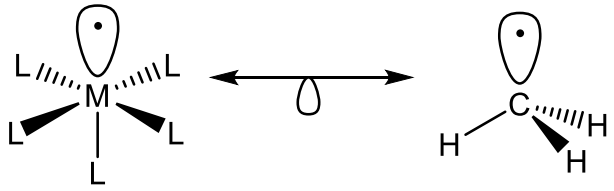

***Figure 1-2**: Isolobal Analogy of d^7-ML_5 to CH_3 fragment*

If two fragments are isolobal they can, theoretically be interchanged, leading to novel compounds. Likewise, phosphorus and the CH fragment are isolobal (**Figure 1-3**) as well as being isoelectronic and both having similar electronegativities, thus, theoretically these two fragments can be interchanged forming new phosphorus containing compounds such as the low coordinate phosphorus compounds, phosphaalkenes and phosphaalkynes.

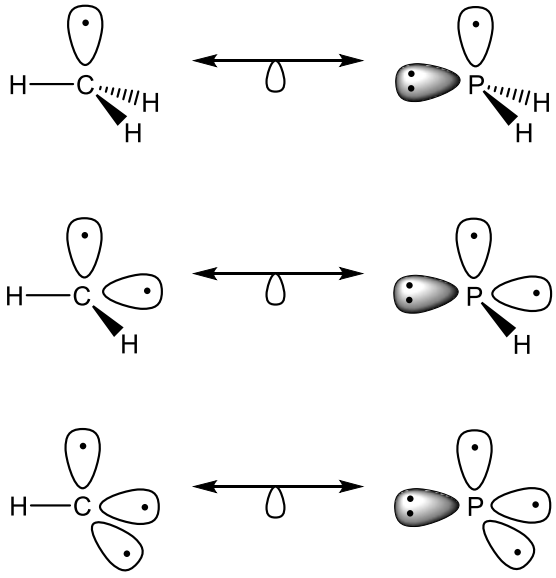

***Figure 1-3:** Isolobal Analogy of phosphacarbons and hydrocarbon fragments.*

Low coordinate phosphorus chemistry, the study where carbon is directly replaced with phosphorus usually forming phosphorus compounds with a coordination number less than

three, thus engaging in multiple bonding to other elements, has been growing over the last 50 years.[1,3] The main interest is in phosphaalkenes and phosphaalkynes (**Figure 1-4**) because the chemistry of these mimics their carbon counterparts, alkenes and alkynes, primarily due to the isolobal analogy.

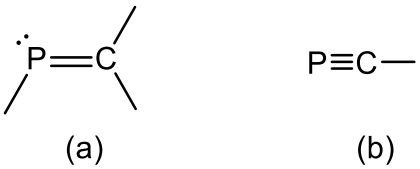

Figure 1-4: *Common Low coordinate phosphorus compounds; (a) phoshalkene, (b) phosphaalkyne.*

1.2 PHOSPHAALKYNES

1.2.1 GENERAL REMARKS ON PHOSPHAALKYNES

Phosphaalkynes are compounds of tervalent phosphorus which contain a P≡C triple bond and were once thought impossible, with Pitzer[5] and Mulliken[6] stating that "elements with a principle quantum number greater than two cannot engage in bonding with orders greater than one, due to being too unstable". This classical view had the rationale that heavy main group elements would have poor *pπ-pπ* overlap (**Figure 1-5**) and consequently not form a sufficient bonding interaction, thus the bonding would be too weak to sustain monomeric compounds leading instead to catenation and the formation of singly bonded rings and cages. This 'double bond' rule has now been disproven as a multitude of compounds containing heavy elements with multiple bonds have been synthesised.

Figure 1-5: *pπ-pπ overlap in light elements (left) and their heavier counterparts (right)*

Phosphaalkynes can be compared to their nitrogen and carbon counterparts (**Figure 1-6**). Comparison of the energies of C≡P and C≡C bonds shows the similarity of the π-systems ($\pi_{C\equiv C}$ = −11.40 eV and $\pi_{C\equiv P}$ = −10.79 eV respectively)[7–9], with the lone pair on the phosphorus atom also allowing comparisons to be drawn between the isolobal and isoelectronic phosphaalkynes and nitriles, however, this relationship is not as apparent as that to alkynes due to the electronegativity differences (C = 2.5, P = 2.2, N = 3.0), a characteristic that controls the reactivity of these species. Consequently, while the C≡N bond is polarized with a partial positive charge on carbon and a partial negative charge on nitrogen, phosphaalkynes show the opposite polarisation. Overall phosphaalkynes are more akin to alkynes than nitriles being in line with the general observation that phosphorus behaves as a "carbon copy".[3,10,11]

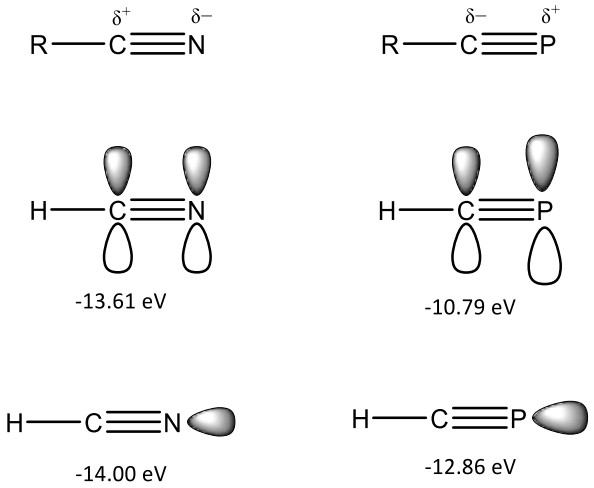

Figure 1-6: *Polarisation and bonding energies of HC≡N and HC≡P.*[3,7–9,12]

1.2.2 PHOSPHAALKYNE SYNTHESIS

The first example of a phosphaalkyne, HC≡P, was synthesised in 1961 by Gier,[13] via the reaction of phosphine gas, PH_3, in a low intensity rotating arc struck between graphite electrodes (**Scheme 1-1**) which was contained in a water-cooled copper reactor.

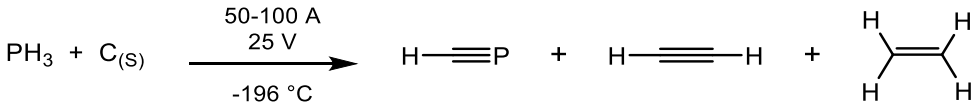

Scheme 1-1: *Synthesis of HCP.*[13]

The reaction evolves a colourless gas, which readily polymerises if stored above -124 °C; both monomer and polymer are pyrophoric. However, later studies have shown an NMR sample in toluene remained unchanged at -70 °C and under reduced pressure HC≡P can be kept at room temperature.[3] Characterisation included infrared spectroscopy and mass spectrometry; the infrared data showed the presence of the C≡P stretching mode at 1265 cm^{-1} and an absence of a H-P stretching mode, both consistent with the formation of HC≡P. The mass spectrum showed a strong molecular ion peak m/z = 44, corresponding to the formation of the cation $[^{1}H\text{-}^{12}C\equiv^{31}P]^{+}$ or $[^{13}C\equiv^{31}P]^{+}$. The connectivity of phosphaethyne was later confirmed by Tyler, using microwave spectroscopy when comparing HC≡P and DC≡P.[14] Within these studies, the bond length of C≡P was determined to be approximately 1.54 Å.

Later, Kroto and Nixon demonstrated an alternative route to HC≡P, although not isolated, supporting the work of Gier.[15–20] They showed that saturated precursors could be used to synthesise phosphaalkynes through double hydrogen halide elimination using a base combined with flash vacuum pyrolysis (**Scheme 1-2**). The products were characterised *in-situ* through microwave spectroscopy. Through this method a range of other members of the phosphaalkyne family have been synthesised.

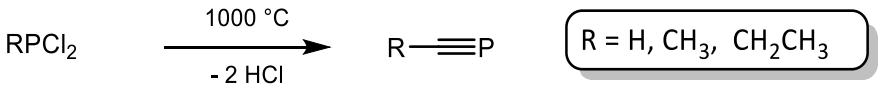

Scheme 1-2: *Synthesis of RC≡P (R = H, CH_3, CH_2CH_3) by flash vacuum pyrolysis.*[15–20]

The flash vacuum pyrolysis technique was further demonstrated by Appel through the elimination of chlorotrimethylsilane from the 1,2-chloro-trimethylsilylphosphaalkenes, Cl-

P=C($SiMe_3$)$_2$ and Cl-P=C($SiMe_3$)(Ph), leading to the *in-situ* observation of PhC≡P and Me_3SiC≡P respectively (**Scheme 1-3**).[21]

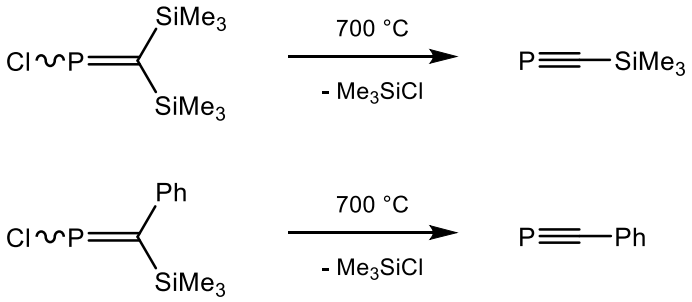

Scheme 1-3: *Synthesis of Me_3SiC≡P and PhC≡P respectively via elimination of chlorotrimethylsilane.*[21]

It was, however, not until 1981 that the chemistry of phosphaalkynes became firmly established due to the work of Becker with synthesis of the first kinetically stable phophaalkyne, ^{t}BuC≡P,[22] an easily handled colourless liquid which is stable under ambient temperatures with a boiling point of 61°C. Becker synthesised the phosphaalkyne by reacting pivaloyl chloride with tris(trimethylsilyl)phosphine to yield a acyl phosphine, which is unstable to silatropic rearrangement forming a phosphaalkene. Subsequent base-induced elimination of hexamethyldisiloxane affords the phosphaalkyne (**Scheme 1-4**).

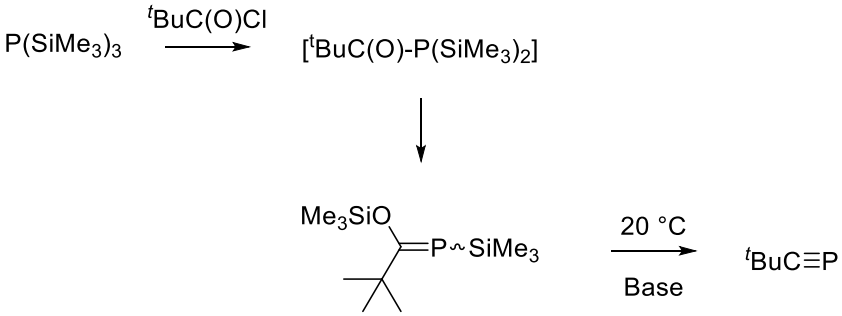

Scheme 1-4: *Synthesis of ^{t}BuC≡P from pivaloyl chloride and P($SiMe_3$)$_3$ followed by a rearrangement and a subsequent base induced elimination of hexamethyldisoloxane.*[22]

In addition, the synthesis of several phosphaalkynes, RC≡P (R= H, Me, Et, Bu, Me_3Si), through flash vacuum pyrolysis, using RCl_2CPH_2 and freshly ground K_2CO_3 at 350 °C was reported by Denis and co-workers (**Scheme 1-5**).[23]

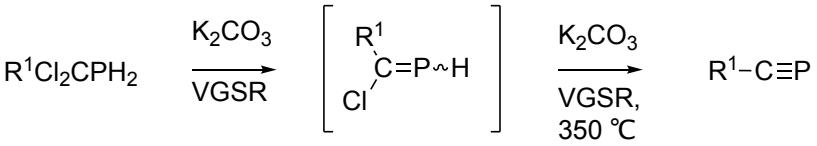

Scheme 1-5: *Synthesis of Phosphaalkynes RCP (R = H, Me, Et, Bu, Me_3Si) by vacuum gas-solid reduction (VGSR).*[23]

Subsequently, Denis reported a synthetic route to phosphaalkynes bearing primary alkyl substituents, through low temperature Lewis base induced rearrangement of the corresponding 1-alkynylphosphines, via the intermediate phosphaallene R-CH=C=PH (**Scheme 1-6**).[24] Although all attempts to characterise this intermediate species by low-temperature NMR were unsuccessful, it was unambiguously proven by chemical trapping using propane-2-thiol. Although this is an efficient approach it is severely limited by the small number of easily available primary 1-alkynyl phosphines. –

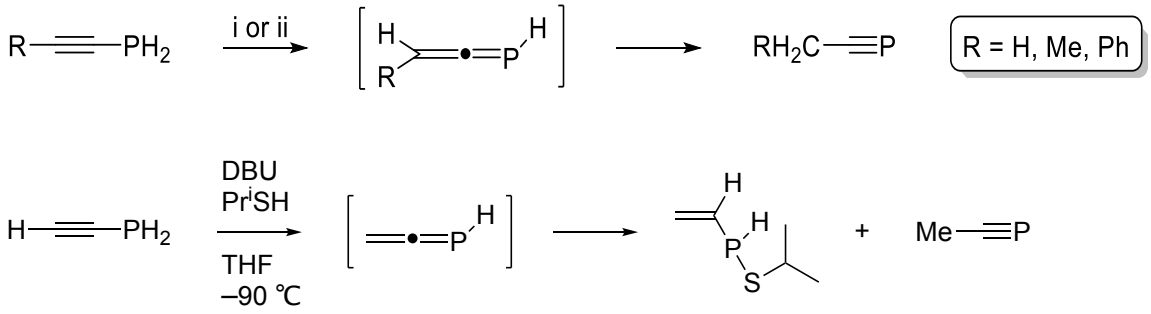

Scheme 1-6*: Top: Synthesis of phosphaalkynes bearing primary alkyl substituents i) NEt_3, 10* ℃ *or DBU, -90* ℃ *in THF, ii) vacuum gas-solid reaction, K_2CO_3, 20* ℃ *(for R = H and Me) Bottom: Chemical trapping of the phosphaallene, R-CH=C=PH, intermediate using propane-2-thiol, where R= H.*[24]

Following from this work the syntheses of primary and secondary alkyl-substituted phosphaalkynes have been reported, through the chemoselective reduction of α-dichlorophosphonates with $AlHCl_2$, followed by the bis-dehydrohalogenation of the resulting α-dichlorophosphines by a strong Lewis base (**Scheme 1-7**).[25] The dehydrohalogenation step is able to be carried out at low temperature allowing accesses to volatile materials as well as reducing the need for special laboratory equipment, making it the only reliable preparation. In addition, the dehydrochlorination route is useful for a range of R groups (R = Me and SiR_3);

though in some cases AgOTf is required to abstract the halide to avoid generating DABCO.HCl, which can subsequently attack the product.[26,27]

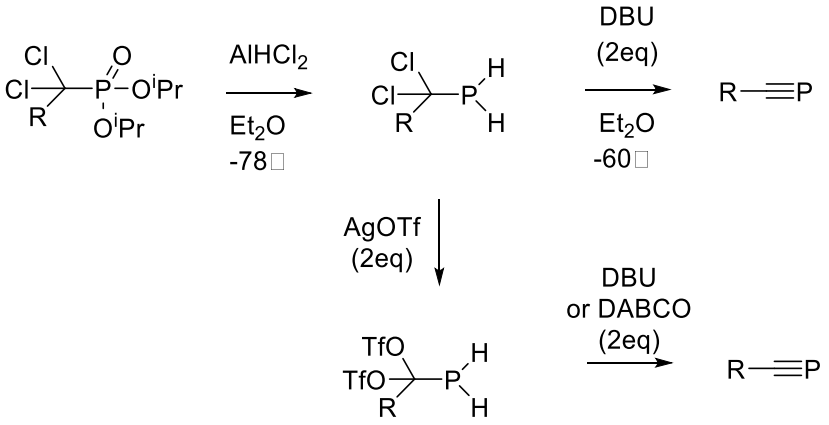

Scheme 1-7: *Synthesis of phosphaalkynes via the chemoselective reduction of the α-dichlorophosphonate with $AlHCl_2$ followed by the bis-dehydrohalogenation of the resulting α-dichlorophosphines by a strong Lewis base.*[25]

Nonetheless, the most routinely used synthetic procedure to phosphaalkynes is still that of Becker, through the elimination of hexamethyldisiloxane from suitable phosphaalkenes.[22] This route has been greatly optimized and generalized by Regitz and co-workers.[28] This seminal procedure has resulted in a library of phosphaalkynes with a variety of different substituents, which are now readily accessible.

1.2.3 PHOSPHAALKYNE PROPERTIES

Phosphaalkynes including HC≡P and ^{t}BuC≡P have been extensively studied both experimentally and theoretically with regard their stability and spectroscopic properties, some of which are summarized below (**Table 1-1**).[29]

Property	H-C≡P	^{t}Bu-C≡P
P≡C bond length, Å	1.5421(5) (microwave)	1.536(2) (microwave) 1.548(1) (X-ray)
Boiling Point, °C	-	61
1st Ionization Potential, eV	10.79[e]	9.70[e]
2nd Ionization Potential, eV	12.86[e]	11.45[e]
NMR, ppm		
^{1}H	2.90[a] ($^{2}J_{PH}$ = 44.0 Hz)	1.15[b] ($^{2}J_{PH}$ = 0.9 Hz)
^{13}C	158.0[a] ($^{1}J_{PC}$ = 56.0 Hz)	158.0[c] ($^{1}J_{PC}$ = 38.5 Hz, $^{2}J_{PC}$ = 18.2 Hz, $^{3}J_{PC}$ = 6.0 Hz)
^{31}P	−32[a,d]	−69.2[c,d]

Table 1-1: *Selected physical properties of H-C≡P and ^{t}Bu-C≡P. [a] CD_2Cl_2, −80 °C. [b] Pure compound. [c] C_6D_6. [d] External H_3PO_4, [e] computational .*[29]

Phosphaalkynes have been studied by NMR spectroscopy and X-ray diffraction. The ^{13}C NMR signals are observed in the region 154-201 ppm, with P-C couplings in the range of 14-56 Hz. In general the ^{31}P NMR resonances are found at low frequency, for example at -32 ppm and -69.2 ppm for HC≡P and ^{t}BuC≡P respectively, but the presence of silyl and aryl groups results in a shift in the ^{31}P NMR resonance to a higher frequency (*ca* 99.4 ppm for $Me_3SiC{\equiv}P$).[30,31] The C≡P bond lengths in HC≡P and ^{t}BuC≡P (**Table 1-1**) have been shown to be longer than their respective carbon and nitrogen analogues (*ca* 1.20 Å and *ca* 1.155 Å respectively).[14,29] This is due to a reduced overlap for the 2pπ-3pπ interaction which was studied further through UV-photoelectron spectra and computational studies, from which the ionization potentials were calculated (**Table 1-1**). These studies showed that ^{t}BuC≡P and HC≡P have first ionization energies at 9.61 eV and 10.79 eV corresponding to the π bond (π(CP)), lower second ionization energies at 11.44 eV and 12.86 eV corresponding to the lone pair (n(P)), and π(CP)-n(P) separations of 1.83 eV and 2.07 eV respectively. In comparison the nitrile analogues were shown to exhibit higher ionization potentials as expected due to the greater electronegativity of nitrogen compared to phosphorus, furthermore, it was shown that nitriles have a significantly smaller π(CN)-n(N) separation compared to the phosphorus counterparts. The increase in π-n

separation in the phosphaalkynes is due to a reduced overlap for the 2pπ-3pπ interaction therefore increasing the bond length and having a destabilisation effect.[7–9,14,29]

The π-n separation is also why there is a difference in the coordination chemistry between phosphaalkynes and nitriles. The majority of nitriles bind to transition metals though the lone pair whereas phosphaalkynes typically, but not exclusively, bind in a side-on manner through the π system, simply because the lone pair of the phosphorus is held in a higher *s*-character orbital compared to the lone pair on the nitrogen in nitriles, therefore it is less available for reactivity.

Typically, phosphaalkynes have a high propensity towards polymerization, which can be attributed to the highly reactive π-system. Traditionally it has been considered that increasing the steric bulk around this π-system will impart kinetic stabilization. For example, phosphaethyne has been shown to be highly reactive and pyrophoric and readily polymerizes at temperatures above −70 °C, whereas, ^{t}BuC≡P is a stable liquid at ambient temperature and is more resilient toward oxygen. However, MeC≡P and Me_3SiC≡P can only be kept for extended periods at -78°C and 4°C respectively, despite the steric bulk of Me_3SiC≡P compared to that of ^{t}BuC≡P. The relative instability of MeC≡P and Me_3SiC≡P can, however, be attributed to the acidity of the Me and the lability Me_3Si groups respectively, rather than the reactivity of the π-system. It may thus be reasoned that sterics alone cannot account the stability of phosphaalkynes and that electronic influences are also a key feature.[32]

1.2.4 REACTIVITY OF PHOSPHAALKYNES

The organic chemistry of phosphaalkynes has been extensively studied and includes 1,2-addition reactions with organomagnesium and organolithium reagents as well as a wide range of cycloadditions ([2+1], [2+2], [2+3] and [2+4]), which has led to the synthesis of a variety of novel organophosphorus compounds.[3,11] Phosphaalkynes also have rich organometallic chemistry and

reactivity which includes metal-assisted oligomerizations and [2+2] cycloadditions.[3,11] This next section will discuss some of these highlights.

ADDITION REACTIONS OF PHOSPHAALKYNES

Protonation of the P≡C triple bond in phosphaalkynes occurs exclusively at the carbon centre despite the presence of the phosphorus lone pair. This has been demonstrated by Regitz and co-workers with the low temperature protonation of both ^{t}BuC≡P and AdC≡P through treatment with various superacid media including FSO_3H/SO_2ClF (**Scheme 1-8**).[10] The initial protonation at the carbon centre leads to a phosphavinyl cation, $RHC{=}P^{+}$ which is rapidly trapped through counterion coordination to afford the corresponding phosphaalkene; when ^{t}BuC≡P is treated with FSO_3H/SO_2ClF minor amounts of isomeric spirocyclotrimer are observed. Protonation at the phosphorus centre was never observed, attributed to the lone pair of the phosphorus being held in a high *s*-character orbital therefore not being available for reactivity, as previously discussed (see section: **1.2.3**).

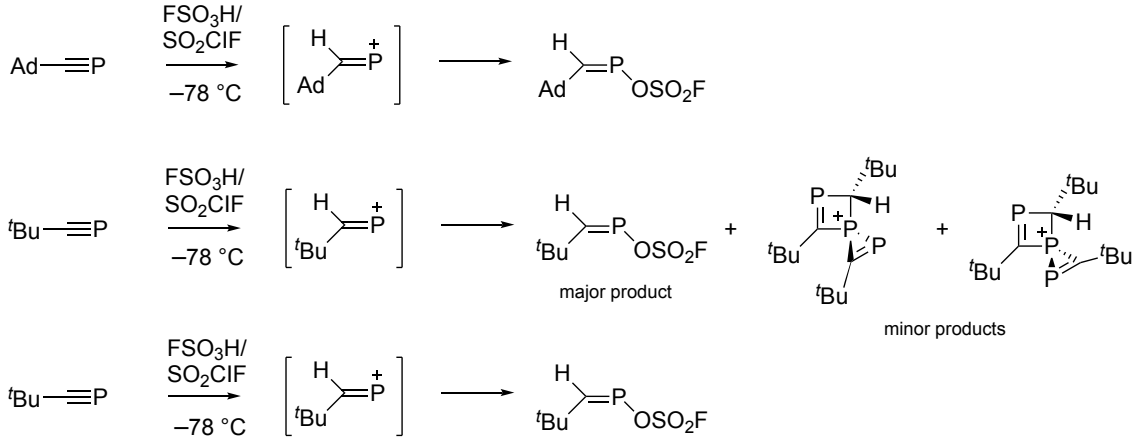

***Scheme 1-8**: Protonation of both ^{t}BuC≡P and AdC≡P through the treatment with various superacid media.*[10]

Phosphaalkynes can also react with nucleophiles and undergo 1,2-addition reactions, for example, halogenophosphaalkenes and dihalophosphanes can be regenerated from the addition of hydrogen halides. In addition, PBr_3 can also undergo 1,2-addtion reactions with ^{t}BuC≡P to yield the products shown below (**Scheme 1-9**). [3,33]

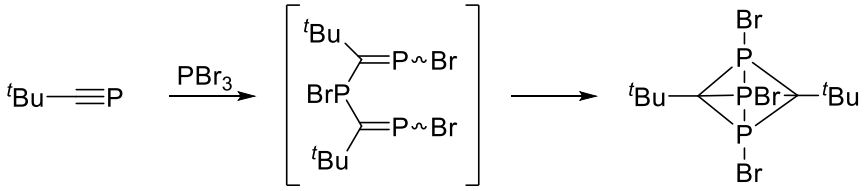

Scheme 1-9: *Reaction scheme of ^{t}BuC≡P with PBr_3.*[3,33]

Organotin hydrides can also undergo 1,2-additions with phosphaalkynes as reported by Regitz in 1998, reacting with an excess of phosphaalkyne in pentane at room temperature for over two weeks to afford the 2-stannyl-substituted 1,2-dihydro-1,3-diphosphetes in good yields (**Scheme 1-10**).[3,34]

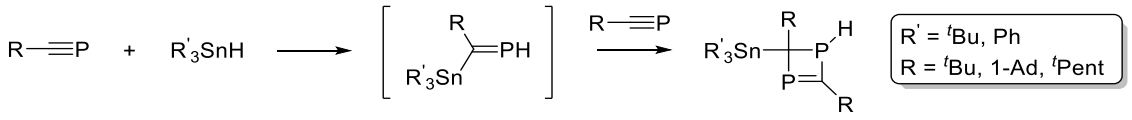

Scheme 1-10*: 1,2-Addition reaction of organotin hydrides with an excess of phosphaalkyne.*[3,35]

Other examples of 1,2-additions include reactions with organo-magnesium and organo-lithium compounds to give phosphavinylmagnesium halides and phosphavinyllithium complexes respectively.[11,36,37] With organolithium reagents the outcome is dependent on the molar ratio of the reagents as shown by Cowley and co-workers (**Scheme 1-11**).[11,36,37] They reported that the reaction of ArC≡P (Ar =2,4,5-^{t}BuC_6H_2) with one equivalent of methyl lithium in THF followed by the addition of water results in the formation of the corresponding phosphaalkene. In comparison when the phosphaalkyne is reacted with two equivalents of methyl lithium the formation of a 1,3-diphosphabutadienyl anion can be achieved. Treatment of the 1,3-diphosphabutadienyl anion with deoxygenated water results in cleavage of one of the P-C bonds yielding equimolar quantities of both the starting material and phosphaalkene, while treatment with alkyl halides affords the 1,3-diphosphabutadiene.[37]

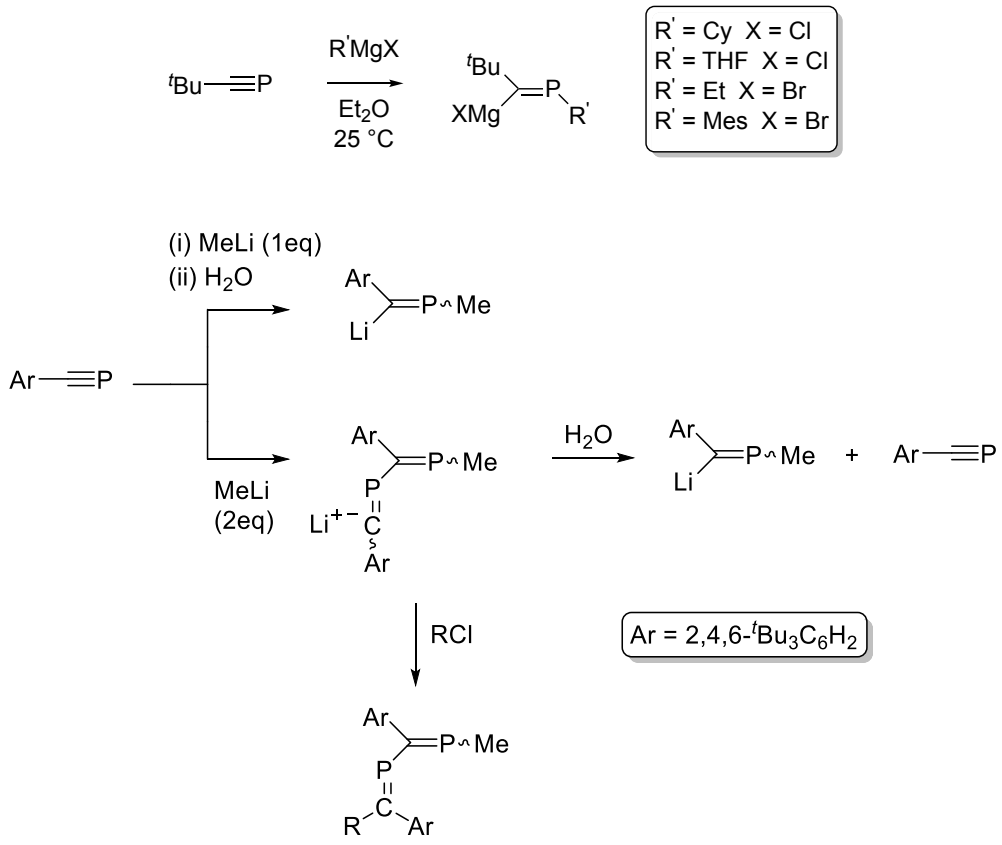

Scheme 1-11: *Top: 1,2-Addition of organomagnesium reagents and phosphaalkynes to give phosphavinylmagnesium halides. Bottom: 1,2-Addition of organolithium reagents and phosphaalkynes to give phosphavinyllithium complexes.*[11,36,37]

CYCLOADDITION REACTIONS OF PHOSPHAALKYNES

The cycloaddition chemistry of phosphaalkynes is extremely well developed with many examples of [2+1] cycloadditions with carbenes,[38] chlorocarbenes,[38] silyenes,[39] germylenes,[40] phosphinidenes[41] and terminal phosphinidene[42] complexes being reported, which offer convenient synthetic routes to phosphorus-containing heterocycles including three-membered ring systems (**Scheme 1-12**).

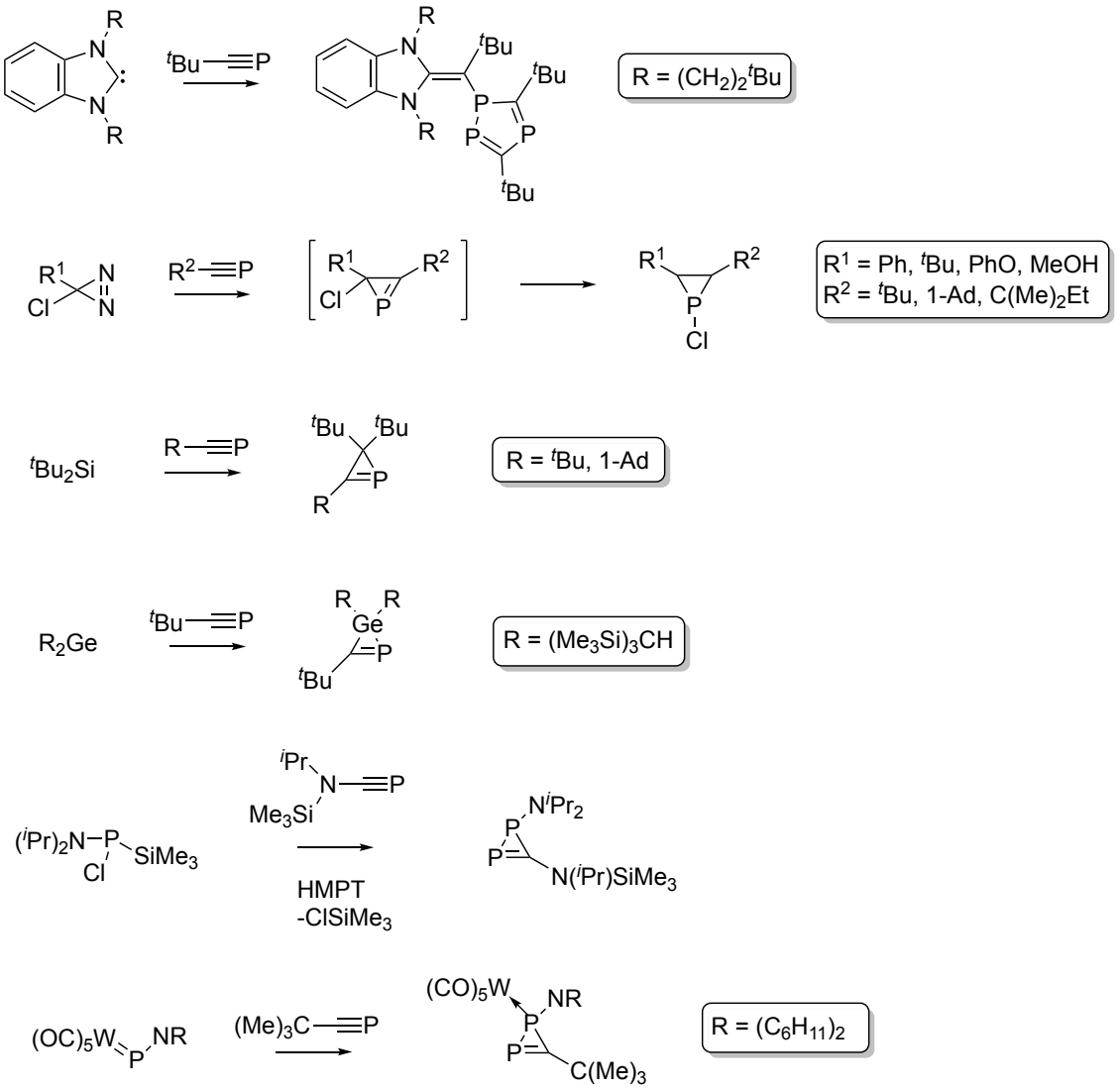

Scheme 1-12: *[2+1] Cycloaddition (a) carbene,*[38] *(b) chlorocarbene,*[38] *(c) silylenes,*[39] *(d) germylenes,*[40] *(e) phosphinidines*[41] *and (f) terminal phosphinidine complexes*[42]

In comparison, [2+2] cycloadditions of phosphaalkynes are relatively rare. However, it has been shown that phosphaalkynes can undergo [2+2] cycloadditions with distannenes,[43] carbenes,[44] metallo-diphosphenes[45] and transition metal imido complexes.[46,47] In 1988, Crowley reported the first example of a phosphadistannacyclobutene, formed by the [2+2] cycloaddition of a distannene and ^{t}BuC≡P (**Scheme 1-13**).[43] The phosphadistannacyclobutene formed was characterised by NMR spectroscopy and X-ray crystallography.

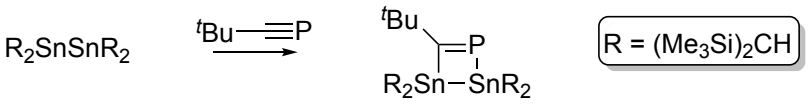

Scheme 1-13: *[2+2] Cycloaddition of distannene and ^{t}BuC≡P* [43]

In 1996, the first 1-phospha-3-molybdacyclobut-2-ene, formed from head-to-tail phosphaalkyne cycloaddition to a metal-carbon double bond of a Schrock-type carbene, was reported (**Scheme 1-14**).[44] The initial step, a [2+2] cycloaddition is followed by a [1,3] migration of an alkoxy group from the molybdenum to the phosphorus, this was the first reported instance of a characterised metal-to-phosphorus ligand migration in such systems. A couple of years later the Weber and Gröbe groups showed that a metallo-diphosphene could undergo a [2+2] cycloaddition with a phosphaalkyne (**Scheme 1-14**).[45]

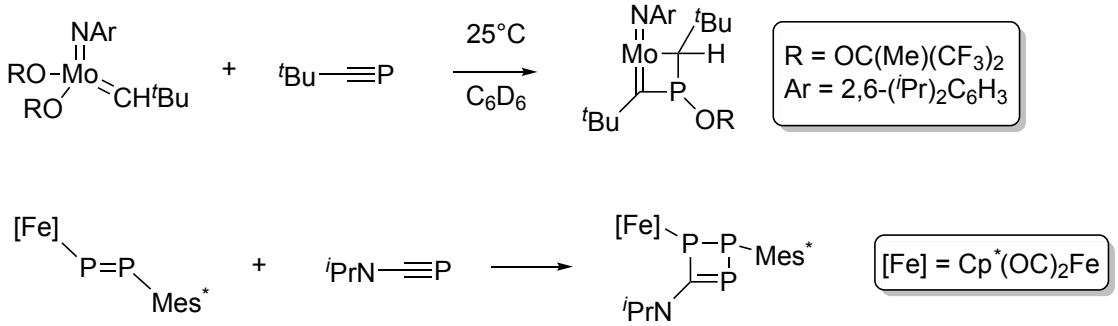

Scheme 1-14: *[2+2] Cycloaddition of: Top: Schrock like carbene.*[44] *Bottom: Metallo-diphosphenes.*[45]

Another example of [2+2] cycoloaddition is that of transition metal imido complexes and phosphaalkynes. Regitz reported the synthesis of 1,3,5-triphosphinines by the trimerization of phosphaalkynes in the coordination sphere of *tert*-butylimidovanadium(V) trichloride via a proposed mechanism involving a [2+2] cycloaddition, although initially no vanadium containing complexes were characterised. Later they reported the isolation of the vanadium(V) intermediate, 1,2,4-azaphosphavanada(V)-cyclobutene, through direct reaction of kinetically stabilized phosphaalkynes and substituted imidovanadium(V) trichloride complexes, RN=VCl_3. (**Scheme 1-15**).[46] In addition, the [2+2] cycloadditions of zirconium(IV) and titanium(IV) imido

complexes and ^{t}BuC≡P (**Scheme 1-15**) have been reported by Cloke and Nixon, with the resulting products being fully structurally characterised.[47]

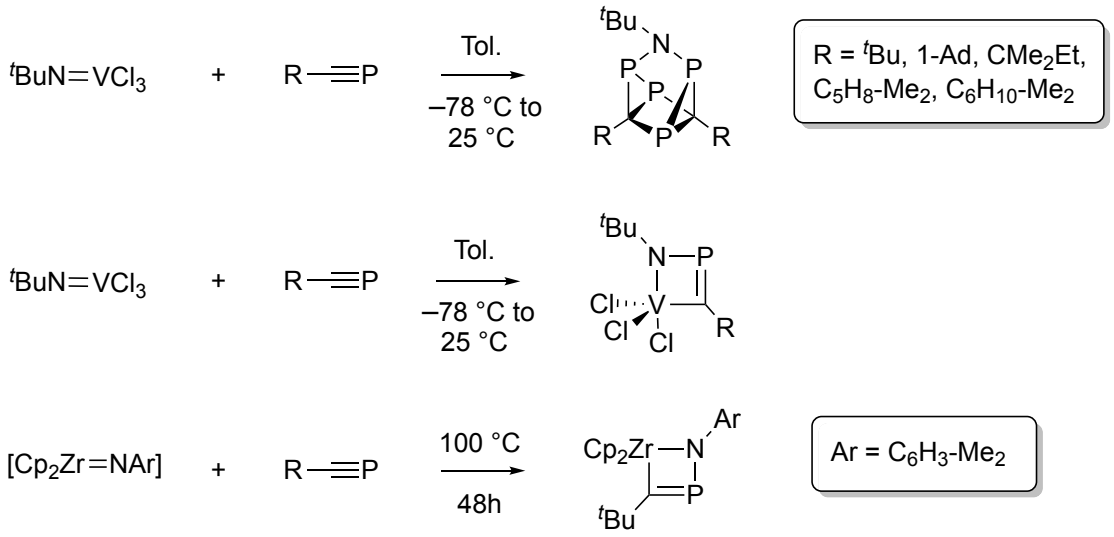

Scheme 1-15: *[2+2] Cycloaddition of vanadium(V)* [46] *and zirconium(IV)* [47] *imido complexes and phosphaalkynes.*

The phosphaalkyne ^{t}BuC≡P has also been shown to undergo codimerization with the λ^{5}-phosphaalkynes, R$_2$P≡CR$'$ (R = Pr$^{i}_2$N, R$'$ = Me$_3$Si) (**Scheme 1-16**), which are generated by *in situ* photolysis of the corresponding diaza- precursors, yielding the stable 1λ^{5},2λ^{3}-diphosphate as a yellow oil, which can undergo further reactivity with the λ^{3} phosphorus atom η^{1}-coordinating to W(CO)$_5$. [48]

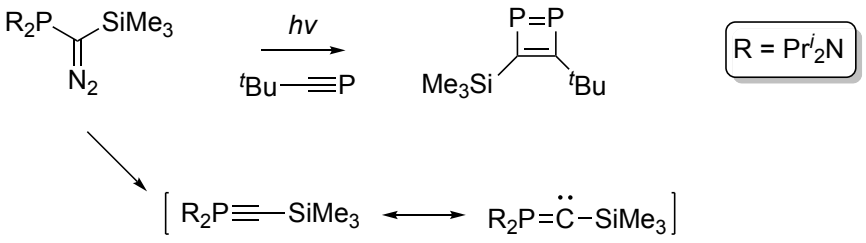

Scheme 1-16: *Codimerization of ^{t}BuC≡P and λ^{5}-phosphaalkyne to yield the stable 1λ^{5},2λ^{3}-diphosphate.*[48]

Other cycloadditions can also occur, for example [2+3] cycloadditions of 1,3-dipole compounds such as nitrile oxides,[49,50] diazoalkanes,[51,49] azides[49,52,53] and selenadiazoles,[54,55] which have been used as a route to a series of heterophospholes, a method used by Regitz in 1987 to prepare the first member of the 1,2,4-thiazaphosphole class of heterocycle (**Scheme 1-17**).[50]

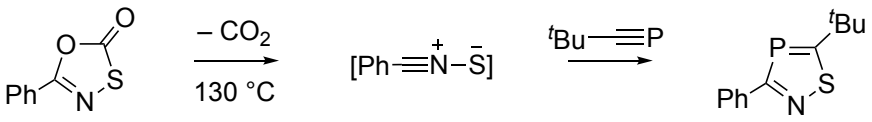

Scheme 1-17: *[2+3] Cycloaddition of phosphaalkyne leading to 1,2,4-thiazaphosphole.*[50]

Phosphaalkynes have also been shown to undergo [2+4] cycloaddtions (**Scheme 1-18**), with the initial cycloadduct being unstable resulting in either the formation of an aromatic phosphine or further reactivity with an additional molecule of the phophaallkyne through an ene-reaction.[3,11]

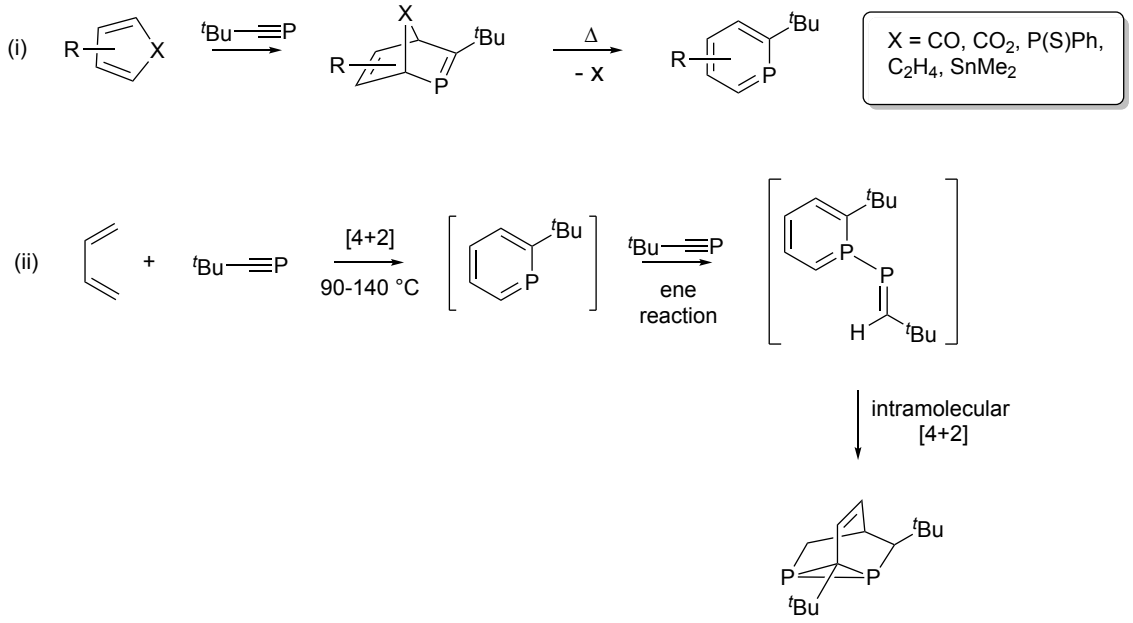

Scheme 1-18: *[2+4] Cycloaddition of phosphaalkyne resulting in (i) aromatic phosphine and (ii) further reactivity with an additional molecule of phophaallkyne through an ene-reaction.*

OLIGOMERISATION REACTIONS

Phosphaalkynes can undergo a variety of cyclo-oligomerisations induced by Lewis acids[56] and transition metals[57,58] as well as thermally[59], generally resulting in complex cage structures. In 1992, Regitz and co-workers reported the first spirocyclotrimerisation of ^{t}BuC≡P in the presence of aluminium trichloride to yield selectively a Lewis acid substituted phosphonium complex (**Scheme 1-19, 1.1^{+})**.[56]

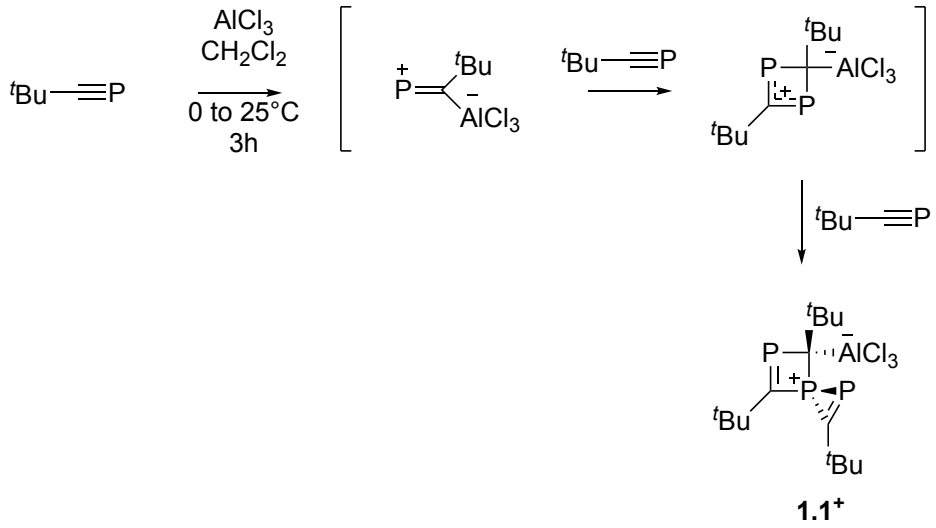

Scheme 1-19: *Spirocyclotrimerisation of ^{t}BuC≡P in the presence of aluminium trichloride to yield selectively the Lewis acid substituted phosphonium complex* ***1.1*****$^{+}$**.[56]

In the presence of DMSO the aluminium trichloride substituent is displaced yielding the spirocyclic $\lambda^5\sigma^4$, $\lambda^3\sigma^2$ diphosphate (**Scheme 1-20**, **1.2**), which rearranges above −45°C to afford the 1,3,5-triphospha Dewar benzene **1.3**; in the presence of ^{t}BuC≡P the tetraphosphatetracycle **1.4** is formed via a homo-Diels-Alder reaction. If the $\lambda^5\sigma^4$, $\lambda^3\sigma^2$ diphosphate rearranges in the presence of excess aluminium trichloride then the isomeric 1,2,5-triphospha Dewar benzene **1.5** is formed which can also be trapped by ^{t}BuC≡P yielding a tetraphosphatetracycle **1.6**.

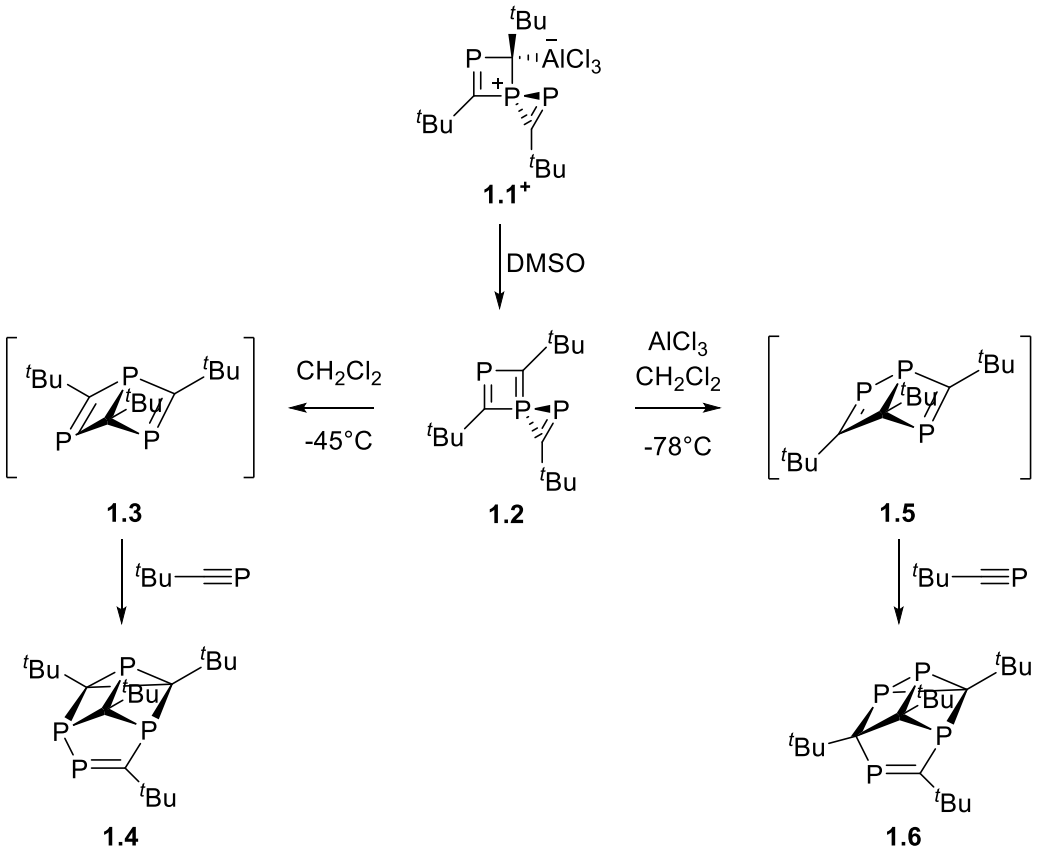

Scheme 1-20: *Synthesis of the spirocyclic $\lambda^5\sigma^4$, $\lambda^3\sigma^2$ diphosphate **1.2** and rearrangement to 1,3,5-triphospha Dewar benzene **1.3** and tetraphosphatetracycle **1.4**. If the $\lambda^5\sigma^4$, $\lambda^3\sigma^2$ diphosphate rearranges in the presence of excess aluminium trichloride 1,2,5-triphospha Dewar benzene **1.5** and tetraphosphatetracycle **1.6** are formed.*[56]

In addition, thermal cyclo-oligomerisation of phosphaalkynes leads to a mixture of complex cage structures.[59] For example, heating ^{t}BuC≡P to 180°C leads to the formation of complex mixtures of tetramers including tetraphosphacubane (**Scheme 1-21**),[59] which has been coordinated to metal centres including $Fe(CO)_4$[60] and $Pt(PR_3)Cl_2$.[61]

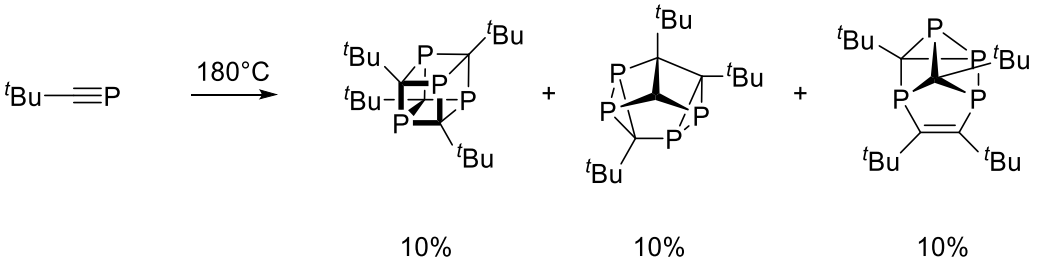

Scheme 1-21: *Thermal cyclo-oligermerisation of ^{t}BuC≡P.*[59]

Transition metals and carbene-like complexes can facilitate the thermal oligomerisation of phosphaalkynes under milder conditions (**Scheme 1-22**).[58] Furthermore, triphosphabenzenes and triphospholides can be afforded through metal-centred cyclotrimerisation and dimerization of phosphaalkynes respectively.[57]

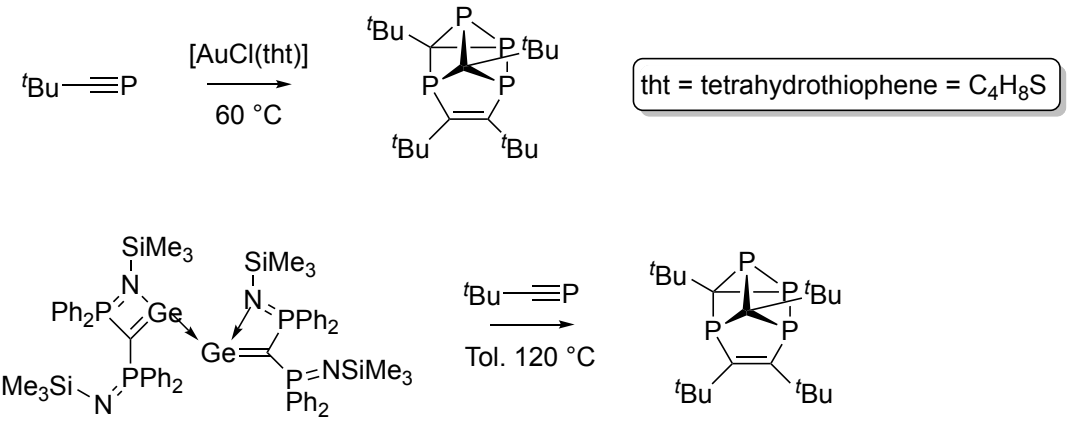

Scheme 1-22: *Metal-catalyzed and carbene-like catalyzed cyclo-oligermerisastion of* ^{t}*BuC≡P forming phosphine oligomers* [58]

1.2.5 COORDINATION CHEMISTRY OF PHOSPHAALKYNES

Phosphaalkynes can coordinate to transition metal centres in a variety of ways (**Figure 1-7**, **a-e**), due to the presence of both the highly reactive π-system and the lone pair on phosphorus.[3,11,57,62,63,64] Typically, η^2-coordination, **b**, is the most common mode observed due to the highly reactive nature of the π-system, yielding complexes analogous to the two electron π-complexes of classical alkynes. This is a direct contrast to the coordination of the isoelectronic nitriles and is a result of the phosphorus lone pair being stabilised compared to the nitrogen lone pair. If there is enough steric bulk provided by the ancillary ligand and the surrounding coordination site then the η^1-coordination of the phosphaalkyne can be achieved. [3,11,57]

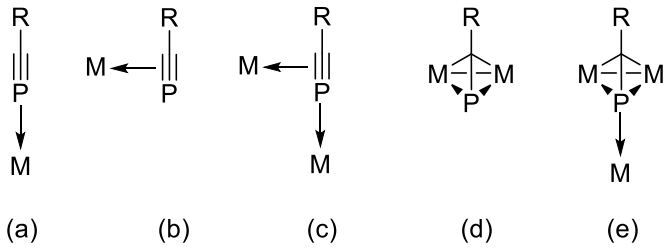

Figure 1-7: *Coordination modes for phosphaalkynes.* [3,11,57]

η^2 PHOSPHAALKYNE COORDINATION

In 1981, Nixon, reported the synthesis and X-ray diffraction studies of the novel platinum complex $Pt(PPh_3)_2(\eta^2\text{-}P{\equiv}C^tBu)$ (**Scheme 1-23**, **1.7**).[62] The coordination resulted in a lengthening of the C≡P bond (1.672(17) Å) compared with that of free phosphaalkyne (1.548(1) Å).

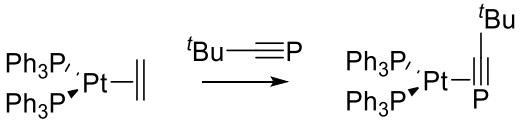

1.7

Scheme 1-23: *Synthesis of the first η^2-coordinated phosphaalkyne complex* ***1.7***.[62]

Later, the synthesis of the first bridging phosphaalkyne complex, $\mu^3\text{-}\eta^2\text{:}\eta^2\text{:}\eta^1$-$[Fe_2(CO)_6Pt(dppe)(^tBuC{\equiv}P)]$ was reported (**Scheme 1-24**).[64] The reaction of $^tBuC{\equiv}P$ with $Pt(dppe)_2$ gave the colourless complex $Pt(dppe)(^tBuC{\equiv}P)$ **1.8** with the phosphaalkyne η^2 -coordinated, subsequent reaction with either $Fe_2(CO)_9$ or $Fe_3(CO)_{12}$ yielded the cherry red trimetallic $\mu^3\text{-}\eta^2\text{:}\eta^2\text{:}\eta^1$-$[Fe_2(CO)_6Pt(dppe)(^tBuC{\equiv}P)]$ **1.9**. Both phosphaalkyne complexes were characterised by NMR studies with the latter also studied by single crystal X-ray diffraction (**Figure 1-8**), which showed that the phosphaalkyne fragment transversely bridged the Fe-Fe bond with the phosphorus atom coordinated to the three metal atoms in the Fe_2Pt ring with the lengthening of the P-C bond to 1.703(6) Å, which is more akin to a P=C double bond than to a triple bond. This was the first established example of this type of bonding for a phosphaalkyne ligand.

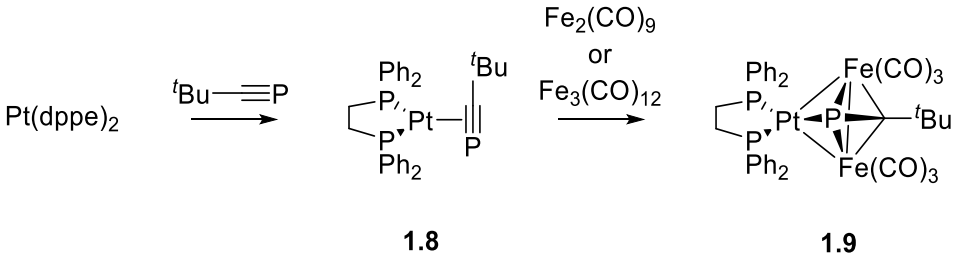

1.8 **1.9**

Scheme 1-24: *Synthesis and reactivity of [Pt(dppe)(ᵗBuC≡P)]* ***1.8*** *yielding μ³-η²-[Fe₂(CO)₆Pt(dppe)(ᵗBuC≡P)]* ***1.9***.[64]

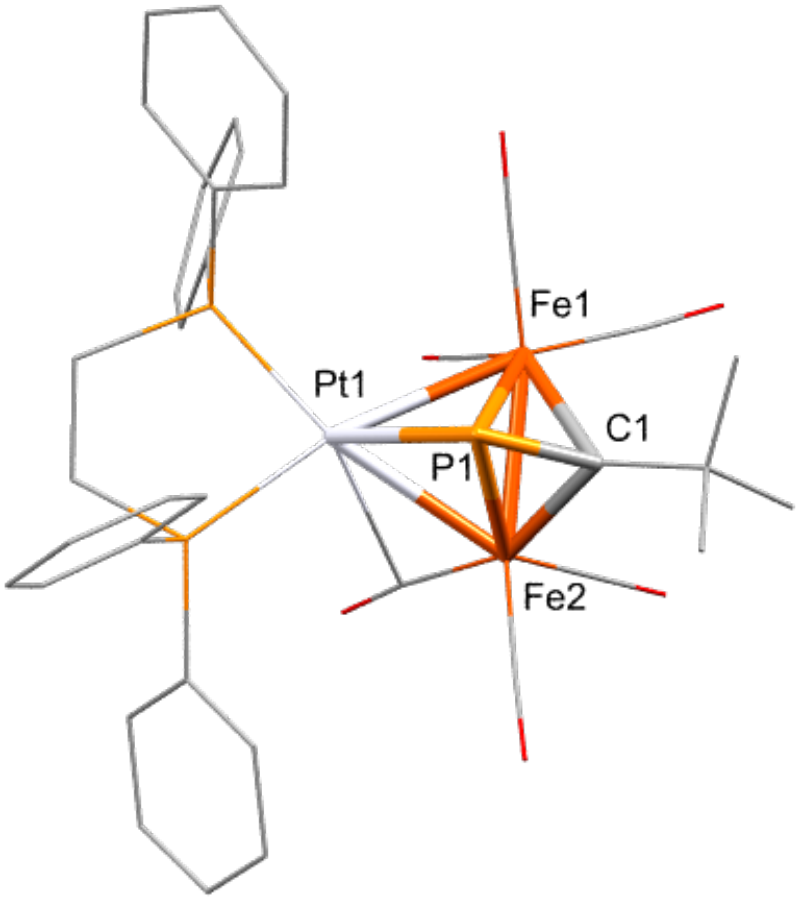

Figure 1-8*: Solid state molecular structure of μ³-η²:η²:η¹-[Fe₂(CO)₆Pt(dppe)(ᵗBuC≡P)]* ***1.9***.[64]

In addition, there have been a variety of other mononuclear complexes with η^2-ligated ^{t}BuC≡P to titanium,[3,57,65] zirconium[3,57,65] and rhodium[3,57](**Scheme 1-25**); while these examples are all 2 electron η^2-bonding, the first mononuclear phosphaalkyne complex with a 4 electron η^2-bonding mode has been reported at molybdenum (**Scheme 1-26**), a type of bonding well established for alkynes.[66]

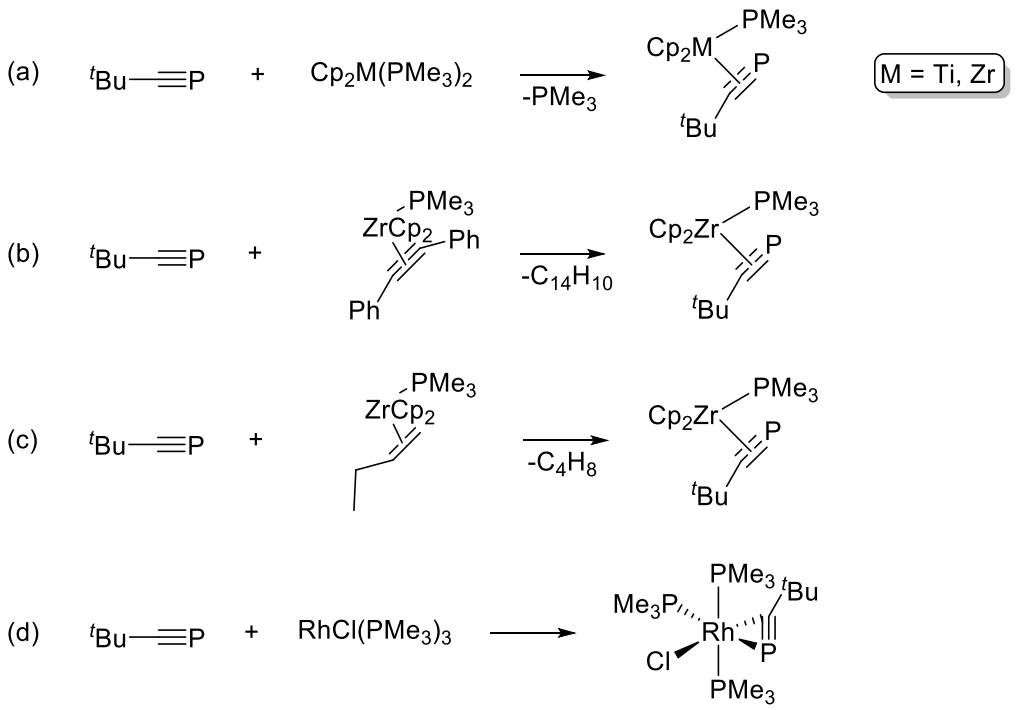

Scheme 1-25: *Synthesis of (a) $Cp_2M(PMe_3)(\eta^2$-^{t}BuC≡P) (M = Ti and Zr),*[3,57,65] *(b) and (c) $Cp_2Zr(PMe_3)(\eta^2$-^{t}BuC≡P)* [3,57,65] *and (d) $RhCl(PMe_3)_3(\eta^2$-^{t}BuC≡P)*[57]

The molybdenum phosphaalkyne complex **1.10**$^+$ was formed through an initial displacement of an alkene in the molybdenum-stilbene precursor followed by the addition of ^{t}BuC≡P at −78 °C, subsequent warming resulted in the η^2-coordination of the phosphaalkyne (**Scheme 1-26**).[66] The ^{31}P{^{1}H} NMR spectrum exhibited two singlet resonances at δ 157.3 and δ 467.8, corresponding respectively to the ancillary bidentate ligand, $[(MeO)_2POBF_2OP(OMe)_2]^-$, and the phosphorus of the four-electron η^2-bonded ^{t}BuC≡P. Furthermore, it was reported that upon addition of a second equivalent of phosphaalkyne, a cycloaddition occurs, forming the η^4-1,3-diphosphacyclobutadiene **1.11**$^+$, in which it was speculated that the bound phosphaalkyne

switched from a four-electron to a two-electron binding mode to accommodate the second equivalent of phosphaalkyne.

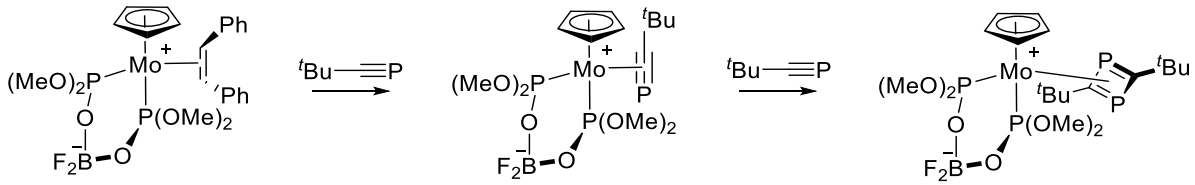

1.10⁺ **1.11⁺**

Scheme 1-26: *Synthesis of the first mononuclear η²-(4e)-phosphaalkyne complex* ***1.10⁺***.[66]

More recently, in 2014, Russell reported the synthesis and characterisation of the first cationic gold(I) complex of a phosphaalkyne (**Scheme 1-27**, **1.12⁺**).[67] The reaction of either ^{t}BuC≡P or AdC≡P with the cationic gold complex [(P(^{t}Bu)$_2$(C$_{12}$H$_9$))Au][SbF$_6$], results in rapid coordination yielding the corresponding η^2-phosphaalkyne complexes which were characterised by NMR and single crystal X-ray-diffraction studies.

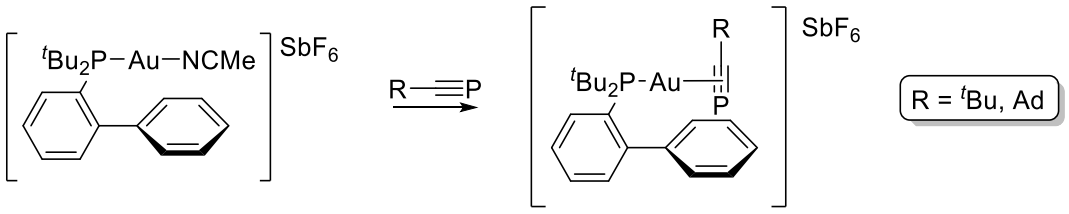

1.12⁺

Scheme 1-27: *Synthesis of the first gold (I) phosphaalkyne complex.*[67]

In the ^{31}P{^{1}H} NMR spectrum two very broad signals were apparent at 72.0 ppm and −22.6 ppm due to the ancillary ligand, ^{t}Bu$_2$P{*o*-biphenyl}, and the coordinated phosphaalkyne respectively. The broadening occurred due to the rapid exchange between the free and coordinated P centres at the metal centre at room temperature on the NMR spectroscopy timescale, this broadening was resolved by undertaking low temperature NMR studies at −40 °C, allowing resolution of the broad signals into doublets with a coupling of 32 Hz (31.9 Hz when R = ^{t}Bu and 32.7 Hz where R = Ad). The crystal structure for the ^{t}BuC≡P complex shows the phosphaalkyne unit is η^2 bound

with a P-Au-phosphaalkyne angle of 168.5(3) °, deviating from linearity reflecting the sterics of the phosphine; the C≡P bond length (1.569(12) Å) is indistinguishable from that of the uncoordinated phosphaalkyne.

η^1 PHOSPHAALKYNE COORDINATION

Phosphaalkynes can also interact with metal centres through the lone pair on the phosphorus. Such complexes are only favoured where the η^2-binding mode is precluded by steric bulk in the ancillary ligand set.

The first unequivocal examples of η^1-coordinated phosphaalkyne complexes were reported by Nixon in 1987, obtained by the displacement of dinitrogen from *trans*-[M(N_2)$_2$($R_2PCH_2CH_2PR_2$)$_2$] (M = Mo and W) (R = *p*-ClC_6H_4, Et, Ph and *p*-Tolyl) with AdC≡P or ^{t}BuC≡P (**Scheme 1-28**).[68] The formation of the η^1-phosphaalkyne complexes **1.13-1.18** was inferred from the $^{31}P\{^1H\}$ NMR spectra, while definitive confirmation was achieved through the crystallographic study of *trans*-[Mo(P≡CAd)$_2$(depe)$_2$] (dppe = $Et_2PCH_2CH_2PEt_2$) **1.17**. The complex contained two *trans*-η^1-coordinated phosphaalkynes with a shortened C≡P bond length of 1.520(12) Å compared to an average value of 1.540(4) Å as observed in the free phosphaalkyne ligands.[14,18]

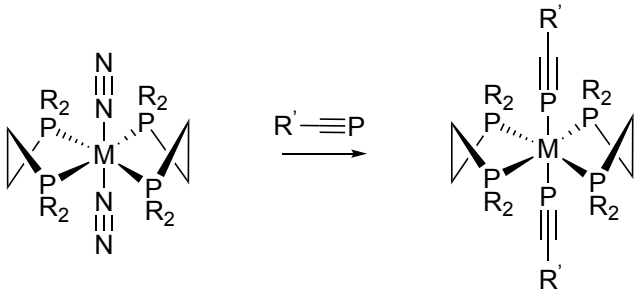

	M	R'	R
1.13	Mo	^{t}Bu	*p*-ClC_6H_4
1.14	Mo	^{t}Bu	Et
1.15	Mo	^{t}Bu	Ph
1.16	Mo	^{t}Bu	*p*-Tolyl
1.17	Mo	Ad	Et
1.18	W	^{t}Bu	Ph

Scheme 1-28: *Synthesis of the first examples of η^1-coordinated phosphaalkyne complexes **1.13-1.18**.*[68]

Further work reported by Nixon showed this concept could be expanded to group VIII metals with the synthesis of *trans*-[FeH(η^1-P≡C^{t}Bu)(dppe)$_2$][BF_4] **1.19.BF_4**, by chloride abstraction from *trans*-[FeHCl(dppe)$_2$] followed by subsequent addition of the phosphaalkyne ^{t}BuC≡P (**Scheme**

1-29).[69] The resulting η^1-phosphaalkyne complex was characterised by $^{31}P\{^1H\}$ NMR spectroscopy which showed two resonances, a quintet at −154 ppm and a doublet at −62 ppm, with a mutual coupling of 36 Hz, assigned to the phosphaalkyne and dppe ligands respectively. The same pattern was also observed for the structurally related complex *trans*-[ReCl(η^1-P≡C^{t}Bu)(dppe)$_2$], which was obtained by displacement of N_2 from *trans*-[ReCl(N_2)(dppe)$_2$].[69]

Anion metathesis of *trans*-[FeH(P≡C^{t}Bu)(dppe)$_2$][BPh_4] allowed crystallographic characterisation as the BF_4 salt **1.19.BF$_4$**. This confirmed the η^1-ligation of the phosphaalkyne *trans*- to the hydride with a notable shortening of the P≡C bond to 1.512(5) Å. This shortening is a direct contrast to the lengthening seen in complexes featuring η^2-coordinated phosphaalkynes and has been rationalised by drawing analogy with isocyanide, carbonyl, organonitrile and dinitrogen ligands, where the electron lone pair orbital involved in the σ coordination to the metal centre has antibonding character to the unsaturated bond. [70]

The reactivity of *trans*-[FeH(P≡C^{t}Bu)(dppe)$_2$][BF_4] **1.19.BF$_4$** in chlorinated solvents was also observed (**Scheme 1-29**). This showed the formation of the η^1-fluorophosphaalkene complex *trans*-[FeH(η^1-PF=CH^{t}Bu)(dppe)$_2$)][$FeCl_2F_2$] **1.20.FeCl$_2$F$_2$**.[69] This was thought to occur through an initial activation of the P≡C bond by coordination to the iron(II) centre, which allowed nucleophilic attack of fluoride ion from the BF_4 counter-ion. The reactivity was replicated by the reaction of either HBF_4 or [H(OEt_2)]BF_4 with *trans*-[FeH(P≡C^{t}Bu)(dppe)$_2$][BF_4] **1.19.BF$_4$**. The resulting η^1-fluorophosphaalkene complex **1.20.FeCl$_2$F$_2$** exhibited a doublet of quintets in the $^{31}P\{^1H\}$ NMR spectrum at 319 ppm ($^1J_{PF}$ = 985 Hz, $^2J_{PP}$ = 38 Hz) and doublet at 79 ppm ($^2J_{PP}$ = 38 Hz) for the phosphaalkene and the dppe scaffold respectively. In the solid state, the phosphaalkene bond has a bond length of 1.66(4) Å, comparable to that of the related fluorophosphaalkene complex, *trans*-[RhCl(PPh_3)$_2$(η^1-PF=C($SiMe_3$)$_2$)] (1.633(10) Å) and shorter than the P=C distance in η^2 phosphaalkenes and the free phosphaalkenes. [71,72]

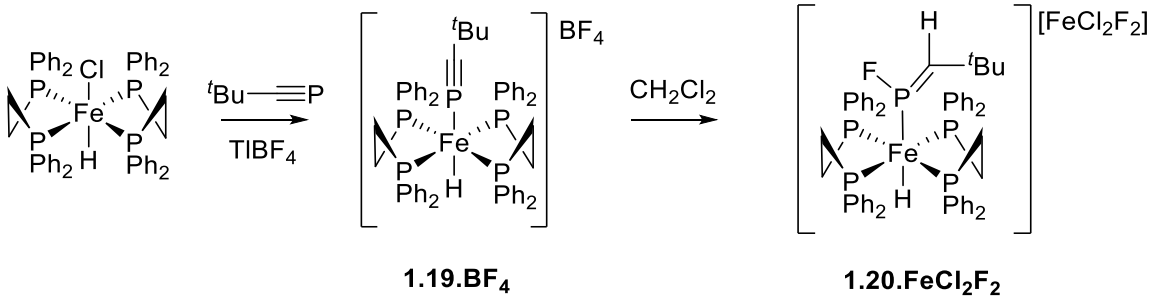

1.19.BF_4 **1.20.$FeCl_2F_2$**

Scheme 1-29: *Synthesis and reactivity in chlorinated solvents of trans-[FeH(P≡C^{t}Bu)(dppe)$_2$][BF_4]* ***1.19.BF_4.***[69]

The rhenium complex *trans*-[ReCl(η^1-P≡C^{t}Bu)(dppe)$_2$] **1.21** shows similar reactivity to *trans*-[FeH(P≡C^{t}Bu)(dppe)$_2$][BF_4] (**Scheme 1-30**), with the formation of a rare example of a phosphorus-bound phosphinidine oxide **1.22,** through a reaction of **1.21** with water. The resulting phosphinidine oxide complex was characterised by both NMR spectroscopy and single crystal X-ray diffraction studies.

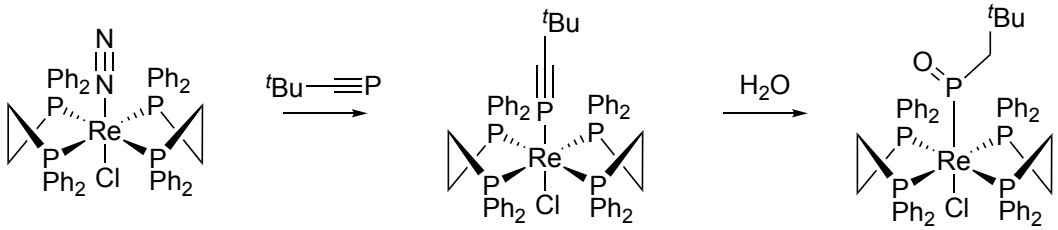

1.21 **1.22**

Scheme 1-30: *Synthesis and reactivity in H_2O of trans-[ReCl(P≡C^{t}Bu)(dppe)$_2$]* ***1.21****.*

1.3 THE 2-PHOSPHAETHYNOLATE ANION

Another aspect of low coordinate phosphorus chemistry which has seen a growth of interest over the last decade is the coordination and reactivity of the 2-phosphaethynolate anion, [P≡CO$^-$], the phosphorus analogue of the cyanate anion, [N≡CO$^-$]. As with the cyanate anion the 2-phosphaethynolate anion exhibits two main resonance forms, the phosphaethynolate and the phosphaketenide form (**Figure 1-9**).[73,74]

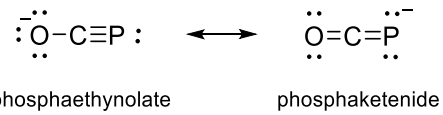

Figure 1-9: *The two main resonance forms of OCP^-.*[73,74]

1.3.1 SYNTHESIS OF THE 2-PHOSPHAETHYNOLATE ANION

The first rational synthesis of OCP^- was developed by Becker and co-workers in 1992.[73–75] They reported the synthesis of $Li(DME)_2(OCP)$ (DME = 1,2-dimethoxyethane) **1.23** by the reaction of lithium *bis*(trimethylsilyl)phosphide ($LiP(SiMe_3)_2$) with dimethyl carbonate (**Scheme 1-31**). The structure of **1.23** was validated through single crystal X-ray diffraction showing a linear anion [O-C-P 178.5(3)°] with P-C and C-O bond length of 1.553(3) and 1.198(4) Å respectively. This short P-C bond length is comparable to that of phosphaalkynes and thus consistent with the phosphaethynolate resonance form. Subsequently other salts were reported, including a family of group II metal *bis*(2-phosphaethynoates), $M(DME)_3(OCP)_2$ (M = Mg **1.24**, Ca **1.25**, Sr **1.26** and Ba **1.27**) which were synthesized in a similar maner to that reported by Becker (**Scheme 1-31**).[76]

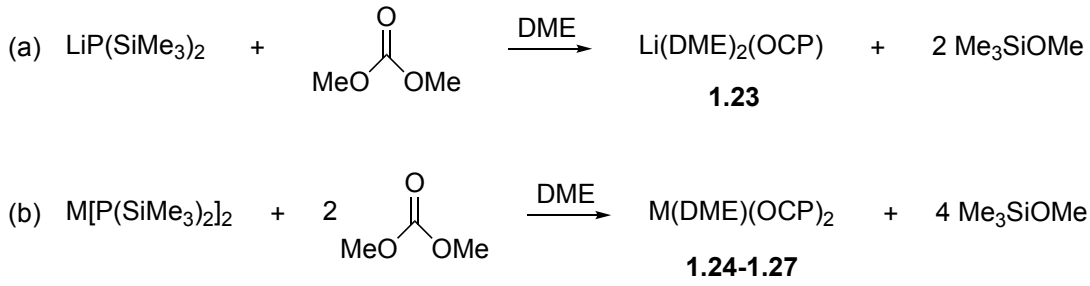

Scheme 1-31: *Synthesis of (a) $Li(DME)_2(OCP)$* ***1.23*** [73,75]

(b) $M(DME)_3(OCP)_2$ (M = Mg ***1.24****, Ca* ***1.25****, Sr* ***1.26*** *and Ba* ***1.27****).*[73,76]

In 2011, Grützmacher and co-workers reported the synthesis of both $Na(DME)_2(OCP)$ **1.28** and $Na(dioxane)_{2.5}(OCP)$ **1.29**, obtained respectively by direct carbonylation of sodium dihydrogen phosphide ($NaPH_2$) and reaction of $NaPH_2$ with ethylenecarbonate (**Scheme 1-32**).[77] Unlike the previously determined structures of $Li(DME)_2(OCP)$[75] and $Ca(DME)_3(OCP)_2$[76] that of

$Na(DME)_2(OCP)$ **1.28** consists of two linear μ_2-bridging OCP^- moieties bound to two $Na(DME)_2$ units through the oxygen atoms forming a central four membered Na_2O_2 ring, with an average C≡P bond length of 1.575 Å, which is comparable to previously discussed phosphaalkynes. In addition, both **1.28** and **1.29** exhibit significant thermal stability with the latter also being air stable and robust to hydrolysis. Most recently Grützmacher and co-workers reported an improved synthesis of $Na(dioxane)_x(OCP)$ (**Scheme 1-32, 1.29**), through the deprotonation of phosphane gas (PH_3) by NaO^tBu and the subsequent reaction of dimethylcarbonate and precipitation by the addition of dioxane. This improved synthesis allows for several-hundred grams of the sodium salt to be synthesized.[73,78]

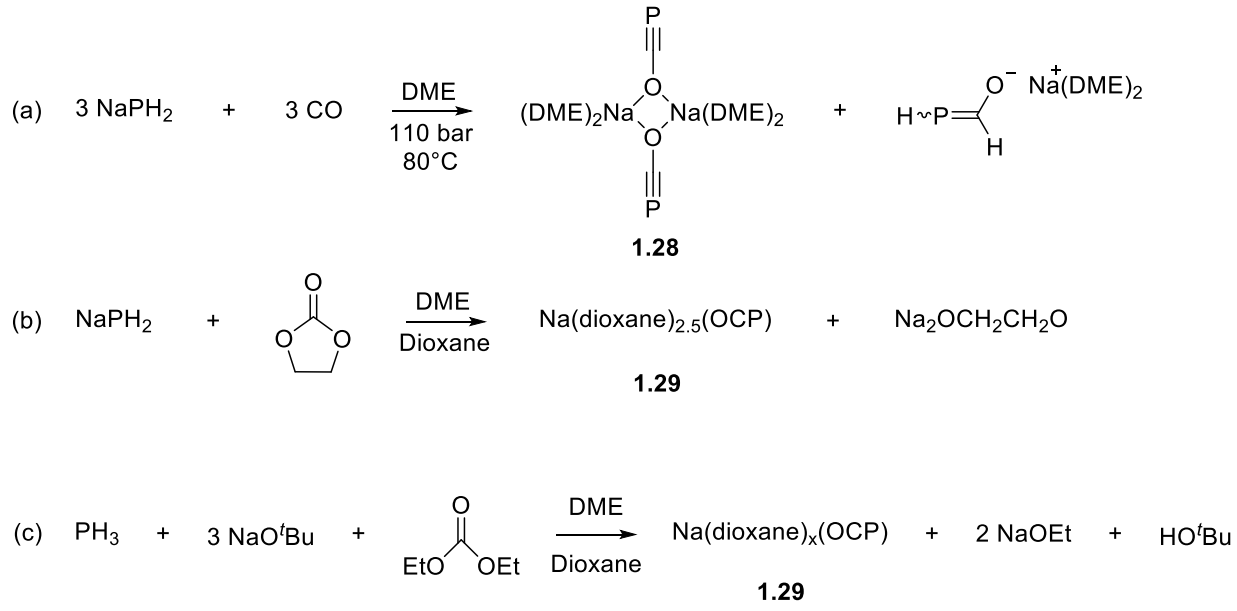

Scheme 1-32: *Synthesis of (a) $Na(DME)_2(OCP)$* ***1.28*** *through direct carbonylation of sodium dihydrogen phosphide ($NaPH_2$) and (b) $Na(dioxane)_{2.5}(OCP)$* ***1.29*** *through the reaction of $NaPH_2$ with ethylenecarbonate.[77] (c) Improved synthesis for $Na(dioxane)_x(OCP)$* ***1.29*** *through the deprotonation of PH_3 by NaO^tBu and the subsequent reaction with dimethylcarbonate.*[73,78]

Cummins and coworkers reported an alternative synthesis for $Na(DME)_2(OCP)$ **1.28** by reaction of carbon dioxide with the borane-capped niobium phosphide anion $[\{(C_6F_5)_3B\}P{\equiv}Nb(N[Np]Ar)_3]^-$ (Ar = 3,5-$C_6H_3Me_2$, Np = neopentyl) (**Scheme 1-33**).[79] The initial $^{31}P\{^1H\}$ NMR studies showed a single resonance at −393 ppm comparable to that reported for the $Li(DME)_2(OCP)$ (-384 ppm).

Upon work-up the sodium salt **1.28** was isolated in a 70% yield with $^{13}C\{^1H\}$ NMR spectroscopy and structural data confirming the formation of the phosphaethynolate salt matching that reported by Grützmacher.[77,79]

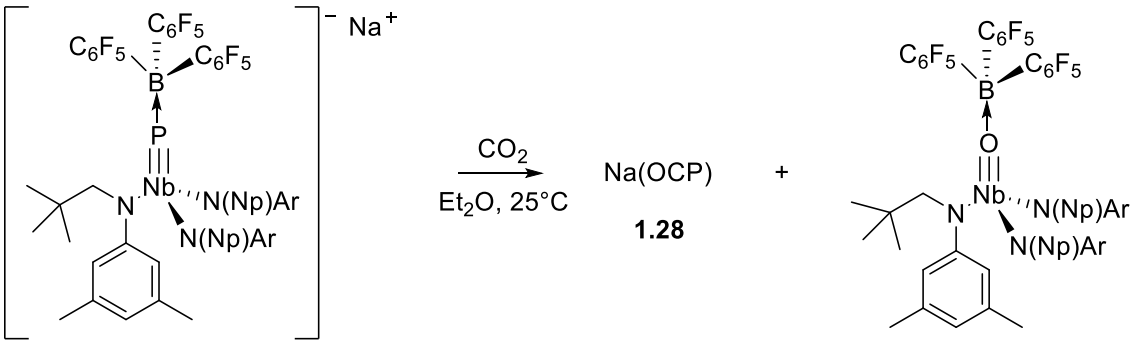

Scheme 1-33: *Synthesis of Na(OCP)* ***1.28*** *through reaction of carbon dioxide with the borane-capped niobium phosphide anion* $[\{(C_6F_5)_3B\}P{\equiv}Nb(N[Np]Ar)_3]^-$ *(Ar = 3,5-*$C_6H_3Me_2$*, Np = neopentyl).*[79]

In 2013, Jupp and Goicoechea described the synthesis of the potassium salt, [K(18-crown-6)][OCP] **1.30**, by a direct carbonylation of DMF solutions of K_3P_7 at 150°C (**Scheme 1-34**).[80] Spectroscopically the potassium salt was comparable to that of the sodium and lithium salts reported, with the $^{31}P\{^1H\}$ NMR spectrum exhibiting a singlet at –397 ppm and the $^{13}C\{^1H\}$ NMR spectrum exhibiting a doublet at 170 ppm. The IR spectrum showed a band at 1730 cm^{-1} arising from the P≡C stretching mode, also consistent with previous literature values. The single crystal X-ray diffraction data revealed a single O-C≡P unit with C-P and O-C bond distances of, 1.579(3) Å and 1.212(4) Å respectively, consistent with a formal C≡P triple bond. The diffraction data also showed a close electrostatic interaction between the phosphorus and the potassium cation (3.383(1) Å). These structural data are comparable to other reported crystal structures and consistent with a phosphaethynolate resonance structure.

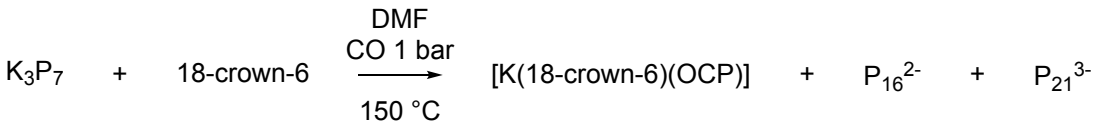

1.30

Scheme 1-34: *Synthesis of [K(18-crown-6)][OCP]* ***1.30*** *by a direct carbonylation of DMF (DMF = N,N-dimethylfomamide) solutions of K_3P_7 at 150°C.*[80]

Sundermeyer and von Hänisch have reported a range of ionic liquids comprising the phosphaethynolate ion and organic cations, obtained by the reaction of organic methylcarbonate salts with $P(SiMe_3)_3$ (**Scheme 1-35**).[81] This has given rise to a variety of highly tuneable salts based on the 2-phosphaethynolate anion, with cations including ammonium and phosphonium. These have been spectroscopically and, in some cases, structurally characterised and show comparable structural properties to previously reported phosphaethynolate anions.

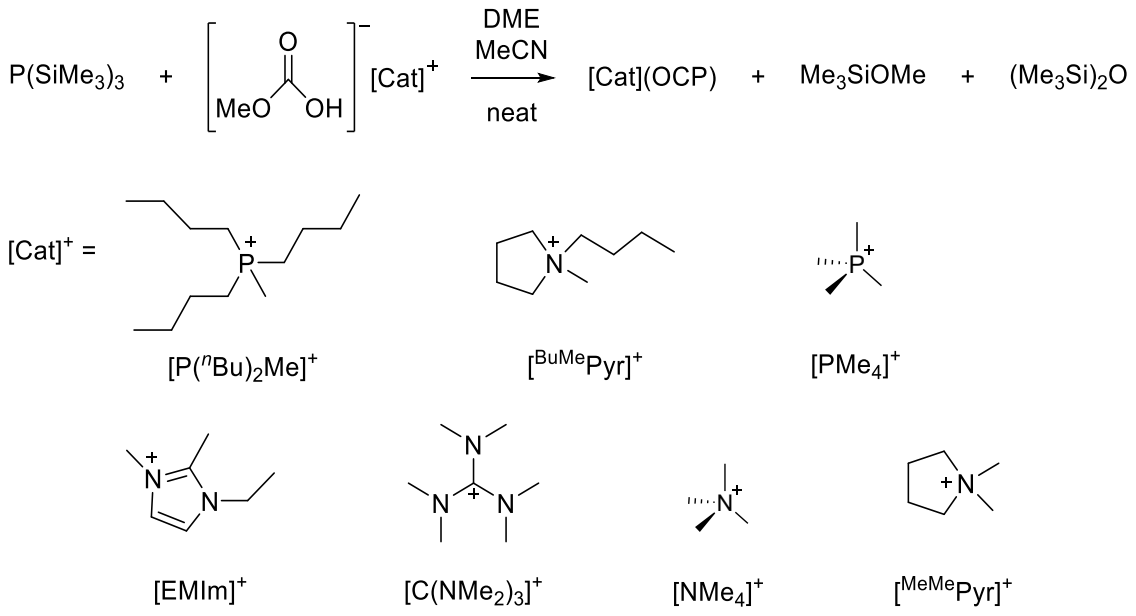

Scheme 1-35: *Synthesis of a range of ionic liquid organic 2-phosphaethynolate salts by the reaction of organic methylcarbonate salts with $P(SiMe_3)_3$.*[81]

1.3.2 CHEMISTRY AND COORDINATION OF THE 2-PHOSPHAETHYNOLATE ANION

The 2-phosphaethynolate anion has been widely studied, including its electrochemistry and coordination to transition metals. It is readily oxidized forming the heterobicyclic dianion, $(P_4C_4O_4)^{2-}$ which was first observed by Becker and co-workers from the reaction of $Li(DME)_2(OCP)$ and sulfur dioxide (**Scheme 1-36**).[82] The $^{31}P\{^1H\}$ NMR spectrum of the dianion shows two triplets at 37 ppm and 81 ppm with a mutual coupling of 32 Hz. The solid-state structure shows that the dianion has a "butterfly" structure containing a central P-P bond. Since this report the analogous sodium salt has been studied using cyclic voltammetry which showed irreversible oxidations at low anodic potentials with the oxidation product being highly stable towards reduction. It was deduced that the stability for the oxidation product towards reduction was due to the insolubility of the product. This insolubility was also reported by Becker for $Li_2(P_4C_4O_4)$ **1.31**, thus, it was hypothesized that the resulting product was the analogous sodium salt, $Na_2(P_4C_4O_4)$ **1.32**.[82,83]

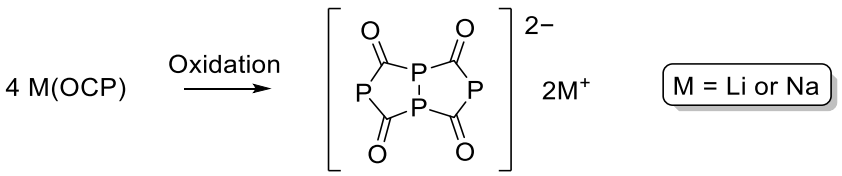

1.31 and **1.32**

Scheme 1-36: *Synthesis of $(P_4C_4O_4)^{2-}$* ***1.31*** *by oxidation of OCP^- with SO_2.*[82,83]

Recently, the reductive dimerization of OCP^- has been explored though treatment of a phosphaethynolate-scandium(III) compound with potassium graphite, resulting in $[K(OEt_2)]_2[(nacnac)Sc(OAr)]_2(OCPPCO)$ (Ar = =2,6-^{i}Pr$_2$C$_6$H$_3$) **1.33**, in which the tetra-anionic $(OCPPCO)^{4-}$ is stabilized by coordination to the two scandium centres (**Scheme 1-37**).[84] The $^{31}P\{^1H\}$ NMR spectra showed a significant change in the electronics of the OCP^- moiety with a shift to a higher frequency of 69.7 ppm compared to –343.5 ppm for the parent phosphaethynolate-scandium(III) compound. The solid-state structure was confirmed through single crystal X-ray

diffraction, which showed the reductive product was the dinuclear-'ate' complex **1.33** where the OCP^- moieties are η^2 bound through the CO and are unified by a single P-P bond.

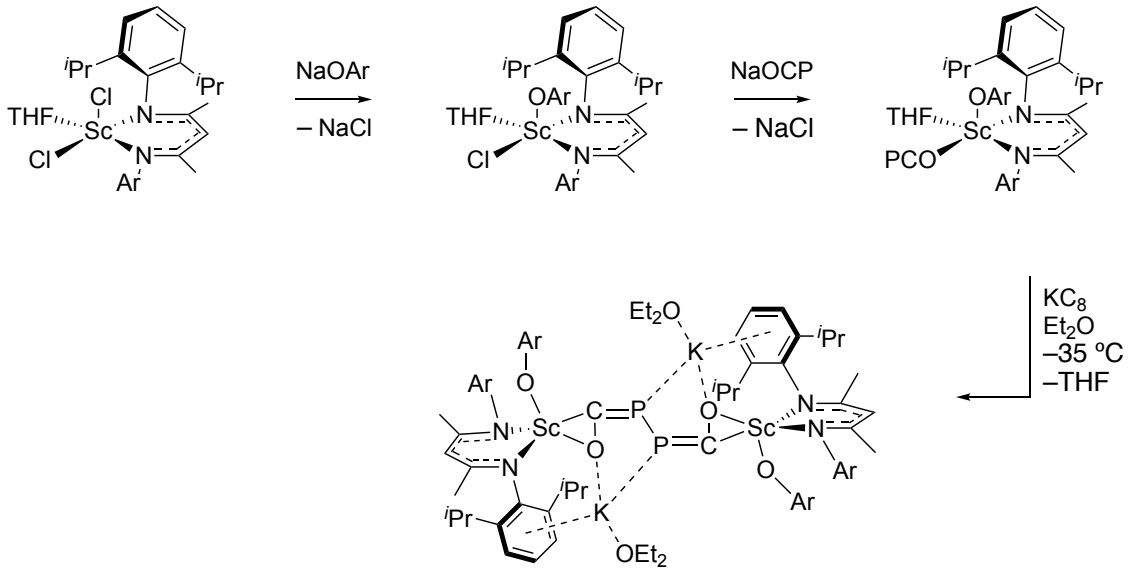

Scheme 1-37: *Synthesis of $[K(OEt_2)]_2$ [(nacnac)Sc(OAr)$_2$(OCPPCO)] (Ar = =2,6-^{i}Pr$_2$C$_6$H$_3$)* ***1.33****.*[84]

The coordination of the 2-phosphaethynolate anion to transition metals and main group element fragments has been studied extensively.[84] Within the resulting complexes the bonding has been shown predominantly to involve coordination through the phosphorus atom, and adoption of the phosphaketenide form, M-P=C=O, for example, (triphos)Re(PCO)(CO_2) (triphos = $MeC(CH_2PPh_2)_3$) **1.34** which was reported by Grützmacher in 2012 (**Scheme 1-38**).[83]

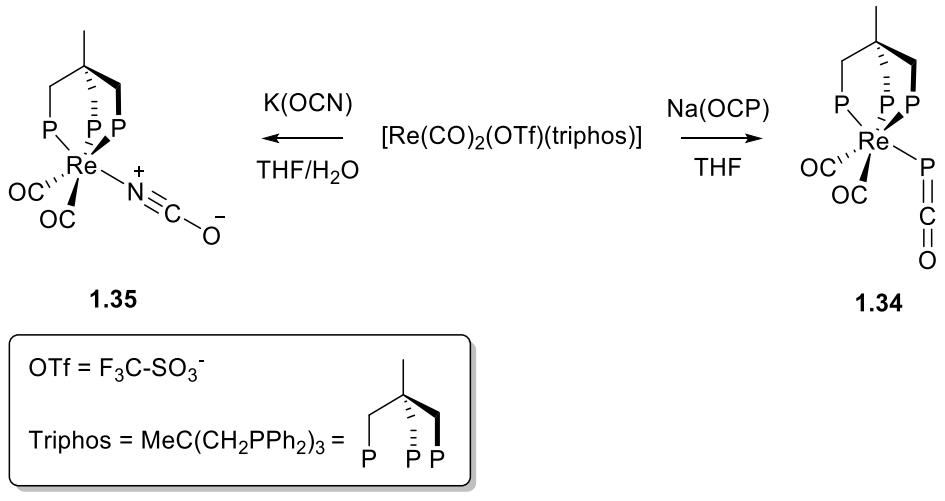

Scheme 1-38: *Synthesis of (triphos)Re(PCO)(CO_2)* ***1.34*** *and (triphos)Re(NCO)(CO_2)* ***1.35*** *(triphos = $MeC(CH_2PPh_2)_3$).*[83]

The bonding within **1.34** was investigated through a combination of X-ray diffraction studies and DFT calculations, alongside its nitrogenous analogue **1.35**, which showed that the bonding with the phosphaketene complex **1.34** has two major differences from **1.35**. The most significant difference is the bent coordination mode with a Re-P-C bond angle of 97.7° compared to the essentially linear coordination of the cyanate (∠Re-N-C of 178.6°).

There have since been multiple other reported complexes where the OCP^- moiety binds through the phosphorus atom, including the recent report of [(nacnac)V(OAr)(PCO)] (nacnac = $[ArNC(CH_3)]_2CH$ and Ar = 2,6-^{i}Pr$_2$C$_6$H$_3$).[85] In addition to the phosphorus-bound OCP^- complexes, it has been noted that OCP^- can bind through the oxygen as well as through the π-system.[73,74]

The formation of the oxygen-bonded phosphaethynolate compounds is favoured for metal centres that are more ionic in character and includes the previously discussed scandium compound [(nacnac)Sc(OAr)(THF)(OCP)] (**Figure 1-10**, **1.36**),[84] and oxophilic actinides e.g. $(amid)_3M(OCP)$ (M = U **1.37**, Th **1.38**; amid = N,N'-bis-(trimethylsilyl)benzamidinate) and [(^{Ad,Me}ArO)$_3$N]U(DME)(OCP)] **1.39**.[86] In these the OCP^- moiety binds through the oxygen atom in a linear fashion with the M-O-C angles approaching 180° with a shortening of the C-P bond and lengthening of the O-C bond. This bonding mode allows for the OCP^- moiety to behave formally as OC≡P, rather than O=C=P$^-$, thus exhibiting phosphaalkyne like reactivity as illustrated by the η^2-coordination of a Ni(COD) fragment (COD = 1,5-cyclooctadiene) to the OCP^- of $(amid)_3Th(OCP)$ (**Figure 1-10**, **1.40**).[87]

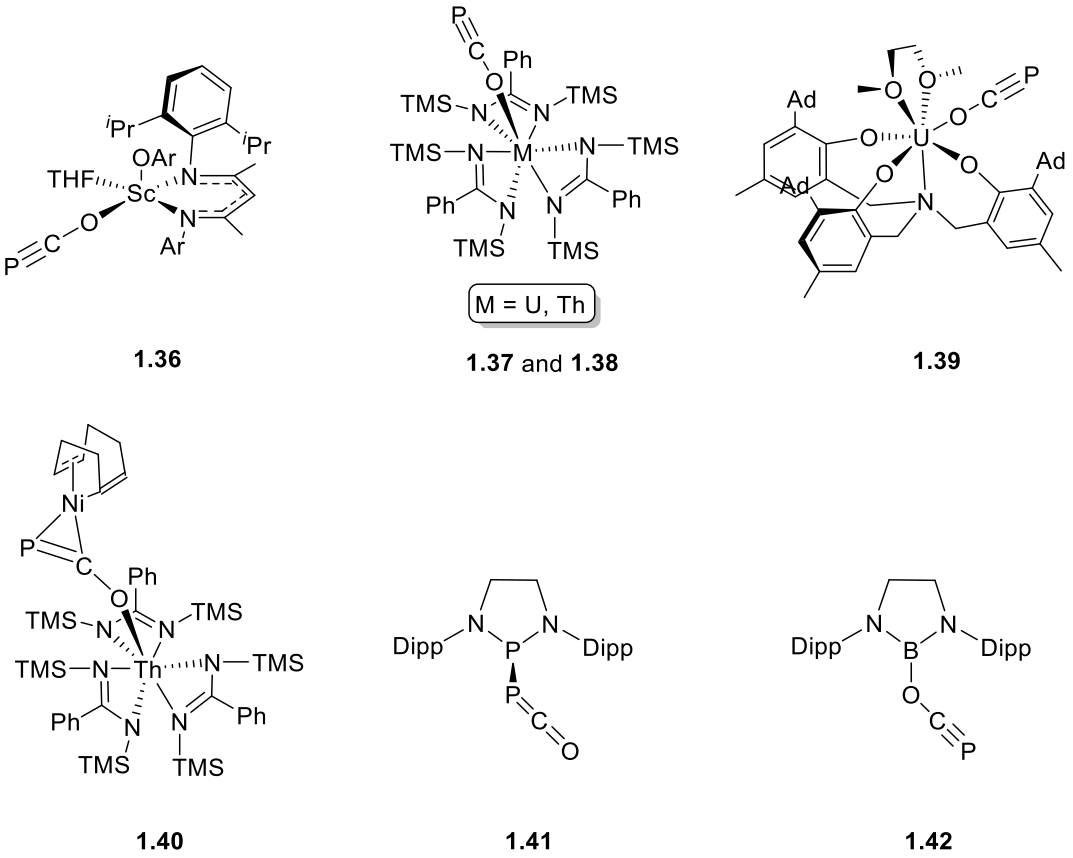

1.36 **1.37** and **1.38** **1.39**

1.40 **1.41** **1.42**

Figure 1-10: *Examples of coordination compounds of the OCP anion [(nacnac)Sc(OAr)(THF)(OCP)]* ***1.36****, (amid)$_3$M(OCP) (M = U* ***1.37****, Th* ***1.38****; amid = N,N′-bis(trimethylsilyl)benzamidinate),*[87] *[(^{Ad,Me}ArO)$_3$N]U(DME)(OCP)]* ***1.39****,*[86] *(amid)$_3$Th(OCP).Ni(COD)* ***1.40****,*[87] *[(CH$_2$)$_2$(NDipp)$_2$]P-(OCP)*[88] *and [(CH)$_2$(NDipp)$_2$]B-(OCP)* ***1.42*** *(Dipp = 2,6-diisopropylphenyl).*

The 2-phosphaethynolate anion can also coordinate to main group elements, as illustrated by the phosphanyl phosphaketene, [(CH$_2$)$_2$(NDipp)$_2$]P-(OCP) (**Figure 1-10, 1.41**).[88] As with the transition metal compounds discussed, the coordination of the OCP$^-$ predominantly occurs through the phosphorus atom, though the boronic system [(CH)$_2$(NDipp)$_2$]B-(OCP) **1.42** is a notable exception, where the OCP$^-$ is bound through the oxygen atom and exhibits phosphaalkyne like reactivity (**Figure 1-10**).[89]

The coordination of OCP$^-$ via the π-system has also been observed, the first example of which, the copper(I) compound (CAAC)Cu(PCO) **1.43** (CAAC = cyclic alkyl amino carbene), was reported by Bertrand and Grützmacher, the structure being authenticated by single-crystal X-ray diffraction confirming the η^2-coordination (**Scheme 1-39**).[90] They also reported that

(CAAC)Cu(PCO) can undergo further reactivity with $B(C_6F_5)_3$ resulting in cyclisation of two OCP^- ligands forming a heterocyclic bridged dimer **1.44** where the $B(C_6F_5)_3$ coordinates to the oxygen lone pairs.[90]

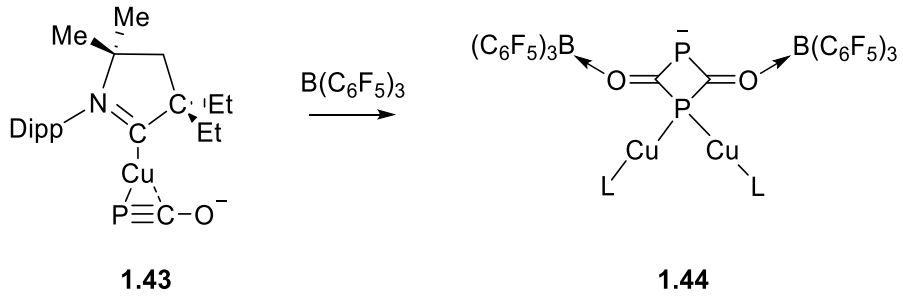

1.43 **1.44**

Scheme 1-39: *Reactivity of (CAAC)Cu(PCO)* ***1.43*** *(CAAC = cyclic alkyl amino carbene) and* $B(C_6F_5)_3$.[90]

Since this report, a silver(I) complex, (ITr)Ag(OCP) (ITr = $[(HCNCPh_3)_2C:]$)[91] and related bimetallic nickel(I) compound, $(\mu^2\eta^5\eta^5\text{-Cp})(\mu^2\eta^2\eta^2\text{-OCP})\{Ni(IPr)\}_2$ (IPr = 1,3-bis(2,6-disopropylphenyl)-imidazol-2-ylidine) **1.45** have been reported, the latter incorporating a bridging OCP^- moiety between the two nickel centres (**Scheme 1-40**).[92] Decarbonylation of the bimetallic nickel(I) compound yields the butterfly compound $(\mu^2\eta^2\eta^2\text{-P}_2)\{Ni(IPr)(CO)\}_2$ (**1.46**) which has been structurally characterised illustrating that the central PP unit is best described as $[P\text{-}P]^{4-}$. Further reactivity has been observed when placed under CO pressure, with P_2 being released which subsequently can be trapped through a Diels–Alder cycloaddition with 2,3-dimethyl-1,3-butadiene which affords 3,4,8,9-tetramethyl-1,6-diphosphabicyclo(4.4.0)deca-3,8-diene. Similar butterfly manganese[93] and titanium[94] systems have also been reported.

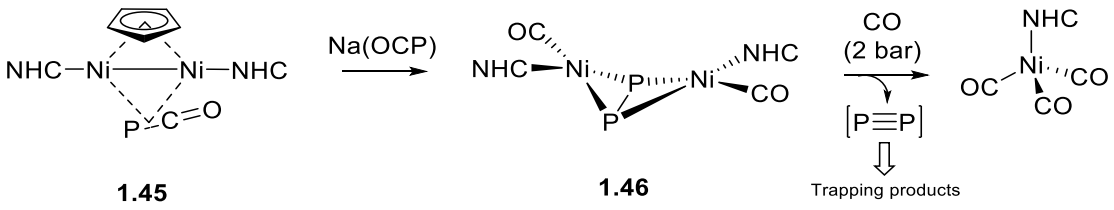

1.45 **1.46**

Scheme 1-40: *Reactivity of* $(\mu^2\eta^5\eta^5\text{-Cp})(\mu^2\eta^2\eta^2\text{-OCP})\{Ni(NHC)\}_2$ *(NHC = IPr = 1,3-bis(2,6-disopropylphenyl)-imidazol-2-ylidine) and NaOCP yielding* $(\mu^2\eta^2\eta^2\text{-P}_2)\{Ni(IPr)(CO)\}_2$.[92]

The 2-phosphaethynolate anion can behave as a phosphide transfer reagent as illustrated by the reaction between a cyclotrisilene and [K(18-crown-6)](OCP), which results in the cleavage of the CP triple bond and the addition of CO and P across the Si=Si double bond. Subsequent photolysis leads to a Si_3P heterocycle (**Scheme 1-41**, **1.47**).[95] The loss of the carbonyl was suggested through the $^{13}C\{^1H\}$ NMR spectrum and X-ray diffraction studies of the product.

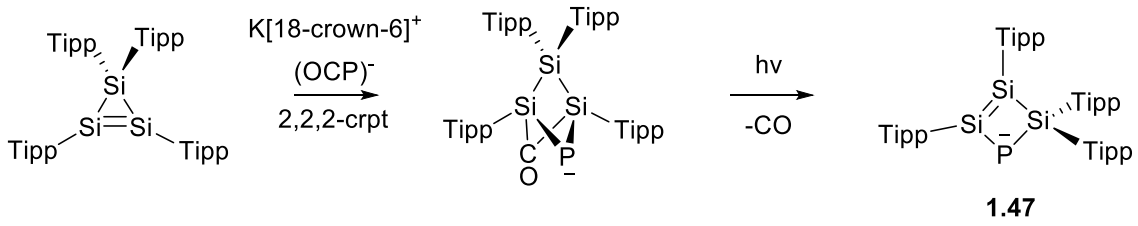

1.47

***Scheme 1-41**: Reactivity of OCP^- towards a cyclotrisilene and subsequent decarbonylation.*[95]

One desirable reactivity of the 2-phosphaethynolate anion that has been particularly sought-after is the deoxygenation to cyaphide, $C{\equiv}P^-$, the simplest, and traditionally elusive, member of the phosphacarbon family.[3,73] In 2017, Meyer and co-workers achieved the reductive deoxygenation of the phosphaethynolate anion with the strongly reducing trivalent uranium(III) aminoalkoxide complex in the presence of a 2.2.2-cryptand, forming the dinuclear μ-oxo bridged structure, [{(((^{Ad,Me}ArO)$_3$N)U(DME)}(μ-O){(((^{Ad,Me}ArO)$_3$N)-U(CP)}] **1.48**, which was unequivocally characterised by X-ray diffraction (**Scheme 1-42**, see also section **1.4.1**).[86] However, this remains the only example of this reactivity with OCP^- to date, although the analogous reaction with $OCAs^-$ has also been reported.[96]

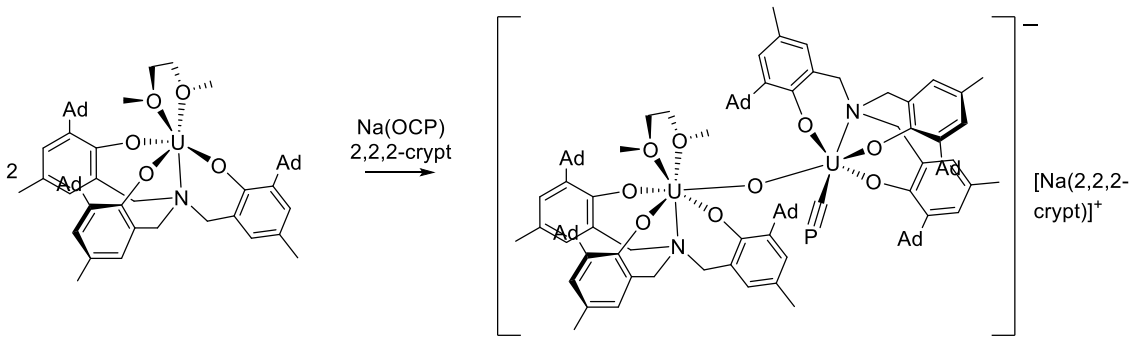

1.48

Scheme 1-42: *Synthesis of [{{{(Ad,Me}ArO)3N)U(DME)}(μ-O){{{(Ad,Me}ArO)3N)-U(CP)}}* ***1.48*** *from the deoxygenation reaction between [{{{(Ad,Me}ArO)3N)U(DME)], NaOCP and 2,2,2,-cryptand.*[86]

1.4 CYAPHIDE

The smallest building block for low-coordinate phosphorus chemistry is the cyaphide anion, $C{\equiv}P^-$, the direct phosphorus analogue of the cyanide anion ($^-C{\equiv}N$). However, unlike the cyanide, efforts to isolate the naked cyaphide as a salt have thus far been ineffective. Indeed, computational studies have demonstrated that the free ion has a C≡P bond length of 1.6 Å, significantly longer than that of ^{t}BuC≡P and more like a double bond.[97,98] These calculations have also shown that the negative charge is 65% localized on the carbon atom, which accounts for the higher gas-phase basicity of $^-C{\equiv}P$ than $^-C{\equiv}N$.[98]

1.4.1 CYAPHIDE COMPLEXES

The first report of a transition metal cyaphide complex was by Angelici in 1992, following the reaction of $[Pd(PEt_3)_4]$ with a platinum phosphaalkene complex (**Scheme 1-43**, **1.49**).[99] The $^{31}P\{^1H\}$ NMR spectra of the mixture exhibited triplet and doublet resonances at 68.8 ppm and 7.3 ppm, with a mutual coupling of 9.1 Hz, seen to imply the presence of $[PtCl(C{\equiv}P)(PEt_3)_2]$. Efforts to isolate $[PtCl(C{\equiv}P)(PEt_3)_2]$ were unsuccessful, however, trapping experiments with $[Pt(PEt_3)_4]$ allowed for isolation of the dimer, $[Cl(Et_3P)_2Pt\text{-}\mu\text{-}\eta^1\text{-}\eta^2\text{-}C{\equiv}P)Pt(PEt_3)_2]$ (**Scheme 1-43, 1.50**) which was unequivocally characterised by single crystal X-ray diffraction. The C≡P triple

bond distance was shown to be 1.666(6) Å, slightly longer than free phosphaalkynes (e.g. 1.536(2) Å for ^{t}BuC≡P) but comparable to the η^2-coordinated phosphaalkyne within the complex, $(PPh_3)_2Pt(\eta^2$-$^{t}BuC{\equiv}P)$ (1.672(17) Å).[99,100] In addition, **1.50** also exhibits Pt-C≡P and Cl-Pt-C bond angles of 144.0(3)° and 178.9(2)° respectively, this slight deviation from linearity is consistent with a slight reduction in bond order.[100]

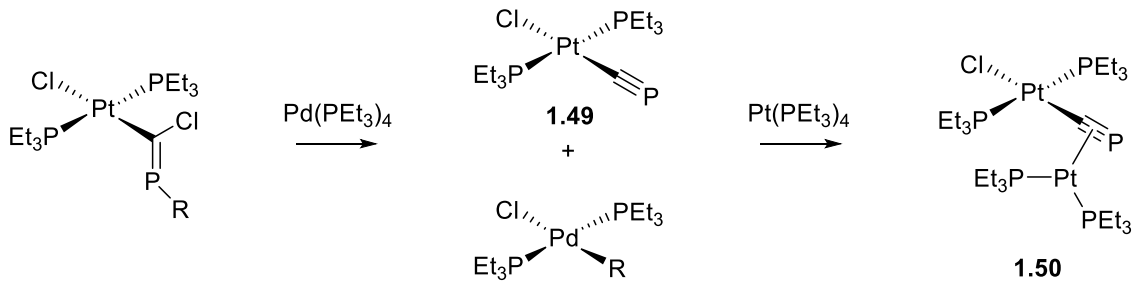

Scheme 1-43: *Synthesis of trans-[PtCl(C≡P)(PEt$_3$)$_2$]* ***1.49*** *and subsequent trapping to afford [Cl(Et$_3$P)$_2$Pt-μ-η^1-η^2-C≡P)Pt(PEt$_3$)$_2$]* ***1.50****.*[99,100]

Despite a series of further studies the discrete cyaphide complex could not be isolated, and it was not until 2006 that an unequivocal example of terminally coordinated cyaphide was described, with Grützmacher's report of *trans*-[RuH(dppe)$_2$(C≡P)] (**Scheme 1-44**, **1.52**). [101] This complex was synthesized through a base-induced desilylative rearrangement of the η^1-phosphaalkyne complex $[RuH(dppe)_2(P{\equiv}CSiPh_3)]^+$ **1.51$^+$**, which was in turn synthesised through the reaction of $Ph_3SiC{\equiv}P$ with $[RuH(dppe)_2]^+$.

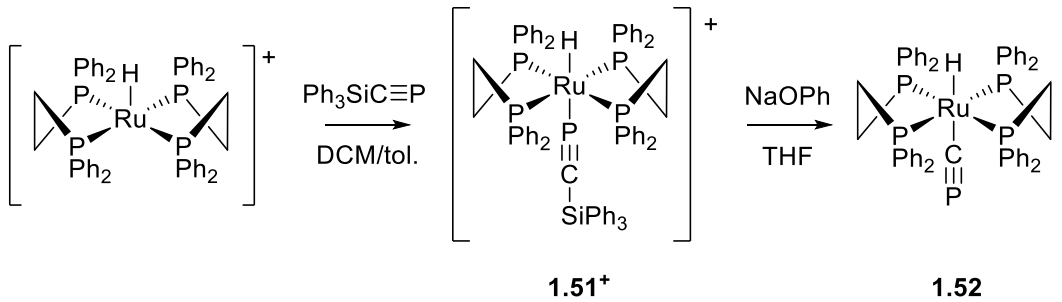

Scheme 1-44: *Synthesis of Grützmacher's η^1-phosphaalkyne* ***1.51$^+$*** *and cyaphide complexes* ***1.52****.*[27]

The initial coordination of the phosphaalkyne was supported by its $^{31}P\{^1H\}$ and ^1H NMR spectra, with the $^{31}P\{^1H\}$ NMR spectrum exhibiting a quintet at 143.8 ppm and a doublet at 60.1 ppm,

with a mutual coupling of 28.7 Hz, corresponding to the $Ph_3SiC{\equiv}P$ and the dppe ligands respectively, and the ^1H NMR spectrum showing a doublet of quintets at −8.13 ppm due to coupling from both the dppe ligands and the η^1 phosphaalkyne. The η^1-phosphaalkyne complex **1.51**$^+$ was also characterised crystallographically, which showed a C≡P bond length of 1.530(3) Å, slightly longer than the free phosphaalkyne, as well as a slightly bent Si-C≡P unit with a bond angle of 165.5 °, attributed to the steric interactions from the dppe ligands.

The base-induced desilylative rearrangement of the η^1-phosphaalkyne **1.51**$^+$ to the cyaphide **1.52** was studied computationally and shown to proceed via nucleophilic attack at the silicon centre forming an isocyaphide complex **1.53**, which then undergoes rearrangement to the cyaphide, via an η^2-coordinated intermediate **1.54**$^+$ (**Scheme 1-45**). An intermediary species in this reaction was observed in situ by $^{31}P\{^1H\}$ NMR, with a quintet at 332 ppm and a doublet at 67.7 ppm with a mutual coupling of J_{PP} = 28 Hz and assigned as the $\lambda^5\sigma^3$-phosphaketenyl-ruthenium complex **1.55**. The identify of this compound was confirmed by X-ray diffraction. This species was, however, found not to lie along the pathway to cyaphide, but rather represent a reversibly formed side product.

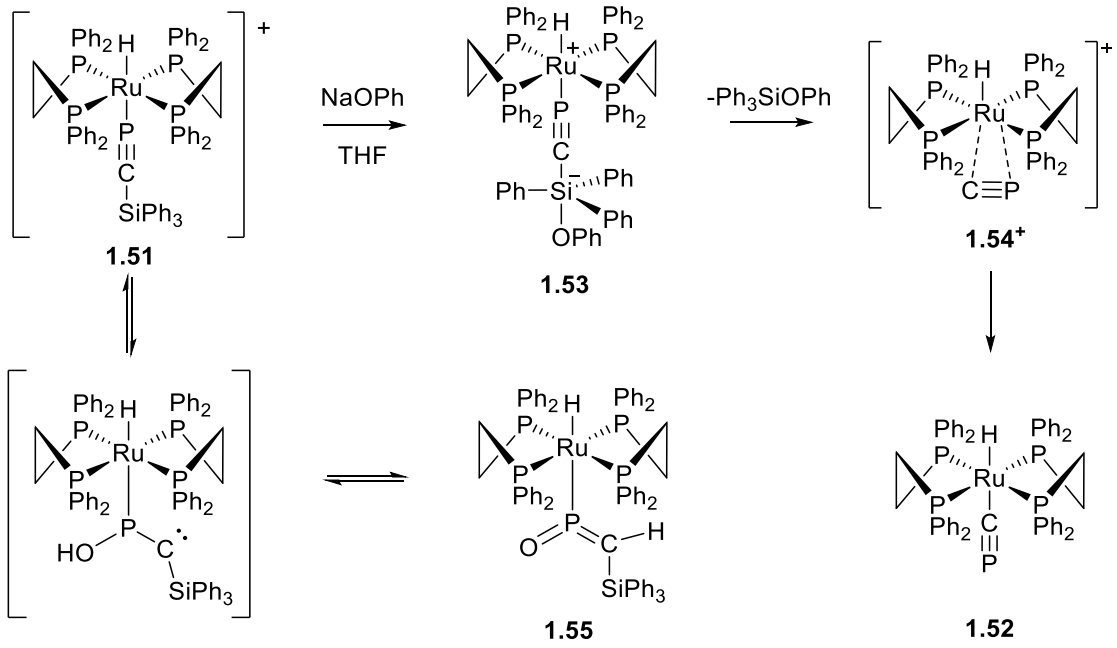

Scheme 1-45*: Postulated scheme for the base-induced desilyative rearrangement.*[27]

The formation of the cyaphide complex **1.52** is apparent from the $^{31}P\{^{1}H\}$ NMR spectrum with a shift to higher frequency of both the cyaphide (165 ppm) and dppe (65.2 ppm) resonances, with a reduced coupling due to a change from $^{2}J_{PP}$ to $^{3}J_{PP}$ interaction. The hydride resonance in the ^{1}H NMR spectrum shifted to -11.2 ppm, with a J_{PH} of 20 Hz. The crystal structure of **1.52** exhibits a C≡P bond length of 1.573(2) Å, slightly longer than that of ^{t}BuC≡P, and the bond angle of the Ru-C≡P unit is near linear, with an angle of 177.9(1)°.

Despite many efforts no further examples were reported until 2012 when Russell and co-workers reported the *in situ* observation of *trans*-[Mo(dppe)$_2$(P≡CSiMe$_3$)(C≡P)]$^-$ **1.57**$^-$ via the isolated *trans*-[Mo(dppe)$_2$(P≡CSiMe$_3$)$_2$] **1.56** (**Scheme 1-46**).[102] The phosphaalkyne complex **1.56** was characterised by $^{31}P\{^{1}H\}$ NMR spectroscopy and X-ray crystallography. The $^{31}P\{^{1}H\}$ NMR spectrum displays a quintet and triplet resonance at 171.7 ppm and 62.8 ppm for the phosphaalkyne and dppe environments respectively, with a mutual coupling of 39 Hz. The crystal structure showed that the two phosphaalkyne units are identical in length, with an associated bond length of 1.540(2) Å, which is notably shorter than that seen in the η^2-coordinated phosphaalkynes.

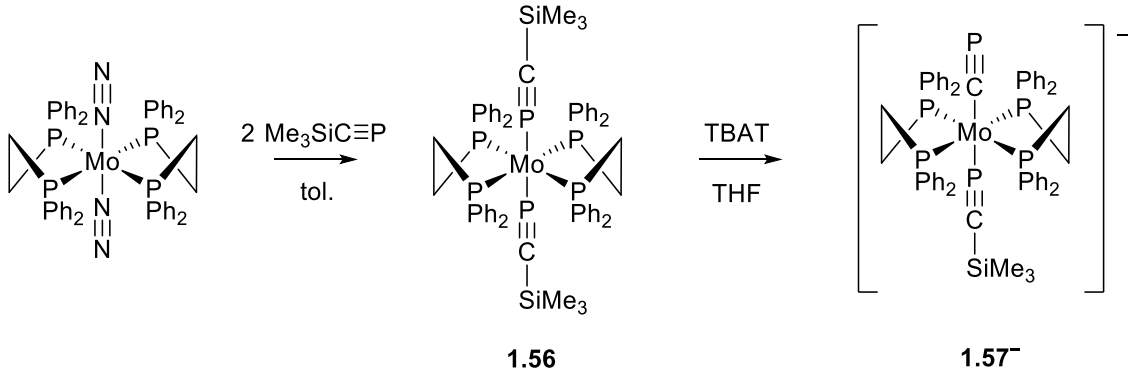

***Scheme 1-46**: Synthesis of trans-[Mo(dppe)$_2$(P≡CSiMe$_3$)(C≡P)]$^-$ **1.57**$^-$ through coordination of Me$_3$SiC≡P to a molybdenum centre , and the conversion to a cyaphide by TBAT (Tetrabutylammonium difluorotriphenylsilicate).*[102]

Treatment of the phosphaalkyne complex with NaOPh and the application of heat resulted in decomposition of the complex. However, treatment with TBAT (Tetrabutylammonium difluorotriphenylsilicate) resulted in the formation of the mixed phosphaalkyne cyaphide complex (**Scheme 1-47, 1.57^{-}**). The $^{31}P\{^{1}H\}$ NMR spectrum showed loss of both the quintet and the triplet resonances and the appearance of a doublet of doublets and two multiplets at 65.5 ppm, 197.8 ppm and 183.0 ppm respectively. In addition, the ^{19}F NMR spectrum showed the presence of Ph_3SiF and Me_3SiF. These data support the removal of one $SiMe_3$ group suggesting a mixed cyaphide phosphaalkyne complex.

In 2014 Crossley and co-workers sought the synthesis and isolation of the first compounds to incorporate the cyaphide ligand as part of an extended π-system as analogous of *trans*-bis acetylides; they reported two conjugated *trans*-cyaphide-alkynyl systems of the type *trans*-$[RuR(dppe)_2(C{\equiv}P)]$ (where R = alkynyl ligand) **1.59 g and h**.[103] The synthesis was effected in similar fashion to that described by Grützmacher, commencing from $[Ru(dppe)_2(\eta^1\text{-}P{\equiv}CSiMe_3)(C{\equiv}CR)]^+$ (**Scheme 1-47**, **1.58$^+$ g and h**). More recently they expanded the series to include a wider range of *trans*-alkynyl groups (**1.59 a-f**), to develop a deeper understanding of the nature and influence of the cyaphide ligand and its interaction with the *trans*-alkynyl fragment (**Scheme 1-47**).[104]

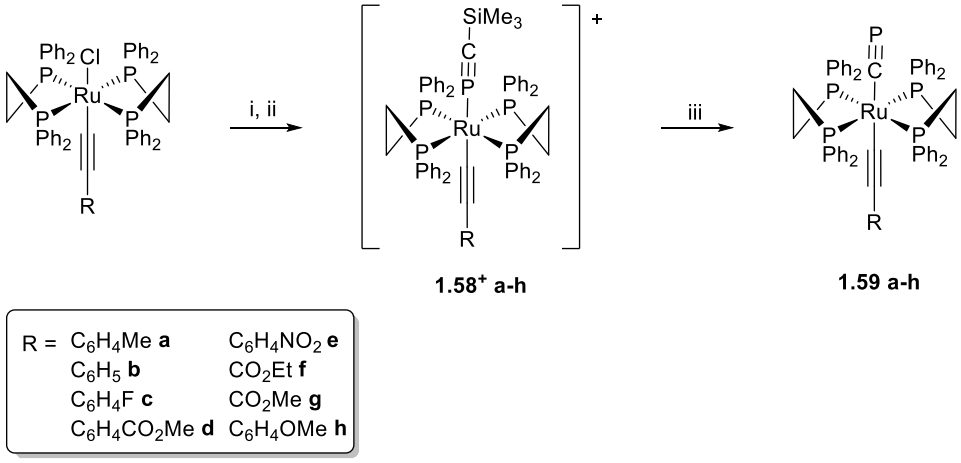

Scheme 1-47: *Synthesis of cyaphide complexes* ***1.59 a-h****. Reagents and conditions: (i) 1 equiv. MX (AgOTf, $AgPF_6$, TlOTf), CH_2Cl_2; (ii) 1.2 equiv. P≡CSiMe₃, CH_2Cl_2/tol., 1h; (iii) 1 equiv. KO^{t}Bu, THF, 1h.*[103,104]

The η^1-phosphaalkyne and cyaphide complexes were studied both spectroscopically (**Table 1-2**) and through X-ray crystallography (**Table 1-3**). The $^{31}P\{^1H\}$ NMR spectra of the η^1-phosphaalkyne complexes exhibit doublet and quintet resonances at *ca* 42 ppm and 110 ppm for the dppe and $Me_3SiC{\equiv}P$ groups respectively.

Selected NMR spectroscopic Data: [Ru(dppe)$_2$(η^1-P≡CSiMe$_3$)(C≡CR)]$^+$

	C_6H_4Me	C_6H_5	C_6H_4F	$C_6H_4CO_2Me$	$C_6H_4NO_2$	CO_2Et	CO_2Me	C_6H_4OMe
$\delta_{P(C\equiv P)}$ [a]	112.3	111.9	111.9	111.0	109.1	108.0 [b]	108.4	113.5
$\delta_{P(dppe)}$ [a]	42.4	42.3	42.0	41.8	41.5	41.3 [b]	41.2	42.4
$\delta_{C(C\equiv P)}$ [a]	188.4	188.6	188.9	190.2	193.5	193.5	192.6	188.2

Selected NMR spectroscopic Data: *trans*-[Ru(dppe)$_2$(C≡P)(C≡CR)]

	C_6H_4Me	C_6H_5	C_6H_4F	$C_6H_4CO_2Me$	$C_6H_4NO_2$	CO_2Et	CO_2Me	C_6H_4OMe
$\delta_{P(C\equiv P)}$ [b]	159.8	160.6	161.7	165.3	170.0	168.3	168.5	159.5
$\delta_{P(dppe)}$ [b]	50.8	50.9	50.8	50.7	50.5	44.6	49.7	50.8
$\delta_{C(C\equiv P)}$ [b]	281.9	281.5	280.8	280.7	279.5	278.7	279.1	281.9

Table 1-2: *Selected NMR spectroscopic data for [Ru(dppe)$_2$(C≡CR)(η^1-P≡CSiMe$_3$)]$^+$ and [Ru(dppe)$_2$(C≡CR)(C≡P)] complexes. [a] solution in $CDCl_3$. [b] solution in CD_2Cl_2.*[103,104]

The conversion to the cyaphide complexes, *trans*-[Ru(dppe)$_2$(C≡P)(C≡CR)], is apparent from the $^{31}P\{^1H\}$ NMR spectra with a shift in the phosphaalkyne and dppe resonances to *ca* 160 ppm and 51 ppm respectively, accompanied by a reduction in the magnitude of coupling for the phosphaalkyne phosphorus centre, which is consistent with a change from a $^2J_{PP}$ to $^3J_{PP}$ interaction. Other spectroscopic data also supported the conversion including the loss of NMR resonances associated with the silyl group and counterion.

For the series of aromatic substituted η^1-phosphaalkynes it was noted that when the remote substituent on the alkyne increases in electronegativity there is a slight decrease in the shift in the $^{31}P\{^1H\}$ NMR resonances, while the opposite is observed in the $^{13}C\{^1H\}$ NMR spectra. This is consistent with the increasing electron acceptor ability of the "Ru(dppe)CCR" fragment which induces polarisation of the P≡C-SiMe$_3$ moiety which is exhibited as desheilding of the carbon and shielding of the phosphorus of the phosphaalkyne moiety. In comparison for the corresponding series of cyaphide complexes the opposite trend was noted with an increase in the shift in the $^{31}P\{^1H\}$ NMR spectra, and a decrease in the $^{13}C\{^1H\}$ NMR spectra.

The molecular connectivity for *trans*-[Ru(η^1-P≡CSiMe$_3$)(dppe)$_2$(C≡CR)]$^+$ (R = CO$_2$Me, C$_6$H$_4$Me and C$_6$H$_4$F) was confirmed through X-ray crystallography (**Table 1-3**). This showed close to linear C–Ru–P bond angles *ca* 173-177° and C≡P bond lengths comparable to that of Grützmacher's η^1-phosphaalkyne complex.[27] The structures of *trans*-[Ru(C≡P)(dppe)$_2$(C≡R)] (R = CO$_2$Me, C$_6$H$_4$F, C$_6$H$_4$CO$_2$Me and C$_6$H$_4$OMe) were also confirmed by X-ray crystallography (**Table 1-3**) showing slight deviation of linearity, which is consistent with that reported by Grützmacher and for *trans*-bisalkynyls.[27] However, the bond length for the C≡P units was shown to be much shorter, and this is thought to be a direct effect of a diminished $d_\pi \rightarrow \pi^*_{(C\equiv P)}$ retrodonation due to the competing *trans*-alkynyl fragment, in comparison to *trans*-hydride.

	$[Ru(dppe)_2(\eta^1\text{-}P{\equiv}CSiMe_3)(C{\equiv}CR)]^+$			*trans*-$[Ru(dppe)_2(C{\equiv}P)(C{\equiv}CR)]$			
	C_6H_4Me	C_6H_4F	CO_2Me	C_6H_4F	CO_2Me	$C_6H_4CO_2Me$	C_6H_4OMe
C≡P	1.515(14)	1.520(5)	1.528(11)	1.493(3)	1.563(7)	1.549(10)	1.544(4)
C-Ru-P_{PC}	175.8(3)	175.6(1)	177.0(3)	174.5(1)	173.8(2)	172.4(4)	171.91(14)

Table 1-3: *Selected X-ray diffraction data for $[Ru(dppe)_2(C{\equiv}CR)(\eta^1\text{-}P{\equiv}CSiMe_3)]^+$ and $[Ru(dppe)_2(C{\equiv}CR)(C{\equiv}P)]$ complexes.*[103,104]

The cyaphide complexes were also studied by DFT calculations along with UV/Vis spectroscopy. This showed that they absorb strongly in the UV region and their electronic spectra are dominated by ligand-to-ligand charge transfer (LLCT) from the C≡C(π) and C≡P(π) to the dppe ancillary ligands, as well as a considerable contribution from intraligand charge transfer (ILCT), $\pi \rightarrow \pi^*$ transition within the C≡P unit. In addition, for the aromatic alkynyl systems, there is also significant contribution from ILCT between the arene and alkynyl fragments. These data alongside DFT studies demonstrated there is a significant influence of the remote *trans*-substituent upon the properties of the cyaphide ligand and appear indicative of some communication between the alkynyl and cyaphide moieties. This is consistent with these *trans*-alkynyl cyaphide complexes being analogous of the *bis*(alkynyl) complexes.

In addition to the *trans*-alkynyl cyaphide complexes Leech and Crossley reported for the first time extended conjugation between multiple cyaphide moieties within the complex $[\{Ru(dppe)_2\}_2\{\mu\text{-}(C{\equiv}C)_2C_6H_4\text{-}p\}(C{\equiv}P)_2]$ **1.61**, which was again obtained from the respective $[\{Ru(dppe)_2\}_2\{\mu\text{-}(C{\equiv}C)_2C_6H_4\text{-}p\}(\eta^1\text{-}P{\equiv}CSiMe_3)_2]^{2+}$ $\mathbf{1.60^{2+}}$ via base-induced desilylation (**Scheme 1-48**).[105]

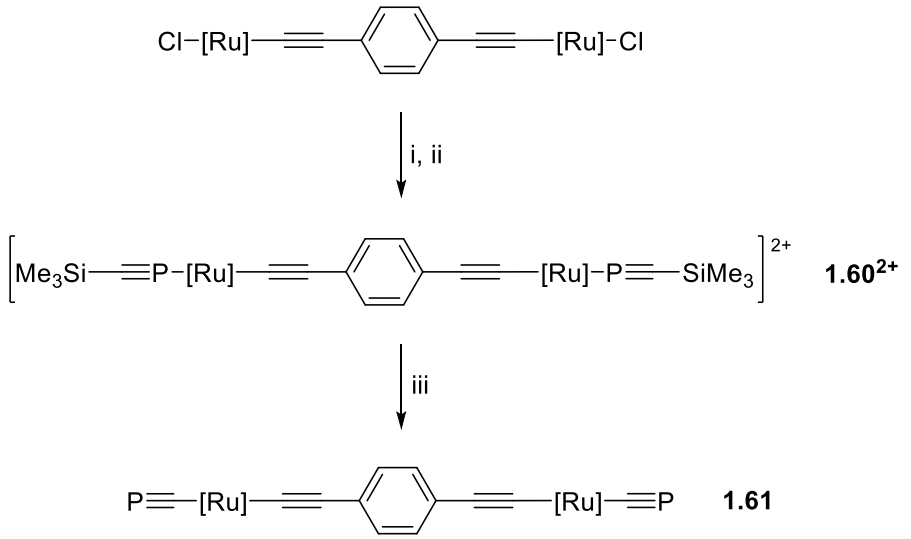

Scheme 1-48: *Synthesis of [{Ru(dppe)$_2$}$_2${μ-(C≡C)$_2$C$_6$H$_4$-p}(C≡P)$_2$]. Reagents and conditions: (i) CH_2Cl_2, 2 AgOTf, (ii) 2 P≡CSiMe$_3$ in toluene, 1 h., (iii) THF, 2 KO^{t}Bu, 1 h. [Ru] = Ru(dppe)$_2$.*[105]

The $^{31}P\{^1H\}$ NMR spectrum for the terminal phosphaalkyne complex **1.60^{2+}** showed two resonances 114.4 ppm and 42.2 ppm with a mutual coupling of J_{PP} 34 Hz, integrating 1:4 for the phosphaalkyne and dppe moieties respectively. The connectivity was further supported through single-crystal X-ray diffraction, showing slight deviations from linearity about the metal centres with P-Ru-C bond angles of 173.4(2)° and 175.3(2)°), consistent with previously synthesised terminal phosphaalkynes.[103]

The spectroscopic data of the cyaphide complex **1.61** showed consistency with previous cyaphide analogous, with the $^{31}P\{^1H\}$ NMR spectrum showing the phosphaalkynyl resonance, at 159.7 ppm and the dppe resonance at 50.7 ppm. The proton and fluorine NMR showed the loss of the silyl and OTf groups respectively.[27,103]

DFT studies of both the η^1-phsphaalkyne and cyaphide complexes showed significant dominance of LLCT and MLCT from the alkynyl bridge and phosphacarbons moieties to the dppe scaffolds with negligible ILCT within the π-system. Overall, it was concluded that there was through-conjugation of two phosphaalkyne moieties for both the η^1-phosphaalkyne and cyaphide complexes.

As previously mentioned (see section: **1.3.2**) Meyer and co-workers reported the formation of a uranium cyaphide complex **1.48**$^{-}$ through the reductive deoxygenation of the phosphaethynolate anion with the strongly reducing trivalent uranium(III) aminoalkoxide complex in the presence of a 2.2.2-cryptand (**Scheme 1-49**).[86]

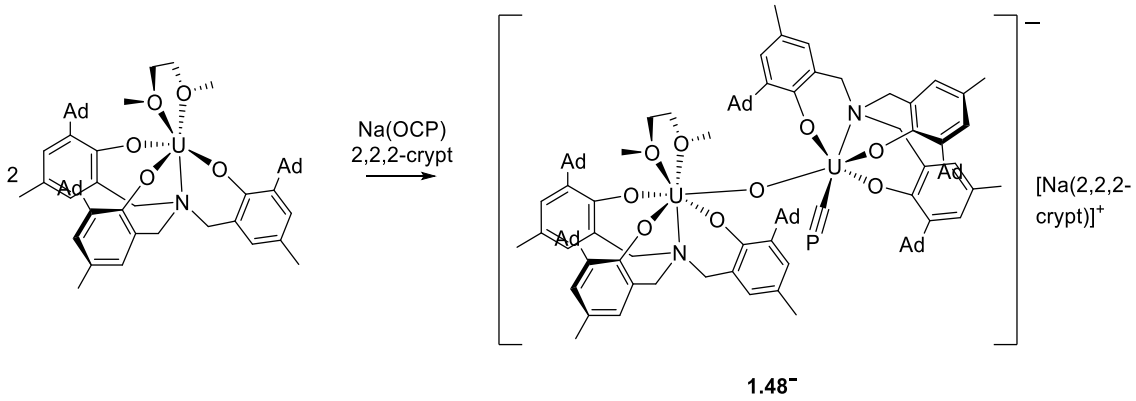

Scheme 1-49: *Synthesis of [{((*^{Ad,Me}*ArO)*$_3$*N)U(DME)}(μ-O){((*^{Ad,Me}*ArO)*$_3$*N)-U(CP)}]* ***1.48***$^{-}$ *from the deoxygenation reaction between [{((*^{Ad,Me}*ArO)*$_3$*N)U(DME)], NaOCP and 2,2,2,-cryptand.*[86]

The $^{31}P\{^{1}H\}$ NMR spectrum for the resulting μ-oxo bridged structure, [{((Ad,Me ArO)$_3$N)U(DME)}(μ-O){((Ad,Me ArO)$_3$N)-U(CP)}] **1.48**$^{-}$ showed one resonance at 265.8 ppm corresponding to the coordinated cyaphide anion, although significantly higher than those reported for the ruthenium systems (*ca* 160 – 165 ppm)[27,103] this was attributed to the paramagnetic nature of uranium(IV). The structure of the μ-oxo bridged complex was unequivocally characterised by X-ray diffraction, showing the cyaphide anion bound *trans*- to a slightly elongated U-N bond (2.643(5) Å) of the supporting N-anchored tris-aryloxide, with a C-P bond length of 1.523(8) Å and a near-to-linear U-C-P angle of 177.5(4)°; these are comparable to previously characterised ruthenium based cyaphides.[27,103]

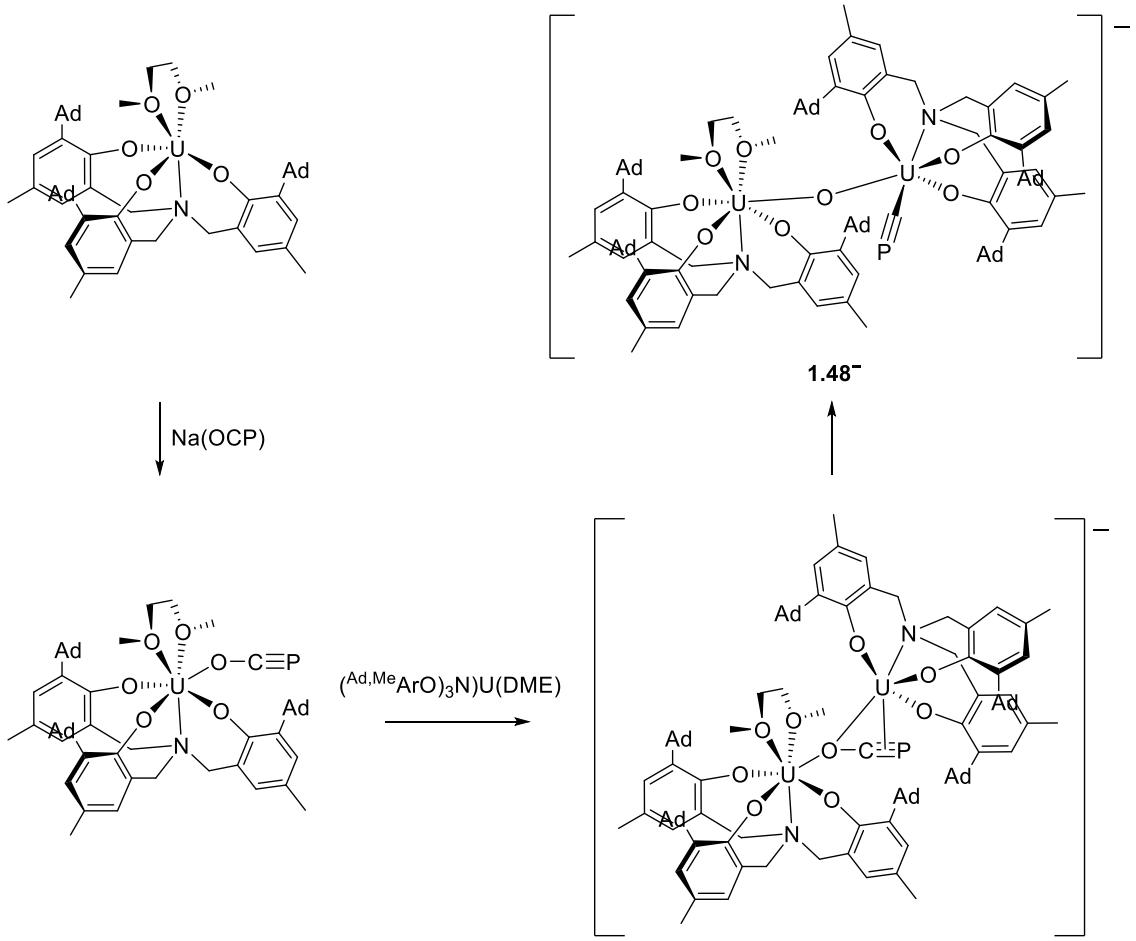

Scheme 1-50: *The mechanism of reaction of [((Ad,MeArO)$_3$N)UIII(DME)] with Na(OCP) from computational studies.*[86]

Computational studies showed that formation of the μ-oxo bridged complex proceeds through two successive one-electron transfer steps (**Scheme 1-50**), the initial step being the reaction of the trivalent precursor, [((^{Ad,Me}ArO)$_3$N)U(DME)], with Na(OCP) to yield a uranium(IV) intermediate with a η^1-OCP^- bound to the uranium centre. The subsequent coordination of a second equivalent of the uranium(III) precursor occurs through the oxygen atom of the bound OCP^- ligand. This results in a one electron reduction of the uranium(III) centre, yielding a key intermediate in which the O-C≡P^- moiety is η^2-coordinated to one uranium centre and μ-oxo bridged to the other. This η^2-activiation leads to a facile O-CP bond cleavage forming the μ-oxo-bridged diuranium(IV/IV) species with the cyaphide ligand η^1-coordinated to one of the uranium centres.

1.5 CONCLUDING REMARKS

As illustrated in the preceding sections, the chemistry and electronic features of cyaphide are an intriguing topic that is only just beginning to be explored. Significant questions remain, particularly regarding the synthesis of novel cyaphide complexes varying the *trans*- ligand and how this influences the reactivity of the cyaphide moiety.

Herein, the incorporation of cyaphide into conjugated monometallic systems is explored, focussing on the synthesis and reactivity of the cyaphide moiety. Furthermore, the synthesis and characterisation of the first *trans*-alkyl and *trans*-halide cyaphide complexes will be discussed alongside their reactivity studies leading to the synthesis of a range of novel cyaphide complexes and unexpected reduction of the ligated cyaphide.

CHAPTER 2 : SYNTHESIS, CHARACTERISATION AND REACTIVITY OF RUTHENIUM *TRANS*-ALKYNYL CYAPHIDE COMPLEXES

2.1 INTRODUCTION

The cyaphide ligand, $^{-}C{\equiv}P$, is of high interest within low coordinate phosphorus chemistry due to the diverse utility of the carbon and nitrogen analogues, acetylide $^{-}C{\equiv}CH$ and cyanide $^{-}C{\equiv}N$ respectively. Although there are a few examples of cyaphide containing compounds in the literature, including the first isolable example, $[RuH(dppe)_2(C{\equiv}P)]$[27] (see section:**1.4.1**), *trans*-$[Mo(dppe)_2(P{\equiv}CSiMe_3)(C{\equiv}P)]^{-}$[102] and a series of *trans*-alkynyl complexes, *trans*-$[RuR(dppe)_2(C{\equiv}P)]$ (where R = alkynyl ligand),[103,104] their properties remain largely unexplored with regard to their electronics and reactivity.

Carbon-rich organometallics, particularly those incorporating σ-alkynyl ligands exhibit a broad selection of desirable electronic, optical, and photoelectronic properties, allowing applications in molecular wires and non-linear optoelectronics.[106–112] Recently, reports have focussed on the acetylide and *bis*-acetylide complexes with the 'Ru(dppe)$_2$' backbone, which have been studied spectroscopically and electrochemically to assess the effects of the introduction of a variety of functionalities on the electronic properties.[109,112]

The introduction of phosphorus, which is a well-established n-type dopant, into conjugated organometallic complexes holds promise with respect to molecular wire design.[3,113–117] Therefore, incorporation of the cyaphide ligand into conjugated organometallic complexes such as in the reported series of *trans*-$[RuR(dppe)_2(C{\equiv}P)]$ (where R = alkynyl ligand) is an ideal starting point for linearly conjugated phosphaorganometallic molecular wires.

Recently, the nature and influence of the cyaphide ligand and its interaction with the *trans*-alkynyl fragment have been studied in the series of *trans*-alkynyl cyaphide complexes.[103–105] This demonstrated there is a significant influence of the remote *trans*- substituent of the alkynyl over

the properties of the cyaphide ligand, indicative of some communication between the alkynyl and cyaphide moieties.

While the reactivity of phosphaalkynes and their complexes has been extensively studied (see section: **1.2.4**) that of cyaphide complexes remains largely unexplored. The first report of reactivity of an isolated cyaphide complex was in 2006 with the observation of exchange of the cyaphide for a chloride when *trans*-[RuH(C≡P)$(dppe)_2$] is stored in chlorinated solvents for prolonged periods of time.[27] Similar observations were reported when samples of *trans*-[Ru(C≡P)(C≡CR)$(dppe)_2$] were dissolved in chloroform, however, this was not investigated further.[118]

The nature of the cyaphidic lone pair has been explored through DFT calculations which showed the lone pair of the cyaphide complexes *trans*-[Ru(C≡P)(C≡CR)$(dppe)_2$] (R = CO_2Me, *p*-An) is held in an orbital of s-character 75 % and p-character 25 %, with the expected polarisation of the C≡P moiety ($C^{\delta-}\equiv P^{\delta+}$).[103] These data are consistent with that of phosphaalkynes more generally (see section: **1.4.1**) therefore, the conclusion was made that the lone pair of the cyaphide ligand is available for reactivity and should behave similarly to that of phosphaalkynes.

Previous work from Crossley and co-workers sought to coordinate the phosphorus lone pair to transition-metal complexes (Pt, Pd and Au), boranes (BPh_3 and $B(C_6F_3)_3$), boron trihalides ($BF_3.Et_2O$), chalcogens and halogens, with many reactions showing limited success.[118,119] Although some success was achieved through the addition of $BF_3.Et_2O$ to *trans*-[Ru(C≡P)(C≡CCO_2Me)$(dppe)_2$], with two major products observed by $^{31}P\{^1H\}$ and $^{11}B\{^1H\}$ NMR spectroscopy, attempts to isolate these complexes as discrete species were unsuccessful.[119]

The effects of the introduction of the cyaphide moiety into conjugated organometallics has been explored and the electronics studied, however, there is little known about how changing the functionality on the *trans*-alkynyl affects the reactivity of cyaphide. This chapter details efforts to probe the reactivity of both the cyaphide lone pair and π-system of a selection of *trans*-alkynyl

cyaphide complexes, *trans*-[RuR(dppe)$_2$(C≡P)]. In addition, the redox behaviour of the cyaphide complexes will be studied through cyclic voltammetry. Furthermore, the synthesis of the first ruthenium cyanide-alkynyl complex, *trans*-[Ru(dppe)$_2$(C≡N)(C≡CPh)]. will be discussed.

2.2 SYNTHESIS OF *trans*-[Ru(dppe)$_2$(C≡P)(C≡CR)]

Previously discussed was the reported synthesis of *trans*-[Ru(dppe)$_2$(η^1-P≡CSiMe$_3$)(C≡CR)]$^+$ (R = C_6H_4Me, C_6H_5, C_6H_4F, $C_6H_4CO_2Me$, $C_6H_4NO_2$, C_6H_4OMe, CO_2Et and CO_2Me) **1.58$^+$ a-h** and their conversion to the cyaphide complexes, *trans*-[Ru(dppe)$_2$(C≡CR)(C≡P)] **1.59a-h** (see section: **1.4.1**).[103,104] Herein, the synthesis of a series of analogous complexes where R is ^{n}Bu, ^{t}Bu and $C_6H_4CO_2Et$ will be discussed alongside the resynthesis of complexes where R is CO_2Et, CO_2Me and C_6H_3-3,5-$(CF_3)_2$[119] for remaining spectroscopic and structural data to be collected and for use in reactivity studies.

2.2.1 SYNTHESIS AND CHARACTERISATION OF *trans*-[Ru(dppe)$_2$(P≡CSiMe$_3$)(C≡CR)]$^+$

The complexes of the type *trans*-[RuCl(C≡CR)(dppe)$_2$] were synthesised using literature methods, then reacted with one equivalent of AgOTf, $AgPF_6$ or TlOTf to effect halide abstraction, subsequent addition of Me$_3$SiC≡P affording the corresponding η^1-phosphaalkyne complexes, *trans*-[Ru(P≡CSiMe$_3$)(C≡CR)(dppe)$_2$]$^+$ (**Scheme 2-1**, **1.58g$^+$, 1.58f$^+$** and **2.1$^+$ a-d**), in good yields (56-93%).

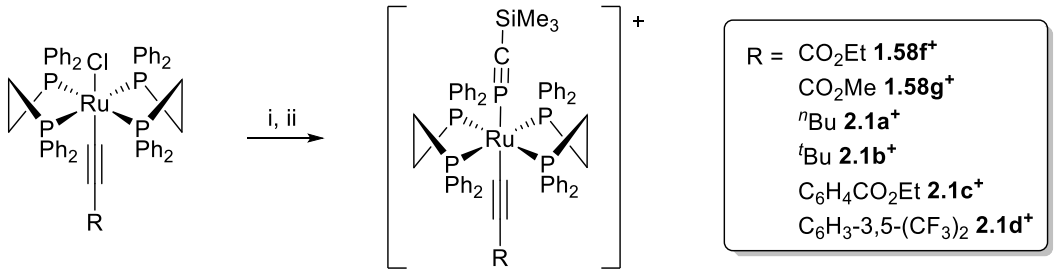

1.58f^{+}, **1.58g**$^{+}$ and **2.1**$^{+}$**a-d**

Scheme 2-1: *Synthesis of η^{1}-phosphaalkyne complexes. Reagents and conditions: (i) 1 equiv. MX (AgOTf, $AgPF_6$, TlOTf), CH_2Cl_2; (ii) 1.2 equiv. P≡CSiMe$_3$, CH_2Cl_2/tol., 1h.*

The complexes **1.58g**$^{+}$**, 1.58f**$^{+}$ and **2.1**$^{+}$ **a-d** were characterised spectroscopically, (**Table 2-1**), the $^{31}P\{^{1}H\}$ NMR spectra being indicative of the η^{1}-coordination of the phosphaalkyne, exhibiting a doublet at 40-45 ppm and quintet at 108-115 ppm, with a mutual coupling of ca 33 Hz, which are assigned to the dppe ancillary ligands and the phosphaalkyne respectively. The ^{1}H NMR and the ^{1}H-^{29}Si HMBC NMR spectra confirm retention of the silyl moiety with resonances in the ranges δ_H –0.05 to –0.20 ppm and δ_{Si} ca –13 ppm

Alkyne Substituent	Compound Number	$^{31}P\{^{1}H\}$ NMR (ppm)		$^{13}C\{^{1}H\}$ NMR (ppm)			^{29}Si NMR (ppm)	^{1}H NMR (ppm)	IR (ν)	
		dppe ($^{2}J_{PP}$, Hz)	C≡P ($^{2}J_{PP}$, Hz)	C≡P ($^{1}J_{CP}$, Hz)	C_{α}≡C	C≡C_{β}	$Si(CH_3)_3$	$Si(CH_3)_3$	C≡P	C≡C
^{n}Bu	**2.1a^{+}**	41.2 (32.4)	114.4 (32.4)	187 (88)	116.0	123.0	−13.7	0.90	1269	2113
^{t}Bu	**2.1b^{+}**	44.6 (33.0)	114.1 (33.0)	-	-	-	-	0.16	1265	2163
CO_2Me	**1.58g^{+}**	41.1 (34.5)	108.1 (34.5)	192.6 (89)[a]	108.8[a]	120.8[a]	−12.3[a]	−0.10	1265[a]	2098[a]
CO_2Et	**1.58f^{+}**	41.3 (35.0)	108.0 (35.0)	193.5 (86)	110.0	123.0	-	−0.10	1268	2094
p-C_6H_4-CO_2Et	**2.1c^{+}**	41.8 (33.0)	110.8 (33.0)	191.0	-	-	-	−0.16	1267	2094
C_6H_3-3,5-$(CF_3)_2$	**2.1d^{+}**	41.6 (32.2)	108.8 (32.2)	191.2 (89)	105.5	112.3	−12.5[b]	−0.05	1276	2092

***Table 2-1**: Selected NMR and IR spectroscopic data for η^{1}-phosphaalkyne complexes **1.58g^{+}, 1.58f^{+}** and **2.1^{+} a-d** ([a] Data from reference 102 and 103, [b] Data from reference 118)*

2.2.2 MOLECULAR STRUCTURE ANALYSIS OF 2.1a$^+$

The identity of **2.1a**$^+$ was further supported through X-ray diffraction studies, with single crystals obtained from a saturated solution of the complex in DCM which had been layered with hexane and left at ambient temperature (**Figure 2-1**). The solid-state structure confirmed the η^1-coordination mode for the phosphaalkyne, lying *trans*- to the hexyne fragment, with C≡C and P≡C bond length of 1.176(10) Å and 1.509(7) Å respectively. The P-C-Si, Ru-P-C and C-Ru-P bond angles of 170.3(6)°, 178.6(4)° and 173.59(18)° demonstrate a slight deviation from linearity, aligning with typical trends for *bis*-alkynyl complexes (*ca* C-Ru-C 172.0 to 180) and within the range considered 'essentially linear'.[120–123] These data are also comparable to those for $[RuH(dppe)_2(P{\equiv}CSiPh_3)]^+$, $[Mo(dppe)_2(P{\equiv}CSiMe_3)_2]$ and *trans*-$[Ru(P{\equiv}CSiMe_3)(C{\equiv}CR)(dppe)_2]^+$ (R = CO_2Me, C_6H_4-*p*-Me and C_6H_4-*p*-F) (**Table 2-2**).[27,102,103,124]

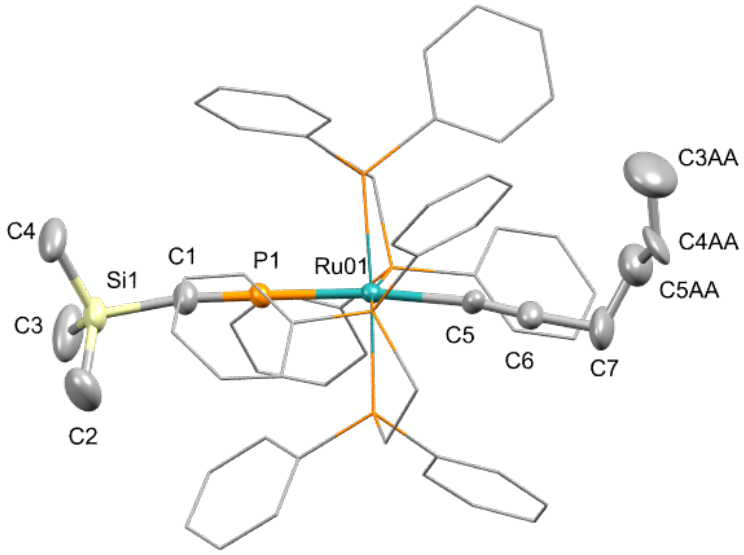

Figure 2-1: *Solid state molecular structure of trans-$[Ru(dppe)_2(C{\equiv}C^nBu)(P{\equiv}CSiMe3)]^+$ (**2.1a**$^+$) in crystals of the PF_6 salt, with thermal ellipsoids at the 50% probability level, hydrogen atoms and PF_6 counterion omitted and the phenyl dppe fragments reduced for clarity. Selected bond lengths (Å) and angles (°)*

	2.1a$^+$	**[RuH(dppe)$_2$(P≡CSiPh$_3$)]$^+$** [a]	**[Mo(dppe)$_2$(P≡CSiMe$_3$)$_2$]** [b]	***trans*-[Ru(P≡CSiMe$_3$)(C≡CR)(dppe)$_2$]$^+$**		
				CO$_2$Me [c]	**C$_6$H$_4$-*p*-Me** [d]	**C$_6$H$_4$-*p*-F** [d]
Ru(01)-C(5)	2.070(7)	-	-	2.082(11)	2.027(9)	2.043(4)
Ru(01)-P(1)	2.2493(16)	2.2485(8)	2.3058(4)	2.274(3)	2.264(3)	2.262(1)
P(1)-C(1)	1.509(7)	1.530(3)	1.540(2)	1.528(11)	1.515(14	1.520(5)
C(1)-Si(1)	1.851(8)	1.825(3)	1.822(2)	1.858(12)	1.851(14)	1.835(5)
C(5)-C(6)	1.176(10)	-	-	1.153(15)	1.197(16)	1.182(6)
P(1)-C(1)-Si(1)	170.3(6)	165.5(2)	179.6(2)	178.3(6)	171.8(10)	171.0(4)
C(5)-Ru(01)-P(1)	173.59(18)	-	-	177.0(3)	174.4(13)	176.0(5)
Ru(01)-P(1)-C(1)	178.6(4)	-	-	175.7(4)	179.6(6)	179.4(2)

Table 2-2: *Selected bond lengths (Å) and angles (°) for* ***2.1a$^+$****, [RuH(dppe)$_2$(P≡CSiPh$_3$)]$^+$* ***1.51$^+$****, [Mo(dppe)$_2$(P≡CSiMe$_3$)$_2$]* ***1.56****, trans-[Ru(P≡CSiMe$_3$)(C≡CR)(dppe)$_2$]$^+$ (R = CO$_2$Me, C$_6$H$_4$-p-Me and C$_6$H$_4$-p-F)* ***1.58a$^+$****,* ***1.58g$^+$*** *and* ***1.58c$^+$****. ([a] data from reference 100, [b] data from reference 101, [c] data from reference 102 and [d] data from reference 103)*

2.2.3 SYNTHESIS AND CHARACTERISATION OF *trans*-[Ru(dppe)$_2$(C≡P)(C≡CR)]

The reaction of the η^1-phosphaalkyne complexes **1.58g$^+$, 1.58f$^+$** and **2.1$^+$ a-d** with a small excess of base (KO^{t}Bu or NaOPh) resulted in desilylative rearrangement of the phosphaalkyne to give the corresponding cyaphide complexes, *trans*-[Ru(dppe)$_2$(C≡CR)(C≡P)] (**Scheme 2-2**, **1.59f, 1.59g** and **2.2a-d**).[103,104]

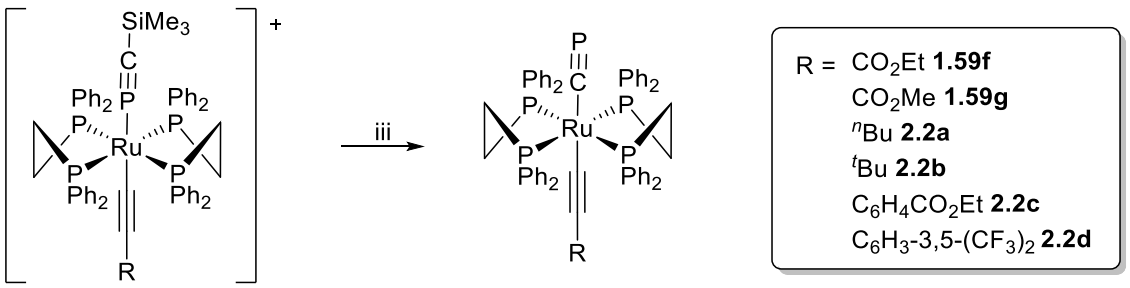

1.59f, **1.59g** and **2.2a-d**

Scheme 2-2: *Synthesis of cyaphide complexes **1.59f, 1.59g** and **2.2a-d**. Reagents and conditions: (iii) 1 equiv. KO^{t}Bu, THF, 1h*

Conversion was typically complete within one hour, with no evidence for the unreacted precursors remaining. The ^{31}P{^{1}H} NMR spectra showed a doublet at *ca* 48 ppm (J_{PP} ≈ 5.0 Hz) for the dppe ancillary ligands and a quintet in the range *ca* 140-170 ppm corresponding to the cyaphide moiety, for which the couplings are not universally resolved (**Table 2-3**). The reduction in magnitude of the J_{PP} coupling constant (from 34 Hz to 5 Hz typically) is consistent with a change from a two, to three-bond coupling and associated with the rearrangement from the M-P≡C to M-C≡P mode. The ^{1}H and ^{1}H-^{29}Si HMBC NMR spectra demonstrated loss of the SiMe$_3$ moiety, while the absence of the counterion was confirmed by ^{19}F NMR spectroscopy. Taken together these data support the conversion of the η^1-phosphaalkynes complexes **1.58g$^+$, 1.58f$^+$** and **2.1$^+$ a-d** to the cyaphide complexes **1.59g, 1.59f** and **2.2 a-d**.

Alkyne Substituent	Compound Number	$^{31}P\{^{1}H\}$ NMR (ppm)		$^{13}C\{^{1}H\}$ NMR (ppm)			IR (ν)	
		dppe ($^{3}J_{PP}$, Hz)	C≡P	C≡P ($^{1}J_{CP}$, Hz)	C_{α}≡C	C≡C_{β}	C≡P	C≡C
^{n}Bu	**2.2a**	50.9 (5.0)	155.5	284.6	118.4	139.5	1241	2090
^{t}Bu	**2.2b**	52.9 (5.1)	142.8	281.1	-	134.2	1251	2083
CO_2Me	**1.59g**	51.6 (5.5)	170.2	279.12[a]	112.4[a]	143.8[a]	1253[a]	2036[a]
CO_2Et	**1.59f**	44.6 (4.7)	168.3	278.7	112.1	141.8	1233	2063
p-C_6H_4-CO_2Et	**2.2c**	50.3 (4.5)	164.9	281.0	114.3	142.3	1268	2057
C_6H_3-3,5-$(CF_3)_2$	**2.2d**	50.9 (5.4)	172.8	280.1[b]	-	123.1[b]	1273[b]	2055[b]

Table 2-3: *Selected NMR and IR spectroscopic data for cyaphide complexes* ***1.59f****,* ***1.59g,*** *and* ***2.2a-d*** *([a] data from reference 102 and 103, [b] data from reference 118)*

2.2.4 MOLECULAR STRUCTURE ANALYSIS OF 1.59f

The cyaphide complex **1.59f** has been previously reported, its identity inferred from spectroscopic data in lieu of the structural data. Single crystals of **1.59f** were ultimately obtained from saturated solution of the complex in benzene at ambient temperature (**Figure 2-2**). The crystallographic data (**Table 2-4**) showed the cyaphide lying *trans*- to the acetylide with C≡C bond length of 1.272(9) Å, an significant elongation compared to *trans*-$[Ru(P{\equiv}CSiMe_3)(C{\equiv}CCO_2Me)(dppe)_2]^+$ (C≡C 1.153(15) Å) and comparable C≡P bond lengths (1.563(7) Å, *vs* 1.528(11) Å). Overall these data matches the general trend seen upon conversion of the η^1-phosphaalkyne ligand into a cyaphide.[27,103,104] The central π-chain shows distortion from linearity with the Ru-C-P and C-Ru-C bonds angles being 169.6(4)° and 173.8(2)° respectively, compared to *trans*-$[Ru(P{\equiv}CSiMe_3)(C{\equiv}CCO_2Me)(dppe)_2]^+$ (Ru-P-C 175.7(4)° and C-Ru-P 177.0(3)°), and is generally in-line with classical *bis*-alkynyl complexes and previously reported cyaphide complexes. (**Table 2-4**).[103,104,120–123] This distortion from linearity of the central π-chains is most pronounced for **1.59f** and is comparable to when R = C_6H_4-*p*-CO_2Me and C_6H_4-*p*-OMe, although it is important to note that this is not observed in all of the reported cyaphides, minimal distortion being observed where R = C_6H_4-*p*-F. Notably, **1.59f** exhibits further deviation at the alkynyl ligand (∠C≡C-C_{ester} 169.5(9)°; d(C-C_{ester}) 1.34(2) Å), which can be attributed to the disorder within the ester group. The reported DFT studies for **1.59f** and for when R = C_6H_4-*p*-OMe indicated that more linear bond angles for the central π-system are favoured in the gas-phase, suggesting that this distortion from linearity is, at least in part, due to the prevalence of packing effects in the solid state. In contrast the computational data for R = C_6H_4-*p*-CO_2Me and R = C_6H_4-*p*-F show good agreement with the experimental data.[103,104,118]

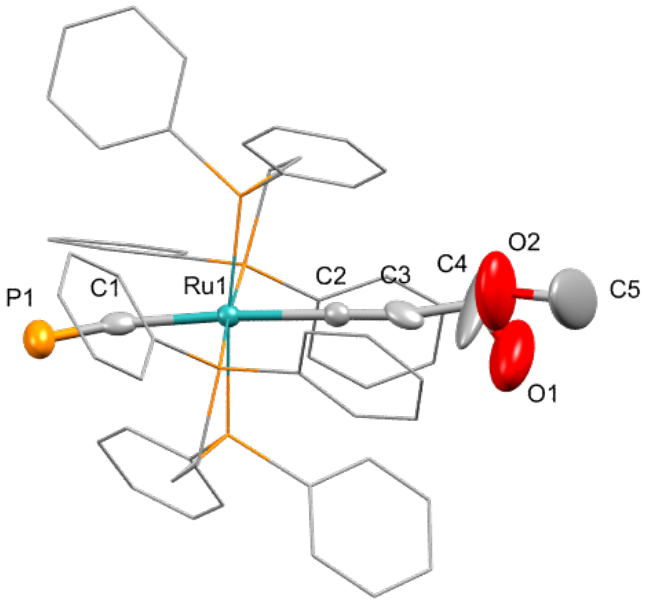

Figure 2-2: *Solid state molecular structure of* ***1.59f*** *crystals of the benzene solvate. Solvent and hydrogen atoms omitted and dppe ligands reduced for clarity, thermal ellipsoids at 50% probability level. The oxygens of the ester group are disordered across multiple sites; hydrogens omitted for clarity.*

			trans-[Ru(C≡P)(C≡CR)(dppe)$_2$]		
	1.59f	**[RuH(dppe)$_2$(C≡P)]^a**	**C$_6$H$_4$-*p*-OMe^b**	**C$_6$H$_4$-*p*-CO$_2$Me^c**	**C$_6$H$_4$-*p*-F^c**
			1.59d	***1.59h***	***1.59c***
Ru(1)-C(1)	2.070(6)	2.057(2)	2.065(4)	2.076(9)	2.118(3)
Ru(1)-C(2)	2.053(5)	-	2.084(3)	2.072(8)	2.054(20)
C(1)-P(1)	1.563(7)	1.573(2)	1.544(4)	1.549(10)	1.493(3)
Alkyne C(2)-C(3)	1.272(9)	-	1.205(5)	1.216(12)	1.216(4)
C(2)-Ru(1)-C(1)	173.8(2)	-	171.91(14)	172.4(4)	174.5(1)
Ru(1)-C(1)-P(1)	169.6(4)	177.9(1)	172.3(2)	172.8(6)	177.8(2)

Table 2-4: *Selected bond lengths (Å) and angles (°) for* ***1.59f****, [RuH(dppe)$_2$(C≡P)]* ***1.52*** *and trans-[Ru(C≡P)(C≡CR)(dppe)$_2$] (R = C$_6$H$_4$-p-CO$_2$Me* ***1.59d****, C$_6$H$_4$-p-OMe* ***1.59h*** *and C$_6$H$_4$-p-F* ***1.59c****). ([a] data from reference 100, [b] data from reference 102 and [c] data from reference 103)*

2.2.5 ELECTROCHEMISTRY OF *trans*-[Ru(C≡P)(C≡CR)(dppe)$_2$]

In order to probe the redox chemistry of the cyaphide complexes, cyclic voltammetry was undertaken for **2.2a**, **2.2c** and **1.59f** as CH_2Cl_2 solutions at a platinum disk working electrode (1mm), with NBu_4PF_6 supporting electrolyte. The cyaphide complexes each exhibit one irreversible oxidation, a quasi-reversible oxidative process and a subsequent irreversible reductive feature, these data have been summarised in (**Table 2-5**).

R Group	Compound Number	Irreversible Reductive Event	Irreversible Oxidative Event	Quasi-reversible event		
		E_{pc} (V)	E_{pa} (V)	E_{pa} (V)	E_{pc} (V)	ΔE (V)
^{n}Bu	**2.2a**	-0.62	-0.02	0.62	0.71	0.09
CO_2Et	**1.59f**	-0.54	0.09	0.67	0.76	0.09
C_6H_4-*p*-CO_2Et	**2.2c**	-0.72	-0.05	0.55	0.66	0.11

Table 2-5: *Cyclic voltammetry data of cyaphide complexes **2.2a**, **2.2c** and **1.59f**. Potentials are reported relative to the ferrocene/ferrocenium (Fc/Fc^+) couple, referenced to the Fc^*/Fc^{*+} couple of doped samples (−0.56 V relative to Fc/Fc^+).*

In all cases an irreversible oxidation event is observed, in general at potentials that become increasingly anodic in line with the electron-withdrawing character of the *trans*-alkyne, and comparable to previously reported *trans*-alkynyl cyaphides, although **2.2c** is an outliner, with a more cathodic oxidation potential of −0.05 V compared to when R is C_6H_4-*p*-CO_2Me (0.16 V).

Direct comparison of the parent chloride complex, *trans*-[RuCl(C≡C^{n}Bu)(dppe)$_2$] to the cyaphide complex **2.2a** (**Figure 2-3**) shows an anodic shift of the oxidative events of *ca* 0.05 V, in line with the cyaphide ligand having a slightly more electron withdrawing character than that of a chloride ligand and is consistent to what has been shown with previously reported *trans*-alkynyl cyaphide complexes (R = $C_6H_4CO_2Me$ E_{pa} = 0.16 V, $E_{1/2}$ [Ru-Cl] = 0.10 V; R = $C_6H_4NO_2$ E_{pa} = 0.58 V, $E_{1/2}$ [Ru-

Cl] = 0.20 V; R = C_6H_4Me E_{pa} = -0.03 V, $E_{1/2}$ [Ru-Cl] = -0.03 V; R = C_6H_4OMe E_{pa} = -0.05 V, $E_{1/2}$ [Ru-Cl] = -0.10 V).[104,119] In addition, the irreversibility of the first oxidation process in **2.2a**, **2.2c** and **1.59f** (**Figure 2-3**) is in accordance to that previously reported for similar systems and suggests instability of the oxidised product consistent with the electron acceptor character for the cyaphide ligand.[104]

However, unlike previously reported cyaphide complexes, **2.2a**, **2.2c** and **1.59f** also show a quasi-reversible process at more anodic potentials similar to that seen previously in *trans*-$RuCl(C{\equiv}CC_6H_4\text{-}R)(dppe)_2$ (R = OMe, C_5H_{11}, Me, H, CO_2Me and NO_2 E_{pa} = 0.69 to 1.07 V).[125] Although these processes have not been unequivocally identified they can be tentatively assigned to the Ru(III)/Ru(IV) redox couple, which is in line with that reported in other octahedral ruthenium systems such as [Ru(β-diketonato)$_3$] compounds (Ru(III/IV) E_{pa} = 0.44 to 1.30V).[126]

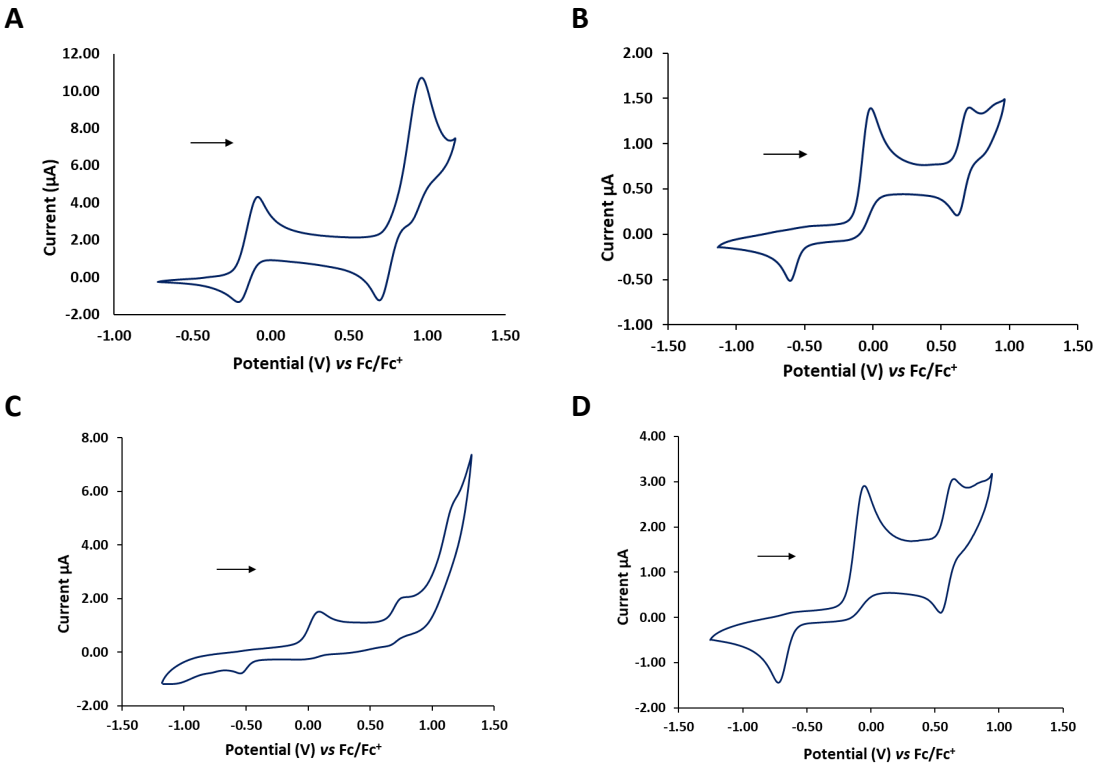

Figure 2-3: *Cyclic Voltammograms for (A) trans-[RuCl(C≡C^{n}Bu)(dppe)$_2$], (B)* ***2.2a****, (C)* ***1.59f****, (D)* ***2.2c****. As solutions in CH_2Cl_2 (0.01M) with [^{n}Bu$_4$N][PF$_6$] supporting electrolyte (0.1 M), 0.1 V s^{-1} scan rate and 5 second equilibrium time. Referenced against decamethylferrocene (−0.56 V relative to ferrocene) in doped samples.*

2.3 REACTIVITY STUDIES OF *trans*-[Ru(C≡P)(C≡CR)(dppe)$_2$]

The synthesis of the platinum cyaphide complex, [PtCl(C≡P)(PEt$_3$)$_2$] **1.49** and the isolated dimer, [Cl(Et$_3$P)$_2$Pt-μ-η^1-η^2-C≡P)Pt(PEt$_3$)$_2$] **1.50** was reported by Angelici, in which **1.50** the cyaphide ligand is η^1-coordinated to one platinum and η^2-coordinated to the second platinum metal centre (see section: **1.4.1**).[99] However, in the *trans*-[Ru(C≡P)(C≡CR)(dppe)$_2$] systems it is believed that the steric hindrance around the cyaphide ligand will prevent η^2-coordination, and therefore force η^1-coordination to a second metal centre engaging the cyaphidic lone pair in reactivity. Therefore, previous reactivity studies have focused on the addition of platinum as well as palladium and gold complexes to attempt to coordinate the phosphorus lone pair.[118] However, initial reactions conducted by others within the group between *trans*-[Ru(C≡P)(C≡CCO$_2$Me)(dppe)$_2$] and [Pt(PPh$_3$)$_2$(C$_2$H$_4$)] showed no reactivity or gave an intractable mixture of products respectively.[118] Gold(I) complexes have demonstrated the ability to ligate low coordinated phosphorus compounds through the lone pair.[127,128] Thus, with the continued aim to coordinate the lone pair of the cyaphide, the addition of gold complexes to the *trans*-alkynyl cyaphide complexes was previously studied, although no reaction was observed.[118]

Building upon these previous studies, the reactivity between *trans*-alkynyl cyaphide complexes and a variety of metal complexes, L$_n$M, was explored under a range of conditions (**Table 2-6**). Multiple *trans*-alkynyl cyaphide complexes were initially studied, with **2.2a** and **1.59g** being the best behaved, therefore these will be the focus of the discussion. The reaction of [Pt$_2$Cl$_4$(PEt$_3$)$_2$] and **2.2a** in DCM was stirred for 24 h at room temperature. The ^{31}P{^{1}H} NMR spectrum showed a singlet at 8.9 ppm attributed to the [PtCl$_2$(PEt$_3$)$_2$] with apparent ^{195}Pt satellites. Also shown are the doublet and quintet resonances at 50.9 ppm and 155.5 ppm for the dppe and C≡P ligands of **2.2a** respectively, demonstrating only a mixture of starting materials. Altering the solvent and stoichiometry resulted in intractable mixtures with evidence for the loss of the C≡P ligand (**Table 2-6**). The reaction of **2.2a** with [Rh(PPh$_3$)$_2$(CO)Cl] in the presence of AgBF$_4$ in *d*-DCM showed no reactivity.

Cyaphide	$[ML_n]$	Conditions	Outcome
2.2a	$PtCl_2(PEt_3)_2$	1: 1, DCM, RT, 24h	• Starting Material
2.2a	$PtCl_2(PEt_3)_2$	1: 1/2 , CD_2Cl_2, RT, 24h	• Loss of C≡P resonance • New doublet resonance at 48 ppm
2.2a	$PtCl_2(PEt_3)_2$	1:1, THF, RT, 24h	• Starting material • New doublet resonance at 48 ppm
2.2a	$PtCl_2(PEt_3)_2$	1:½, C_6D_6, RT, 24h	• Intractable mixture of products
1.59f	$PtCl_2(PEt_3)_2$	1: 1, DCM, RT, 24h	• Loss of C≡P resonance • New doublet resonance at 48 ppm
2.2a	$RhCl(CO)(PPh_3)_2$ + $AgBF_4$	1: 1:1, CD_2Cl_2, RT, 24h	• Starting Material

Table 2-6: *Summary of the reaction reagents and conditions and their outcomes for $[ML_n]$ = Pt or Rh.*

No reaction was observed between **2.2a** and $AuCl(PPh_3)$ in line with previous studies.[118] In contrast, **1.59g** was reacted with one equivalent of $AuCl(PPh_3)$ on a NMR scale in deuterated DCM for 18 h, resulting in changes in the $^{31}P\{^1H\}$ NMR spectrum, which showed a broad singlet at 49.2 ppm and a sharp singlet at 47.3 ppm integrating in a 4:1 ratio respectively. These data are similar to those previously noted upon reaction of *trans*-$[Ru(dppe)_2(C{\equiv}CCO_2Et)(C{\equiv}P)]$ with $AuCl(PPh_3)$ in the presence of $AgBF_4$.[118] The $^{31}P\{^1H\}$ NMR spectrum also shows a C≡P resonance at 146.3 ppm, a significant shift from that of **1.59g** (ca 173.9 ppm). Overall, these data are suggestive of some reaction, albeit not well defined. Attempts to isolate and characterise the product have been unsuccessful with decomposition occurring routinely.

Reactivity towards silver salts was also studied, reacting **1.59g** with one equivalent of $AgPF_6$ in CD_2Cl_2, which resulted in the instant formation of a brown precipitate. The $^{31}P\{^1H\}$ NMR spectrum, obtained for the crude product after 18 h showed the loss of the C≡P resonance and the appearance of a singlet at 41.6 ppm and a septet at −144.2 (attributed to PF_6), alongside multiple low intensity peaks obscured by the baseline; these data suggest breakdown of the cyaphide complex. Further experiments were carried out to potentially trap the leaving cyaphide through the addition of Me_3SiCl and MeI to yield Me_3SiCP or MeCP respectively. Conducting the reaction in the presence of Me_3SiCl yielded a new broad multiplet in the baseline at 101 ppm, while with MeI three resonances were observed, a singlet at 47 ppm, a doublet at 46 ppm and a quintet at −144.2 (attributed to PF_6). These species could not be isolated, and the data thus remains inconclusive.

The reactivity of **2.2a** towards $AgPF_6$ was also investigated, the $^{31}P\{^1H\}$ NMR spectrum showing a new resonance at 82.8 ppm and a slightly shifted cyaphide (146 ppm) with a corresponding dppe resonance (50.9 ppm) integrating in a 2:1:4 ratio respectively, in addition, a resonance associated with PF_6 (−144 ppm.) is also present. Although there is a slight shift in the cyaphide resonance there is not enough evidence to suggest any lone pair coordination, however, the appearance of the new signal at 82.8 ppm could be a result of the cyaphide reacting. Attempts to isolate the product were unsuccessful and further reactions introducing either Me_3SiCl or MeI gave no further indication to the products' identities.

2.4 SYNTHESIS OF *trans*-[Ru(C≡CPh)(C≡N)(dppe)$_2$]

Though innumerable *bis*-alkynyl complexes exist with which the cyaphide-alkynyls can be compared, there are currently no suitable cyanide analogous. The synthesis of complexes of the type *trans*-[Ru(C≡CR)(C≡N)(dppe)$_2$] was therefore investigated, to allow for a direct comparison of ligated cyaphide with cyanide. It is noteworthy that previous synthetic attempts via salt metathesis of sodium cyanide with *trans*-[RuCl(C≡CPh)(dppe)$_2$] have given a mixture of starting material and the *bis*-acetylide complex, *trans*-[Ru(C≡CPh)$_2$(dppe)$_2$].[119]

2.4.1 SYNTHESIS OF *trans*-[Ru(C≡CPh)(C≡N)(dppe)$_2$] 2.3

Treatment of *trans*-[RuCl(C≡CPh)(dppe)$_2$] with TlOTf in DCM for 1 hour followed by filtration and subsequent addition of NaCN yielded a pale brown solid (**Scheme 2-3**). The $^{31}P\{^1H\}$ NMR spectrum showed a mixture of two products, with two singlet resonances at 54.5 ppm and 55.0 ppm integrating in a 15:1 ratio assigned as **2.3** and the parent chloride complex, *trans*-[RuCl(C≡CPh)(dppe)$_2$] respectively, while the ^1H NMR spectra showed resonances consistent with the dppe ligands and one acetylide being present. The presence of the cyanide ligand was confirmed by Infra-Red spectroscopy which showed a characteristically strong peak at 2059 cm^{-1} for the C≡N stretch, thus these data are in general consistent with the formation of *trans*-[Ru(C≡CPh)(C≡N)(dppe)$_2$] **2.3** which was ultimately confirmed by X-ray diffraction data.

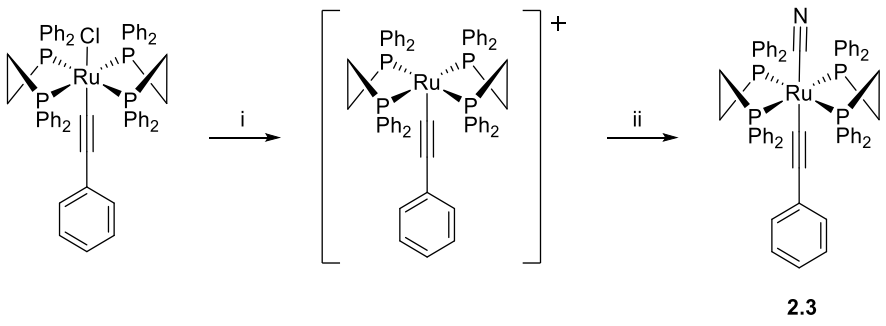

2.3

Scheme 2-3: *Synthesis of trans-[Ru(C≡N)(C≡CPh)(dppe)$_2$] **2.3**. Reagents and conditions: (i) 1 eq. TlOTf, DCM, 1h, RT, (ii) excess NaCN, DCM, 18h, RT.*

2.4.2 MOLECULAR STRUCTURE OF *trans*-[Ru(C≡CPh)(C≡N)(dppe)$_2$] 2.3

Crystals from a concentrated sample of the reaction mixture in DCM and layered with hexanes were grown. The solid-state structure (**Figure 2-4**) was conclusive in showing the formation of **2.3** with a C≡N trans to the phenylactylide fragment, apparently co-crystallised with two equivalents of TlOTf. The structure suffers from appreciable disorder and involves a superposition of the cyanide moiety and the precursor chloride. Consequently, though connectivity is adequately defined, structural parameters are unreliable.

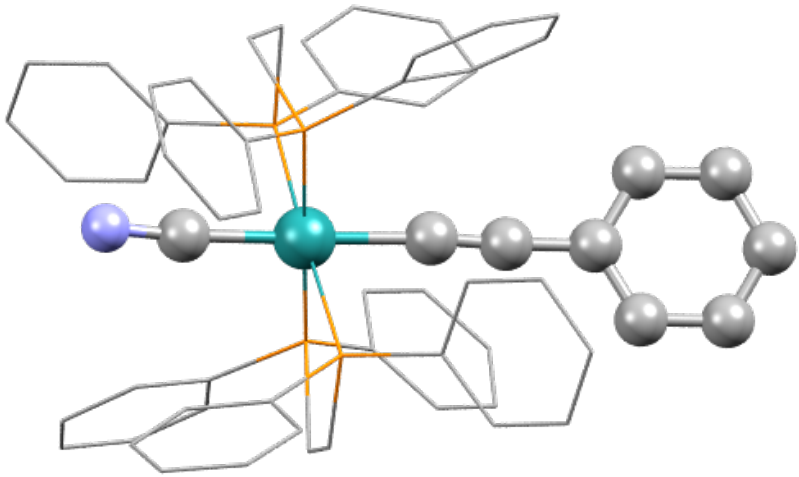

Figure 2-4: *Solid state molecular structure of trans-[Ru(C≡N)(C≡CPh)(dppe)$_2$]* ***2.3*** *showing connectivity only, due to high levels of disorder. The chloride, hydrogens and TlOTf molecules removed for clarity.*

2.5 CONCLUDING REMARKS

The synthesis of the η^1-phosphaalkyne **1.58f**$^+$ and **1.58g**$^+$ and **2.1**$^+$ **a-d** and cyaphide complexes **1.59f**, **1.59g** and **2.2a-d** has been achieved and the compounds characterised through NMR and Infra-Red spectroscopy. Complexes **2.1a**$^+$ and **1.59g** were additionally characterised through X-ray diffraction showing characteristic features comparable to previously reported analogous systems. Cyclic voltammetry was used to study the electrochemical behaviour of **2.2a**, **1.59f** and **1.59g**, with all exhibiting an irreversible oxidative peak with an additional quasi-reversible oxidative feature. In addition, **2.2a** showed an anodic shift compared to its parent chloride complex, demonstrating a slightly greater electron-withdrawing capacity of the C≡P ligand in comparison to the chloride.

Initial investigations into the possible reactivity of ligated cyaphide have been undertaken with multiple attempts to coordinate to metal centres (Pt, Pd, Au, Ag and Rh) the majority of which were unsuccessful. However, the reaction of **1.59g** with AuCl(PPh_3) showed some promise with the $^{31}P\{^1H\}$ NMR spectra showing a significant shift of the C≡P resonance to 146.3 ppm from 173.9 ppm, but further investigations are required in order to fully characterise the resultant complex.

The synthesis of the first example of a *trans*-[Ru(C≡CR)(C≡N)$(dppe)_2$] complex, **2.3** , was achieved through treatment of *trans*-[RuCl(C≡CPh)$(dppe)_2$] with TlOTf in DCM and subsequent addition of NaCN. Spectroscopic data support the formation of **2.3** and the connectivity was confirmed through X-ray diffraction. However, additional work is needed to optimise the synthetic procedure to yield pure product in order to gain full characterisation data and to study the complex further.

CHAPTER 3 : SYNTHESIS AND REACTIVITY OF THE FIRST *TRANS*-ALKYL AND *TRANS*-HALIDE CYAPHIDE COMPLEXES

3.1 INTRODUCTION

As previously discussed, (see section: **2.3**) the controlled reactivity of the cyaphide complexes remains unknown with most examples either appearing inert or being prone to decomposition with the loss of the cyaphide ligand. This has not only limited the ability to study the reactivity of the lone pair and π-system of the cyaphide moiety but has also precluded the post-synthetic modification of such complexes, with all known cyaphide complexes to date requiring the cyaphide ligand to be installed in the final step. The range of accessible complexes is thus significantly limited by the availability of the precursors of the type *trans*-$[RuR(dppe)_2]^+$ and their susceptibility to the coordination of the η^1-P≡CSiMe$_3$ ligand, which due to the low basicity of the phosphaalkyne lone pairs cannot be assured.

In order to continue to probe the reactivity of the cyaphide moiety a simplified system of the type *trans*-$[RuR(dppe)_2(C{\equiv}P)]$ (R = alkyl) was sought. It was believed that simplifying the ligand *trans* to the cyaphide might reduce unwanted side reactions when seeking coordination on the cyaphide lone pair. However, there are no precedent examples of alkyl cyaphide complexes in the literature and previous attempts within the Crossley group to synthesise an appropriate precursor to enable pre-coordination of the η^1-P≡CSiMe$_3$ ligand have been unsuccessful.

Herein, the synthesis and reactivity studies of the first such complex, *trans*-$[RuMe(dppe)_2(C{\equiv}P)]$, will be discussed. Moreover, investigations of the reactivity of *trans*-$[RuMe(dppe)_2(C{\equiv}P)]$ has revealed a facile means to access a series of *trans*-halide cyaphides which can ultimately be exploited for post-synthetic modification, allowing the expansion of the organometallic and coordination chemistry of cyaphides.

3.2 *TRANS*-ALKYL CYAPHIDE COMPLEXES

3.2.1 SYNTHESIS AND CHARACTERISATION OF *trans*-[RuMe(dppe)$_2$(C≡P)]

Trans-[RuMe(dppe)$_2$]$^+$ (**3.1$^+$**) was prepared by methide abstraction from *trans*-[RuMe$_2$(dppe)$_2$], itself obtained via a modification of a literature preparation (**Scheme 3-1**).[129–131] The optimised two-step synthetic procedure consists of reacting [RuCl(dppe)$_2$]OTf with one and a half equivalents of Me$_2$Mg in THF or diethyl ether to yield *trans*-[Ru(Me)$_2$(dppe)$_2$], and subsequent addition of one equivalent of TlOTf to afford [RuMe(dppe)$_2$]OTf as a purple solid. The spectroscopic data for *trans*-[Ru(Me)$_2$(dppe)$_2$] and [RuMe(dppe)$_2$]OTf were in accordance with the literature.[131]

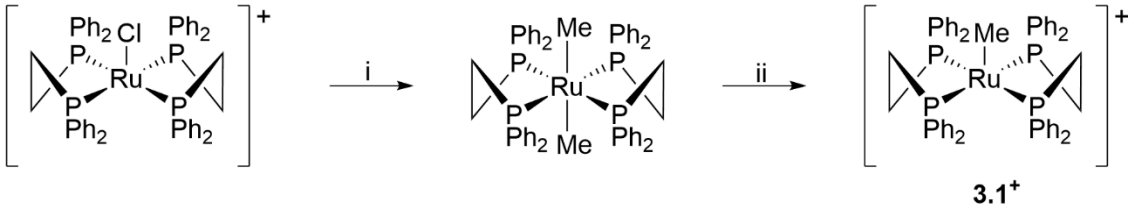

***Scheme 3-1**: Preparation of [RuMe(dppe)$_2$]OTf **3.1$^+$**. Reagents and conditions: (i) 1.5 eq. Me$_2$Mg, THF, 18h, RT. (ii) 1eq. TlOTf, DCM, 1h, RT.*

The reaction of a DCM solution of **3.1$^+$** and Me$_3$SiCP at ambient temperature for 1 hour gave the corresponding η^1-phosphaalkyne complex, *trans*-[Ru(Me)(P≡CSiMe$_3$)(dppe)$_2$]$^+$ (**3.2$^+$**). In addition to signals characteristic of the η^1 phosphaalkyne and dppe fragments, a quintet (121 ppm, J_{PP} = 28 Hz) and a doublet (46.3 ppm, J_{PP} = 28 Hz) in a 1:4 ratio respectively, the $^{31}P\{^1H\}$ NMR spectrum also showed two triplets (47.8 ppm and 57.6 ppm J_{PP} =12.1 Hz). Although the identity of these species giving rise to these triplets was not determined it was thought to be due to **3.2$^+$** being unstable in chlorinated solvents. Altering the solvent to toluene resulted in a mixture of the desired product and starting material, while optimal results were achieved by combining **3.1$^+$** as a suspension in 1,4-dioxane with a toluene solution of Me$_3$SiCP, which affords *trans*-[Ru(P≡CSiMe$_3$)(Me)(dppe)$_2$]$^+$ (**3.2$^+$**) in good yields of 71% (**Scheme 3-2**).

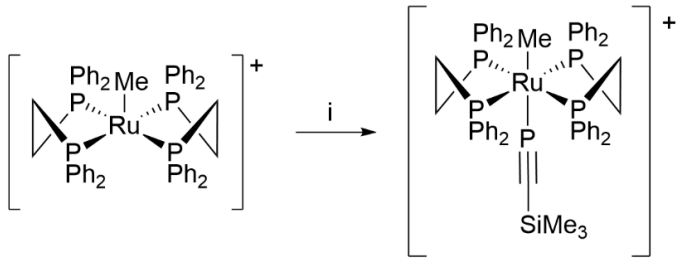

3.1⁺ **3.2⁺**

Scheme 3-2: *Synthesis of trans-[Ru(P≡CSiMe$_3$)(Me)(dppe)$_2$]$^+$ (**3.2**$^+$). Reagents and conditions: (i) Excess P≡CSiMe$_3$ in toluene, 1,4-dioxane, 1h, RT*

Treatment of **3.2**$^+$ with one equivalent of KO^{t}Bu yielded a yellow solid, identified as *trans*-[Ru(Me)(C≡P)(dppe)$_2$] (**3.3**), after one hour at room temperature. However, optimal results were achieved using 1.2 equivalents of NaOPh, at −30°C for between 1-5 minutes, which afforded **3.3** in enhanced yields and purity (**Scheme 3-3**). The spectroscopic data for **3.3** are consistent with the previously synthesised cyaphides with the $^{31}P\{^1H\}$ NMR spectrum showing a doublet (58.9 ppm, J_{PP} = 4.0 Hz) and quintet at (177.9 ppm), assigned as the dppe ancillary ligands and the cyaphide respectively, the multiplicity and coupling constant being consistent with the retention of the *trans*- geometry. The ^1H NMR spectrum showed the retention of the methyl group at −2.31 ppm and the loss of the silyl group, while the ^{19}F NMR spectrum demonstrated the absence of the triflate counterion. In addition, in the Infra-red spectrum a C≡P stretching frequency is observed (ν_{CP} = 1271 cm^{-1}) comparable to that observed for the *trans*-alkynyl cyaphide complexes.[103,124]

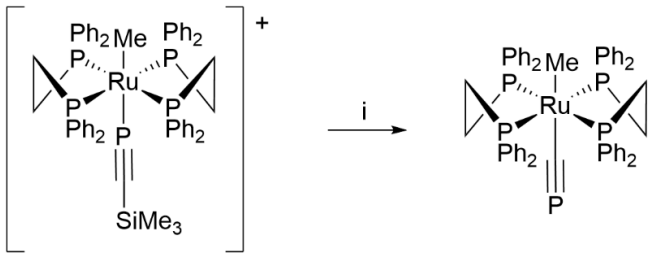

3.2⁺ **3.3**

Scheme 3-3: *Synthesis of trans-Ru(Me)(C≡P)(dppe)$_2$ **(3.3)**. Reagents and conditions: 1.2 eq. NaOPh, THF, −30°C, 1-5 minutes.*

3.2.2 MOLECULAR STRUCTURE ANALYSIS OF 3.3

The Identity of **3.3** was ultimately confirmed through X-ray diffraction. These data unequivocally confirmed the connectivity for **3.3**, but disorder about the cyaphidic carbon centre precludes any significant discussion of the C≡P distance (1.392(8) Å) which appears shortened compared to previously discussed examples.[103–105] In addition, the Ru-C_{CP} bond is notably longer, although still within the range for ruthenium acetylide systems recorded in the CCDC.[132] Furthermore the Ru1-C2 bond length (2.238(6) Å) is comparable to those reported for *trans*-[Ru$(CH_3)_2$(dmpe)$_2$], *trans*-[Ru(CH_3)(C≡CPh)(dmpe)$_2$] and *trans*-[Ru(CH_3)(C≡C^{t}Bu)(dmpe)$_2$] (2.236(3) Å, 2.247(2) Å and 2.2213(8) Å respectively).[27,103–105,129]

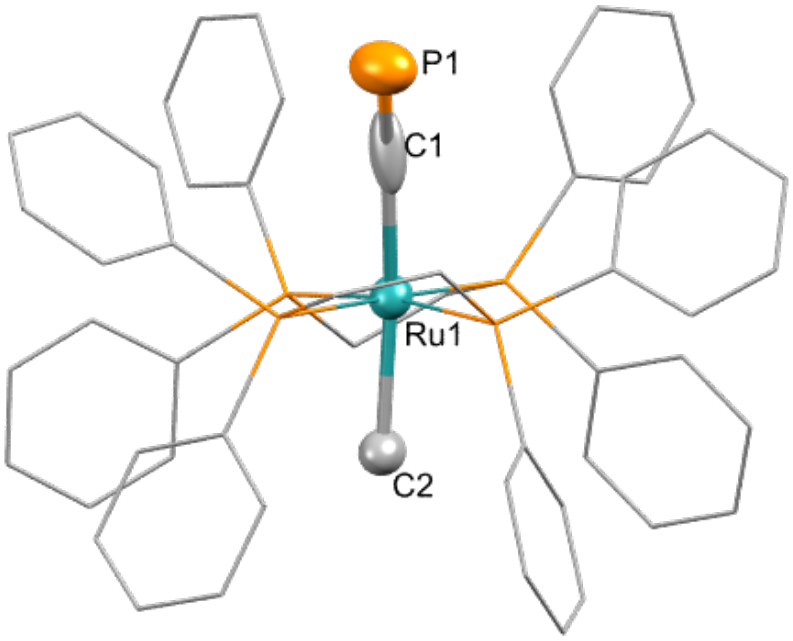

Figure 3-1: *Solid state molecular structure of* ***3.3****. Hydrogen atoms omitted and dppe ligands reduced for clarity, thermal ellipsoids at 50% probability level. C1 is disordered across two sites (90%/10%) but not readily modelled, distorting the C≡P distance. Selected bond lengths (Å) and angles (°): Ru1-C1 2.186(8), Ru1-C2 2.238(6), C1-P1 1.392(8), C2-Ru1-C1 171.2(3) and Ru1-C1-P1 165.5(5).*

3.3 ATTEMPTED SYNTHESIS OF *trans*-[RuR(dppe)$_2$]OTf (R = Et, Bn)

With the successful synthesis of *trans*-[Ru(Me)(C≡P)(dppe)$_2$] from the [RuMe(dppe)$_2$]OTf salt, the ethyl analogue was sought to extend the series of alkyl cyaphide complexes. However, the reaction of [RuCl(dppe)$_2$]OTf with one and half equivalents of Et_2Mg in THF, led to an intractable mixture of products with the predominant species being characterised as a hydride (δ_H −19.0 ppm). This is most likely to arise from a β-hydride elimination reaction from an initially formed, *trans*-[Ru(Et)(dppe)$_2$]OTf. Other attempts including using half an equivalent of Et_2Mg in THF or diethyl ether, with the intention to synthesise the *trans*-Ru(Et)(Cl)(dppe)$_2$ led to the same mixture of intractable products. More attempts featuring changing the reaction times and temperatures were also unsuccessful. In addition, the reaction between [RuCl(dppe)$_2$]OTf and KBn in toluene also led to an intractable mixture of products including a comparable hydride-containing species.

3.4 REACTIVITY STUDIES OF *trans*-[RuMe(dppe)$_2$(C≡P)]

With *trans*-[Ru(Me)(C≡P)(dppe)$_2$] in hand efforts were made to engage the cyaphidic lone pair in reactivity. The reaction between **3.3** and [$Pt_2(PEt_3)_2Cl_4$] resulted in a change in the $^{31}P\{^1H\}$ NMR spectrum, with a shift in the C≡P resonance from 186 ppm to 135.7 ppm, though the latter is devoid of any ^{195}Pt satellites. In addition, a multitude of other signals appeared including two new singlets at 47 ppm and at 28.8 ppm corresponding to the dppe ligands and the platinum starting material respectively, alongside apparent decomposition products including *trans*-[RuMe(dppe)$_2$]$^+$ and free PEt_3 which were observed as singlets at 56 ppm and 15 ppm respectively. These NMR data suggest the reaction to be unsuccessful.

The reaction of **3.3** with gold and silver was also studied. Comparable to the *trans*-alkynyl cyaphides the reaction of **3.3** with [AuCl(PPh_3)] in the presence of $AgBF_4$ resulted in loss of the cyaphide resonance. In addition, the $^{31}P\{^1H\}$ NMR spectrum of the crude product showed three

singlets, δ_P 47, δ_P 29 and δ_P 25 which exhibited no mutual coupling. In the absence of the $AgBF_4$ a shift in the cyaphidic resonance was observed in the $^{31}P\{^1H\}$ NMR spectra from 186 ppm to 136 ppm, which could suggest potential reactivity of the cyaphide ligand, also a peak at 47 ppm was present which was assigned to the dppe scaffold which integrated 4:1 to the cyaphide resonance. The reaction of **3.3** with $AgPF_6$ resulted in comparable data with the $^{31}P\{^1H\}$ NMR spectra exhibiting resonances at 136 ppm and 47 ppm, with an additional quintet at −142 ppm for the PF_6. Overall, these spectroscopic data for the reactions of **3.3** with [AuCl(PPh_3)] and $AgPF_6$ are inconclusive as to whether η^1-coordination of the phosphorus lone pair has been achieved, or merely some complex decomposition, in line with the previous platinum reaction. Additional attempts to coordinate the lone pair through the reaction between **3.3** and $RhCl(CO)(PPh_3)_2$ in the presence of $AgBF_4$, as well as with [FeCp(η^6-Tol)]PF_6 and $B(PPh_3)_3$, failed to show any evidence of reactivity with only starting material apparent in both the $^{31}P\{^1H\}$ and ^1H NMR spectra.

Attempts were also made to engage the C≡P π-system in cycloadditions chemistry, reacting **3.3** with furan while heating to reflux and varying the solvent failed to effect any change, the $^{31}P\{^1H\}$ and ^1H NMR spectra showed only starting material present. In addition, reactions of **3.3** with the nucleophilic reagents MeMgCl, LiMe and $NaBH_4$ were attempted to engage the cyaphide moiety in chemistry, however, these resulted in no observable reactivity.

In further efforts to achieve chemistry of the cyaphide fragment, the coordination of zinc was considered, given its relatively extensive acid/base chemistry with phosphine donors, for example, $ZnX_2(PR_3)_2$ (X = Cl, Br, I and R = Ph, Et, Bu and Cy) and $ZnBr_2(PMe_2Ph)_2$.[133–136] In addition, zinc has been shown to coordinate to triphenylphosphine in the reaction of R-C≡C-I and Et_2Zn in the presence of PPh_3 forming a phosphine-ligated zinc acetylide dimer.[137] In this later example the zinc was shown to also coordinate to the π-system of the acetylide anion (**Figure 3-2**); given that phosphaalkynes have been shown to have similar chemistry to alkynes, zinc may have the

potential to coordinate to not only the phosphorus lone pair but also the cyaphide π-system. Thus, the reactivity of **3.3** towards zinc complexes was studied.

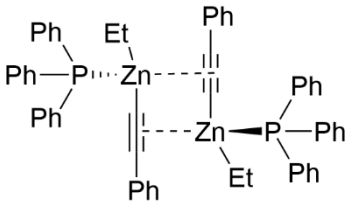

Figure 3-2: *Left:* Phosphine-ligated acetylide zinc dimer.[137]

Initially **3.3** was reacted with $ZnBr_2(PPh_3)_2$ in a 1:1 ratio in THF for 18 h yielding an orange solid. The $^{31}P\{^1H\}$ NMR spectrum showed a resonance consistent with the cyaphide moiety at 135 ppm, and the dppe ligands at 46 ppm, integrating in a 1:4 ratio. Also present was a broad peak at −6.7 ppm integrating to 2 phosphorus atoms, this is assigned to free PPh_3 liberated from the $ZnBr_2(PPh_3)_2$. The other major peak present in the spectrum is a singlet at 56 ppm assigned to $[RuMe(dppe)_2]^+$.

Further reactions of **3.3** with $ZnBr_2$ and PPh_3 (5 mol%) in both THF and DCM gave comparable results, although no resonance for $[RuMe(dppe)_2]^+$ was observed in the $^{31}P\{^1H\}$ NMR spectrum. The ^1H NMR spectrum demonstrated the retention of the dppe ligands, but the apparent loss of the resonance associated with the σ-methyl ligand. This was replaced by a new resonance at −0.83 ppm, which, though not definitively identified, is consistent with Zn−Me derivatives, as might result from Me/Br metathesis.[138–140] Crystallographic data ultimately confirmed the identity of the product as *trans*-$[RuBr(dppe)_2(C{\equiv}P)]$ **3.4**. The analogous reactions between **3.3** and ZnX_2 (X = Cl or I) with PPh_3 (5 mol%) afforded *trans*-$[RuCl(dppe)_2(C{\equiv}P)]$ **3.5** and *trans*-$[RuI(dppe)_2(C{\equiv}P)]$ **3.6** (**Scheme 3-4**). Both **3.5** and **3.6** are also obtained from the reaction of **3.3** with Me_3SiCl or MeI respectively, although these methods are less amenable to the isolation of the product in sufficient purity.

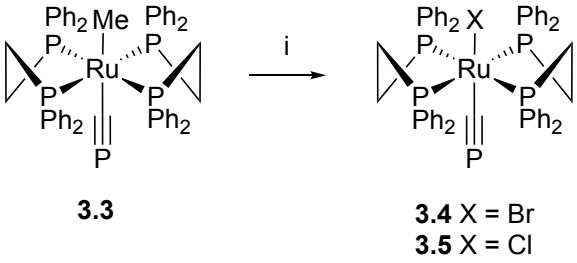

3.3

3.4 X = Br
3.5 X = Cl

Scheme 3-4: *Synthesis of trans-[RuX(dppe)$_2$(C≡P)].*

Reagents and conditions: ZnX_2, PPh_3 (5 mol%), THF or DCM, RT, 18 h.

Though the mechanism for this reaction has not been probed it would appear to be the first example of zinc halide-mediated halogen/methyl exchange at a transition metal. It appears that the reaction requires the presence of at least catalytic PPh_3, implying that $ZnX_2(PPh_3)_2$, formed *in situ*, is the active species. The involvement of HX, arising from adventitious water, can be excluded, on the basis that the reagents were scrupulously dried, and the reactions were carried out under strict anaerobic conditions. Moreover, *in situ* studies showed no evidence for the release of CH_4,[141] while the reaction of **3.3** with stoichiometric amounts of HCl yields only small amounts of **3.5** alongside numerous unidentified species, with excess of HCl cleaving the cyaphide moiety completely, affording $Ru(dppe)_2Cl_2$ as the sole identifiable product.

3.5 T*RANS*-HALO CYAPHIDE COMPLEXES

3.4.1 SYNTHESIS AND CHARACTERISATION OF *trans*-[RuX(dppe)$_2$(C≡P)] (X = Cl, Br or I)

The cyaphide complexes **3.4**-**3.6** have since been further characterised. The $^{31}P\{^1H\}$ NMR spectra in each case showed a characteristic cyaphide resonance (135.4 ppm **3.4**, 132.0 ppm **3.5** and 140.0 ppm **3.6**) and the corresponding dppe resonances (44.8 ppm **3.4**, 46.2 ppm **3.5** and 42.1 ppm **3.6**) (**Table 3-1**). The cyaphide carbon could not be resolved in the $^{13}C\{^1H\}$ NMR spectra for **3.4** and **3.6,** however, the spectrum for **3.5** showed the cyaphide carbon at 265.4 ppm. In

addition, the Infra-Red spectra confirmed the retention of the cyaphide ligand with stretching frequencies at 1249 cm^{-1} for **3.4** and 1250 cm^{-1} for **3.5** and **3.6**.

X	Compound	$^{31}P\{^{1}H\}$ NMR (ppm)		$^{13}C\{^{1}H\}$ NMR (ppm)	IR (ν)
		dppe ($^{3}J_{PP}$, Hz)	C≡P	C≡P	C≡P
Cl	**3.5**	46.2 (4.2)	132.0	265.4	1250
Br	**3.4**	44.8 (4.3)	135.4	-	1249
I	**3.6**	42.1 (br)	140.0	-	1250

Table 3-1: *Selected NMR and IR spectroscopic data for cyaphide complexes **3.4-3.6***

3.4.2 MOLECULAR STRUCTURE OF *trans*-[RuX(dppe)$_2$(C≡P)] (X = Cl, Br)

The identities of **3.4** (**Figure 3-3**) and **3.5 (Figure 3-4)** were ultimately confirmed through X-ray diffraction study of single crystals obtained from concentrated solutions of **3.4** and **3.5** in DCM layered with hexanes. These data confirmed the *trans* arrangement of the cyaphide and halide, which are mutually disordered and refined equally between the two sites. Both **3.4** and **3.5** exhibit PC-Ru-X bond angles which are near to perfectly linear (177.1(2)° **3.4**, 175.1(5)° **3.5**) as observed in *trans*-[RuH(dppe)$_2$(C≡P)] (177.9(1)°). In addition, the C≡P bond distances, (1.544(10) Å **3.4**, 1.638(17) Å **3.5**) are comparable to previously reported systems (*ca trans*-[RuH(dppe)$_2$(C≡P)] 1.530(3) Å,[27] *trans*-[Ru(C≡P)(C≡CR)(dppe)$_2$] (R = C_6H_4-p-CO_2Me **1.59d**, CO_2Me **1.59f**, C_6H_4-p-OMe **1.59h** and C_6H_4-p-F **1.59c**) 1.549(10) Å, 1.563(7) Å, 1.544(4) Å and 1.493(3) Å[103,104] respectively). In contrast, the Ru-C_{CP} distance in both cases appear shortened although more significantly in **3.5** (1.687(16) Å, **3.5** *cf.* 1.901(9) Å **3.4**,) compared to known cyaphides (*trans*-[RuH(dppe)$_2$(C≡P)] 2.057(2) Å,[27] **1.59h** 2.065(4) Å, **1.59d** 2.076(9) Å, **1.59c** 2.118(3) Å and **1.59f** 2.070(6) Å[103,104]). This significant shortening in the Ru-C_{CP} in **3.5** is thought to be due to the high levels of disorder across the Cl-Ru-CP unit. In addition, the Ru-X linkages (2.690(2) Å **3.4**,

2.556(2) Å **3.5**) lie in the middle or towards the longest known in the CCDC (X = Br (2.45-2.75 Å); X = Cl (2.30-2.60 Å)).[132]

	3.4	**3.5**
Ru(1)-C(1)	1.901(9)	1.687(16)
Ru(1)-X	2.690(2)	2.556(2)
C(1)-P(1)	1.544(10)	1.638(17
X-Ru(1)-C(1)	177.1(2)	175.1(5)
Ru(1)-C(1)-P(1)	175.8(5)	177.4(10)

Table 3-2: *Selected bond lengths (Å) and angles (°) for* ***3.5*** *and* ***3.6.***

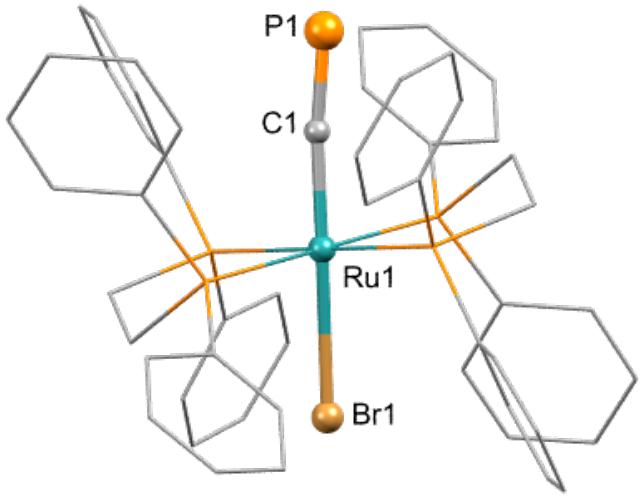

Figure 3-3: *Solid state molecular structure of* ***3.4****. Hydrogen atoms omitted and dppe ligands reduced for clarity, thermal ellipsoids at 50% probability level. Br and C≡P are refined across two sites (50%/50%) such that the Ru atom sits on the inversion centre; equivalent atoms are generated by symmetry transformation.*

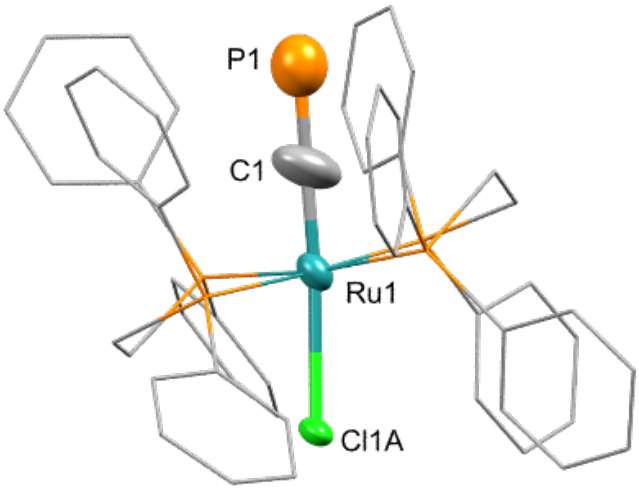

Figure 3-4: *Solid state molecular structure of* ***3.5****. Hydrogen atoms omitted and dppe ligands reduced for clarity, thermal ellipsoids at 50% probability level. Cl and C≡P are refined across two sites (50%/50%) such that the Ru atom sits on the inversion centre; equivalent atoms are generated by symmetry transformation.*

3.6 CONCLUDING REMARKS

The synthesis of *trans*-[RuMe(dppe)$_2$(P≡CSiMe$_3$)]$^+$ **3.2**$^+$ and *trans*-[RuMe(dppe)$_2$(C≡P)] **3.3** have been achieved and the compounds characterised through NMR and Infra-Red spectroscopy. Structural data for **3.3** exhibit features characteristic of previously reported analogues. Comparable to the *trans*-alkynyl cyaphide complexes the initial attempts to coordinate the phosphorus lone pair of **3.3** to metal centres (Pt, Pd, Au, Ag and Rh) were unsuccessful. However, the reactions between **3.3** and ZnX_2 (X = Cl, Br, I) in the presence of PPh_3 afforded a series of *trans*-halo cyaphide complexes *trans*-[RuX(dppe)$_2$(C≡P)] (X = Cl **3.4**, Br **3.5** or I **3.6**), through what would appear to be the first example of zinc halide-mediated halogen/methyl exchange at a transition metal. The formation of this series is notable given that they have previously been inaccessible by more “traditional” routes and present obvious targets for post synthetic modification.

CHAPTER 4 : CONTROLLED REACTIVITY OF *trans*-[RuBr(dppe)$_2$(C≡P)]: ISOLATION OF THE 5-COORDINATE [Ru(dppe)$_2$(C≡P)]$^+$

4.1 INTRODUCTION

The synthetic scope of cyaphide complexes has been limited, due to the requirement of the cyaphide ligand to be installed in the final step, which is significantly restricted by the availability of precursors of the type *trans*-[RuR(dppe)$_2$]$^+$. Even where such salts are available, their ability to coordinate to the η^1-P≡CSiMe$_3$ ligand, the lone pair of which has relatively low basicity, cannot be assured. Consequently, the ability to effect post-synthetic modification of cyaphide complexes would be a significant advance, one that has typically been precluded by the instability of cyaphide complexes.[57,72]

The formation of the series of *trans*-halo cyaphide complexes *trans*-[RuX(dppe)$_2$(C≡P)] (X = Cl **3.5**, Br **3.4** and I **3.6**) is notable, given that they have previously been inaccessible by more "traditional" routes, with [Ru(dppe)$_2$Cl]$^+$ being essentially inert toward Me$_3$SiC≡P. Indeed, only trace levels of *trans*-[RuCl(dppe)$_2$(P≡CSiMe$_3$)]$^+$ can be observed and only by generating [Ru(dppe)$_2$Cl]$^+$ *in situ* in the presence of a large excess of Me$_3$SiC≡P, enabling the trapping of [Ru(dppe)$_2$Cl]$^+$ prior to its relaxation to a trigonal-bipyramidal geometry. This has previously impeded the access to this series of cyaphides which present obvious targets for post synthetic modification.

Herein, the reactivity of *trans*-[RuBr(dppe)$_2$(C≡P)] (**3.4**) will be discussed including its role in the synthesis, isolation and characterisation of the first 5-coordinate complex, [Ru(C≡P)(dppe)$_2$]OTf (**4.1**$^+$). Moreover, the susceptibility of **4.1**$^+$ toward ligand addition at the vacant coordination site will be discussed.

4.2 CONTROLLED REACTIVITY OF *trans*-[RuBr(dppe)$_2$(C≡P)]

The reactivity of the cyaphide complex *trans*-[RuBr(dppe)$_2$(C≡P)] **3.4** was studied to probe its versatility for post synthetic modification. Indeed, this was illustrated with the reaction of THF solutions of **3.4** with Me_2Mg which afforded some evidence for the regeneration of *trans*-[RuMe(dppe)$_2$(C≡P)] **3.3**. The reaction of **3.4** and Et_2Mg to synthesise the ethyl analogue, *trans*-[RuEt(dppe)$_2$(C≡P)] was unsuccessful, resulting in spectroscopic data comparable to those for *trans*-[RuH(dppe)$_2$(C≡P)], viz.: δ_P 157, 65 and δ_H −11.2, with a significant shift in the cyaphide resonance being observed (*ca.* 165 ppm), albeit not probed this presumably arises from interactions of the cyaphide moiety with magnesium salts present in the reaction mixture. Although the mechanism for this has not been studied it is believed this may be occurring through one of two potential pathways. The first possibility is the presence of trace MgH_2, a known contaminant of Et_2Mg formed during the desolvation process under high temperature and reduced pressure, which then acts as a nucleophilic hydride source.[142,143] However, due to the overlap of the signature resonance with the THF signal the presence of the MgH_2 was not identified in the ^{1}H NMR spectrum. The second possibility would be that due to the co-ordinately saturated ruthenium system and the reduced nucleophilicity of Et_2Mg compared to Me_2Mg, the hydride source arises from β-elimination within the Et_2Mg (**Scheme 4-1**). This has been seen in the reduction of ketones using $^iPr_2Mg$, although there are no comparative examples of this at transition metals.[144,145] Overall, extensive mechanistic studies, which were not pursued, are needed to confirm the hydride source.

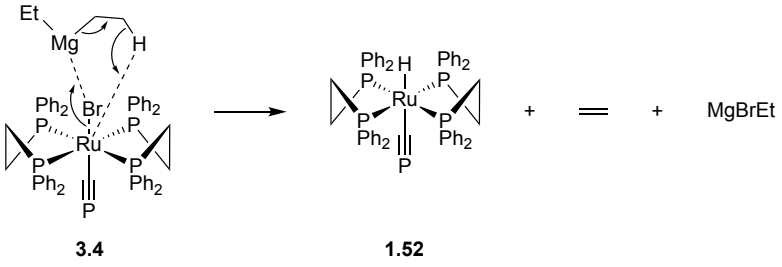

3.4 **1.52**

Scheme 4-1: *Potential mechanism for the reaction of **3.4** and Et_2Mg resulting in the formation of trans-[RuH(dppe)$_2$(C≡P)].*

Reactions between **3.4** and PhMgBr, LiC≡CPh, LiC≡CSiMe$_3$ or NaCN (**Scheme 4-2**) were also explored, but again proved ineffective, with no observable spectroscopic changes. Presumably this in part reflects the coordinate saturation of **3.4**, coupled in the case of LiC≡CPh and LiC≡CSiMe$_3$ with a propensity to aggregate, preventing the lithium assisting with abstraction of the bromide. Furthermore, for the reaction between **3.4** and NaCN, the lack of solubility of the salt was a major contributing factor for no observable reaction.

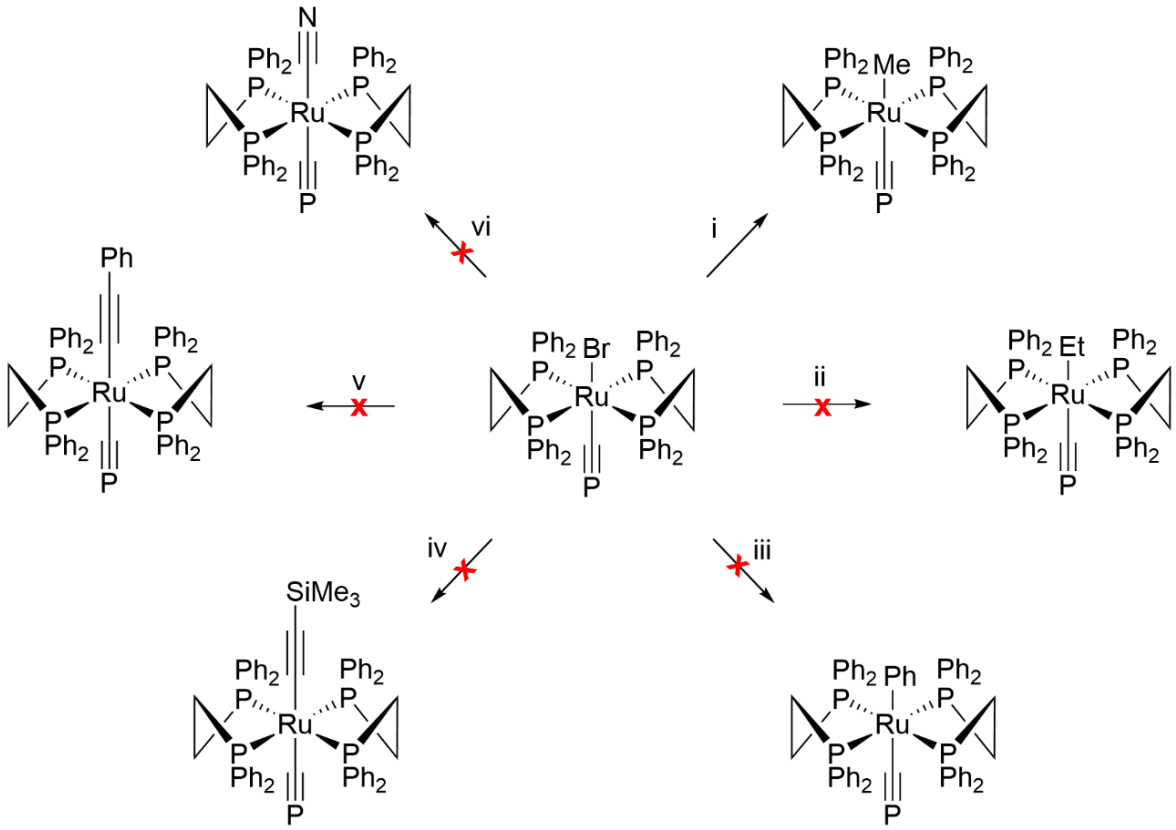

Scheme 4-2: *Reactivity of trans-[RuBr(dppe)$_2$(C≡P)]* ***3.4****. Reagents and Conditions: (i) Me$_2$Mg, THF, RT, 1 hour. (ii) Et$_2$Mg, THF, RT, 18 h. (iii) PhMgBr, THF, RT, 18 h. (iv) LiC≡CSiMe$_3$, THF, RT, 18 h. (v) LiC≡CPh, THF, RT, 18 h. (vi) NaC≡N, THF, RT, 18 h.*

In view of these results, it was clear that pre-abstraction of the bromide would be necessary to enable reaction with nucleophiles. To this end the reaction of **3.4** with LiC≡CPh was conducted with the addition of TlOTf, which proceeds readily to afford *trans*-[Ru(C≡CPh)(dppe)$_2$(C≡P)], as confirmed spectroscopically. During the transformation a brief colour change to purple was observed, presumably resulting from the transient formation of a 5-coordinate species. This would seem to imply that the cyaphide ligand remains somewhat stable within a less encumbered coordination sphere. In light of this observation attempts were made to isolate this intermediate.

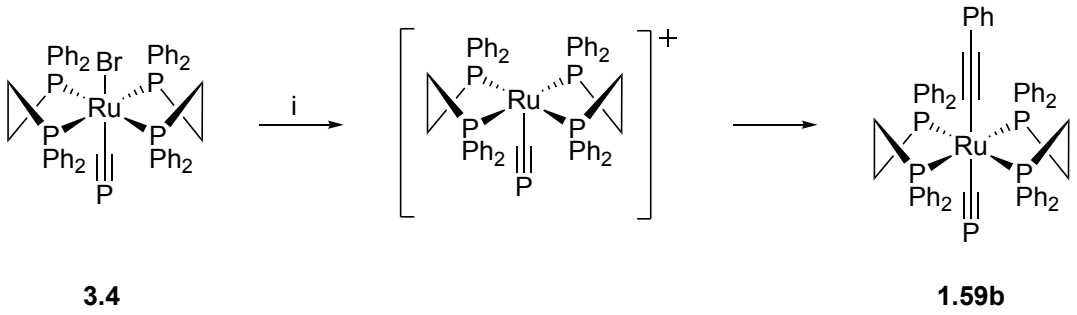

3.4 **1.59b**

Scheme 4-3*: Synthesis of trans-Ru(C≡CPh)(dppe)$_2$(C≡P) via suggested 5-coordinate species. Reagents and Conditions: (i) 1 eq. TlOTf, DCM, LiC≡CPh.*

4.3 THE 5-COORDINATE CYAPHIDE COMPLEX: [Ru(dppe)$_2$(C≡P)]OTf

4.3.1 SYNTHESIS AND CHARACTERISATION of [Ru(dppe)$_2$(C≡P)]OTf

The reaction of **3.4** with stoichiometric amounts of TlOTf, resulted in an immediate colour change from yellow to deep purple with the formation of a white precipitate. The $^{31}P\{^1H\}$ NMR spectrum of the isolated product showed a quintet and a doublet at 154 ppm and 52.1 ppm for the cyaphide and dppe resonances respectively, with a mutual coupling of 7.2 Hz. The chemical and magnetic equivalence of the dppe ligands suggest their retention in the equatorial plane, consistent with a square-pyramidal geometry, in which the cyaphide ligand is in the axial position. The triflate counter ion is apparent from the ^{19}F NMR spectrum and appears uncoordinated; this was further supported by using $AgPF_6$ in place of TlOTf which gave identical

spectroscopic data for the complex. The $^{13}C\{^1H\}$ NMR and Infra-Red spectra provide further evidence for the retention of the cyaphide moiety, which is apparent as a resonance at δ_C 265 ppm and a stretch at 1242 cm^{-1} respectively. The identity of the 5-coordinate, $[Ru(dppe)_2(C{\equiv}P)]OTf$ (**4.1**$^+$) was ultimately confirmed by X-ray diffraction studies (see section: **4.3.2**).

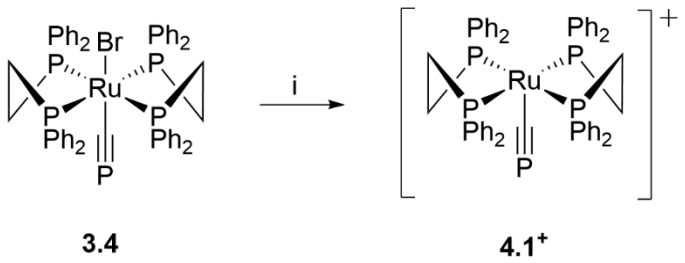

3.4 **4.1**$^+$

Scheme 4-4: *Synthesis of trans-$[Ru(C{\equiv}P)(dppe)_2]OTf$ (**4.1**$^+$). Reagents and conditions: (i) 1 eq TlOTf, DCM, 1 hour.*

With the aim of synthesising **4.1**$^+$ via a more direct method, methide abstraction from **3.3** and hydride abstraction from *trans*-$[RuH(dppe)_2(C{\equiv}P)]$ were also attempted. However, treatment of **3.3** with TlOTf or *trans*-$[RuH(dppe)_2(C{\equiv}P)]$ with Ph_3CBF_4, both proved ineffective, with no evidence of formation of **4.1**$^+$. Moreover, the reaction of **3.3** with Brookhart's acid, $[H(OEt_2)][BAr^f{}_4]$, resulted in demethylation with trace levels of methane (broad singlet at 0.21 ppm; **Figure 4-1**) observed in the ^1H NMR spectrum,[146] although, no resonances associated with **4.1**$^+$ and a multitude of signals due to decomposition were also observed. Furthermore, the $^{31}P\{^1H\}$ NMR spectrum showed an intractable mixture of products and was devoid of any cyaphidic resonances**.**

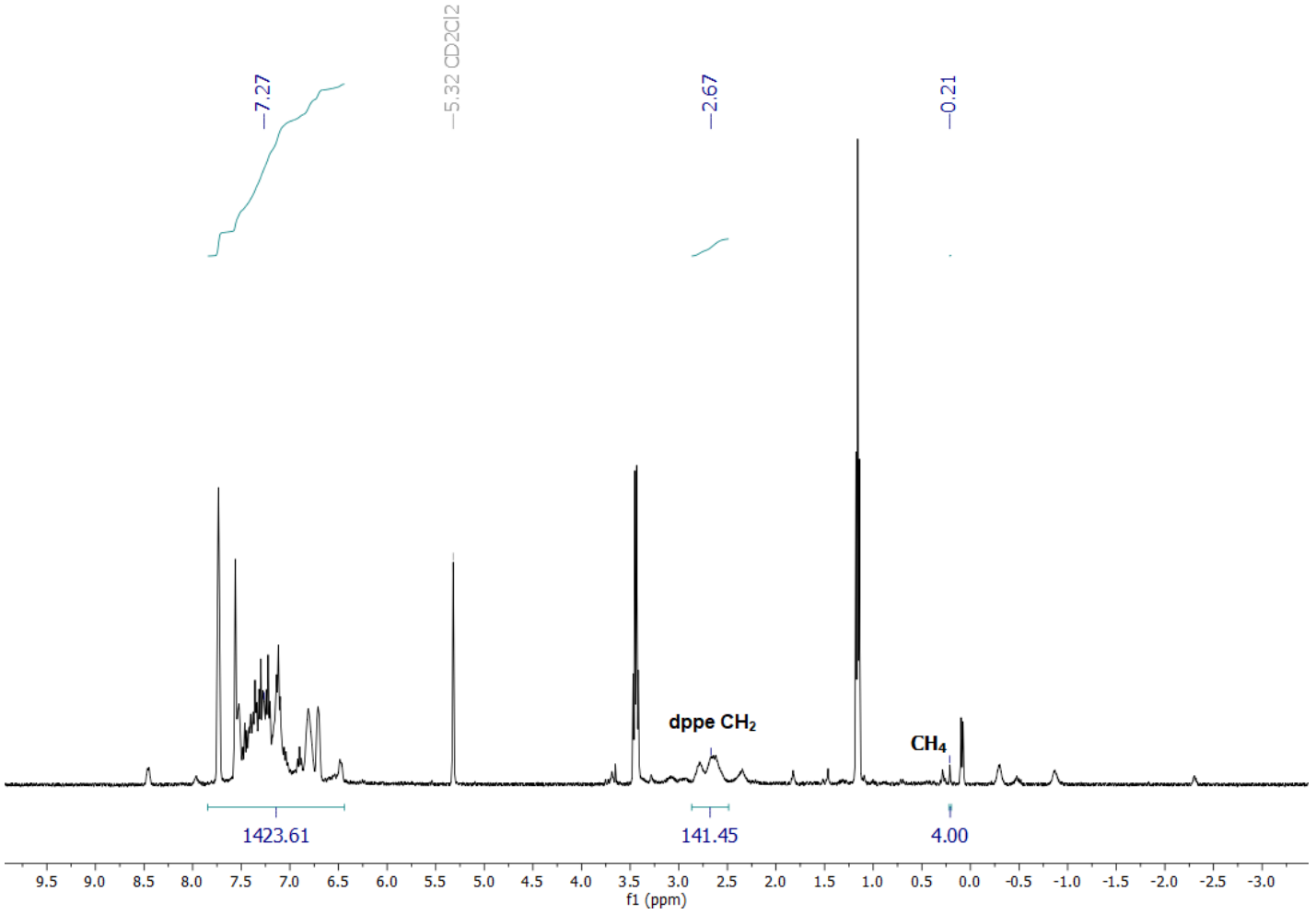

Figure 4-1: *^{1}H NMR of in situ reaction of **3.3** with $[H(OEt_2)_2][BAr^f{}_4]$ (1 equiv.) in CD_2Cl_2 for ca 72 h*

4.3.2 MOLECULAR STRUCTURE OF [Ru(dppe)$_2$(C≡P)]OTf

These data (**Figure 4-2**) confirmed that **4.1**$^+$ adopts a square-pyramidal geometry, which appears stabilised through π stacking between the dppe phenyl rings, resulting in a vacant coordination site *trans* to the cyaphide ligand. The square-pyramidal geometry has a flattened basal plane from which the mutually *trans* phosphines are displaced by ± 5.5° consistent with examples of square-pyramidal ruthenium complexes with similarly bulky ancillary ligand sets, (**4.1**$^+$, C-Ru-P, 85.84(13)°, 86.481(13)°, 94.26(12)° and 94.88(12)°) [*cf*. ([RuH(dppe)$_2$]BPh$_4$, H-Ru-P 85° and 94°) and ([RuCl$_2$(P(C$_6$H$_4$-CH$_3$)$_3$], P-Ru-Cl 108.48(3)°, 94.29(3)° and P-Ru-P 99.21(3)°, 102.36(3)°)].[147,148]

There are no direct comparators of ruthenium or any other group 8 or 9 metal with either ethynyl or cyanide ligands in the apical site of a square base pyramid, with only a few examples where the alkynyl or cyano ligand adopts a basal coordination site.[149,150,159,151–158] Thus, the most closely related comparator to **4.1**$^+$ is Grützmacher's cyaphide complex *trans*-[RuH(dppe)$_2$(C≡P)], in which the hydride ligand imparts minimal steric perturbation.[27] Indeed, **4.1**$^+$ and *trans*-[RuH(dppe)$_2$(C≡P)] exhibit almost identical C≡P bond lengths (1.573(4) Å vs 1.573(2) Å), although the Ru-CP linkage is considerably shorter in **4.1**$^+$ (1.904(4) Å vs 2.057(2) Å), which can be explained by the lack of hydridic *trans*-influence strengthening the Ru-CP bond.

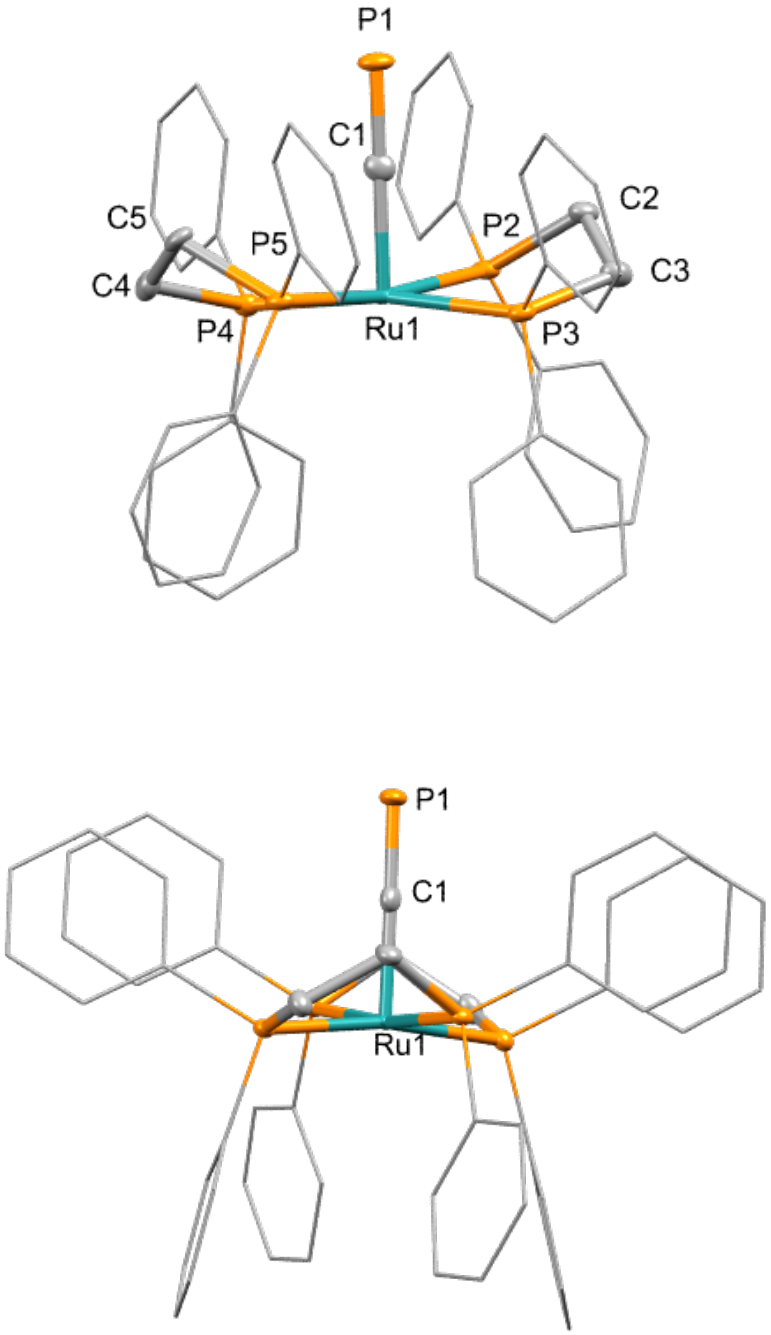

Figure 4-2: *Solid state molecular structure of* ***4.1***$^{+}$*. Hydrogen atoms and triflate counterion omitted and dppe ligands reduced for clarity, thermal ellipsoids at 50% probability level. Within the lower projection (illustrating π stacking between the dppe ligands), C2/C5 appear to be superimposed onto the Ru1− C1 bond. Selected bond lengths (Å) and angles (°): P1−C1 1.573(4), C1−Ru1 1.904(4), Ru1−P2 2.363(1), Ru1−P3 2.380(1), Ru1−P4 2.379(1), Ru1−P5 2.351(1); P1−C1−Ru1 178.9(2), P2− Ru1−P3 81.31(3), P2−Ru1−P4 99.16(4), P3−Ru1−P5 99.91(4), P4−Ru1−P5 80.86(3), C1−Ru1−P2 86.48(13), C1−Ru1−P3 94.26(12), C1−Ru1−P4 94.88(12), C1−Ru1−P5 85.84(13).*

4.4 REACTIVITY OF 4.1

The 5-coordinate cyaphide complex, **4.1**$^{+}$ is an obvious candidate for nucleophilic addition to access novel complexes, including many that have previously defied synthesis through more classical routes. Indeed, the 5-coordinate cyaphide **4.1**$^{+}$ was reacted with a range of nucleophiles resulting in the synthesis of novel cyaphide complexes **4.2**$^{+}$-**4.10**$^{+}$ (**Scheme 4-5**).

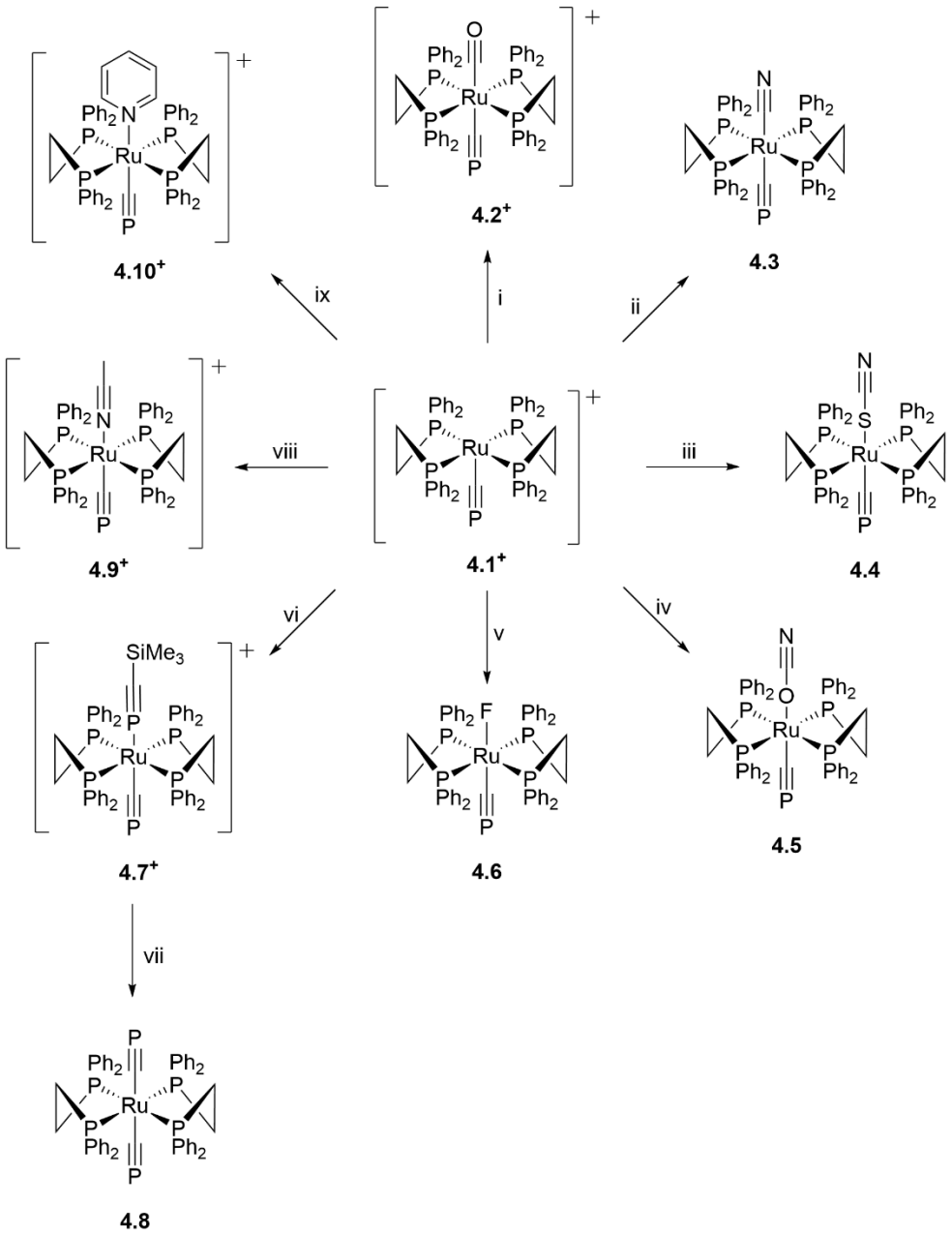

Scheme 4-5: *Synthesis of* ***4.2***$^{+}$ *to* ***4.10***$^{+}$*. Reagents and Conditions: (i) CO, DCM, 2 mins (ii) NaCN, THF, 18h (iii) KSCN, DCM, 18 h (iv) KOCN, DCM, 18 h (v) CsF, DCM, 1h (vi) Excess Me_3SiCP, 1,4-Dioxane, 1h (vii) 1.3 eq. NaOPh, THF, -30°C, 1-5 mins (viii) Acetonitrile, 1h (ix) Pyridine, 18h.*

4.4.1 SYNTHESES AND CHARACTERISATION OF REACTIVITY PRODUCTS

The addition of CO to **4.1**$^+$ to yield *trans*-[Ru(C≡O)(dppe)$_2$(C≡P)]OTf (**4.2**$^+$) was chosen as an initial target as the *trans*-carbonyl serves as a convenient reporter for the electronic character of the cyaphide ligand; such complexes have previously been inaccessible, due to difficulties in the installation of the η^1-P≡CSiMe$_3$ *trans* to the carbonyl ligand. However, bubbling CO through a DCM solution of **4.1**$^+$ effects an instantaneous colour change from purple to yellow; subsequent removal of volatiles under reduced pressure yields **4.2**$^+$ as a pale-yellow solid. The $^{31}P\{^1H\}$ NMR spectrum exhibited a quintet at 181 ppm and a doublet at 43.6 ppm with a mutual coupling of 10 Hz and the $^{13}C\{^1H\}$ NMR spectrum showed a broad multiplet at 249 ppm for the cyaphide moiety and a quintet at 200.5 ppm (J_{CP} = 10 Hz, 4 Hz) for the carbonyl. Both the cyaphide and carbonyl are also apparent in the IR spectrum at ν_{CP} 1261 cm^{-1} and ν_{CO} 1980 cm^{-1} respectively. The carbonyl stretch of **4.2**$^+$ is comparable to the limited range of *trans*-[Ru(dppe)$_2$(CO)(C≡CR)] (ν_{CO} 1977-1984 cm^{-1}) and to more general ruthenium(II) alkynylcarbonyl complexes, consistent with the alkynyl-like character of the cyaphide moiety. The cyaphide stretching frequency (ν_{CP} 1261 cm^{-1}) is higher than previously reported cyaphides, suggestive of a stronger C≡P bond which is consistent with a reduction in $\pi_{Ru} \rightarrow \pi^*_{CP}$ contribution as a consequence of competitive back-bonding to the more potently π-acidic *trans*- carbonyl ligand.

The 5-coordinate cyaphide **4.1**$^+$ also lends itself to salt metathesis reactions with sodium, potassium and caesium salts (NaCN, KSCN, KOCN and CsF) affording access to the neutral complexes, *trans*-[Ru(C≡N)(dppe)$_2$(C≡P)] **4.3**, *trans*-[Ru(SC≡N)(dppe)$_2$(C≡P)] **4.4**, *trans*-[Ru(OC≡N)(dppe)$_2$(C≡P)] **4.5** and *trans*-[RuF(dppe)$_2$(C≡P)] **4.6**. The *trans*-cyano cyaphide complex, **4.3**, exhibits the expected $^{31}P\{^1H\}$ NMR spectroscopic data with a broad quintet at 161.3 ppm and a doublet at 51.1 ppm with a mutual coupling of 5.1 Hz for the cyaphide and dppe ligands respectively. The IR spectrum confirmed the installation of the cyano ligand with a characteristic C≡N band at 2075 cm^{-1} comparable to *trans*-[RuCl(C≡N)(dppe)$_2$] (ν_{CN} 2068 cm^{-1})[160] and a C≡P stretch at 1245 cm^{-1}. The reactions of **4.1**$^+$ with KSCN and KOCN to yield **4.4** and

4.5, both result in $^{31}P\{^{1}H\}$ NMR spectroscopic data consistent with successful reaction; broad multiplets at 148 ppm (**4.4**) and 142 ppm (**4.5**) and a doublet at 47 ppm (J_{PP} = 4.7 Hz) (**4.4** and **4.5**). For **4.5** the spectrum shows additional resonances within the baseline corresponding to **4.1**$^{+}$ and unidentified side products. However, due to poor solubility of both **4.4** and **4.5** further purification and characterisation (including carbon NMR spectroscopy and X-ray diffraction) were unable to be obtained.

The reaction of **4.1**$^{+}$ and CsF yields **4.6** which exhibits chemical shifts in line with those of the previously discussed *trans*-halo cyaphide complexes **3.4**, **3.5** and **3.6**, with the $^{31}P\{^{1}H\}$ NMR spectrum exhibiting a doublet at 45.5 ppm (J_{PP} = 15.5 Hz) and doublet of quintets at 125.6 ppm (J_{PP} = 15.5 Hz, J_{PF} = 70 Hz) for the dppe and cyaphide ligands respectively. The loss of the triflate counter ion and the presence of the *trans*-fluoride are confirmed by the ^{19}F NMR spectrum which shows only a doublet of multiplets at 400 ppm (J_{PF} = 70 Hz and 7 Hz). Within the series of *trans*-halo cyaphides a trend is observed in the shifts of cyaphide resonances in the $^{31}P\{^{1}H\}$ NMR spectra (*ca* 125.6 ppm **4.6**, 132.0 ppm **3.5**, 135.4 ppm **3.4** and 140.0 ppm **3.6**) which shows the stronger the π-donor ability of the halogen the lower the chemical shift of the resonance.

With the ability of **4.1**$^{+}$ to undergo the addition of nucleophiles as previously discussed, it was considered whether **4.1**$^{+}$ would react similarly with the lone pair of the phosphaalkyne, P≡CSiMe$_3$, to yield the mixed phosphaalkyne-cyaphide complex *trans*-[Ru(P≡CSiMe$_3$)(dppe)$_2$(C≡P)]$^{+}$ **4.7**$^{+}$, the ruthenium analogue of Russell's *in-situ* observed *trans*-[Mo(P≡CSiMe$_3$)(C≡P)(dppe)$_2$]$^{-}$.[102] Indeed, the reaction proceeded as expected, with **4.7**$^{+}$ being apparent from the $^{31}P\{^{1}H\}$ NMR spectrum, which showed a doublet of doublets at 39.5 ppm ($^{2}J_{PP}$ = 32 Hz and $^{3}J_{PP}$ = 10 Hz) and two quintets at 108 ppm ($^{2}J_{PP}$ = 32 Hz) and 154 ppm ($^{3}J_{PP}$ = 10 Hz), integrating in a 4:1:1 ratio, for the dppe, Me$_3$SiC≡P and C≡P ligands respectively, a comparable splitting pattern to that observed for *trans*-[Mo(Me$_3$SiC≡P)(C≡P)(dppe)$_2$]$^{-}$.[102] The ^{1}H NMR and the ^{1}H-^{29}Si HMBC NMR spectra confirm the presence of the silyl moiety with a resonance at δ_H

−0.13 ppm and *ca* δ_{Si} −12.5 ppm respectively. In addition, the ^{19}F NMR spectrum confirmed the triflate anion.

Unlike *trans*-[Mo(P≡CSiMe$_3$)(C≡P)(dppe)$_2$]$^-$, **4.7**$^+$ can undergo base-induced desilyative rearrangement upon the reaction with 1.3 equivalents of NaOPh to yield the *bis*-cyaphide complex *trans*-[Ru(C≡P)$_2$(dppe)$_2$] **4.8**, which was isolated in good yields. The $^{31}P\{^1H\}$ NMR spectrum showed a broad triplet at 49.6 ppm ($^3J_{PP}$ = 4.7 Hz) and a broad multiplet at 186 ppm, integrating in a 4:2 ratio, corresponding to the dppe and C≡P ligands respectively. Notably the cyaphidic resonance is at the highest chemical shift yet observed and is comparable to that seen for the *trans*-carbonyl system **4.2**$^+$. The ^1H NMR spectrum supports the loss of the silyl moiety and the IR spectrum shows the C≡P stretch at a significantly lower wavenumber compared to the previously reported cyaphide complexes at 1227 cm^{-1}. Unfortunately, due to the highly insoluble nature of **4.8** the C≡P resonance was unable to be resolved in the $^{13}C\{^1H\}$ NMR spectrum although these data did confirm the loss of the counter ion. In addition, definitive confirmation by X-ray diffraction has so far been elusive.

With the amenability of **4.1**$^+$ to coordinate to the lone pair of the phosphaalkyne, it was hypothesised that nitrogen lone pairs would also coordinate. The reaction of **4.1**$^+$ and acetonitrile yielded *trans*-[Ru(N≡CMe)(dppe)$_2$(C≡P)]$^+$ **4.9**$^+$ with the $^{31}P\{^1H\}$ NMR spectrum exhibiting a broad multiplet at 168 ppm and doublet 47.6 ppm ($^3J_{PP}$ = 5.7 Hz) integrating in a 4:1 ratio. The $^{13}C\{^1H\}$ NMR spectrum confirmed the coordination of the acetonitrile with a C≡N resonance at 125 ppm and the C≡P resonance at 258 ppm.

Other nitrogen donors, 4,4′-bipyridine and pyridine were reacted with **4.1**$^+$, with the latter resulting in successful coordination yielding *trans*-[Ru(NC$_5$H$_5$)(dppe)$_2$(C≡P)]$^+$ **4.10**$^+$. The $^{31}P\{^1H\}$ NMR spectrum showed the cyaphidic resonance at 161 ppm (J_{PP} = 5 Hz) with the corresponding dppe resonance at 50 ppm; also present are unidentified singlet resonances at 72 ppm, 49 ppm

and -9.5 ppm. The reaction of **4.1**$^{+}$ and 4,4′-bipyridine was also tested however no reaction was observed.

Overall, the spectroscopic data for **3.4-3.6** and **4.2**$^{+}$**-4.10**$^{+}$ reveal a general trend in the chemical shift within the cyaphide moiety that correlate to the donor/acceptor capacity of the *trans*-ligand (**Table 4-2**). The more π-acidic in nature of the *trans*-ligand the higher the chemical shift of the cyaphide resonance within the $^{31}P\{^{1}H\}$ NMR spectra, ranging over 60 ppm with *trans*-CO complex **4.2**$^{+}$ exhibiting the highest chemical shift (*ca* 181 ppm) and the *trans*-fluoride cyaphide complex, **4.6** exhibiting the lowest shift (*ca* 125.6 ppm). Notably, the *bis*-cyaphide complex **4.8** exhibits a slightly higher chemical shift (*ca* 186 ppm) but serves as a poor comparator and offers no meaningful information. This trend has been reported for the series of *trans*-alkynyl cyaphide systems with a slight increase in the chemical shift with more electron withdrawing nature of the terminal alkynyl substituent, although this is less pronounced ranging over 10 ppm.[104] In addition, for the *trans*-alkynyl cyaphide systems the opposite trend was noted in the $^{13}C\{^{1}H\}$ NMR spectra, unfortunately due to the lack of data for the full series of **3.4-3.6** and **4.2**$^{+}$**-4.10**$^{+}$ no comparison can be made. Overall, these spectroscopic data show a significant long-range influence of the *trans*-ligand upon the cyaphide moiety as was previously suggested on the basis for the *trans*-alkynyl cyaphide complexes.[104]

Trans-Substituent	Compound Number	$^{31}P\{^{1}H\}$ NMR (ppm)		$^{13}C\{^{1}H\}$ NMR (ppm)		^{19}F NMR (ppm)	IR (ν)	
		dppe ($^{3}J_{PP}$, Hz)	C≡P ($^{3}J_{PP}$, Hz)	C≡P	C≡O or C≡N	OTf/F (J_{PF}, Hz)	C≡P	C≡O or C≡N
C≡O	**4.2^{+}**	43.6 (10.0)	181.0 (10.0)	249.0	200.5		1261	1980
C≡N	**4.3**	51.1 (5.1)	161.3 (5.1)	*	-	-	1245	2075
SC≡N	**4.4**	47.0 (4.7)	148.0	*	*	-	-	-
OC≡N	**4.5**	47.0 (4.7)	142.0	*	*	-	-	-
F	**4.6**	45.5 ($^{3}J_{PP}$ = 15.5, J_{PF} = 70)	125.6 (15.5)	247.0	-	400.0 (70)	1259	-
P≡CSiMe$_3$	**4.7^{+}**	39.5 ppm ($^{2}J_{PP}$ = 32 and $^{3}J_{PP}$ = 10)	108.0 ($^{2}J_{PP}$ = 32), 154.0 ($^{3}J_{PP}$ = 10)	*	-			-
C≡P	**4.8**	49.6 ($^{3}J_{PP}$ = 4.7)	186.0	*	-	-	1227	-
N≡CMe	**4.9^{+}**	47.6 (5.7)	168.0	258.0	125.0		1255	-
NC$_5$H$_5$	**4.10^{+}**	50.0 (5.0)	161 (5.0)	-	-	-	-	-

Table 4-1: *Selected NMR and IR spectroscopic data for trans-[Ru(dppe)$_2$(C≡P)L] / trans-[Ru(dppe)$_2$(C≡P)L]$^{+}$ complexes* ***4.2^{+}-4.10^{+}****. Values marked '*' could not be assigned.*

Trans- Substituent	Compound Number	$^{31}P\{^{1}H\}$ NMR (ppm), C≡P
C≡P	**4.8**	186.0
C≡O	**4.2**$^{+}$	181.0
Me	**3.3**	177.9
C≡C-C_6H_3-3,5-CF_3	**2.3d**	172.8
C≡CCO_2Me	**1.59g**	170.2[b]
C≡C-*p*-C_6H_4-NO_2	**1.59e**	170.0[b]
C≡CCO_2Et	**1.59f**	168.3[b]
N≡CMe	**4.9**$^{+}$	168.0
C≡C-*p*-C_6H_4-CO_2Me	**1.59d**	165.3[b]
H	**1.52**	165.0[a,c]
C≡C-*p*-C_6H_4-CO_2Et	**2.3c**	164.9
C≡C-*p*-C_6H_4-F	**1.59c**	161.7[b]
C≡N	**4.3**	161.3
NC_5H_5	**4.10**$^{+}$	161.0
C≡C-C_6H_5	**1.59b**	160.6[b]
C≡C-*p*-C_6H_4-Me	**1.59a**	159.8[b]
C≡C-*p*-C_6H_4-OMe	**1.59h**	159.5[b]
C≡C^{n}Bu	**2.3a**	154.0
-	**4.1**$^{+}$	154.0
P≡C$SiMe_3$	**4.7**	108.0 and 154.0
SC≡N	**4.4**	148.0
C≡C^{t}Bu	**2.3b**	142.8
OC≡N	**4.5**	142.0
I	**3.6**	140.0
Br	**3.4**	135.4
Cl	**3.5**	132.0
F	**4.6**	125.6

Table 4-2: *Selected NMR data for cyaphide complexes, trans-[Ru(dppe)$_2$(C≡P)L], unless otherwise solutions in CD_2Cl_2 [a] Data from reference 100, [b] Data from reference 102 and 103 , [c] solutions in d8-THF.*

4.4.2 MOLECULAR STRUCTURE CHARACTERISATION OF REACTIVITY PRODUCTS

The cyaphide complexes, **4.2**$^+$, **4.3**, **4.6** and **4.9**$^+$ have been structurally characterised through X-ray diffraction of single crystals grown from either slow evaporation of concentrated solution in benzene or DCM layered with hexanes.

The structural data for **4.2**$^+$ (**Figure 4-3**) warrant caution, due to the disorder of C≡P and C≡O ligands which also differ between two independent molecules within the cell, thus are modelled across two positions and required the respective carbon atoms be modelled isotropically. In addition, **4.3** exhibits disorder of the nitrogen of the C≡N ligand which required the nitrogen to be modelled isotropically. Despite this disorder these data showed short C≡P bond lengths of 1.53(2) Å and 1.465(6) Å for **4.2**$^+$ and **4.3** respectively with the latter being significantly shorter than previously discussed *trans*-alkynyl and halo cyaphide complexes. Furthermore, both **4.2**$^+$ and **4.3** exhibit slightly elongated Ru-CP bond lengths of 2.06(2) Å and 2.047(6) Å, with the *trans*-C≡N and C≡O bond lengths, 1.331(7) Å (*cf.* 1.240(3) Å, *trans*-[RuCl(C≡N)(dppe)$_2$]) and 1.14(2) Å (*cf.* [Ru{P═CH(SiMe$_2$R)}Cl(CO)(PPh$_3$)$_2$] (R = Me 1.183(12) Å, Ph 1.143(3) Å, *p*-Tol 1.163(4) Å)) respectively.[161] Overall the relatively long Ru-CP and the truncated C≡P bond lengths along with the opposing trend for the C≡O and C≡N ligands, would generally indicate that the previously noted acceptor character of the C≡P ligand, although appreciable with respect for alkynyls, is weak compared to that of C≡O and C≡N, supporting that the C≡P ligand is more akin to the alkynyl ligand but with a slightly enhanced acceptor character.

The comparison of the X-ray diffraction data of **4.6** (**Figure 4-4**) to those of **3.4** and **3.5** show no appreciable trend with the Ru-C_{CP} and C≡P bond lengths as the *trans*- halide is swapped, with distances 1.944(3) Å and 1.584(3) Å for **4.6** (*cf.* 1.901(9) Å and 1.544(10) Å **3.4**, 1.687(16) Å and 1.638(17) Å **3.5**). In addition, the Ru-X bond length in **4.6**, 2.168(1) Å, is comparable to other Ru-F bonds (*cf.* [Ru(dppe)$_2$F$_2$] 2.1729(18) Å).[162]

The X-ray data for **4.9**$^+$ (**Figure 4-4**) showed the acetonitrile ligand is end-on coordinated with a C≡P bond length of 1.576(6) Å and a Ru-C bond length, 1.974(6) Å, comparable to the previously reported cyaphides. The data also showed a N≡C bond length of 1.137(8) Å which is near identical to that seen in free acetonitrile (1.141(2) Å)[163], *cis*-[Ru(dppm)$_2$(N≡CEt)Cl]PF$_6$ (1.13(1) Å)[164] and *trans*-[Ru(dppm)$_2$(N≡CMe)H]BF$_4$ (1.122(4) Å)[165], also shown is a Ru-N bond length of and 2.113(5) Å which is within the range for reported Ru-N bonds (1.940-2.36 Å).[166]

Comparable to that seen in the *trans*-alkynyl cyaphide complexes the linearity of the central π-systems of the series of cyaphide complexes varies depending on the *trans*- ligand. Both **4.3** and **4.9**$^+$ exhibit slight deviation from linearity with the central π-system of **4.3** having Ru-C-P (175.2(4)°), C-Ru-C (174.71(2)°) and Ru-C-N (169.1(4)°) bonds angles, and **4.9**$^+$ having C-Ru-N (174.2(2)°), P-C-Ru (174.1(4)°) and C-N-Ru (173.4(5)°) bond angles. In addition for **4.3** the Ru-C-N bonds angle, 169.1(4)°, appears significantly distorted from linearity compared to the literature cyanide complex *trans*-[RuCl(C≡N)(dppe)$_2$] (176.9(9)°).[160] In comparison **4.2**$^+$ shows very little distortion from linearity with Ru-C-P, C-Ru-C and Ru-C-O bonds angles, 176.0(13)°, 178.3(7)° and 177.8(17)°. In addition, **4.6** also exhibits a near perfect linear central π-system with Ru-C-P and F-Ru-C bond angles of 177.65(17)° and 176.12(8)° (*cf.* X-Ru-C, 177.1(2)° **3.4**, 175.1(5)° **3.5**).

The structural data for **3.4**, **3.5**, **4.2**$^+$, **4.3**, **4.6** and **4.9**$^+$ have revealed general trends in the C≡P and Ru-C bond lengths, with these being typically dependent on the π-donor/acceptor capacity of the *trans*-ligand. The structural data for **4.2** and **4.3** where the *trans* ligands C≡O and C≡N respectively, exhibit shorter C≡P bonds (*ca* **4.2** 1.53(2) Å, **4.3** 1.465(6) Å) and longer Ru-C bond lengths (*ca* **4.2** 2.06(2) Å, **4.3** 2.047(6) Å), are representive of the π-acceptor nature of these ligands. In comparison, when the *trans* ligands are more π-donating, **4.9**$^+$, **3.4**, **3.5** and **4.6** the C≡P bond lengths have been shown to be longer (*ca* **4.9**$^+$ 1.576(6) Å, **4.6** 1.584(3) Å, **3.4** 1.544(10) Å, **3.5** 1.638 (17) Å) and the Ru-C bond lengths shorter (*ca* **4.9**$^+$ 1.974(6) Å, **4.6** 1.944(3) Å, **3.4**

1.901(9)) Å, **3.5** 1.687(16) Å). Overall this trend, albeit subtle compared to that of the trend seen for the phosphorus NMR chemical shifts, aligns with the previously noted acceptor character of the C≡P ligand.[104]

	4.2$^+$	**4.3**	**4.6**	**4.9$^+$**
Ru(1)-C(1)	2.06(2)	2.047(6)	1.944(3)	1.974(6)
Ru(1)-C(2)	1.888(19)	2.091(6)	-	-
Ru(1)-N(1)	-	-	-	2.113(5)
Ru(1)-Cl(1)	-	-	-	-
Ru(1)-F(1)	-	-	2.168(1)	-
C(1)-P(1)	1.53(2)	1.465(6)	1.584(3)	1.576(6)
C(2)-O(1)	1.14(2)	-	-	-
C(2)-N(1)	-	1.331(7)	-	1.137(8)
C(2)-C(3)	-	-	-	-
C(2)-Ru(1)-C(1)	178.3(7)	174.71(19)	-	-
F(1)-Ru(1)-C(1)	-	-	176.12(8)	-
N(1)-Ru(1)-C(1)	-	-	-	174.1(2)
Ru(1)-C(1)-P(1)	176.0(13)	173.2(4)	177.65(17)	174.1(4)
Ru(1)-C(2)-O(1)	177.8(17)	-	-	-
Ru(1)-C(2)-N(1)	-	169.1(4)	-	-
Ru(1)-N(1)-C(2)	-	-	-	173.4(5)

***Table 4-3**: Selected bond lengths (Å) and angles (°) for **4.2**$^+$, **4.3**, **4.6**, **4.9**$^+$ and trans-[RuCl(C≡N)(dppe)$_2$] (Reference #128)*

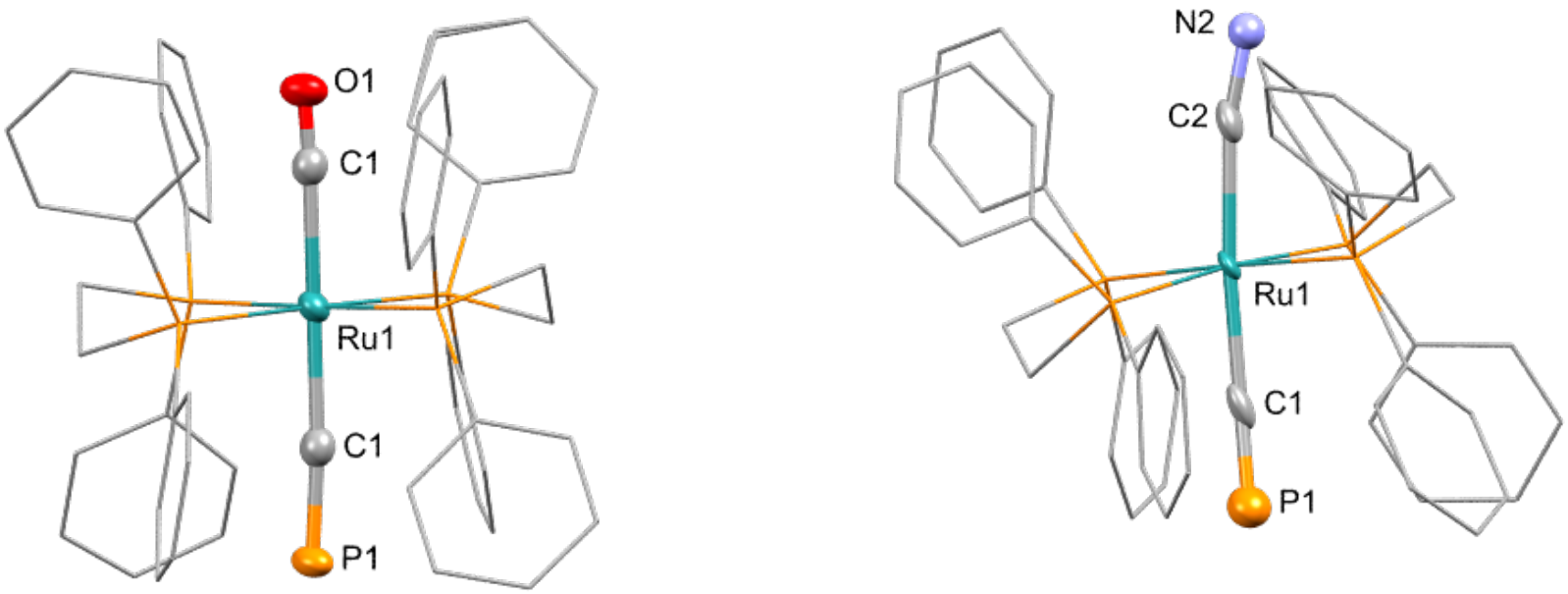

Figure 4-3: *Solid state molecular structure of* ***4.2***$^{+}$ *and* ***4.3.*** *Hydrogen atoms and triflate counterion omitted and dppe ligands reduced for clarity, thermal ellipsoids at 50% probability level. For* ***4.2***$^{+}$ *the asymmetric unit comprises two half cations with the CO and CP ligands modelled across two positions (50% occupancy); this disorder requires that the respective carbon atoms are modelled isotopically. For* ***4.3*** *disorder of the C≡N ligand requires that the respective nitrogen atom is modelled isotopically.*

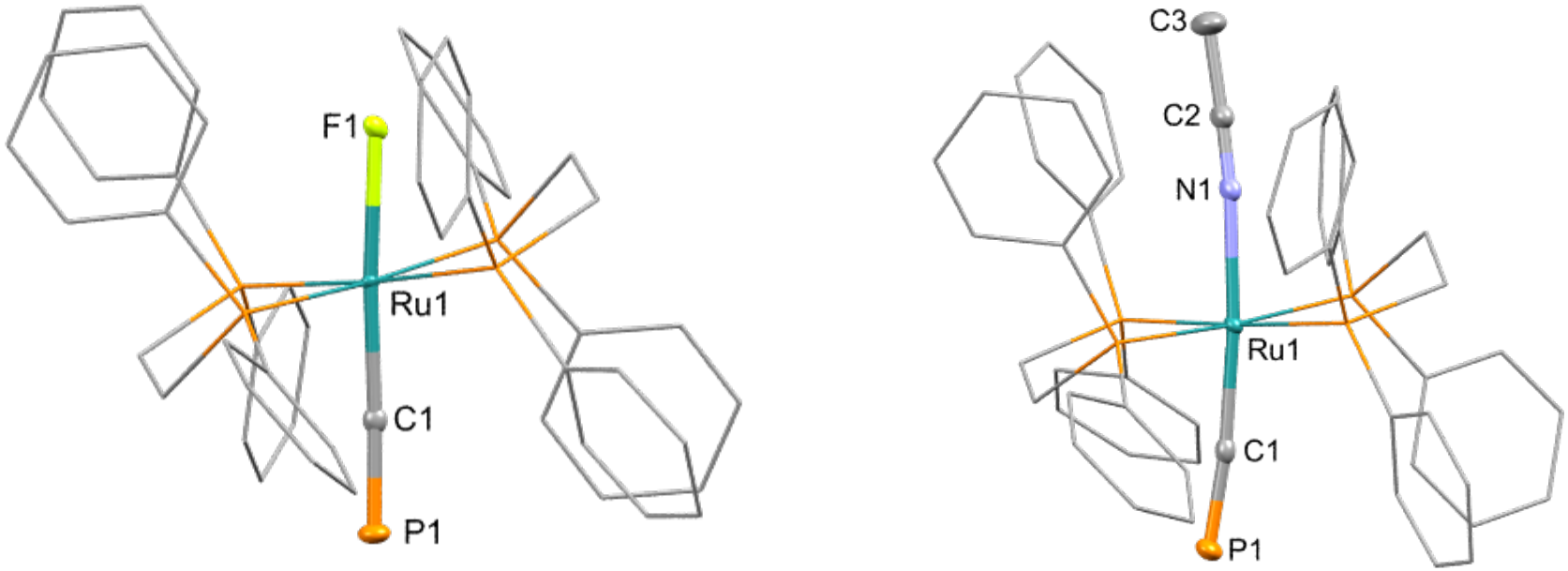

Figure 4-4: *Solid state molecular structure of* ***4.6*** *and* ***4.9***$^{+}$*. Hydrogen atoms and triflate counterion omitted and dppe ligands reduced for clarity, thermal ellipsoids at 50% probability level.*

4.5 ANCILLARY LIGAND SUBSITUTION

There are still very few reports of transition metal cyaphide complexes and all except the first example observed *in situ* by Angelici, *trans*-[Pt(PEt_3)$_2$Cl(C≡P)], are held within a sterically encumbered coordination sphere.[99] This steric encumbrance allows for formation of the parent η^1-phosphalkyne complex and seems to direct the desilylative rearrangement to form the cyaphide. However, having increased steric bulk around the cyaphide moiety not only restricts the reactivity of the π-system and phosphorus lone pair but also limits the type of complexes where cyaphide ligand can be used. Therefore, to engage the true reactivity and the scope of cyaphide complexes the steric encumbrance needs to be reduced, thus it was sought to displace the dppe ancillary ligands with less sterically encumbering ligands.

4.5.1 TRIMETHYLPHOSPHINE

The reaction between DCM solutions of [Ru(dppe)$_2$(C≡P)]$^+$ **4.1$^+$** and PMe_3 was studied with a range of stoichiometries. The initial reaction of **4.1$^+$** with PMe_3 in a 1:1 ratio in CD_2Cl_2 in a J-Young NMR tube, resulted in a colour change from purple to a pale yellow over a period of 1 hour. The initial spectroscopic data (**Figure 4-5**) showed only **4.1$^+$** and free PMe_3, however, after 18 h the $^{31}P\{^1H\}$ NMR spectrum exhibited three broad multiplets at 153.9 ppm, 153.7 ppm and 144.5 ppm, integrating roughly in a 0.5:0.5:0.5 ratio, which are consistent with cyaphidic resonances. Furthermore, a doublet at 53 ppm and two doublets of multiplets at 48 ppm and −20 ppm were observed, integrating roughly in a 2:2:2 ratio, with the more complex pattens sharing a mutual coupling of 210 Hz. Also present are two independent peaks, a quartet at −28 ppm (J = 30 Hz) and quintet at −35 ppm (J = 23 Hz) both integrating to 1 respectively, which are associated with two other PMe_3 environments. In addition, a singlet at −13 ppm is observed which is associated with free dppe. Overall, these data are suggestive of successful coordination of the PMe_3, albeit resulting in multiple products, with the two doublets of multiplets alongside the presence of

free dppe being indicative of coordination of two PMe_3 groups and the displacement of one of the dppe ligands yielding $[Ru(PMe_3)_2(dppe)(C{\equiv}P)]^+$ (**4.12**$^+$). Furthermore, the multiplets at −28 ppm or −35 ppm both seem consistent with a PMe_3 group *trans*- to the cyaphide moiety and the formation of $[Ru(PMe_3)_3(dppe)(C{\equiv}P)]^+$ (**4.13**$^+$). However, the resonances do not integrate consistently against any individual cyaphide signal, which may reflect subtle isomeric differences, though data are inconclusive.

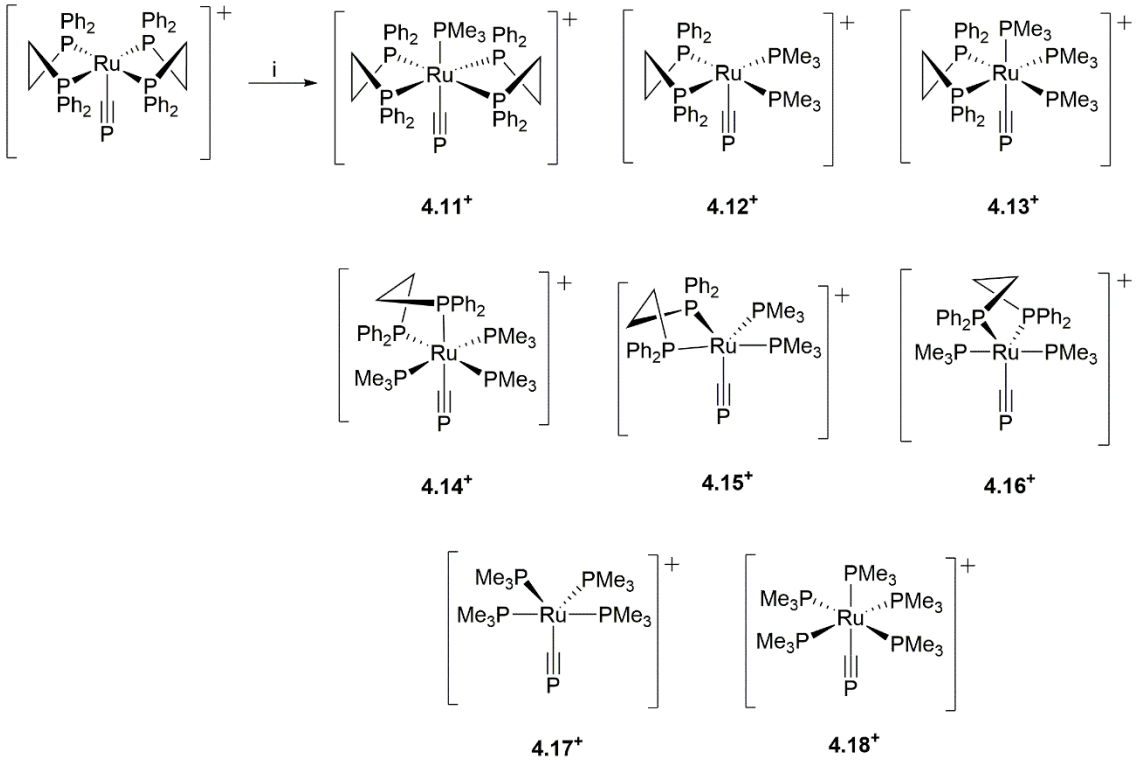

Scheme 4-6: *Possible products of the reaction of* ***4.1***$^+$ *and* PMe_3*: [Ru(*PMe_3*)$_{1+x}$(dppe)$_{2-x}$(C≡P)]OTf (where x = 0, 2 or 4) (****4.11***$^+$*-****4.18***$^+$*). Reagents and Conditions:* ***4.1***$^+$*, DCM,* PMe_3 *(Varying the equivalents), RT, 18 h.*

The reaction of **4.1**$^+$ and three equivalents of PMe_3 gave the same set of resonances in the $^{31}P\{^1H\}$ NMR spectrum associated with the products $[Ru(PMe_3)_2(dppe)(C{\equiv}P)]^+$ (**4.12**$^+$) and $[Ru(PMe_3)_3(dppe)(C{\equiv}P)]^+$ (**4.13**$^+$) (**Figure 4-6**). Also present are multiple new resonances; singlets at 31 ppm and 30 ppm, a doublet at −12 ppm and a doublet of doublets at −17 ppm, although the identity of these have not been assigned, furthermore, the ^1H NMR spectrum confirmed the presence of multiple methyl groups.

To drive the reaction to completion, **4.1**$^{+}$ was reacted with excess PMe_3. The $^{31}P\{^{1}H\}$ NMR spectrum (**Figure 4-7**) showed a broad singlet at 112 ppm and two sets of doublets of multiplets at 39 ppm and −10 ppm, integrating in a 1:2:2 ratio, which appear to be associated with the cyaphide, dppe and PMe_3 ligands respectively. In addition, three singlets at 37 ppm, 34 ppm and 24 ppm are also present integrating 0.5:0.8:0.2 respectively, with a singlet at −13 ppm, integrating to 2 associated with free dppe. The ^{1}H NMR showed the presence of coordinating dppe and multiple methyl groups. Overall, these data are consistent with the loss of one dppe ligand, and broadly consistent with the formation of **4.12**$^{+}$, $[Ru(PMe_3)_2(dppe)(C{\equiv}P)]OTf$, however, the significant shift in the resonances compared to the initial reaction (**4.1**$^{+}$ and 1 equivalent of PMe_3), for which **4.12**$^{+}$ was believed to be the major product, raises the question whether the triflate counter ion coordinates in the vacant site. Furthermore, the cyaphide resonance is at a significantly lower frequency than any previously reported and discussed examples, which could suggest alterations within the cyaphide moiety.

Furthermore, **4.1**$^{+}$ was reacted in neat PMe_3 which was filtered and followed by subsequent washing with benzene to remove any excess PMe_3, before drying under reduced pressure resulting in a cream solid. This resulted in full consumption of **4.1**$^{+}$ with the $^{31}P\{^{1}H\}$ NMR spectrum (**Figure 4-8**) showing multiple resonances including those previously seen; 153.7 ppm (*br m*), 144.3 ppm (*br m*), 48 ppm (*dm*), −20 ppm (*dm*), −28 ppm (*q*) and −35 ppm (*quint*). In addition to these, two singlets at 51 ppm and 37 ppm, a doublet of multiplets at 25 ppm and a multiplet of multiplets at 20 ppm are also observed. Additionally, the ^{1}H NMR spectrum confirmed the presence of multiple methyl groups. Overall, these data suggest the formation of multiple products. Despite all these reactions resulting in multiple products further characterisation was undertaken on the cream solid isolated from the reaction of **4.1**$^{+}$ and neat PMe_3. The ^{19}F NMR showed the triflate counter ion still present and the IR spectra of the product showed the C≡P stretch at 1260 cm^{-1} comparable to previous cyaphides discussed.

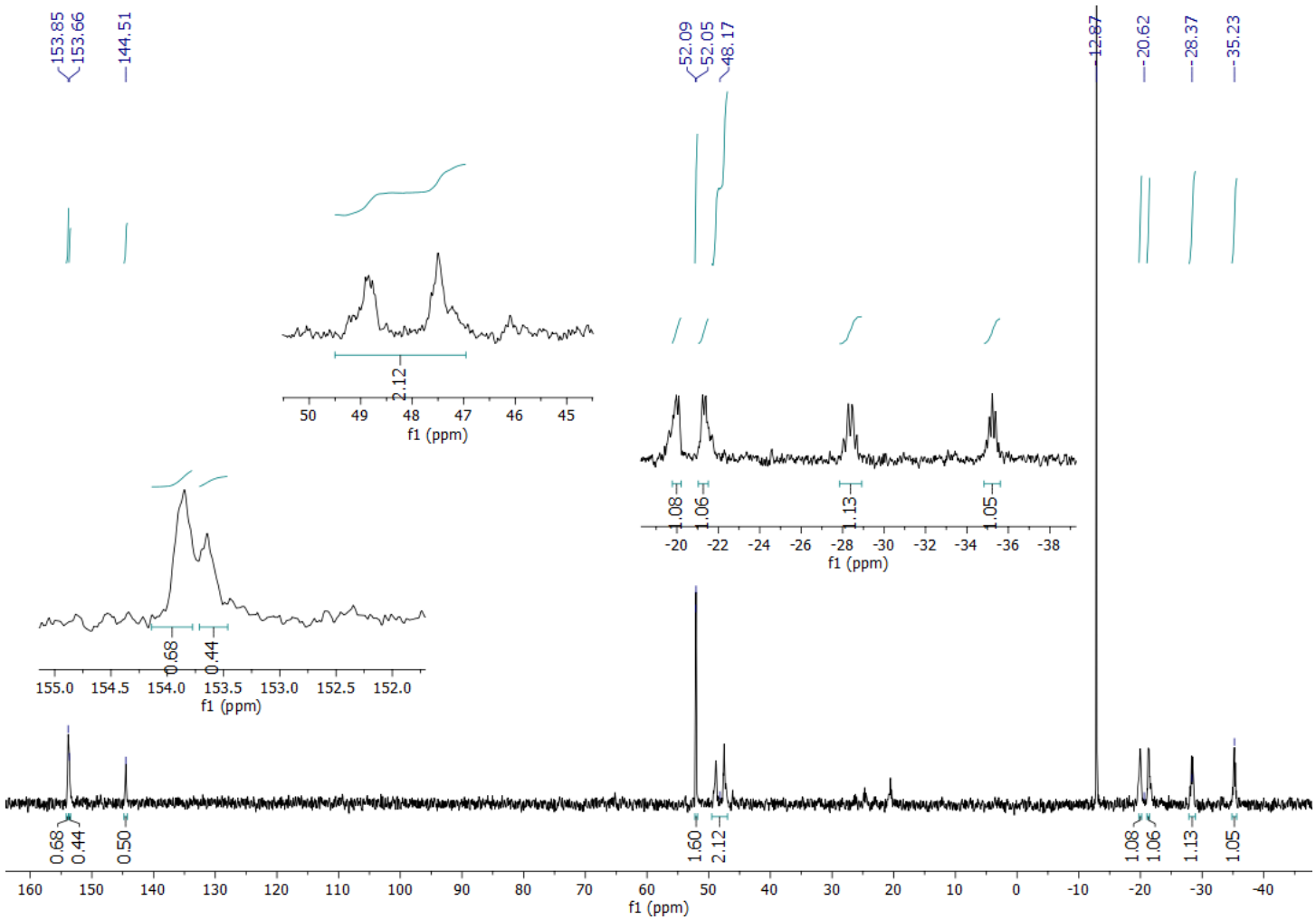

Figure 4-5: *The $^{31}P\{^{1}H\}$ NMR spectrum for the reaction of* ***4.1***$^{+}$ *and 1 eq. of* PMe_3 *in* CD_2Cl_2.

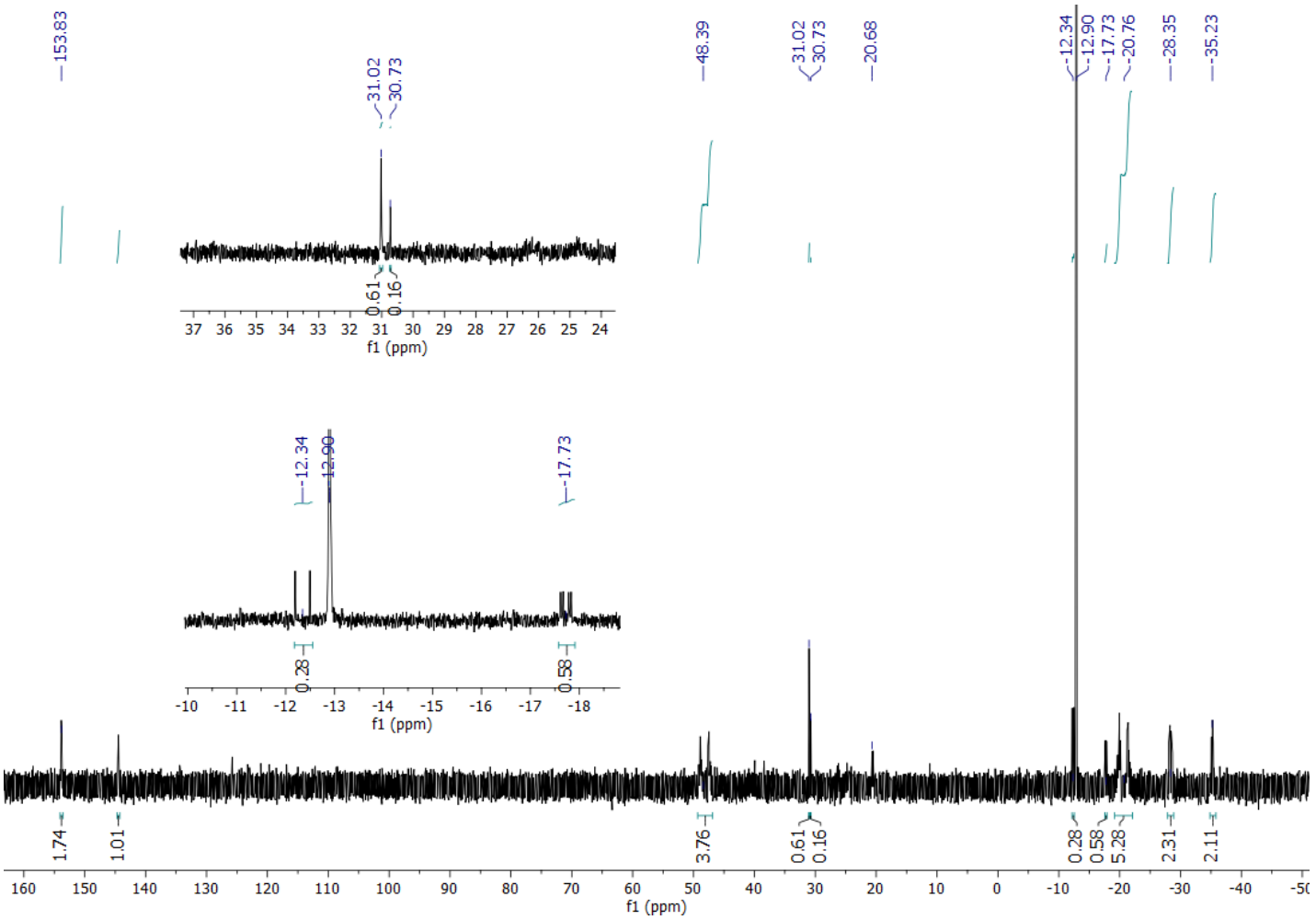

Figure 4-6: *The $^{31}P\{^{1}H\}$ NMR spectrum for the reaction of* ***4.1***$^{+}$ *and 3 eq. of* PMe_3 *in* CD_2Cl_2.

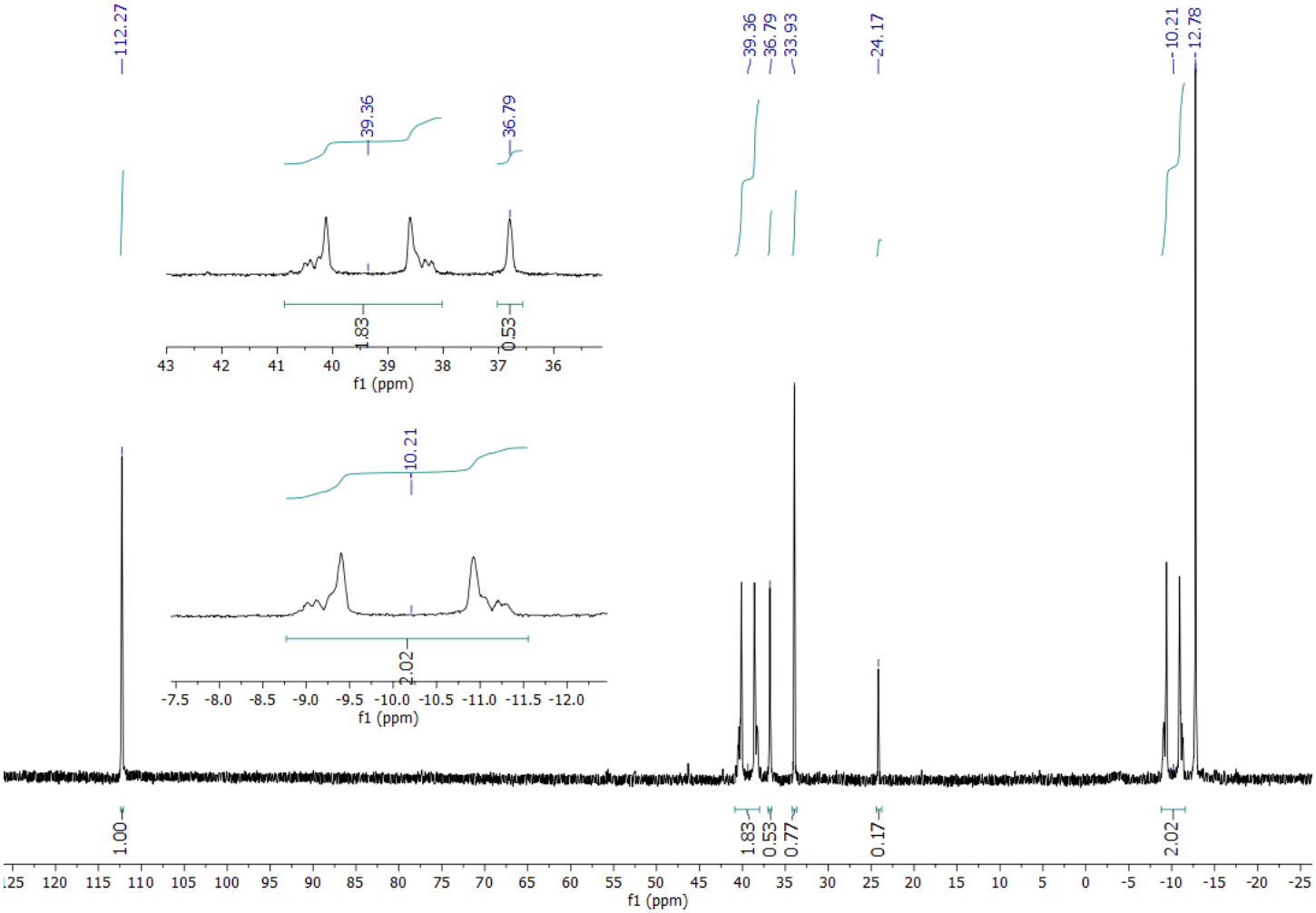

***Figure 4-7**: The $^{31}P\{^{1}H\}$ NMR spectrum for the reaction of **4.1**$^{+}$ and excess of PMe_3 in CD_2Cl_2.*

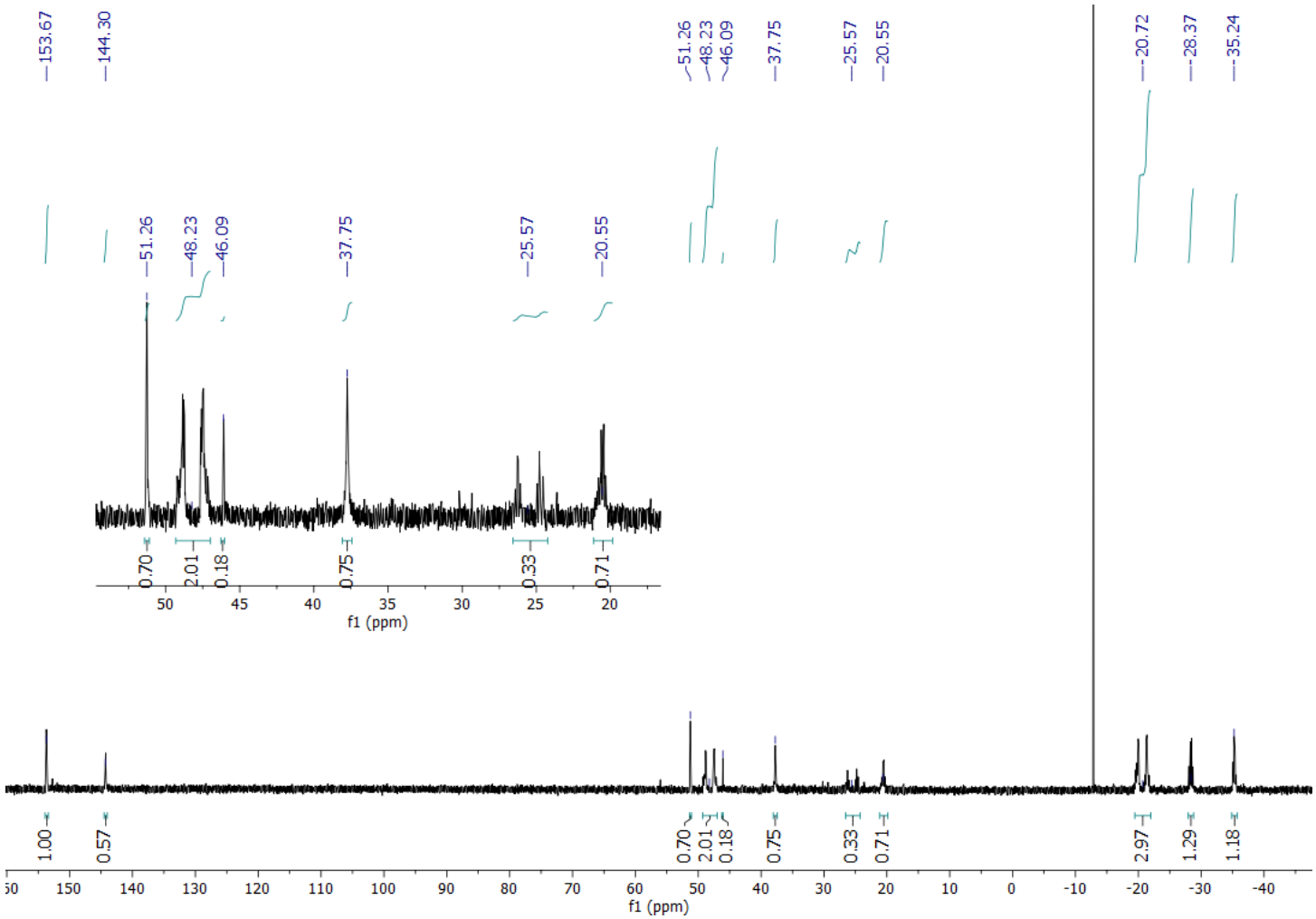

Figure 4-8: *The $^{31}P\{^{1}H\}$ NMR spectrum for the reaction of* ***4.1***$^{+}$ *and excess* PMe_3 *neat.*

Overall, the spectroscopic data showed no evidence for the formation of many of the possible products (**4.11**$^+$, **4.14**$^+$, **4.16**$^+$, **4.17**$^+$ and **4.18**$^+$) with limited evidence for the formation of **4.12**$^+$, **4.13**$^+$ and **4.15**$^+$ with the formation of **4.12**$^+$ seeming the most favourable. However, it is unclear whether the vacant coordination site of **4.12**$^+$ is occupied by the OTf counter ion or not. Despite the uncertainty in the identity of the product the X-ray diffraction data for crystals grown from slow evaporation of the reaction mixture of 3 equivalents of PMe_3 (**Figure 4-9**) showed the formation of **4.14**$^+$, where the C≡P ligand is sitting *trans* to one of the dppe phosphines and the three PMe_3 ligands are sitting in the equatorial positions alongside the other dppe phosphine. The geometry of the phosphine ligands might reflect the π-acceptor character of the cyaphide moiety preferring the increased electron density of the dx^2-y^2 orbital achieved by the three PMe_3 donors lying in the equatorial plane. These data show **4.14**$^+$ exhibits a C≡P bond length of 1.548(10) Å with a Ru-CCP bond length of 2.030(10) Å comparable to previously discussed cyaphides.

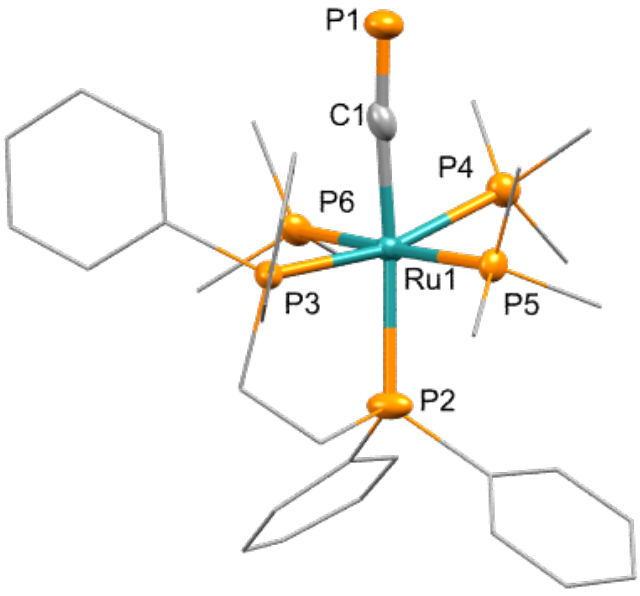

Figure 4-9: *Solid state molecular structure of* ***4.14***$^+$***.*** *Hydrogen atoms and triflate counterion omitted and dppe ligands reduced for clarity, thermal ellipsoids at 50% probability level. Selected bond lengths (Å) and angles (°): Ru1-C1 (2.030(10)), C1-P1 (1.548(10)), Ru1-P2 (2.446(2)), Ru1-P3 (2.372(2)), Ru1-P4 (2.415(3)), Ru1-P5 (2.409(2)), Ru1-P6 (2.406(2)), C1-Ru-P2 (171.4(3)), P1-C1-Ru (175.0(6))*

4.5.2 IN PURSUIT OF CYCLOPENTADIENYL DERIVATIVES AND UNEXPECTED REDUCTION CHEMISTRY

Given the prevalence of complexes of the type MCp(dppe)((C≡C)$_n$R')) in molecular wire chemistry,[90,106,107,167–172] compounds of the type RuCp(dppe)(C≡P) are particularly attractive targets and have been recently sought by the Crossley group, however, the synthesis of such complexes via established routes has proven unsuccessful. Thus, due to the reaction of **4.1**$^+$ with PMe_3 resulting in the displacement of the dppe ligands, it was postulated that **4.1**$^+$ could be a convenient starting point to synthesise RuCp'(dppe)(C≡P) (Cp' = Cp and Cp*).

The reaction between **4.1**$^+$ and potassium pentamethylcyclopentadienide for 18 h at room temperature, resulted in no reaction. However, the reaction of **4.1**$^+$ and lithium cyclopentadienide in deuterated benzene resulted in new resonances in the $^{31}P\{^1H\}$ NMR spectrum at 140 ppm and 50.9 ppm for the cyaphide moiety and dppe ligands which integrate in a 1:4 ratio. In addition, two broad multiplets at 141 ppm (*dm*) and 134 ppm (*m*), integrating in a 0.7:0.4 ratio, alongside these there are multiple resonances in the range of 40-88 ppm that have multiplicity in line with that seen in trigonal bipyramidal ruthenium complexes, however, the identity of these resonance have been unable to be confirmed, although some are likely to be attributed to decomposition.[173,174] The ^1H NMR spectrum shows no LiCp present, although alongside multitude resonances, there is a new singlet at 4.82 ppm which is consistent with a coordinated Cp ligand. Crystals were sought to aid identification, however, the X-ray diffraction of the crystals grown yielded an unexpected product [(Ru(dppe)$_2$)$_2$(CPPC)] (**4.19**) (**Figure 4-10**).

These data showed **4.19** (**Table 4-4**) is a dimer with a central Ru-C-P-P-C-Ru chain. Also shown is a change from the square pyramidal structure of **4.1**$^+$ to a trigonal bipyramidal geometry, comparable to that of [RuCl(dppe)$_2$]OTf. These data also show shortened Ru-C1 and extended C1-P1 bond lengths of 1.864(9) Å and 1.678(9) Å (*ca* **4.1**$^+$ Ru-C1 1.904(4) Å and C1-P1 1.573(4) Å), the latter being comparable to a P=C double bond, as observed in phosphaalkenes (*cf.* η^5-

$(C_5Me_5)(CO)_2FeP=C(SiMe_3)Ph$ 1.665(6) Å and η^5-$(C_5Me_5)(CO)_2FeP=C(SiMe_3)_2$ 1.680(9) Å).[175–177] These data alongside a P1-P1 bond length of 2.281(4) Å are comparable to those seen in carbene stabilized diphosphorus compounds (*cf.* L:P-P:L, L = :C{N(2,4,6-$Me_3C_6H_2$)-CH}$_2$, C1-P1 1.754(3) Å and P1-P1 2.1897(11) Å).[178] In addition, the P1-P1 bond length is only slightly longer than that of tetrahedral P_4 (*ca* 2.21 Å).[179] Furthermore the shortened Ru-C1 bond length (1.864(9) Å) is in line with that observed in ruthenium Fischer type carbene complexes (*cf*. $[RuCl_2(PPh_3)_2(=C(H)Ph)]$ 1.833(4) Å,[180] $[RuCl_2(=C(H)SC_6H_4Me\text{-}p)(PCy_3)_2]$ 1.826(6) Å,[181] $[RuCl_2(=C(H)SePh)(PCy_3)_2]$ 1.825(3) Å [181]); overall, these data are consistent with a Ru=C=P-P=C=Ru bridging unit.

Selected bond lengths (Å) and angles (°) for **4.16**

Ru1-C1	1.864(9)	**C1-Ru1-P2**	90.8(3)
C1-P1	1.678(9)	**C1-Ru1-P3**	137.7(3)
P1-P1	2.281(4)	**C1-Ru1-P4**	88.2(3)
Ru-C1-P1	175.4(6)	**C1-Ru1-P5**	122.4(3)
C1-P1-P1	103.9(4)	**P2-Ru-P4**	177.23(9)
P3-Ru-P5	99.88(9)	**P3-Ru-P2**	81.73(9)
P5-Ru-P4	83.63(9)	**P5-Ru-P2**	99.09(9)

Table 4-4**: Selected bond lengths (Å) and angles (°) for **4.19

More interestingly these C1-P1 and P1-P1 bond lengths 1.678(9) Å and 2.281(4) Å are comparable to those of the first example of diisophosphaethynolate ligand, OCPPCO, stabilized by two scandium centres, $[K(OEt_2)]_2$ [(nacnac)Sc(OAr)]$_2$(OCPPCO) (Ar = 2,6-^{i}Pr$_2$C$_6$H$_3$) (**Figure 4-11**), synthesised via the reductive coupling of a Sc-OCP precursor, this scandium diisophosphethynolate complex showed a P-P single bond length of 2.227(3) Å and a C-P double bond length of 1.705(4) Å.[84]

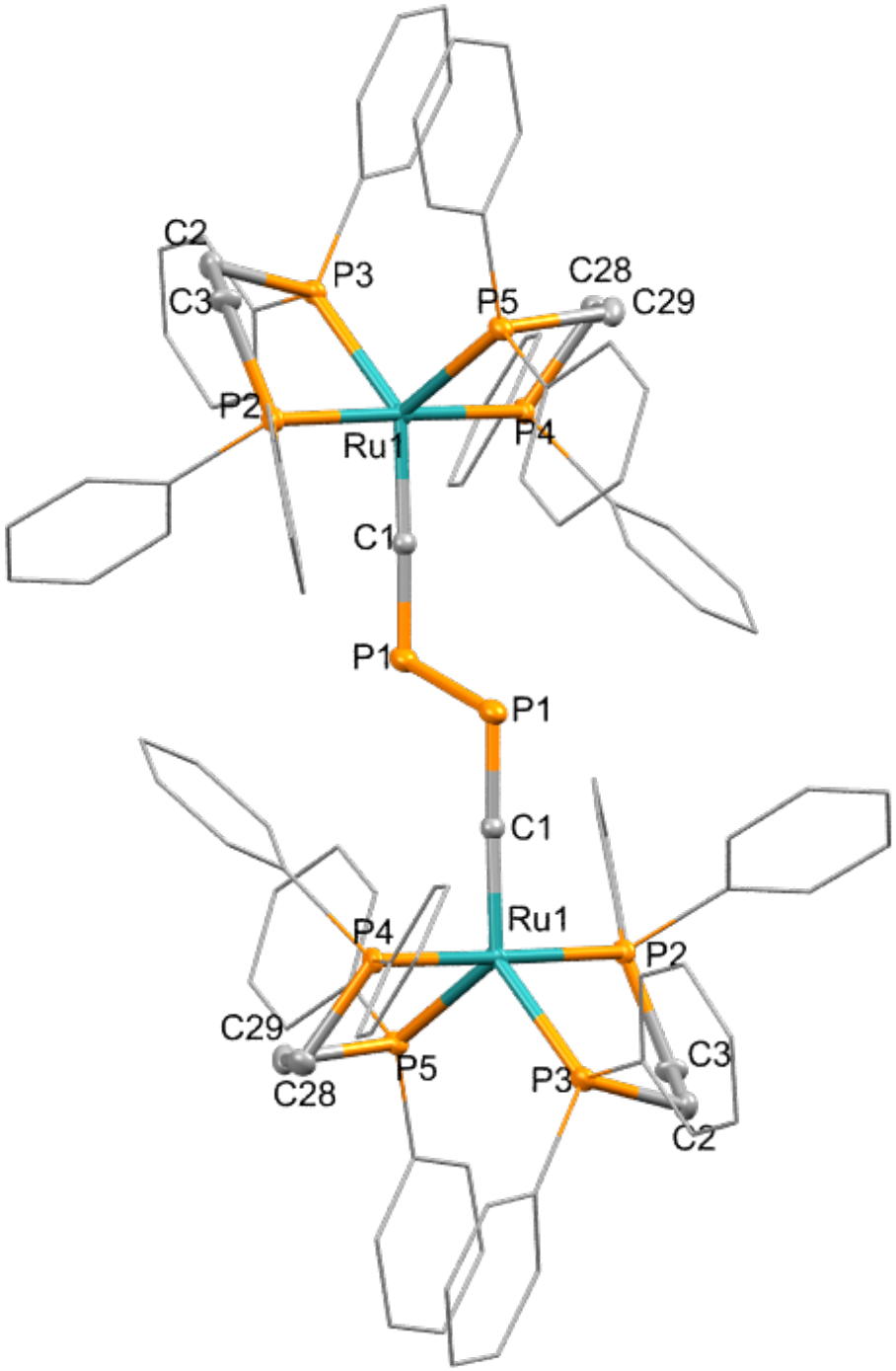

***Figure 4-10**: Solid state molecular structure of **4.19.** Hydrogen atoms and triflate counterion omitted and dppe ligands reduced for clarity, thermal ellipsoids at 50% probability level.*

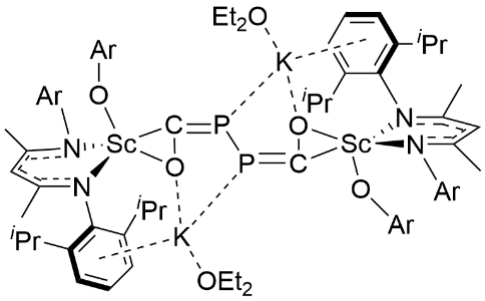

Figure 4-11: *[K(OEt$_2$)]$_2$ [(nacnac)Sc(OAr)]$_2$(OCPPCO) (Ar = 2,6-^{i}Pr$_2$C$_6$H$_3$).*[84]

The formation of **4.19** [(Ru(dppe)$_2$)$_2$(CPPC)] presumably results from the reduction of **4.1**$^+$ mediated by the Cp$^-$ anion. The use of the Cp anion as a reductant has been well documented in the preparation of both transition metal and lanthanide complexes, with excess of the anion yielding the corresponding M(II) metallocene complexes.[182–188] However, this is the first example of the reduction of a cyaphide complex and indeed reactivity of the cyaphide ligand. Therefore, selective synthesis of the reduction product was sought.

The reaction of **4.1**$^+$ with sodium naphthalenide was studied with the resulting crude ^{31}P{^{1}H} NMR spectrum exhibiting multiple new resonances including broad multiplets at 147 ppm, 136 ppm and 118 ppm and two singlets at 48 ppm and 47 ppm; also present are a multitude of peaks in the baseline. These peaks within the baseline include a doublet of doublet of multiplets at 57.9 ppm and a doublet of multiplets at −29.8 ppm, which integrate in a 1:1 ratio with a mutual coupling of *ca* 320 Hz, consistent with the *trans*- disposed phosphorus centres of a trigonal bipyramidal geometry.[173,174] Furthermore, there are two additional doublet of doublet of multiplets at 56.4 ppm and 55.6 ppm, which also integrate in a 1:1 ratio, which can be assigned to the two equatorial phosphorus centres. Overall, these baseline resonances are consistent with the formation of a trigonal bipyramidal complex and are comparable to literature ruthenium complexes (*cf* [*fac*-Ru{OC(O)CMe=CH$_2$-κ^1*O*}Cl(PPh$_3$)$_3$] δ_P 7.33 (2P), 28.35 (1P)[174]; [*fac*-Ru{OC(O)Ph$_2$-κ^1*O*}Cl(PPh$_3$)$_3$] δ_P 29.29 (2P), 50.75 (1P)[174]; [Ru(η^3-C$_3$H$_5$)(OCOCF$_3$)(PEt$_3$)$_3$] δ_P 18.2 (2P), 44.6 (1P)[173]; [Ru(η^3-C$_3$H$_5$)(OCOCF$_3$)(PMe$_3$)$_3$] δ_P −2.8 (2P), 28.7 (1P)[173]). Despite no definitive

evidence these baseline resonances integrate against the broad multiplet at 118 ppm roughly in a 4:1 ratio, consistent with a change of geometry and the possible reduction of **4.1**$^{+}$.

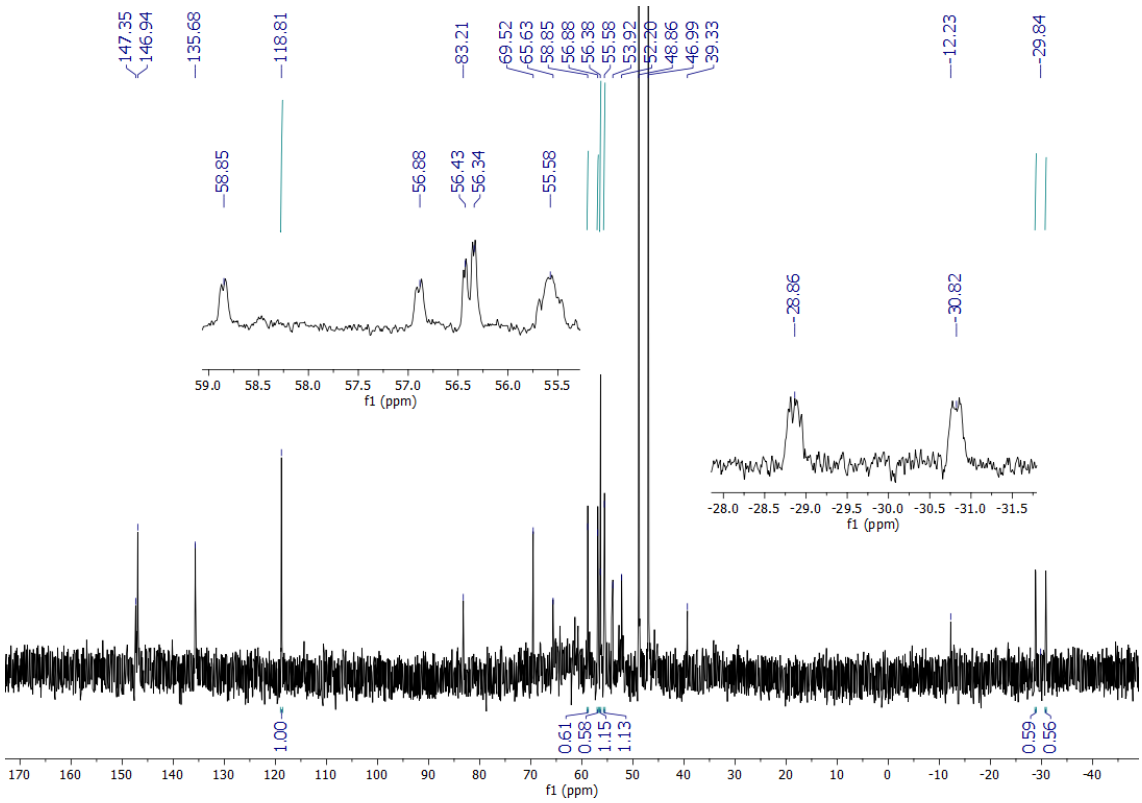

Figure 4-12: *The $^{31}P\{^{1}H\}$ NMR spectrum for the reaction of **4.1**$^{+}$ and sodium naphthalenide.*

Attempts to clean the reaction mixture up proved unsuccessful; however, slow evaporation of a benzene solution yielded crystals and the X-ray diffraction data of these confirmed the connectivity of one of the products formed from the reaction, albeit low quality data precluded detailed analysis of geometric parameters (**Figure 4-13**). Despite this these data showed two trigonal bipyramidal ruthenium centres forming a dimer with a central four membered Na_2P_2 ring (**4.20**), in which the two sodium atoms are both η^2 bound to the π-system of one of the cyaphide moieties and η^1 to the lone pair of the other cyaphide. In addition, these data show Ru-C and P-C bond lengths of 1.94(3) Å and 1.60(3) Å respectively, which is consistent with the retention of the triple bond character of the cyaphide ligand and the central Ru-C≡PNa_2P≡C-Ru

unit. Overall, although not definitive, these data could be consistent with the product seen in the baseline of the previously discussed $^{31}P\{^{1}H\}$ NMR spectrum which is in line with the trigonal-bipyramidal geometry of **4.20**.

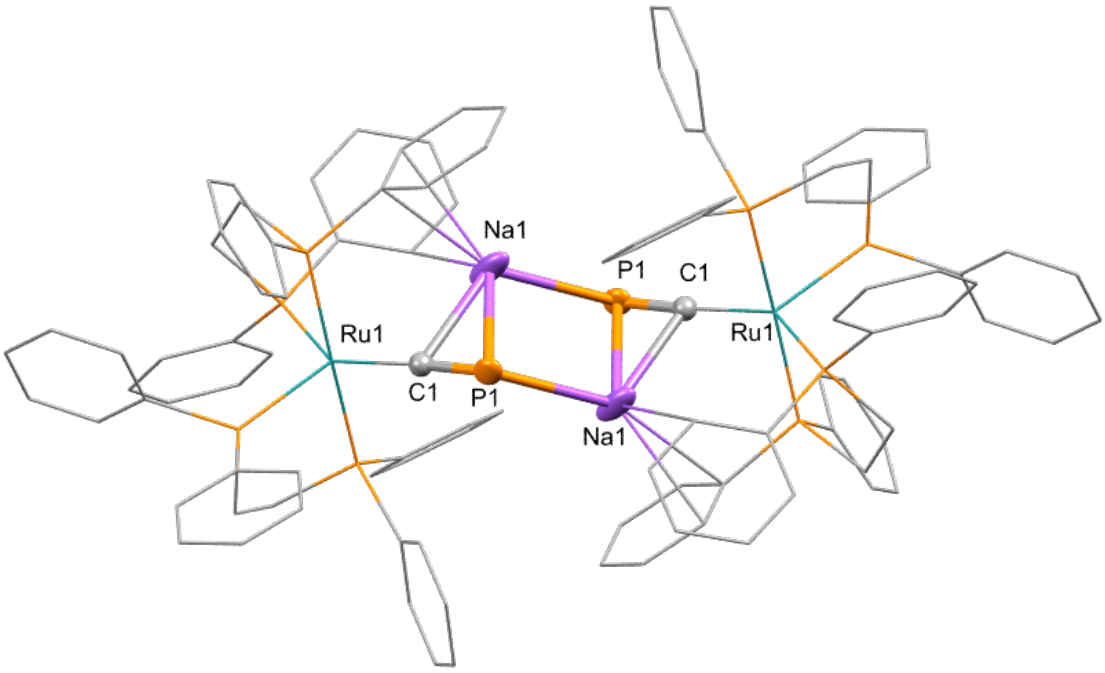

Figure 4-13: *Solid state molecular structure showing the connectivity of* ***4.20*** *Hydrogen atoms and dppe ligands reduced for clarity.*

The central Na_2P_2 ring of **4.20**, is reminiscent of the niobium phosphide sodium dimer reported by Cummings in 2004, which was synthesised by the reduction of the dinuclear bridging diphosphide complex $[(\mu^2{:}\eta^2,\eta^2\text{-}P_2)\{Nb(N[Np]Ar)_3\}_2]$ using Na/Hg (**Scheme 4-7**).[189] In view of this the reduction of **4.1**$^+$ with Na/Hg was attempted, yielding a crude $^{31}P\{^{1}H\}$ NMR spectrum that was comparable to that of the sodium naphthalenide reaction, albeit cleaner, showing multiplet resonances at 166 ppm, 146 ppm and 135 ppm and singlets at 66 ppm, 48 ppm and 47ppm. The resonances at 166 ppm and 66 ppm are attributed to the synthesis of Grützmacher's cyaphide, *trans*-$[RuH(dppe)_2(C{\equiv}P)]$, which was confirmed through the ^{1}H NMR with a hydride resonance present at −11 ppm. Also present in the ^{1}H NMR spectrum is a resonance at −6 ppm, which is associated with a second hydride complex, the identity of which is unknown. In addition, the

resonances at 146 ppm and 48 ppm have been attributed to **4.1**$^{+}$, with the slight shift due to switching solvents from CD_2Cl_2 to THF. Further experiments have yielded identical results though definitive identification remains elusive.

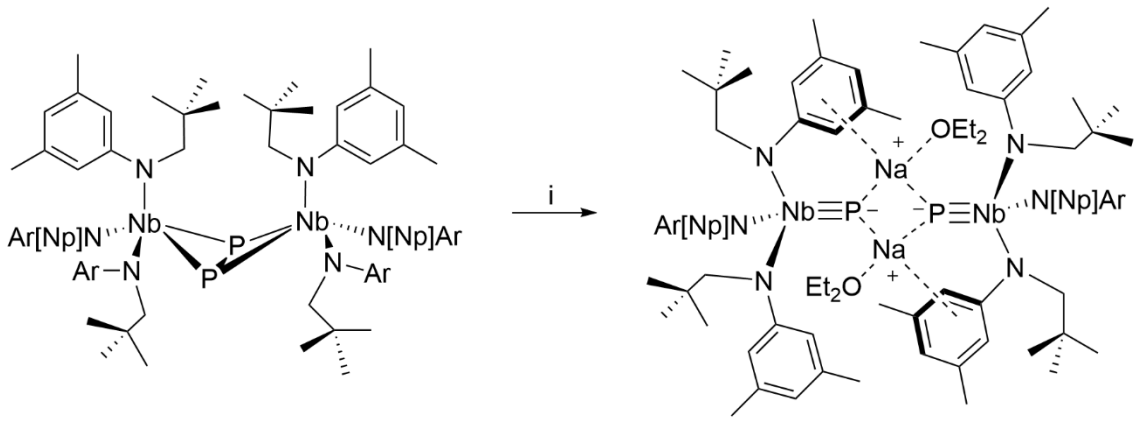

Scheme 4-7: *Reported reaction of reduction of the dinuclear bridging diphosphide complex [(μ^2:η^2,η^2-P_2){Nb(N[Np]Ar)$_3$}$_2$] using Na/Hg. Reagents and conditions: (i) Na/Hg, THF (ii) Et_2O, -35°.*[189]

4.5.3 REACTIVITY OF 4.1^{+} AND TRISPYRAZOLYLBORATE

With the continued aim to synthesise a cyaphide complex with alternative ancillary ligands, **4.1**$^{+}$ was reacted with potassium trispyrazolylborate (KTp) resulting in new resonances in the $^{31}P\{^{1}H\}$ NMR spectrum at 131 ppm as well as at 65 ppm and 46 ppm; also present is a resonance consistent with free dppe. However, the ^{1}H NMR spectrum, alongside a multitude of resonances, showed resonances consistent with the retention of the coordinated dppe ligands, in addition, no resonances were present that could be related to the trispyrazolylborate ligand. Overall, the spectroscopic evidence is suggestive of decomposition and unsuccessful binding of the trispyrazoylborate ligand; further repeats of the reaction including with the bulkier potassium tris(3,5-dimethyl-1-pyrazolyl)borate resulted in the same outcome.

4.6 CONTINUED LIGAND ADDITION TO 4.1$^+$: PRELIMINARY RESULTS

Further reactivity of **4.1**$^+$ has been studied, including the reaction of **4.1**$^+$ with trimethylsilyl acetylene with the aim to synthesise the first cyaphide complex with a *trans*- vinylidene, *trans*-[Ru(=C=CH(SiMe$_3$))(C≡P)(dppe)$_2$]OTf **4.21**$^+$ (**Scheme 4-8**). The ^{31}P{^{1}H} NMR spectrum of the reaction mixture showed a significant shift in the quintet resonance of the cyaphide to 238 ppm with the associated dppe doublet at 45 ppm, with a mutual coupling of 10 Hz. In addition, a singlet at 45.6 ppm is present although not assigned. The ^{1}H NMR showed the retention of the dppe scaffold and the presence of the trimethylsilyl group with a singlet at 0.20 ppm, furthermore, a quintet at 1.90 ppm (J ≈ 2 Hz) is observed, which is consistent with previously reported ruthenium vinylidene complexes.[125] Unfortunately, purification attempts resulted in decomposition thus further characterisation was unable to be obtained.

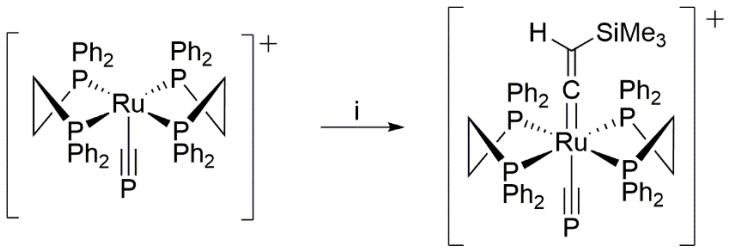

4.21$^+$

***Scheme 4-8**: Synthesis of trans-[Ru(=C=CH(SiMe$_3$))(C≡P)(dppe)$_2$]$^+$ **4.21**$^+$. Reagents and conditions: (i) trimethylsilyl acetylene, DCM, RT, 4 h.*

Previously discussed was the reaction of **3.4** with LiC≡CPh in the presence of TlOTf, resulting in the formation of *trans*-[Ru(C≡CPh)(C≡P)(dppe)$_2$], with spectroscopic data matching those known.[119] Analogous independent reactions of **4.1**$^+$ with LiC≡CSiMe$_3$ and NaC≡CH were carried out with the aim to synthesise *trans*-[Ru(C≡CSiMe$_3$)(C≡P)(dppe)$_2$] **4.22** and *trans*-[Ru(C≡CH)(C≡P)(dppe)$_2$] **4.23** respectively (**Scheme 4-9**), both of which have been sought, unsuccessfully, using other methods.[119] However, despite the success of the reaction of **4.1**$^+$ and LiC≡CPh, the reaction of **4.1**$^+$ and LiC≡CSiMe$_3$ resulted in no reaction after 18 h, while the reaction of **4.1**$^+$ and NaC≡CH resulted in the formation of an intractable mixture of products which

included resonances in the $^{31}P\{^{1}H\}$ NMR spectrum consistent with *trans*-[RuH(C≡P)(dppe)$_2$] and **3.4**. Further reaction attempts resulted in decomposition.

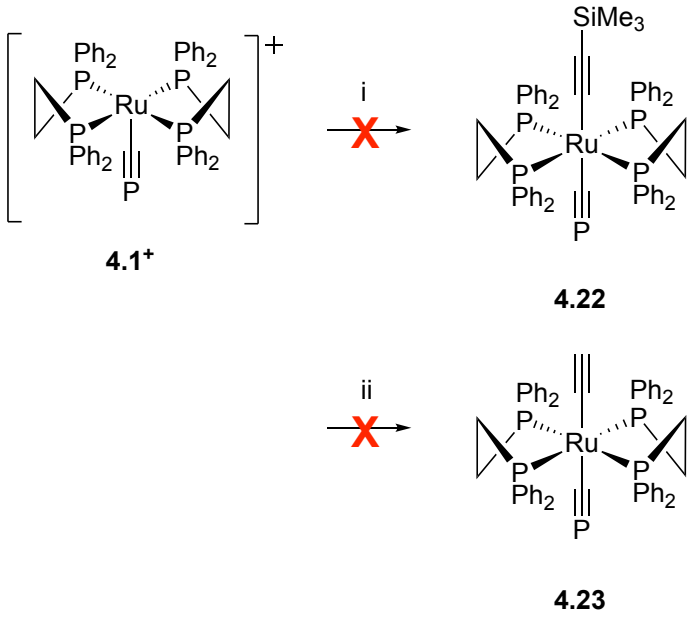

4.1$^+$ **4.22** **4.23**

Scheme 4-9: *Attempted synthesis of trans-[Ru(C≡CSiMe$_3$)(C≡P)(dppe)$_2$]* ***4.22*** *and trans-[Ru(C≡CH)(C≡P)(dppe)$_2$]* ***4.23****.*

Reagents and conditions: (i) LiC≡CSiMe$_3$, THF, RT, 18 h. (ii) NaC≡CH, DCM, RT, 18 h.

Previously Crossley and Leech reported the synthesis of the first extended through-conjugated bimetallic cyaphide complex, [{Ru(dppe)$_2$}$_2${μ-(C≡C)$_2$C$_6$H$_4$-*p*}(C≡P)$_2$] alongside the corresponding phosphaalkyne complex.[105] Therefore, it was sought to exploit **4.1$^+$** in the synthesis of new trimetallic, [{Ru(dppe)$_2$}$_3${μ-(C≡C)$_3$C$_6$H$_3$}(C≡P)$_2$] **4.24** and bimetallic complexes [{Ru(dppe)$_2$}$_2${μ-(C≡C)$_2$C$_4$H$_2$S}(C≡P)$_2$] **4.25** (**Scheme 4-10**) .

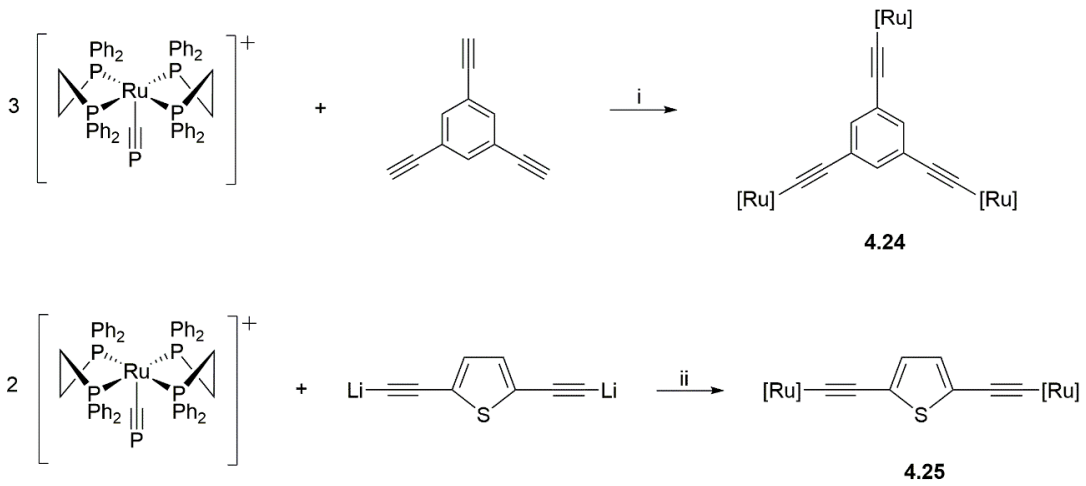

Scheme 4-10: *Attempted synthesis of [{Ru(dppe)$_2$}$_3${μ-(C≡C)$_3$C$_6$H$_3$}(C≡P)$_2$]* ***4.24*** *and [{Ru(dppe)$_2$}$_2${μ-(C≡C)$_2$C$_4$H$_2$S}(C≡P)$_2$]* ***4.25****. Reagents and conditions: (i) Excess DBU, DCM, RT, 16 h (ii) THF, 18 h, RT.*

The resulting $^{31}P\{^1H\}$ NMR spectrum for the attempted synthesis of **4.24** exhibited a cyaphidic resonance at 132 ppm and dppe resonance at 46 ppm; these data are inconsistent with the formation of **4.24**, with the cyaphidic resonance expected to be at significantly higher frequency (*cf. trans*-[Ru(C≡CPh)(dppe)$_2$(C≡P)] δ_P 160.4, [{Ru(dppe)$_2$}$_2${μ-(C≡C)$_2$C$_6$H$_4$-p}(C≡P)$_2$] δ_P 159.7). However, the ^{1}H NMR spectrum showed no resonances present for the aromatic protons from the conjugated alkyne. Furthermore, an alternative synthetic pathway was attempted by reacting **4.1$^+$** with the lithiated alkyne although this was unsuccessful. In addition, the attempted synthesis of **4.25** resulted in the formation of intractable mixtures.

In collaboration with K. G. Pearce (Sussex) a series of other ligand addition reactions were studied. The reaction of **4.1$^+$** and 4-cyanoisophthalic acid to yield **4.26$^+$** was attempted (**Scheme 4-11**). The crude $^{31}P\{^1H\}$ NMR spectrum exhibited two new resonances at 164 ppm and 46 ppm for the cyaphide and dppe respectively, in addition a small amount of starting material was also present. These data are comparable to those of **4.9$^+$** (168 ppm, 47.6 ppm) and are suggestive of successful coordination of the 4-cyanoisophthalic acid via the nitrogen lone pair. The ^{1}H NMR also showed the presence of acidic protons at 3.03 ppm confirming the presence of the 4-cyanoisophthalic acid.

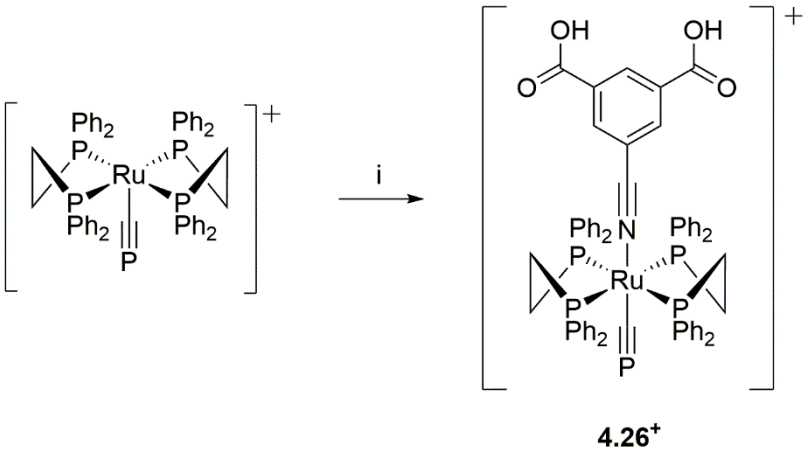

4.26$^+$

Scheme 4-11: *Attempted synthesis of trans-[Ru(N≡C-($C_6H_3(CO_2OH)_2$)(dppe)$_2$(C≡P)]OTf,* ***4.26$^+$****. Reagents and Conditions: (i) 4-cyanoisophthalic acid, CD_2Cl_2, 1 hour, RT.*

Other initial test reactions were conducted, with **4.1$^+$** reacted independently with $P(SiMe_3)_3$, $P(SiMe_3)_2H$ and $[C_6H_4\text{-}1,2\text{-}P_2BPh][Li_2(TMEDA)_2]$[190] all of which resulted in observable changes in the spectroscopic data and the retention of the cyaphidic resonance.

The reaction of **4.1$^+$** and $P(SiMe_3)_3$ resulted in significant changes in the $^{31}P\{^1H\}$ NMR spectrum, with a cyaphidic multiplet at 178 ppm, a doublet at 48 ppm (J_{PP} = 24 Hz) and a quintet at −104 ppm (J_{PP} = 24 Hz), integrating in a 1:4:1 ratio; also present are resonances for **4.1$^+$**. The resonance at −104 ppm was shown in the proton-coupled ^{31}P NMR as a quartet of quintets (J_{PP} = 24 Hz, J_{PH} = 340 Hz). These data are consistent with the synthesis of *trans*-[Ru(PH_3)(C≡P)(dppe)$_2$]OTf (*cf*. [RuCl(TFA)(PH_3)(CO)(PPh_3)$_2$] δ_P −90.1, J_{PP} = 24.5 Hz, J_{PH} = 381.6 Hz; [RuCl(H)(PH_3)(CO)(PPh_3)$_2$] δ_P −136.0, J_{PP} = 17.3 Hz, J_{PH} = 310.6 Hz; [RuCl(Ph)(PH_3)(CO)(PPh_3)$_2$] δ_P −129.4, J_{PP} = 10.0 Hz, J_{PH} = 318.6 Hz)[191], presumably from *in-situ* formation of PH_3 reacting with **4.1$^+$**. The ^1H NMR spectrum provides further evidence for the formation of *trans*-[Ru(PH_3)(C≡P)(dppe)$_2$]OTf, with a doublet of quintets at 1.94 ppm (J_{PH} = 340 Hz and 4 Hz) for the *trans*-PH_3 ligand, also present are resonances associated with the dppe ligands. The reaction of **4.1$^+$** and $P(SiMe_3)_2H$ resulted in a comparable $^{31}P\{^1H\}$ NMR spectrum with an additional broad singlet present at 115 ppm, which

has unable to be identified. Additional reactions are needed to isolate and further characterise *trans*-[Ru(PH_3)(C≡P)(dppe)$_2$]OTf, which were impeded due to time constraints.

The reaction of **4.1**$^+$ and [1,2-P_2BPh-C_6H_4][Li_2(TMEDA)$_2$][190] resulted in two new resonances in the crude $^{31}P\{^1H\}$ NMR spectrum, a doublet of multiplets at 135 ppm (J ≈ 6.0 Hz, 3.0 Hz) and a broad multiplet at 47 ppm, integrating in a 1:4 ratio. In addition, there are two multiplets at 65 ppm and 48 ppm, as well as a singlet for free dppe at −12 ppm, integrating in a 0.7:0.8:0.3 ratio. Furthermore, there is no evidence of the free ligand [1,2-P_2BPh-C_6H_4][Li_2(TMEDA)$_2$] (56 ppm), although one of the multiplets present at 65 ppm and 48 ppm may be consistent with the coordination of the ligand. Overall, these data suggest the formation of two products, one of which retains the cyaphide moiety, however, further evidence is needed to assign the identities of these. Indeed, for all three cases further characterisation and investigations are needed to assign the products from these reactions.

4.8 CONCLUDING REMARKS

The cyaphide complex, **3.4** has shown to be an important precursor for post synthetic modification, with the reaction between **3.4** and Me_2Mg showing the reformation of **3.3**. In addition, **3.4** has been shown to be susceptible to halide abstraction affording a discrete 5-coordinate complex cation, [Ru(dppe)$_2$(C≡P)]$^+$, **4.1**$^+$. Isolable in bulk as the triflate salt, **4.1**$^+$ is the first complex to feature a terminally ligated cyaphide within a flexible coordination sphere with **4.1**$^+$ adopting a square-pyramidal geometry.

The 5-coordiante cyaphide complex **4.1**$^+$ exhibits a readily accessible vacant coordination site, which is susceptible to nucleophiles such as LiC≡CPh which offers access to previously reported alkynyl complexes. In addition, ligand addition to this vacant coordination site has yielded a series of novel cyaphide complexes which are unable to be obtained via more "traditional" routes. These include *trans*-[Ru(R)(dppe)$_2$(C≡P)]$^+$, (R = C≡O **4.2**$^+$, P≡C$SiMe_3$ **4.7**$^+$, C≡NCH_3 **4.9**$^+$ and NC_5H_5 **4.10**$^+$) and *trans*-[Ru(R)(dppe)$_2$(C≡P)], (R = C≡N **4.3**, F **4.6**, SC≡N **4.4**, OC≡N **4.5** and C≡P **4.8**)

which have been characterised through multinuclear NMR spectroscopy, with **4.2**$^{+}$, **4.3**, **4.4** and **4.9**$^{+}$ also structurally characterised by X-ray diffraction, which show comparable data for the C≡P bond lengths and the R-Ru-CP bond angles. In addition, **4.4** has shown to be in line with that of the chloride and bromide analogues and **4.3** and **4.9**$^{+}$ showed C≡N bond lengths consistent with literature ruthenium cyanide and acetonitrile complexes respectively.

The reaction of **4.1**$^{+}$ and PMe_3 has yielded the structurally characterised $[Ru(PMe_3)_3(dppe)(C{\equiv}P)]^{+}$ **4.14**$^{+}$, the first example of dppe ligand displacement whilst maintaining the cyaphide moiety. However, further studies into purification and isolation are needed to further study and characterise **4.14**$^{+}$ alongside the other possible products from the reaction.

Furthermore, in the attempt to displace one of the dppe ligands with a cyclopentadiene ligand, **4.1**$^{+}$ was shown to undergo unexpected reduction chemistry, with the reaction of **4.1**$^{+}$ and LiCp resulting in the dimer $[(Ru(dppe)_2)_2(CPPC)]$ (**4.19**), which was identified through X-ray diffraction; these data showed a trigonal bipyramidal structure with a central C-P-P-C unit. Additionally, in further investigations to explore the reduction chemistry, the reaction of **4.1**$^{+}$ with sodium naphthalide resulted in the structurally characterised Na_2P_2 centred dimer, $[Ru(C{\equiv}PNa)(dppe)_2]_2$ (**4.20**), which was shown to retain the triple bond character of the cyaphide ligand. Overall, further work is needed to optimise the synthesis and fully characterise these reduction products.

CHAPTER 5 : COMPUTATIONAL, ELECTROCHEMICAL AND SPECTROELECTROCHEMICAL STUDIES OF CYAPHIDE COMPLEXES

5.1 INTRODUCTION

The *trans*-alkynyl cyaphide complexes have been previously studied through DFT and cyclic voltammetry in order to gain understanding about the electronics of the cyaphide moiety. These studies demonstrated frontier molecular orbitals analogous to that of the *bis*(alkynyl) complexes, and a significant influence of the remote *trans*- substituent upon the properties of the cyaphide ligand which appeared indicative of some communication between the alkynyl and cyaphide moieties. Furthermore, the DFT and cyclic voltammetry studies of [{Ru(dppe)$_2$}$_2${μ-(C≡C)$_2$C$_6$H$_4$-*p*}(η^1-P≡CSiMe$_3$)$_2$]$^{2+}$ **1.60**$^+$ and [{Ru(dppe)$_2$}$_2${μ-(C≡C)$_2$C$_6$H$_4$-*p*}(C≡P)$_2$] **1.61** showed through-conjugation of two phosphaalkyne moieties.

To gain further understanding of how the *trans* ligand affects the electronic behaviour of the cyaphide moiety, a combination of DFT, UV-vis spectroscopy, cyclic voltammetry and spectroelectrochemistry of the cyaphide complexes *trans*-[Ru(C≡O)(dppe)$_2$(C≡P)]$^+$ (**4.2**$^+$) and *trans*-[Ru(R)(dppe)$_2$(C≡P)] (R = Me (**3.3**), Br (**3.4**), C≡N (**4.3**), C≡P (**4.8**)), as well as the 5-coordinate cyaphide complex *trans*-[Ru(dppe)$_2$(C≡P)]$^+$ (**4.1**$^+$), will be discussed.

5.2 DFT STUDIES

The ground state geometries for the cyaphide complexes **3.3**, **3.4** and **4.1**$^+$ were optimised using DFT methods, at the B3LYP level of theory (6-31G for H, C, P and Br and LANL2DZ for Ru). The starting points for these calculations were their respective solid-state structures. The calculated bond lengths and bond angles (**Table 5-1**) are in close agreement with the solid-state structures of **3.3**, **3.4** and **4.1**$^+$. In general, the gas-phase optimised geometries revealed a slightly greater degree of linearity around the metal centre alongside slightly elongated C≡P bond lengths for **3.3** and **3.5**, this is consistent with the presence of crystal packing forces in the solid state, and

the absence of intermolecular interactions in the gas phase and is comparable to that seen in the DFT calculations for the *trans*-alkynyl cyaphide complexes.

	3.3		**3.4**		**4.1$^+$**	
	Exp	**Calc**	**Exp**	**Calc**	**Exp**	**Calc**
Ru(1)-C(1)	2.186(8)	2.05302	1.901(9)	1.96178	1.904(4)	1.92055
Ru(1)-R	2.238(6)	2.26808	2.690(2)	2.75316	-	-
C(1)-P(1)	1.392(8)	1.58751	1.544(10)	1.58261	1.573(4)	1.57881
R-Ru(1)-C(1)	171.2(3)	172.88372	177.1(2)	174.67649	-	-
Ru(1)-C(1)-P(1)	165.5(5)	173.19038	175.8(5)	178.64055	178.9(2)	179.99847

Table 5-1: *Selected key bond lengths (Å) and bond angels (°) from both experimental data and DFT calculations of* ***3.3****,* ***3.4*** *and* ***4.1$^+$***

3.3

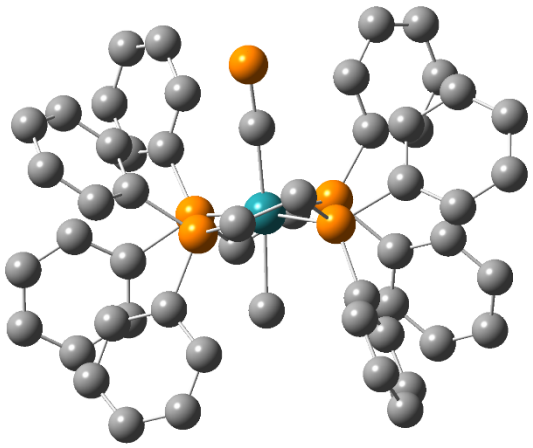

3.4

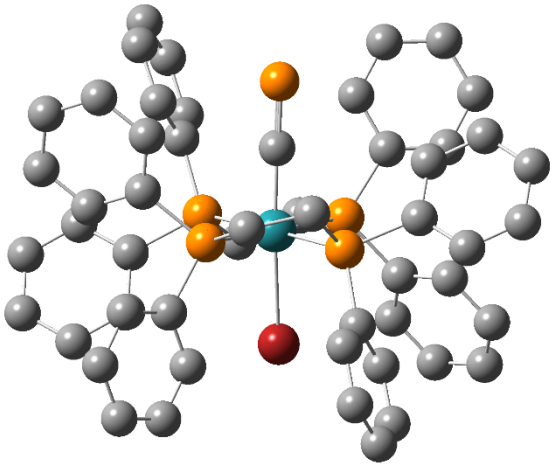

4.1^{+}

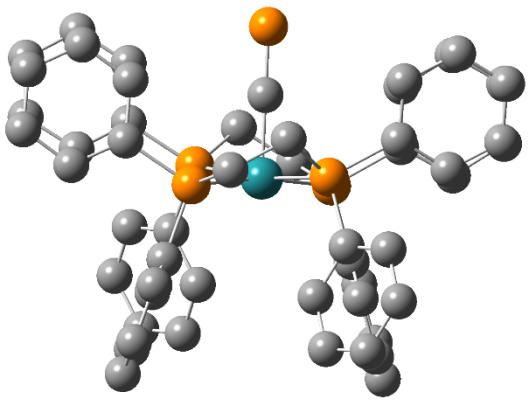

Figure 5-1: *DFT Optimised structures for* ***3.3****,* ***3.4*** *and* ***4.1^{+}****. Hydrogen atoms have been omitted for clarity.*

The DFT calculations were able to identify some of the key electronic features of these cyaphide complexes. The frontier molecular orbitals (**Figure 5-2**) for **3.3** (**Figure 5-3**), **3.4** (**Figure 5-4**) and **4.1**$^+$ (**Figure 5-5**) are comparable to those seen in the previously reported *trans*-alkynyl cyaphide complexes with the HOMO and HOMO-1 being heavily associated with the π-orbitals of the C≡P bond (≈ 50-60%) and the ruthenium d-orbitals (≈ 30-40%), while the LUMO and LUMO+1 are predominantly based on the dppe ancillary ligands. However, for **4.1**$^+$ the HOMO and LUMO are significantly lower in energy than **3.3** and **3.4** (-7.56 eV and -4.38 eV) with the LUMO, although predominantly centred on the dppe ancillary ligands (43%), also having a significant contribution from the dz^2 orbital on the ruthenium centre (41%). In addition, unlike that reported for the *trans*-alkynyl cyaphide complexes, **3.3** and **3.4**, the LUMO of **4.1**$^+$ also exhibits σ-antibonding contribution (16%) for the cyaphide moiety.

Comparable to the precedent *trans*-alkynyl cyaphide complexes the LUMO for **3.3**, **3.4** and **4.1**$^+$ is appreciably separated from the HOMO (Δ*E* 3.62 eV **3.3**, 3.59 eV **3.4**, 3.18 eV **4.1**$^+$) with the higher energy orbitals being almost exclusively dppe ligand based. For both **3.3** and **3.4** the C≡P π* orbitals appreciably contribute to L+15/16 (0.35 eV) and L+17/18 (0.36 eV) respectively, comparable to that of the *trans*-alkynyl systems (L+18/19/20, 0.28 eV to 0.59 eV), while for **4.1**$^+$ the C≡P π* orbitals contribution at significantly lower energy at the L+12/13 (-2.66 eV).

In comparison to the *trans*-alkynyl cyaphide complexes where the lone pair lies *ca* 1.6 eV below the HOMO in either HOMO-6 or HOMO-7, the phosphorus lone pair of the cyaphide moiety for **3.3**, **3.4** and **4.1**$^+$ is appreciably more stabilised lying at -2.84 eV, -3.06 eV and -3.18 eV below the HOMO in HOMO-22, HOMO-24 and HOMO-22 respectively.

3.3

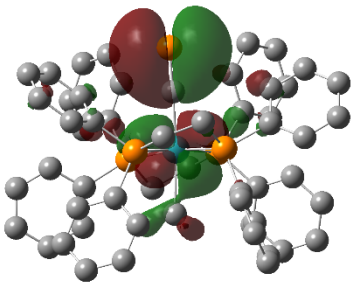

HOMO
-4.53 eV

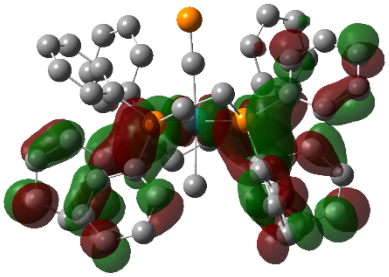

LUMO
-0.91 eV

3.4

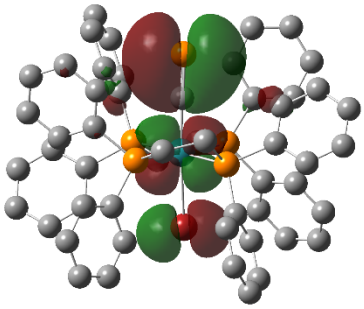

HOMO
-4.72 eV

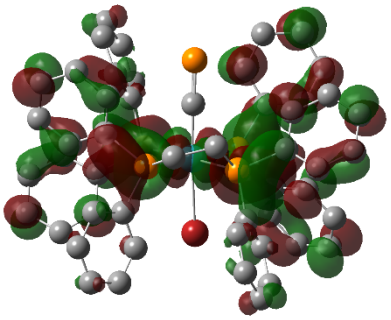

LUMO
-1.13 eV

4.1^{+}

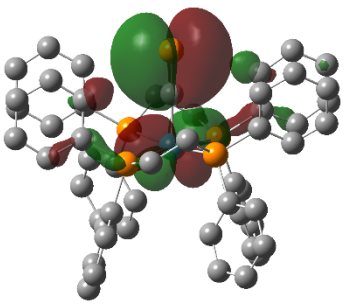

HOMO
-7.56 eV

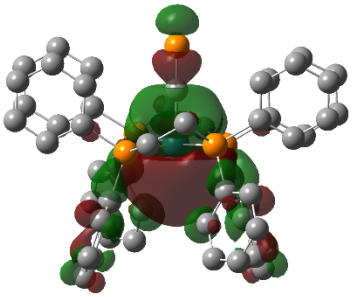

LUMO
-4.38 eV

Figure 5-2: *Calculated frontier molecular orbitals for* ***3.3****,* ***3.4*** *and* ***4.1^{+}****.*

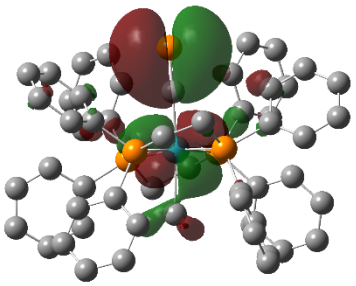

HOMO
-4.53 eV

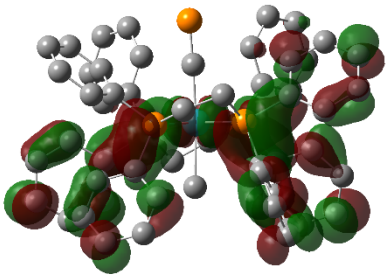

LUMO
-0.91 eV

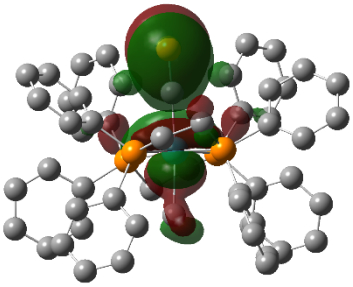

HOMO-1
-4.65 eV

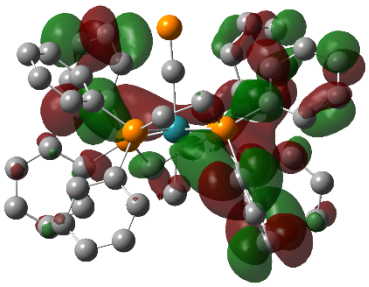

LUMO+1
-0.68 eV

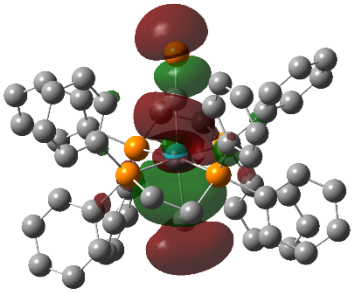

HOMO-2
-5.3 eV

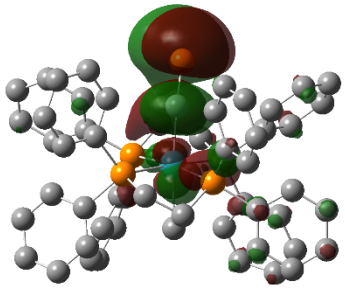

LUMO+16
0.35 eV

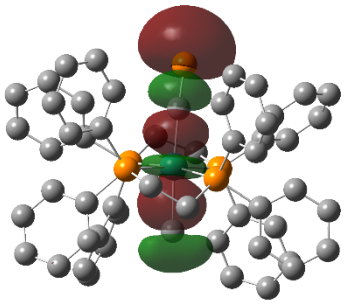

HOMO-22
-7.37 eV

Figure 5-3: *Calculated molecular orbitals for* ***3.3****.*

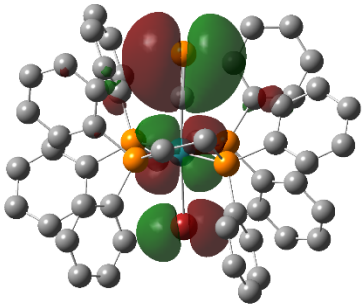

HOMO
-4.72 eV

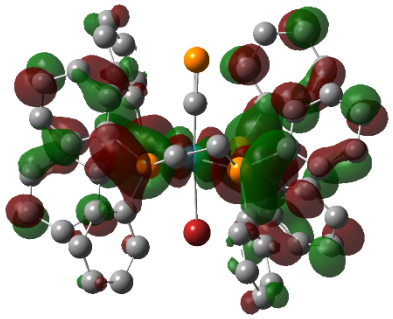

LUMO
-1.13 eV

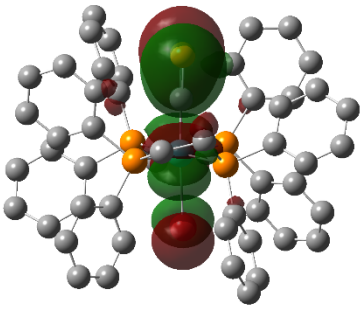

HOMO-1
-4.82 eV

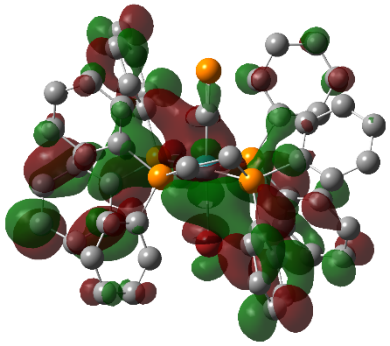

LUMO+1
-0.77 eV

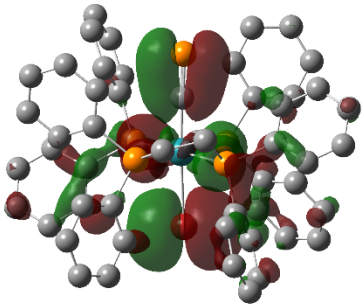

HOMO-2
-5.67 eV

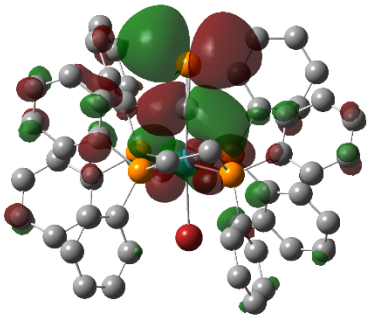

LUMO+18
0.36 eV

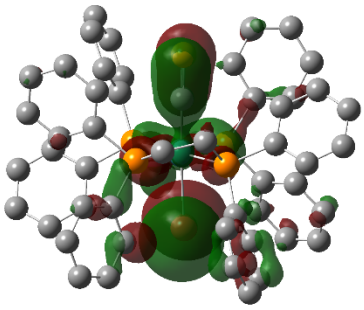

HOMO-3
-5.75 eV

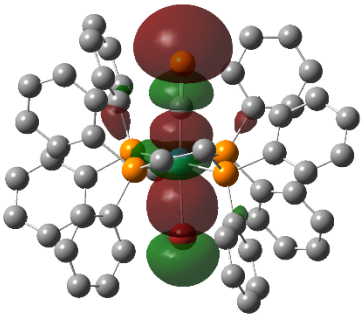

HOMO-24
-7.78 eV

***Figure 5-4**: Calculated molecular orbitals for **3.4**.*

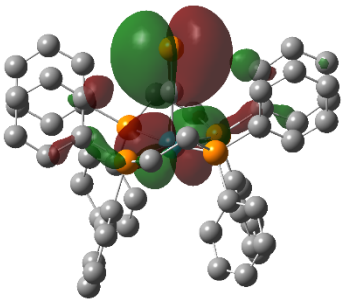

HOMO
-7.56 eV

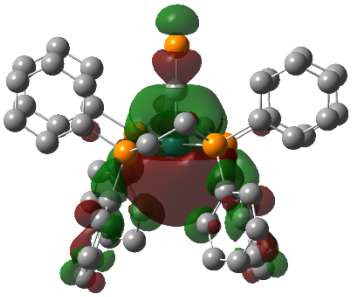

LUMO
-4.38 eV

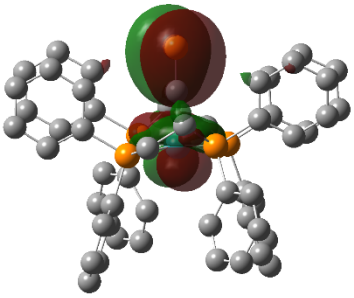

HOMO-1
-7.75 eV

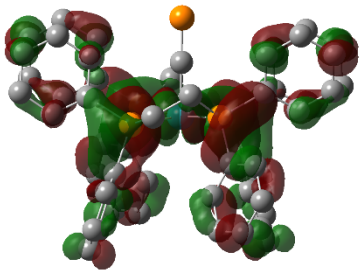

LUMO+1
-3.46 eV

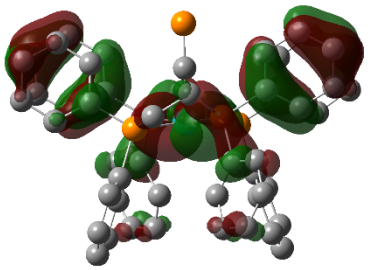

HOMO-2
-8.61 eV

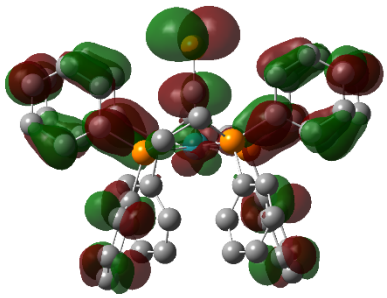

LUMO+12
-2.66 eV

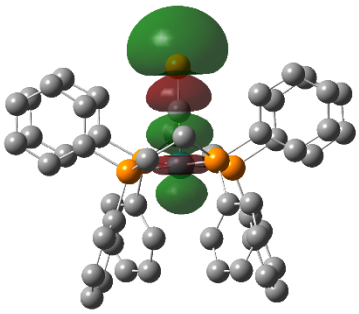

HOMO-22
-10.36 eV

Figure 5-5: *Calculated molecular orbitals for* ***4.1***$^{+}$.

5.3 UV-VIS SPECTROSCOPY

The UV-Vis spectra of **3.3**, **3.4** and **4.1**$^{+}$ all exhibit high energy features between 200 nm and 400 nm. The assignment of these UV-Vis spectral features was assisted by TD-DFT calculations, with the first 100 excited states computed with a cpcm solvent model (CH_2Cl_2) at the B3LYP/3-21G level of theory. It is important to note that previous studies in the Crossley group have determined this level of theory to be appropriate for general assignment of electronic spectra for systems of this type.[103,104]

The UV-vis spectrum of **3.3** (**Figure 5-6**) exhibits three high energy features between 210 nm and 300 nm. The first at 215 nm is dominated by inter-ligand charge transfer (ILCT) between the dppe ancillary ligands with some ligand to metal charge transfer (LMCT) from the methyl and cyaphide ligands to the ruthenium centre, augmented by metal to ligand charge transfer (MLCT) and ligand to ligand charge transfer (LLCT) from the ruthenium and cyaphide to the dppe ligands. In addition, these MLCT and LLCT bands are the predominant features for the absorbance at 240 nm. A further weak feature at 290 nm is also observed and tentatively assigned as MLCT from the ruthenium to the dppe ligands and to the $\pi^*_{C\equiv P}$ orbitals.

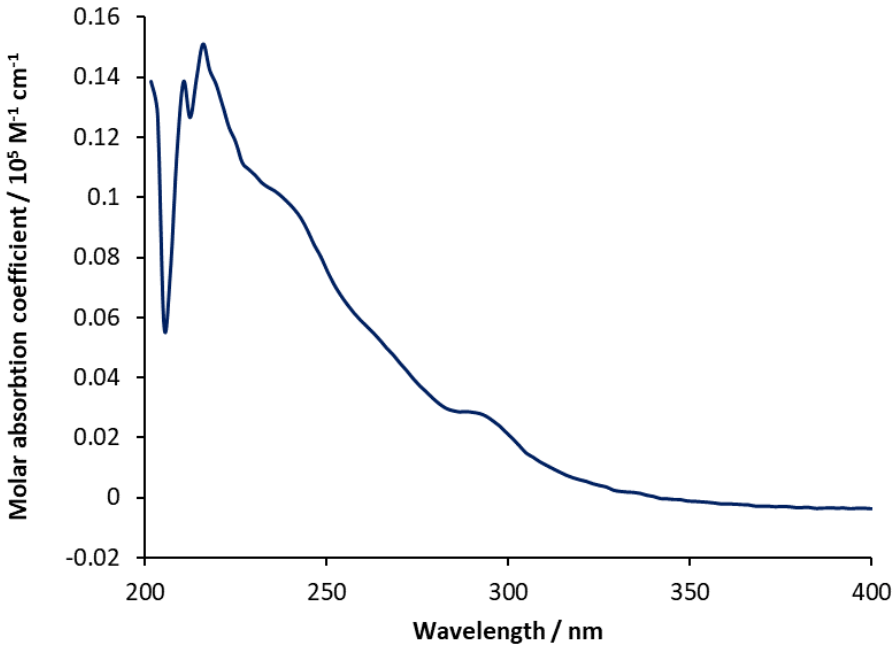

Figure 5-6: *UV-vis spectra for* ***3.3****. Obtained in an OTTLE cell. Conditions: 0.001 M solutions of analyte and 0.1M solutions of electrolyte [^{n}BuN][PF_6] in DCM and a path length of 0.2 mm. Note: Initial UV-spectra from the spectroelectrochemistry experiment.*

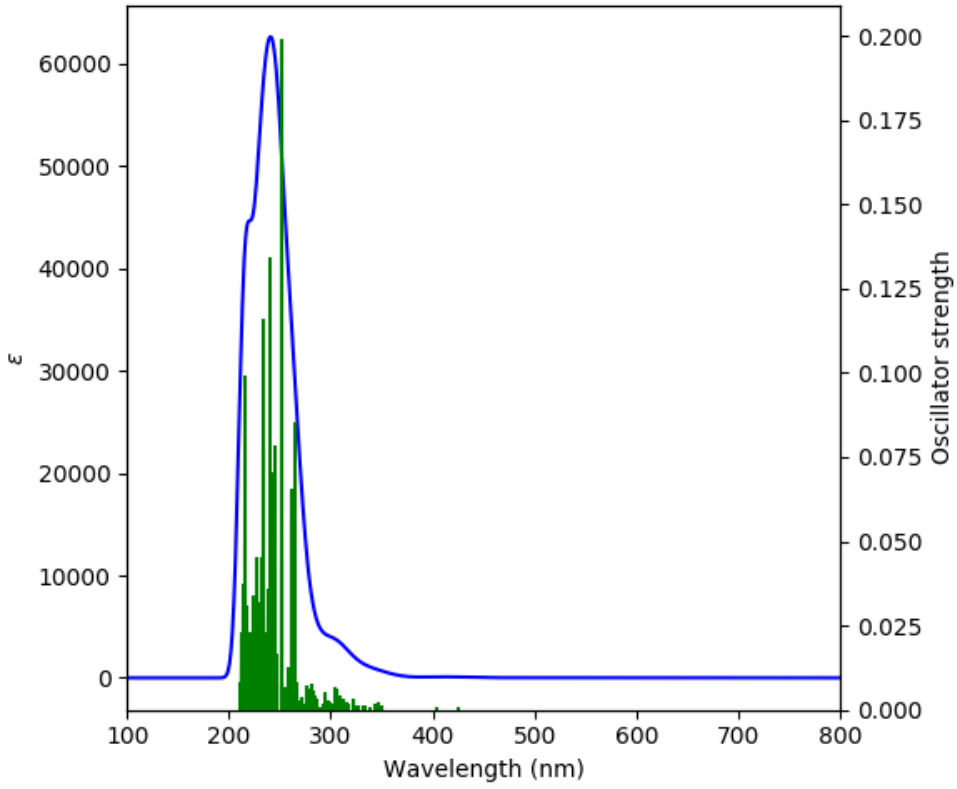

Figure 5-7: *Calculated UV-vis spectra for* ***3.3.***

Similarly, the UV-vis spectrum of **3.4** (**Figure 5-8**) exhibits multiple high energy features with bands at 220 nm, 230 nm, 245 nm and 270 nm. Comparable to those of **3.3** the first features at 220 nm and 230 nm are dominated by ILCT between the dppe ancillary ligands. In addition, there are smaller contributions from LLCT from the cyaphide/bromide to the dppe ligands and for the band at 220 nm there is notable contribution from LLCT between the bromide and the $\pi^*_{C\equiv P}$ orbitals. The band at 245 nm has significant contributions from MLCT to the dppe ligands alongside ILCT between the dppe ligands and the band at 270 nm is dominated by LLCT from the Br and C≡P to the dppe ancillary ligands with small contributions from ILCT between the $\pi_{C\equiv P}$ orbitals (HOMO) to the $\pi^*_{C\equiv P}$ orbitals (LUMO+17/18).

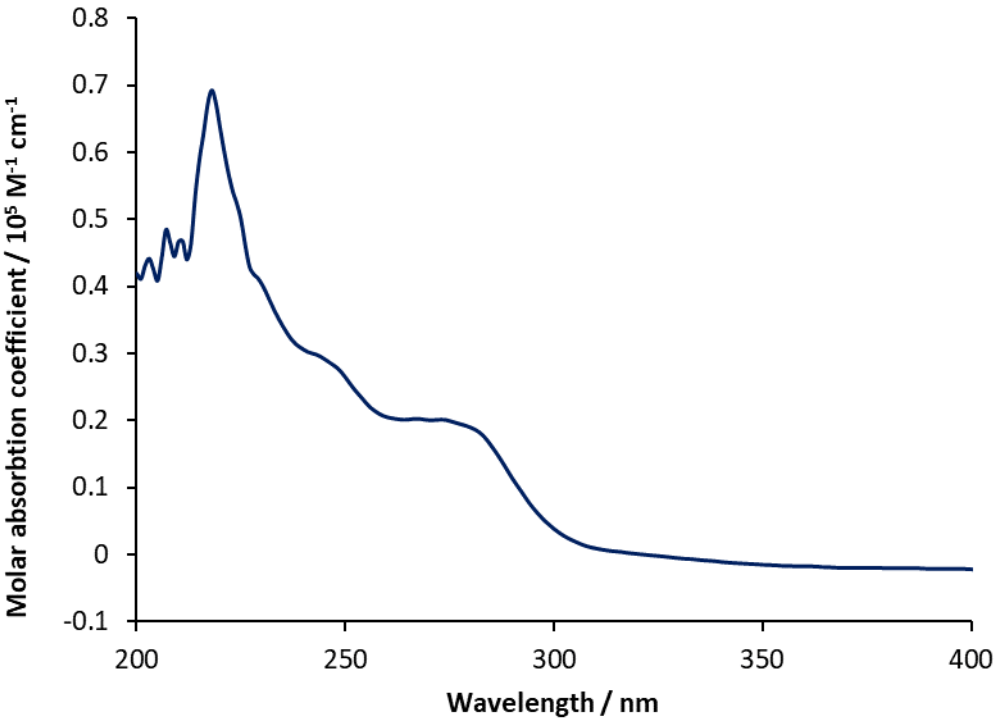

Figure 5-8: *UV-vis spectra for* ***3.4****. Obtained in an OTTLE cell. Conditions: 0.001 M solutions of analyte and 0.1M solutions of electrolyte [^{n}BuN][PF_6] in DCM and a path length of 0.2 mm. Note: Initial UV-spectra from the spectroelectrochemistry experiment.*

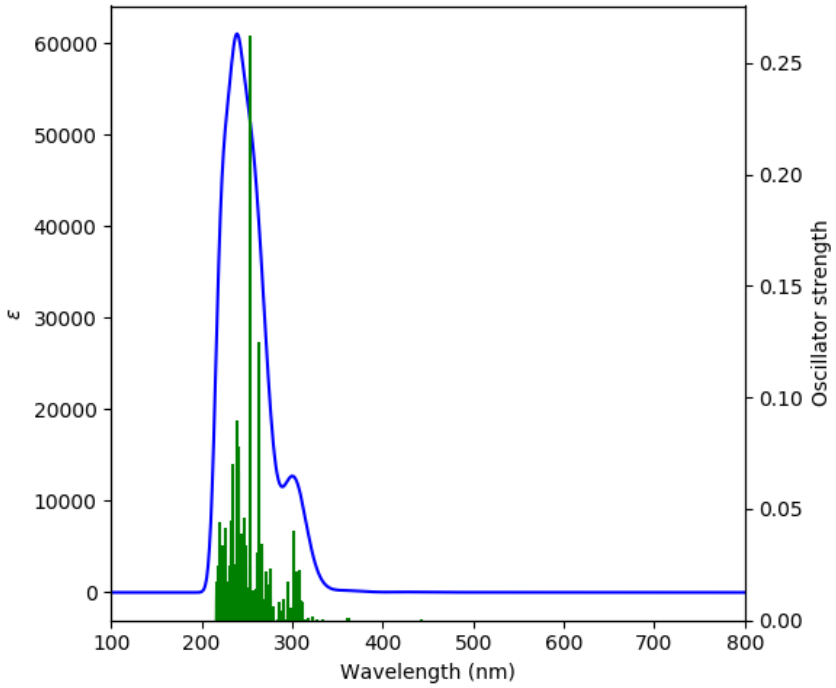

Figure 5-9: *Calculated UV-vis spectra for* ***3.4.***

The 5-coordinate cyaphide complex **4.1**$^{+}$ (**Figure 5-10**) shows a different UV-vis profile compared to **3.3** and **3.4** and is consistent with the significant difference in colour with **4.1**$^{+}$ being deep purple and **3.3** and **3.4** being bright yellow. However, the UV-vis spectrum of **4.1**$^{+}$ still exhibits comparable high energy features at 200 nm to 220 nm, which are comparable to that of **3.3** and **3.4**, which are dominated by ILCT between the dppe ancillary ligands as well as by MLCT from the metal d-orbitals to the dppe π-systems. In addition, there are two weak features at 260 nm and 300 nm, the former arising predominantly from LMCT from the dppe π-system to the d-orbitals on the metal centre with a small contribution from ILCT between the dppe ligands, and the later feature at 300 nm arising from LLCT from the dppe to cyaphide and MLCT from the dppe. Unlike for that of **3.3** and **3.4,** the observed feature at 300 nm has no contribution of transitions to the $\pi^*_{C\equiv P}$ orbitals.

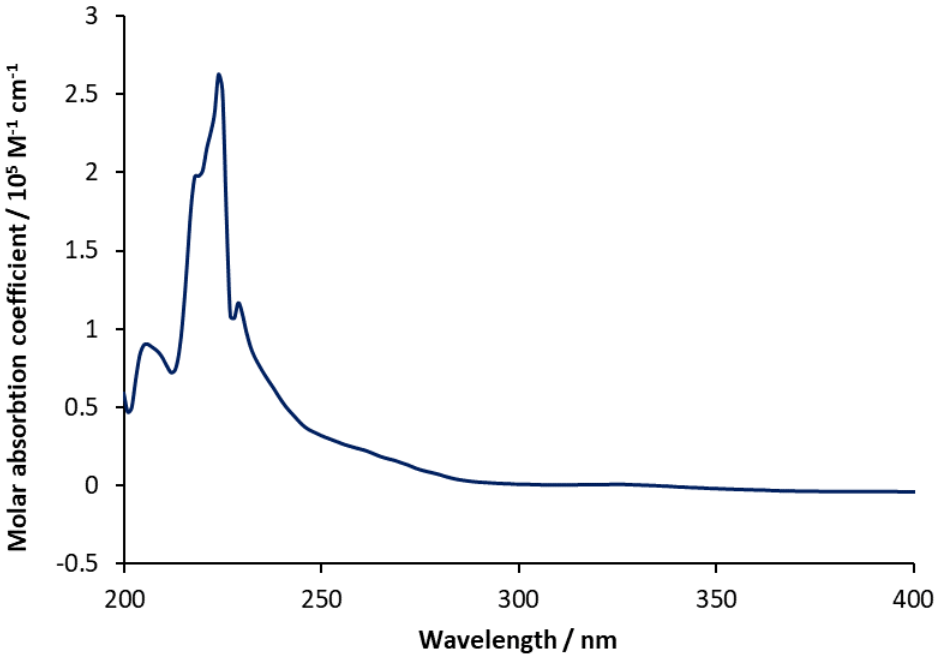

Figure 5-10: *UV-vis spectra for* ***4.1***$^{+}$*. Obtained in an OTTLE cell. Conditions: 0.001 M solutions of analyte and 0.1M solutions of electrolyte [*^{n}*BuN][PF*$_6$*] in DCM and a path length of 0.2 mm. Note: Initial UV-spectra from the Spectroelectrochemistry experiment.*

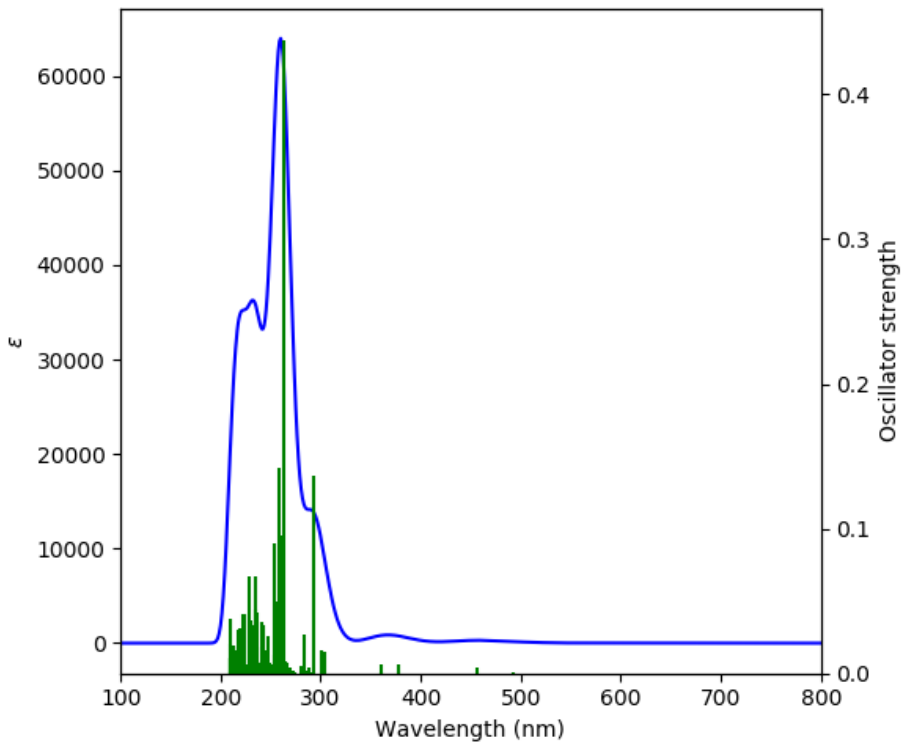

Figure 5-11: *Calculated UV-vis spectra for* ***4.1***$^{+}$***.***

5.4 ELECTROCHEMISTRY

The electrochemical behaviours of the cyaphide complexes *trans*-[RuMe(dppe)$_2$(C≡P)] **3.3**, *trans*-[RuCl(dppe)$_2$(C≡P)] **3.5**, *trans*-[RuBr(dppe)$_2$(C≡P)] **3.4**, *trans*-[Ru(dppe)$_2$(C≡P)]OTf **4.1$^+$**, *trans*-[Ru(C≡N)(dppe)$_2$(C≡P)] **4.3** and *trans*-[Ru(dppe)$_2$(C≡P)$_2$] **4.8**, have been studied by cyclic voltammetry as CH_2Cl_2 solutions at a platinum disk working electrode (1.6 mm), with NBu_4PF_6 supporting electrolyte. The table (**Table 5-2**) summarises the key features of the cyclic voltammograms for **3.3**, **3.4**, **3.5**, **4.1$^+$**, **4.3** and **4.8**.

R Group	Compound Number	Irreversible Reductive Event(s)	Irreversible Oxidative Event(s)
		E_{pc} (V)	E_{pa} (V)
Me	**3.3**	−1.08	0.02
Br	**3.4**	−1.25	0.61
Cl	**3.5**	−0.83	0.06
-	**4.1$^+$**	−0.64 and 2.00	−0.31 and 0.50
CN	**4.3**	−0.89	0.36
CP	**4.8**	−0.93	0.16 and 1.11

Table 5-2: *Cyclic voltammetry data of cyaphide complexes **3.3**, **3.4**, **3.5**, **4.1$^+$**, **4.3** and **4.8**. Potentials are reported relative to the ferrocene/ferrocenium (Fc/Fc$^+$) couple, referenced to the Fc*/Fc*$^+$ couple of doped samples (−0.56 V relative to Fc/Fc$^+$).*

The complexes **3.3**, **3.4** and **3.5** (**Figure 5-12** and **Figure 5-13**) exhibit a single irreversible oxidation process (0.02 V **3.3,** 0.61 V **3.4**, 0.06 V **3.5**) consistent with a one electron oxidation from Ru(II) to Ru(III), alongside a reductive process (-1.08 V **3.3**, -1.25 V **3.4**, -0.83 V **3.5**). This irreversible oxidative behaviour is comparable to that seen in the *trans*-alkynyl cyaphide complexes and the oxidative and reductive potentials for both **3.3** and **3.5** lie within the range

for these precedent examples (E_{pa}: −0.05 to 0.58 V, E_{pc}: 0.09 to −1.89 V). In comparison **3.4** exhibits an oxidation event at a more anodic potential (0.61 V) which is comparable to the *trans*-alkynyl complexes, but is significantly more positive than that of the other *trans*-halo complexes.[104] In addition, compared to $RuCl_2(dppe)_2$ ($E_{1/2}$ = 0.37 V, $RuCl_2(dppe)_2$), the oxidative feature for **3.4** is at a more negative potential.[192] The lower oxidation potential of **3.3** (0.02 V) compared to the *trans*-halo cyaphides **3.4** and **3.5** (0.61 V and 0.06 V) is in line with the σ donor character of the methyl ligand and the acceptor character of the halide ligands.

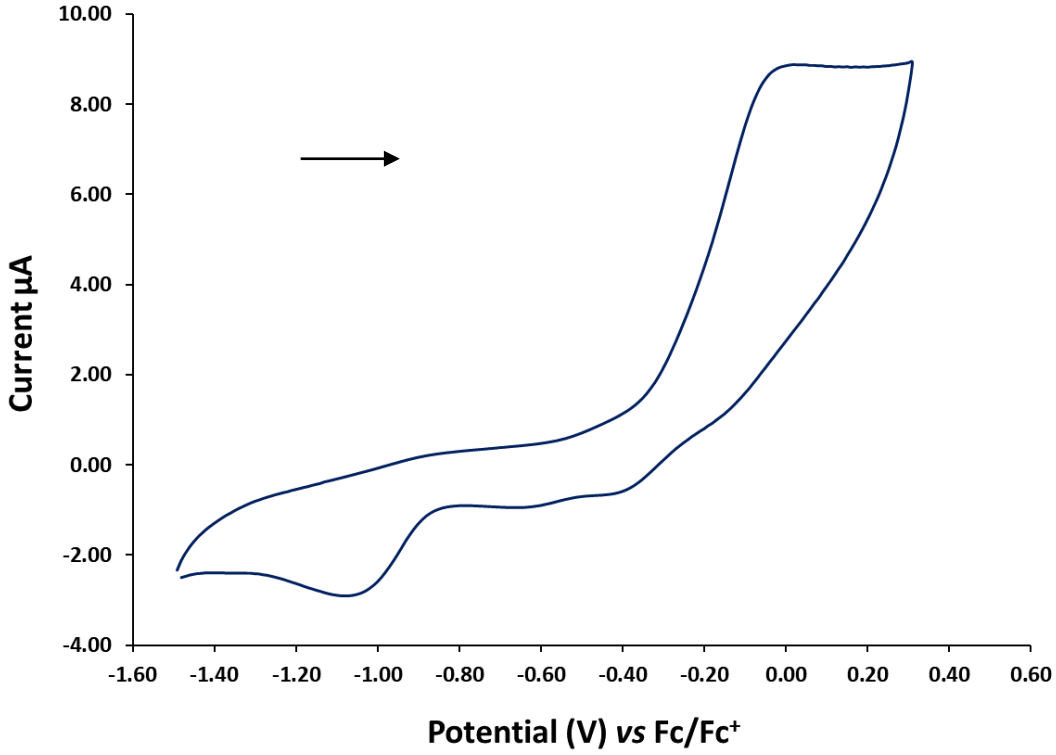

Figure 5-12: *Cyclic Voltammogram for **3.3** as a solution in CH_2Cl_2 (0.01M) with $[^nBu_4N][PF_6]$ supporting electrolyte (0.1 M), 0.1 V s^{-1} scan rate and 5 second equilibrium time. Referenced to the Fc^*/Fc^{*+} couple of doped samples (−0.56 V relative to Fc/Fc^+).*

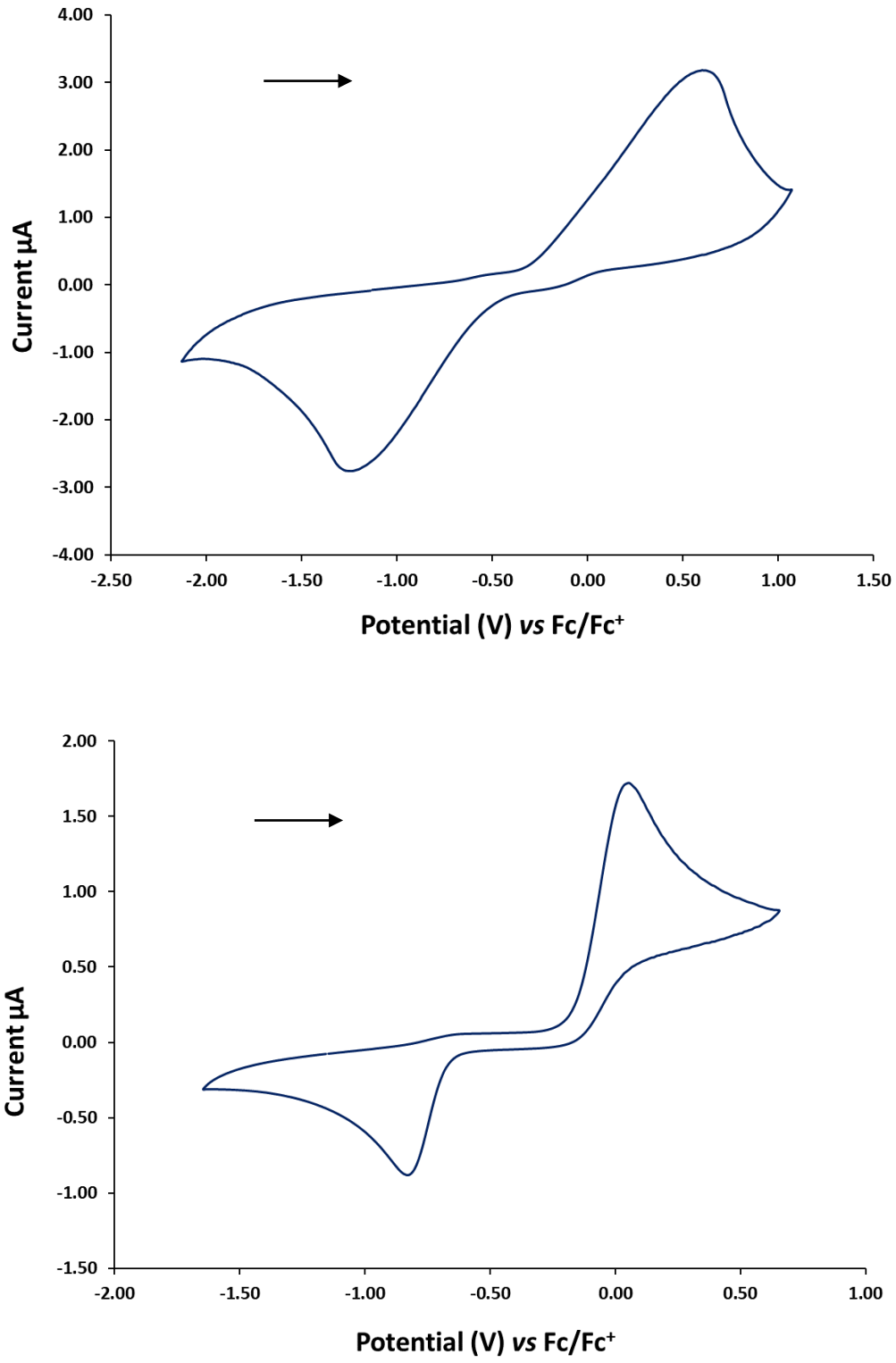

Figure 5-13: *Cyclic Voltammograms for* ***3.4*** *and* ***3.5*** *as solutions in CH_2Cl_2 (0.01M) with $[^nBu_4N][PF_6]$ supporting electrolyte (0.1 M), 0.1 V s^{-1} scan rate and 5 second equilibrium time. Referenced to the Fc*/Fc*+ couple of doped samples (−0.56 V relative to Fc/Fc+).*

The Cyclic Voltammogram of $[Ru(dppe)_2(C{\equiv}P)]^+$ **4.1**$^+$ (**Figure 5-14**) is significantly different to the previously discussed examples and shows an irreversible oxidative peak at 0.50 V and a reductive peak at −2.00 V, alongside a weaker psudoreversible process ($E_{1/2}$ = 0.48 eV). In comparison to the *trans*-alkynyl cyaphides (E_{pa}: −0.05 to 0.58 V, E_{pc}: 0.09 to −1.89 V)[104] and **3.4** (E_{pa}: 0.61 V. E_{pc}: -1.25 V), the first oxidation event is significantly more cathodic with the second oxidation event occurring at a comparable potential. However, it is the main reductive feature at −2.00 V, observed prior to the oxidation events (**Figure 5-15**), that is of significant importance and interest as it is consistent with the observed chemical reduction of the 5-coordinate cyaphide complex (See Section: **4.5.2**).

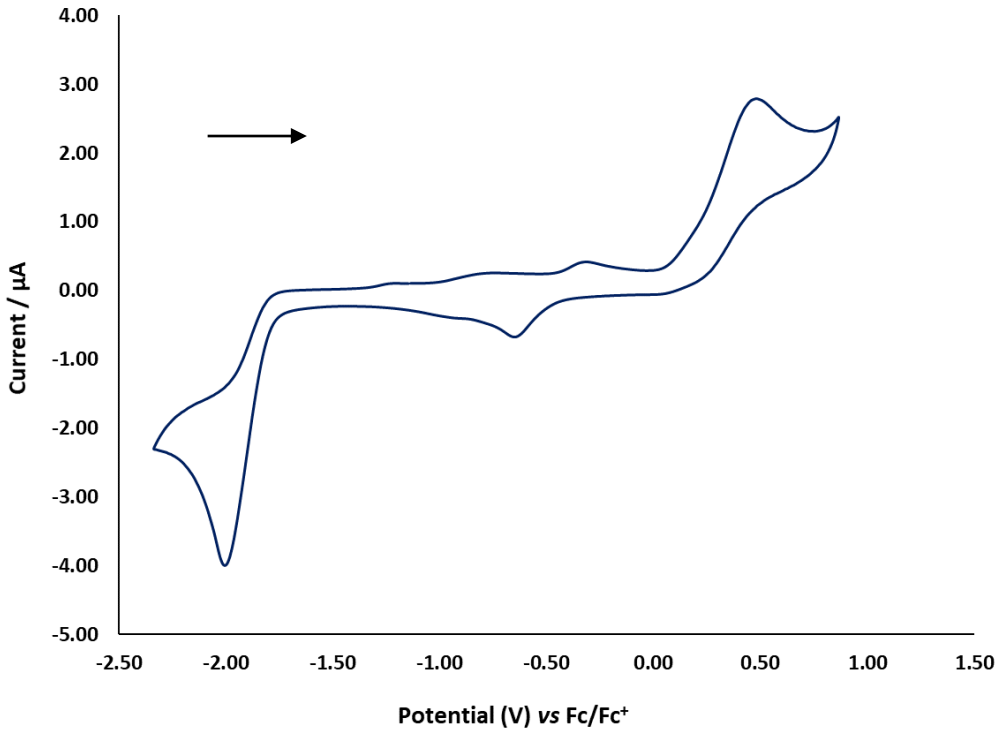

Figure 5-14: *Cyclic Voltammogram for* ***4.1***$^+$ *as a solution in* CH_2Cl_2 *(0.01M) with* $[^nBu_4N][PF_6]$ *supporting electrolyte (0.1 M), 0.1 V* s^{-1} *scan rate and 5 second equilibrium time, oxidative scan first. Referenced to the Fc*/Fc*$^+$ couple of doped samples (−0.56 V relative to Fc/Fc$^+$).*

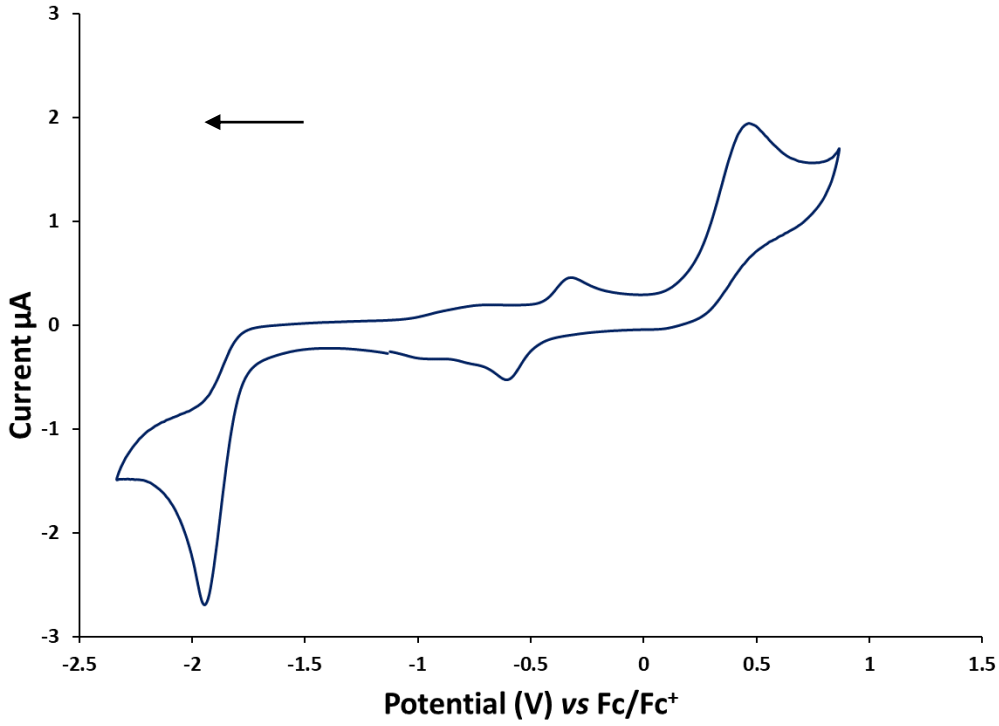

Figure 5-15: *Cyclic Voltammogram for* ***4.1***$^{+}$ *as a solution in* CH_2Cl_2 *(0.01M) with* $[^{n}Bu_4N][PF_6]$ *supporting electrolyte (0.1 M), 0.1 V* s^{-1} *scan rate and 5 second equilibrium time, reductive scan first. Referenced to the Fc*/Fc**$^{+}$ *couple of doped samples (−0.56 V relative to* Fc/Fc^{+}*).*

The Cyclic Voltammogram for *trans*-[Ru(C≡N)(dppe)$_2$(C≡P)] **4.3** (**Figure 5-16**) exhibits two irreversible redox events at (E_{pa} = 0.36 V and E_{pc} = −0.89 V) which correspond to the oxidation of Ru(II) to Ru(III) and the reduction of Ru(III) to Ru(II) respectively. These data are generally comparable to the *trans*-alkynyl cyaphides (E_{pa}: −0.05 to 0.58 V, E_{pc}: 0.09 to −1.89 V)[104] with the oxidation event (E_{pa} = 0.36 V) lying towards the top end of the range. This is consistent with the anodic shift of the oxidation potential seen when the electron-withdrawing character of arene substituent of the *trans*-alkynyl cyaphide complexes increases, as well as the relative electron-withdrawing character of the cyanide ligand. In comparison to the data reported for RuH(dppe)$_2$(C≡N) (E_{pa} = 0.28 V and E_{pc} = −1.47 V)[119] and RuH(dppe)$_2$(C≡P) (E_{pa} = −0.11 V)[119] the oxidative and reductive events for **4.3** lie at more anodic potentials which is consistent with the electron withdrawing nature of both the cyaphide and cyanide moiety.

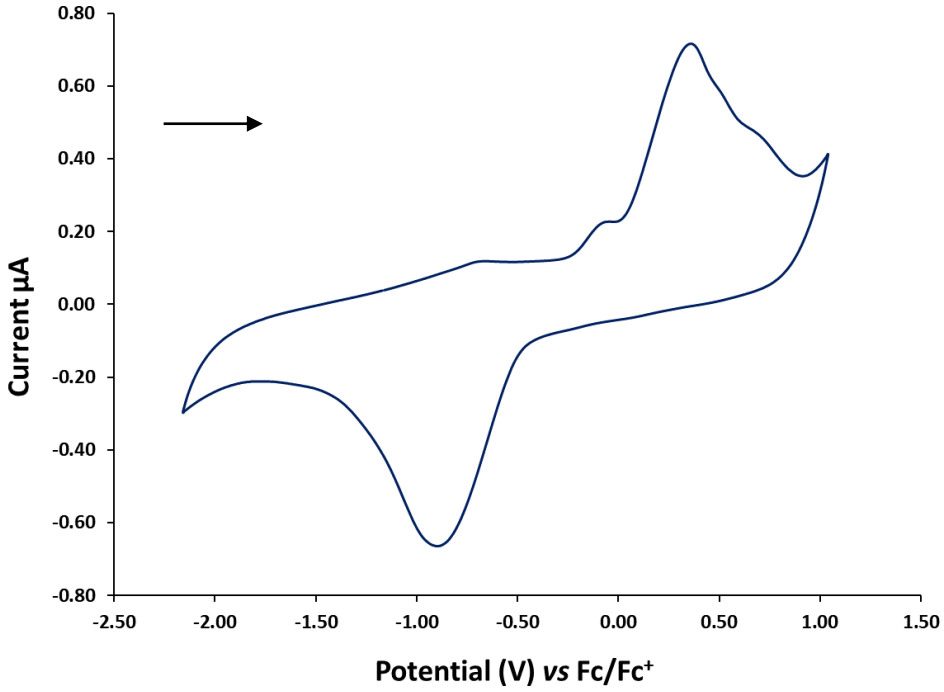

Figure 5-16: *Cyclic Voltammogram for* ***4.3*** *as solutions in CH_2Cl_2 (0.01M) with [^{n}Bu$_4$N][PF$_6$] supporting electrolyte (0.1 M), 0.1 V s^{-1} scan rate and 5 second equilibrium time. Referenced to the Fc*/Fc*$^+$ couple of doped samples (−0.56 V relative to Fc/Fc$^+$).*

The complex *trans*-[Ru(dppe)$_2$(C≡P)$_2$] **4.8** (**Figure 5-17**) exhibits two oxidative events at 0.16 V and 1.11 V, the first corresponding to the Ru(II/III) couple, alongside a reductive event at −0.93 V. Comparative to that seen in **4.3** and RuH(dppe)$_2$(C≡P) a shift to a more positive potential is observed for the oxidative event. Interestingly, when directly comparing the potentials of the main oxidation events of **4.3** (E_{pa} = 0.36 V) and **4.8** (E_{pa} = 0.16 V), the potential of **4.3** is more positive which is consistent with the relative electronegativities of nitrogen and phosphorus (3.0 *vs* 2.1) and is consistent with that seen in the comparison of RuH(dppe)$_2$(CN) (E_{pa} = 0.28 V) to RuH(dppe)$_2$(CP) (E_{pa} = −0.11 V). The second oxidation event seen in **4.8** has been associated with the Ru(III/IV) oxidation as seen in the *trans*-alkynyl cyaphides (See section: **2.2.5**), ruthenium bis(acetylides) complexes and [Ru(β-diketonato)$_3$] compounds (Ru(III/IV) E_{pa} = 0.44 to 1.30V).[125,126]

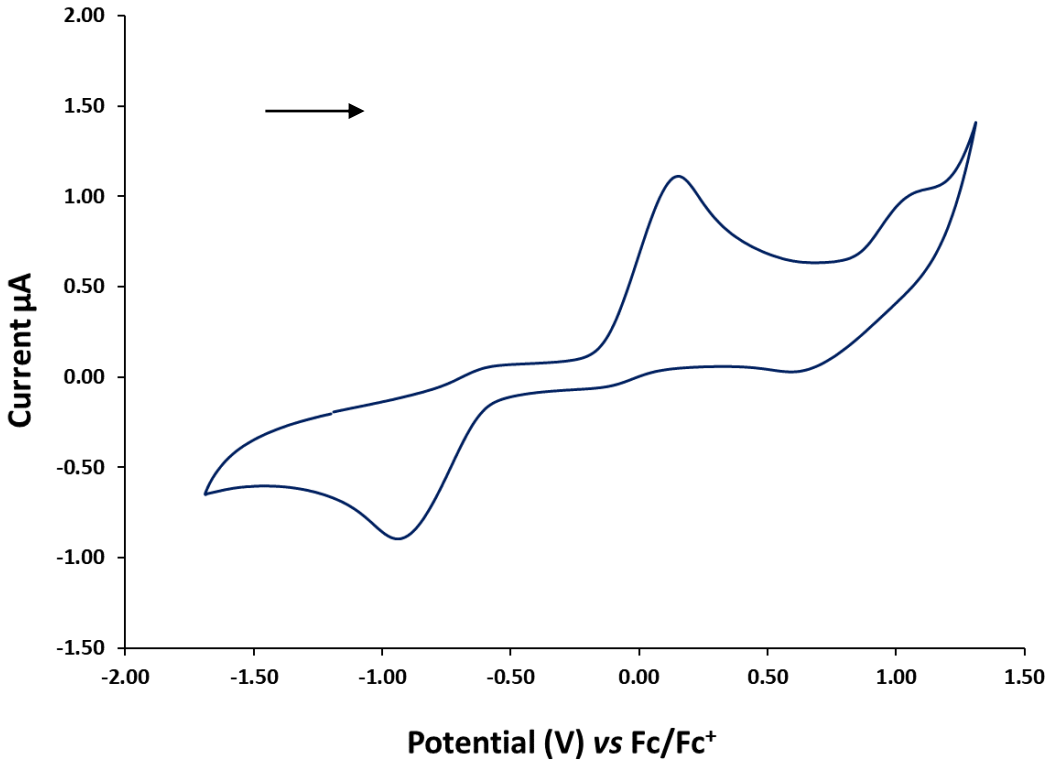

Figure 5-17: *Cyclic Voltammogram for **4.8** as a solution in CH_2Cl_2 (0.01M) with [^{n}Bu$_4$N][PF$_6$] supporting electrolyte (0.1 M), 0.1 V s^{-1} scan rate and 5 second equilibrium time. Referenced to the Fc*/Fc*$^+$ couple of doped samples (−0.56 V relative to Fc/Fc$^+$).*

5.5 SPECTROELECTROCHEMISTRY

The spectroelectrochemistry of **3.3**, **3.4**, **4.1**$^{+}$ and **4.8** was studied to observe the changes in the UV-vis and IR spectrum upon oxidation (**3.3**, **3.4** and **4.8**) and reduction (**4.1**$^{+}$), in order to gain insight into the electro-generated species. The spectroelectrochemistry experiments were carried out using an OTTLE cell with DCM solutions of 0.1 mol dm^{-3} of electrolyte and 0.001 mol dm^{-3} of analyte. In all of **3.3**, **3.4**, **4.1**$^{+}$ and **4.8** there were significant changes within the recorded UV-vis spectra upon oxidation/reduction however, there was no observable changes within the IR spectra.

The solutions of **3.3 and 3.4** (**Figure 5-18**, **––Start**) exhibit near-UV absorptions at 210-290 nm tailing off into the visible region with a shoulder at 300/280nm, with no observable absorbance after this point. Upon oxidation (**––Peak Oxidation**) the UV-spectrum for **3.3** shows a shift in the shoulder feature at 300 nm to a lower wavelength, 250 nm, tailing off at 310 nm. In addition, a significant absorption at 390 nm is detected upon oxidation. In contrast **3.4** exhibits a decrease in absorption in the near-UV region with a slight shift in the shoulder feature to increased wavelengths upon oxidation (**––Peak Oxidation**); furthermore, a significant absorption at 400 nm is observed comparable to that seen for **3.3**. In the UV-spectra for both **3.3** and **3.4** the intensity of the absorption at 390 nm/400 nm reduces after the oxidation event is complete (**––After Oxidation**) while the shoulder feature moves to lower energy for **3.3**, in contrast for **3.4** and the near-UV absorptions at 210-290 nm remain changed. Furthermore, for both **3.3** and **3.4**, during the oxidation the development of a feature around 500-510 nm is observed. For **3.3** upon reduction (**––After Reduction**) the absorption at 390 nm and the shoulder feature are lost with strong near-UV absorptions at 210-310 nm tailing off into the visible region, in comparison no changes were observed for **3.4** upon reduction.

The formation of the new feature upon oxidation at 390-400 nm for both **3.3** and **3.4** is probably due to transitions into the SOMO (HOMO for non-oxidised) which are most likely to be transitions into the cyaphide π-orbitals and the ruthenium metal centre. The changes in the UV-spectra upon the reduction event are in the near-UV region which in the neutral complexes is predominantly due to excitations to the LUMO and higher energy orbitals. The energy of the orbital involved in the reduction event (SOMO) can be estimated using the equation below (***Equation 1***) using the reductive potential, relative to the Fc/Fc^{+} couple:[193–198]

$$E = -\left(4.8 + E_{pc}\right) \qquad \textit{Equation 1}$$

Therefore, the energy of the SOMO for **3.3** and **3.4** can be estimated as E = −3.72 eV and E = −3.55 eV respectively. The energies of these orbitals lie close to that of the calculated HOMO for **3.3** and **3.4**, which are based on the ruthenium metal centre and cyaphide ligand, suggestive of no significant changes in the energy of the frontier orbitals upon oxidation and reduction during the electrochemical studies. However, caution needs to be taken as further calculations and experiments will be needed to fully identify the nature of these transitions.

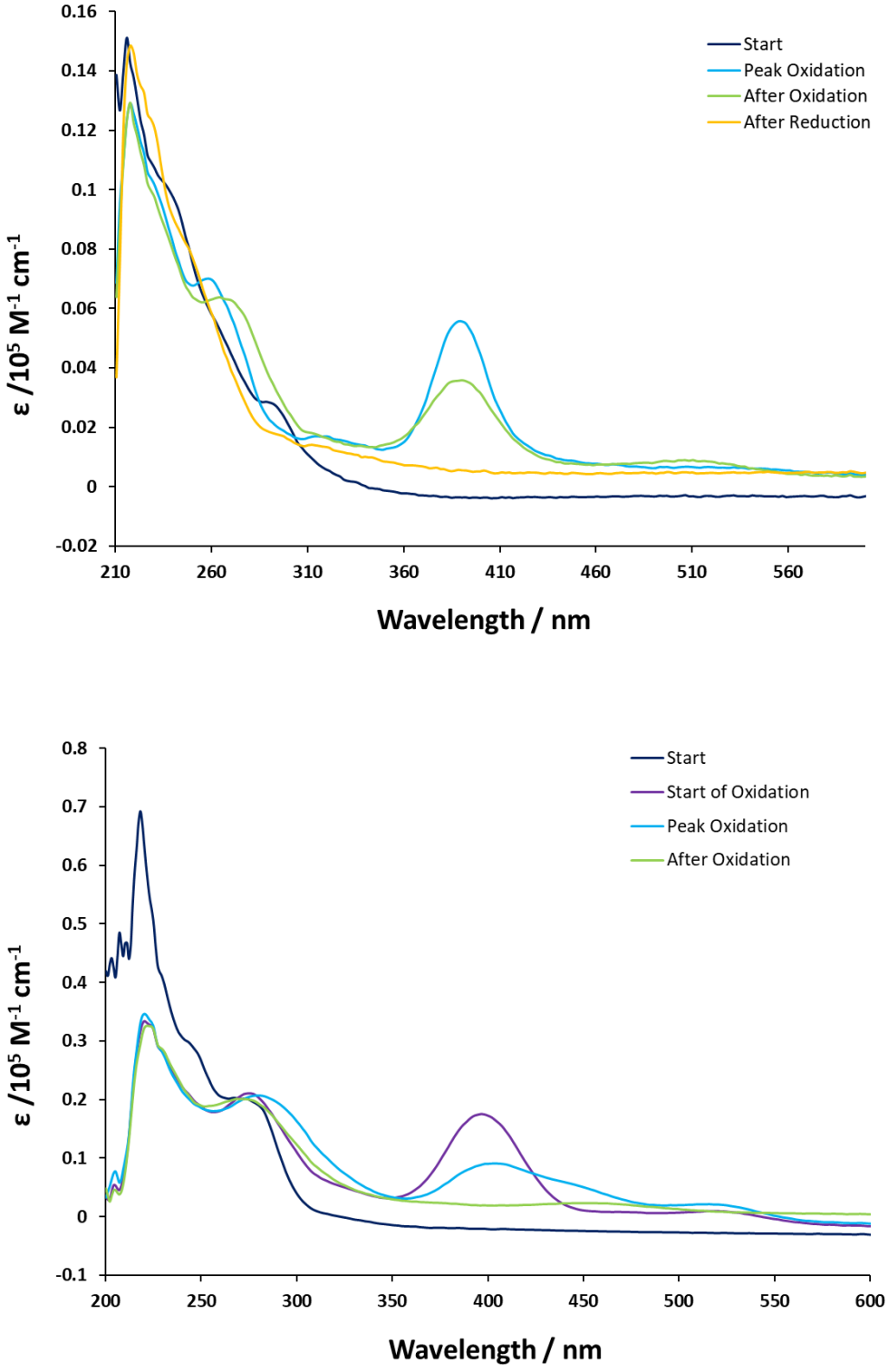

Figure 5-18: *Electronic absorption changes in the UV-vis spectra recoded during the irreversible oxidation and reduction events of* ***3.3*** *(Top) and* ***3.4*** *(Bottom) in an OTTLE cell. Conditions: 0.001 M solutions of analyte and 0.1M solutions of electrolyte [^{n}BuN][PF_6] in DCM.*

Unlike the previously studied, neutral 6-coordinate complexes, **3.3** and **3.4**, the purple DCM solution of **4.1**$^{+}$ exhibits no significant changes in the absorption spectra above 300 nm upon reduction or oxidation, with all the notable changes occurring in the near-UV range 210-230 nm (**Figure 5-19**). Upon the first reduction event (**––1st Reduction**) there is a significant increase in the molar absorption coefficient for the excitation at 217 nm, which then drops back after the event occurs. During the second reduction event (**––2nd Reduction**), the more significant reduction event seen in the cyclic voltammetry experiments, an increase in the absorption at 225 nm is observed. On the reverse scan, (**––1st Oxidation** / **––After 2nd Oxidation**) less significant changes occur in the UV-vis spectrum, with a reduction in the absorption at 225 nm and a slight increase in the absorption in the range 250-290 nm. The changes within the UV-vis spectrum upon reduction may be related to but cannot be assigned to the rearrangement from square based pyramidal to trigonal pyramidal geometry seen upon chemical reduction of **4.1**$^{+}$ (See section: **4.5.2**) without further calculations which were precluded by time constraints.

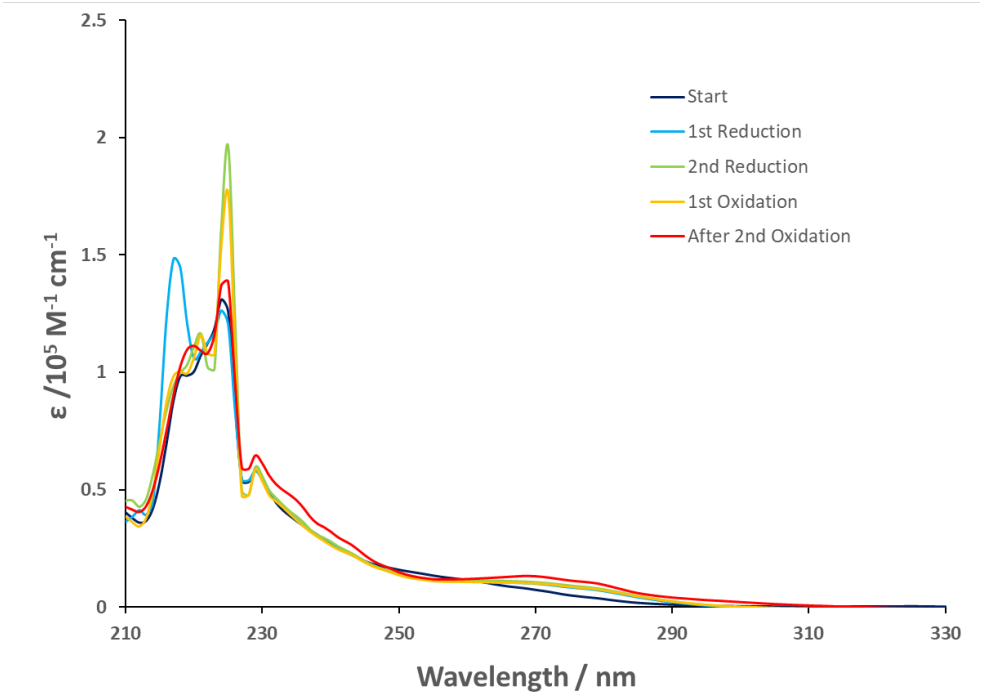

Figure 5-19: *Electronic absorption changes I the UV-vis spectra recoded during the irreversible oxidation and reduction events of* ***4.1***$^{+}$ *in an OTTLE cell. Conditions: 0.001 M solutions of analyte* ***4.1***$^{+}$ *and 0.1M solutions of electrolyte [*^{n}*BuN][PF*$_6$*] in DCM.*

The spectroelectrochemistry of **4.8** (**Figure 5-20**) was also studied and these spectroscopic data show that the pale-yellow DCM solution of **4.8** (**––Start**) exhibits near-UV absorptions at 210-350nm tailing off into the visible region, with no absorbance after this point. Upon oxidation (**––1st Oxidation**, **––2nd Oxidation**) a new absorption at 400-450 nm is observed comparable to that seen in **3.3** and **3.4**, which then reduces in intensity when the event is completed, in contrast an increase in intensity is observed for the near-UV peak at 210 nm (**––After Oxidation**). Upon reduction (**––Reduction**) this increase in absorption of the near-UV peak reduces in intensity which reduces further after the reduction event is over (**––After Reduction**). In addition, the IR spectrum was also monitored but showed no change. Overall, the spectroelectrochemistry of **4.8** is comparable to that of **3.3** and **3.4** and although no calculations on **4.8** have been undertaken the similarities in the resulting UV-vis spectra could suggest similar oxidative and reductive behaviour.

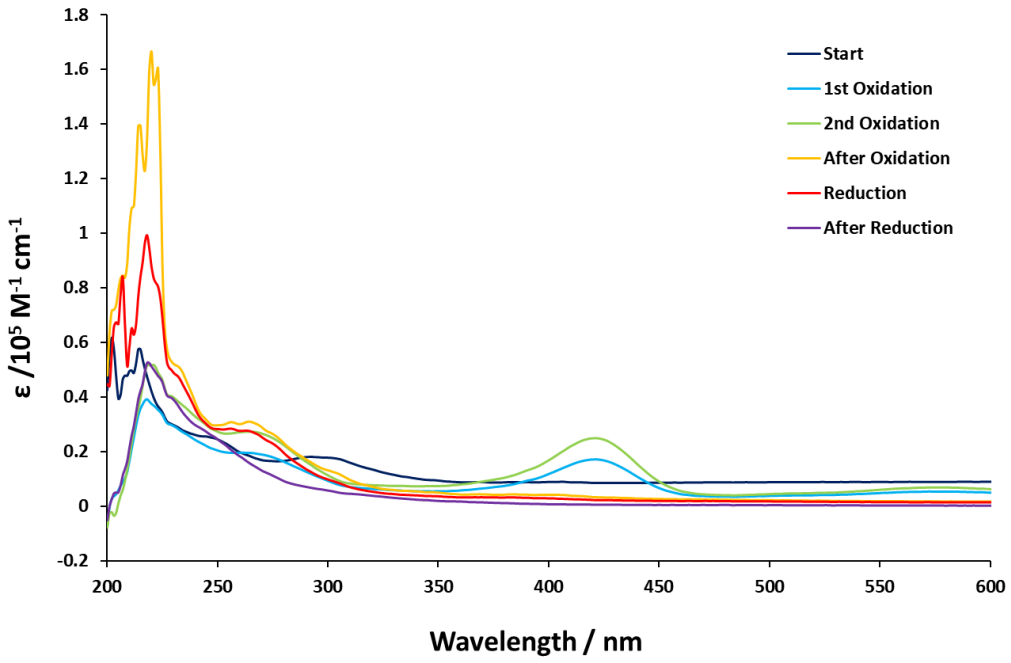

Figure 5-20: *Electronic absorption changes in the UV-vis spectra recoded during the irreversible oxidation and reduction events of* ***4.8*** *in an OTTLE cell. Conditions: 0.001 M solutions of analyte* ***4.8*** *and 0.1M solutions of electrolyte [^{n}BuN][PF_6] in DCM.*

5.6 CONCLUDING REMARKS

The DFT calculations have shown the frontier molecular orbitals of the cyaphide complexes, *trans*-[RuMe(dppe)$_2$(C≡P)] **3.3**, *trans*-[RuBr(dppe)$_2$(C≡P)] **3.4** and [Ru(dppe)$_2$(C≡P)]$^+$ **4.1**$^+$ to be comparable to those seen in the previously reported *trans*-alkynyl cyaphide complexes, with the HOMO/HOMO-1 being heavily associated with the π-orbitals of the C≡P bond and the ruthenium d-orbitals, while the LUMO/LUMO+1 is based on the dppe ancillary ligands. In addition, the calculations showed the frontier orbitals of **4.1**$^+$ to be significantly lower in energy and the LUMO having contribution from the dz^2 orbital on the ruthenium centre and σ-antibonding contribution for the cyaphide ligand. Furthermore, the UV-Vis spectra of the cyaphide complexes, **3.3**, **3.4** and **4.1**$^+$ were studied and exhibit high energy features between 200 nm and 400 nm and are in alignment with the computed spectra through TD-DFT calculations.

The electrochemistry **3.3**, **3.4**, **4.1**$^+$, **4.3** and **4.8** and spectroelectrochemistry of **3.3**, **3.4**, **4.1**$^+$ and **4.8** were studied to gain insight into the oxidative and reductive species. The cyclic voltammagrams for cyaphide complexes **3.3**, **3.4**, **4.3** and **4.8**, exhibited independent irreversible oxidation and reduction events for the Ru(II)/Ru(III) redox couple, with **4.1**$^+$ also exhibiting a pseudoreversible process, albeit weak. Furthermore, for **4.1**$^+$ the irreversible reductive feature (*ca* −2.00 V) was shown to be consistent with the observed chemical reduction of the 5-coordinate cyaphide complex. The spectroelectrochemistry studies of **4.1**$^+$ showed significant changes in the near-UV region upon reduction, although without further calculations which were precluded by time constraints, no definitive conclusions can be made. The spectroelectrochemistry of **3.3**, **3.4** and **4.8** was also undertaken; these showed the formation of a new feature upon oxidation at 390-400 nm which is most likely associated with transitions to both the cyaphide and ruthenium, also observed is a reduction in the strong absorption bands in the near-UV region which may be due to transitions from the SOMO to the LUMO. However, further calculations are needed to fully understand and conclude the nature of these transitions

CHAPTER 6 : EXPERIMENTAL

GENERAL EXPERIMENTAL PROCEDURES

Unless otherwise stated all materials were prepared and handled under an inert atmosphere (N_2 or Ar) using standard Schlenk line techniques or MBaun glove-box (catalytically purified N_2 or Ar). Solvents were distilled under N_2 from potassium (THF, toluene, benzene, 1,4-dioxane), sodium-potassium alloy (pentane, hexane, diethyl ether), calcium hydride (DCM, acetonitrile), or Mg/I_2 (methanol), degassed and stored under argon over potassium mirrors (pentane, hexane, toluene and diethyl ether), 4 Å molecular sieves (DCM, diethyl ether, benzene, 1,4-dioxane and THF) or 3 Å molecular sieves (methanol). Deuterated solvents for NMR spectroscopy were purchased from Goss Scientific (Cambridge) and were degassed using freeze-pump-thaw and heated under reflux over calcium hydride ($CDCl_3$, CD_2Cl_2) or potassium (d_8-THF, C_6D_6), then vacuum transferred and stored in ampoules under a nitrogen or argon atmosphere in the glove-box.

The following reagents were purchased from Sigma-Aldrich, Fisher Scientific, Fluorochem, or Acros organics, and used as supplied: AgOTf, $AgPF_6$, TlOTf, $NaPF_6$, CaH_2, dppe, $[FeCp_2][PF_6]$, $HC{\equiv}CC_6H_3$-3,5-CF_3, $HC{\equiv}CC_6H_5$, $HC{\equiv}C^tBu$, $HC{\equiv}C^nBu$, $HC{\equiv}CCO_2Me$, $HC{\equiv}CCO_2Et$, ^{n}BuLi (in hexanes, 2.5 M), PPh_3, $RuCl_3.3H_2O$, $[^NBu_4][PF_6]$ (electrochemical grade), and $ZnBr_2$. The following were purified prior to use as detailed: DABCO, $[FeCp_2]$, $[FeCp^*_2]$, and KO^tBu by sublimation, PCl_3, $Me_3SiC{\equiv}CH$, and Me_3SiCH_2Cl by distillation and DBU was dried over KOH for 48 h and purified by distillation. Anhydrous ZnX_2 were further purified by extended heating at >200 °C under high vacuum (10^{-7} mbar) and sublimation (>250 °C, 10^{-7} mbar)

TMSC≡P,[30,31] $HC{\equiv}CC_6H_4$-CO_2Et,[199] $RuCl_2(PPh_3)_3$,[125] $[RuCl(dppe)_2]OTf$,[125] 1,3,5-triethynylbenzene[200] and Me_2Mg[201] were prepared by literature methods. The compounds 2,5-diethynlthiophene,[202]

NaCN (Acros organics), CO (BOC), $NaBH_4$ (Sigma), $NaBPh_4$, NaC≡CH, NaOPh, $[Pd(PPh_3)_2Cl_2]$[203] $AuCl(PPh_3)$[204] were readily available in the lab.

Caution! Thallium(I) salts have acute toxicity through ingestion and inhalation, with potential long-term health impacts. Ensure that proper containment and personal protective equipment are used when handling these materials and all residues containing thallium are collected and labelled.

CHARACTERISATION DETAILS

The NMR spectra were recorded on a Varian VNMRS 400 spectrometer (^1H 399.5 MHz; ^{13}C 100.25 MHz; ^{19}F; 375.87 MHz, ^{31}P 161.7 MHz; ^{29}Si 79.4 MHz) and referenced to external $SiMe_4$, $CFCl_3$, or 85% H_3PO_4 as appropriate. Carbon spectra were assigned with reference to 2D (HSQC, HMBC) spectra, and all heteronuclear NMR spectra were recorded at 303 K unless otherwise stated.

UV-Vis spectra were recorded on either a Thermo Spectronic UV300 or a Perkin Elmer Lambda 265 instrument. IR spectra were recorded on a Perkin Elmer Spectrum One instrument in the solid state. Mass spectra were recorded by Dr A. Abdul-Sada of the University of Sussex departmental service, and elemental analyses were obtained from the London Metropolitan University Analytical Service, Elemental Microanalysis Ltd and Mikronanalytisches Labor Pascher.

Single crystal X-ray diffraction data were recorded on an Agilent Xcalibur Eos Gemini Ultra diffractometer with a CCD plate detector using Cu Kα (λ = 1.54184 Å) radiation. Structure solution and refinement were performed using SHELXT[205] and SHELXL,[206] respectively, running under Olex-2.[207]

ELECTROCHEMICAL DETAILS

Cyclic voltammetry studies were conducted under argon or nitrogen atmosphere in the glove box using an EmStat3+ Blue potentiostat under computer control at 298 K. Sample concentrations of 0.001 M (2 cm^3 DCM) were used throughout, alongside either 0.1 M [^{n}Bu$_4$][PF_6] or 0.1M [^{n}Bu$_4$][BArF] supporting electrolyte concentrations. All experiments were conducted using a standard three-electrode setup comprising of a platinum disc (1.6 mm) working electrode, platinum wire counter electrode, and a silver wire pseudoreference electrode. Potentials are reported relative to the [$FeCp_2$] 0/+ redox couple through the addition of an internal standard of either ferrocene or decamethylferrocene ($FeCp^*_2$, E½ = −0.56V vs ferrocene) unless otherwise stated.

Spectroelectrochemical studies were carried out under an argon atmosphere using an OTTLE Cell (Optically Transparent Thin Layer Electrode; Pt mesh working electrode, silver pseudo reference and Pt wire counter electrode) and EmStat3+ Blue potentiostat under computer control at 298 K. Sample concentrations of 0.001 M (5 cm^3 DCM) were used throughout, alongside either 0.1 M [^{n}Bu$_4$][PF_6] or 0.1M [^{n}Bu$_4$][BArF] supporting electrolyte concentrations.

CALIBRATION OF Me_3SiCP

$Me_3SiC{\equiv}P$ was synthesised following the literature procedure as a toluene solution and calibrated quantitatively using $^{31}P\{^1H\}$ NMR spectroscopy. To a measured volume of $Me_3SiC{\equiv}P$ solution (*ca* 0.4 cm^3), a known quantity of PPh_3 (*ca* 5 mg) in C_6D_6 was added. The solution was mixed in a Youngs' NMR tube until homogeneous. The $^{31}P\{^1H\}$ NMR spectrum was then recorded, with a d_1 relaxation delay of 56 seconds. Concentration was then calculated by integral comparison of the two resonances.

DFT CALCULATIONS

Calculations were performed using Gaussian 09 Revision D.01[208] running on the Sussex High Performance Cluster. Results were visualised using Gaussview 5.0; orbital contributions and UV-Vis spectra were obtained using GaussSum.[209] Geometries were optimised with the functional B3LYP, using Lanl2dz for Ru and 6-31G for all other atoms. Stationary points were characterised using frequency calculations and confirmed as minima on the basis of no imaginary frequencies. Excited states were calculated using TD-DFT with the first 100 excited states computed with a cpcm solvent model (DCM) with the B3LYP functional, using 3-21G on all atoms.

EXPERIMENTAL DETAILS FOR CHAPTER 2

SYNTHESIS OF *trans*-[RuCl(C≡CR)(dppe)$_2$]

Trans-[RuCl(C≡C^{n}Bu)(dppe)$_2$]

1-Hexyne (0.49 mL, 4.26 mmol) was degassed by freeze-thaw and DCM (*ca* 5 mL) was added. The solution was added to [RuCl(dppe)$_2$]OTf (2.00 g, 2.06 mmol) dissolved in DCM (20 mL) and left to stir overnight (*ca* 18 h), resulting in a colour change from red to brown. Solvent was removed under reduced pressure to afford a light brown solid, which was washed with hexane (3 x 15 mL) and dried under reduced pressure to afford *trans*-[RuCl(dppe)$_2$(=C=CH(^{n}Bu)]OTf. Yield: 1.714 g, 1.47 mmol, 71%. ^{1}H NMR ($CDCl_3$): δ_H 7.45 (4H, *m* (br), C_6H_5), 7.31 (8H, *t*, *J* = 7.0 Hz, C_6H_5), 7.23 (16H, *m* (br), C_6H_5), 7.06 (8H, *t*, *J* = 7.8 Hz, C_6H_5), 2.81 (8H, *m* (br), C_2H_4), 2.30 (1H, *quint*, *J* = 2.5 Hz, =C=CH), 1.46 (2H, *q*, *J* = 7.6 Hz, CH_2), 0.90 (2H, *m*, CH_2), 0.74 (3H, *t*, *J* = 7.3 Hz, CH_3). ^{31}P{^{1}H} NMR ($CDCl_3$): δ_P 42.3 (4P, *s*, $Ph_2PCH_2CH_2PPh_2$)

Trans-[RuCl(dppe)$_2$(=C=C(H)-^{n}Bu)]OTf (1.686 g, 1.45 mmol) in DCM (10 mL) was stirred until in solution (*ca* 5 min.) before DBU (0.45 mL, 3.01 mmol) was added, and the reaction mixture left to stir for 3 h. Removal of solvent under reduced pressure afforded a brown solid, which was

washed with methanol (3 x 15 mL) and dried under reduced pressure to afford a yellow-coloured solid. ^{1}H NMR ($CDCl_3$): δ_H 7.36 (16H, *m*, *J* = 29.7 Hz, C_6H_5), 7.21 (8H, *m, J* = 7.4 Hz, C_6H_5), 7.02 (16H, *q*, *J* = 7.1 Hz, C_6H_5), 3.51 (3H, *s*, OCH_3), 2.92 (8H, *t*, *J* = 6.6 Hz, C_2H_4), 2.23 (2H, *m*, C_2H_4), 1.50 (4H, *m*, C_2H_4), 1.14 (2H, *m,* CH_3). $^{31}P\{^{1}H\}$ NMR ($CDCl_3$): δ_P 48.3 (4P, s, $Ph_2PCH_2CH_2PPh_2$)

***Trans*-[RuCl(C≡C^{t}Bu)(dppe)$_2$]**

[RuCl(dppe)$_2$]OTf (1.72 g, 1.59 mmol) in DCM (20 mL) was stirred until in solution (*ca* 5 min.) before *tert*-butyl acetylene (0.4 mL, 3.27 mmol) was added, and the reaction mixture left to stir overnight (*ca* 18 h), resulting in a colour change from red to brown. The solution was filtered into hexanes (20 mL) forming a pink precipitate. Filtration yielded *trans*-[RuCl(dppe)$_2$(=C=CH(^{t}Bu)]OTf. Yield: 1.347 g, 1.16 mmol, 73%. ^{1}H NMR ($CDCl_3$): δ_H 7.5 (4H, *t*, *J* = 7.69 Hz, C_6H_5), 7.4 (8H, *m* (br), C_6H_5), 7.3 (8H, *t*, *J* = 7.48 Hz, C_6H_5), 7.2 (8H, *m* (br), C_6H_5), 7.0 (8H, *t*, *J* = 7.63 Hz, C_6H_5), 2.81 (8H, *m* (br), C_2H_4), 2.40 (1H, *m (br)*, =C=CH), 0.5 (9H, *s*, CH_3). $^{31}P\{^{1}H\}$ NMR ($CDCl_3$): δ_P 40.5 (4P, *s*, $Ph_2PCH_2CH_2PPh_2$).

Trans-[RuCl(dppe)$_2$(=C=CH(^{t}Bu))]OTf (1.347 g, 1.16 mmol) in DCM (15 mL) was stirred until in solution (*ca* 5 min.) before DBU (0.25 mL, 1.16 mmol) was added, and the reaction mixture left to stir for 3 h. Solvent was removed under reduced pressure, affording a brown solid, which was washed with degassed acetone (3 x 10mL) yielding a yellow solid. Yield: 0.927 g, 0.912 mmol, 79%. ^{1}H NMR (CD_2Cl_2): δ_H 8.2 (8H, *m (br),* C_6H_5), 7.3 (4H, *t*, *J* = 7.39 Hz, C_6H_5), 7.1 (12H, *m (br),* C_6H_5), 6.9 (8H, *t*, *J* = 7.6 Hz, C_6H_5), 6.7 (8H, *m (br),* C_6H_5), 2.92 (8H, *t*, *J* = 6.6 Hz, C_2H_4), 1.0 (9H, *s*, CH_3). $^{31}P\{^{1}H\}$ NMR (CD_2Cl_2): δ_P 52.3 (4P, *s*, $Ph_2PCH_2CH_2PPh_2$).

***Trans*-[RuCl(C≡CCO$_2$Me)(dppe)$_2$]**

[RuCl(dppe)$_2$]OTf (2.00 g, 2.06 mmol) in DCM (20 mL) was stirred until in solution (*ca* 5 min.) before methyl propiolate (0.2 mL, 2.25 mmol) was added, and the reaction mixture left to stir overnight (*ca* 18 h), resulting in a colour change from red to brown. Solvent was removed under reduced pressure to afford a light brown solid, which was washed with hexane (3 x 20 mL) and dried under reduced pressure to afford *trans*-[RuCl(dppe)$_2$(=C=CH(CO$_2$Me]OTf. Yield: 1.894 g, 1.63 mmol, 79%. ^{1}H NMR ($CDCl_3$): δ_H 7.45 (4H, *t*, *J* = 7.14 Hz, C_6H_5), 7.33-7.22 (20H, *m* (br), C_6H_5), 7.15 (8H, *m* (br), C_6H_5), 7.07 (8H, *t*, *J* = 7.7 Hz, C_6H_5), 3.44 (1H, *q*, *J* = 2.5 Hz, =C=CH), 3.07 (3H, *s*, OCH_3),), 2.85 (8H, *m (br)*, C_2H_4). ^{31}P{^{1}H} NMR ($CDCl_3$): δ_P 40.1 (4P, *s*, $Ph_2PCH_2CH_2PPh_2$)

Trans-[RuCl(dppe)$_2$(C=CH(CO$_2$Me))]OTf (5.018 g, 5.11 mmol) in DCM (10 mL) was stirred until in solution (*ca* 5 min.) before DBU (1.0 mL, 6.68 mmol) was added, and the reaction mixture left to stir for 3 h. Removal of solvent under reduced pressure afforded a brown solid, which was washed with degassed acetone (3 x 20 mL) and dried under reduced pressure to afford a cream-coloured solid. Yield: 1.085 g, 1.31 mmol, 26%. ^{1}H NMR ($CDCl_3$): δ_H 7.36 (16H, *m*, *J* = 29.7 Hz, C_6H_5), 7.21 (8H, *m, J* = 7.4 Hz, C_6H_5), 7.02 (16H, *q*, *J* = 7.1 Hz, C_6H_5), 3.51 (3H, *s*, OCH_3), 2.68 (8H, *t*, *J* = 6.6 Hz, C_2H_4). ^{31}P{^{1}H} NMR ($CDCl_3$): δ_P 48.1 (4P, s, $Ph_2PCH_2CH_2PPh_2$)

***Trans*-[RuCl(C≡CCO$_2$Et)(dppe)$_2$]**

[RuCl(dppe)$_2$]OTf (1.50 g, 1.55 mmol) in DCM (20 mL) and stir in solution (*ca* 5 min.) before ethyl propiolate (0.3 mL, 3.06 mmol) was added, and the reaction mixture left to stir overnight (*ca* 18 h), resulting in a colour change from red to brown. Solvent was removed under reduced pressure to afford a light brown solid, which was washed with hexane (3 x 15 mL) and dried under reduced pressure to afford *trans*-[RuCl(dppe)$_2$(=C=CH(CO$_2$Et)]OTf. Yield: 1.396 g, 1.2 mmol, 77%. ^{1}H NMR ($CDCl_3$): δ_H 7.36 (4H, *t*, *J* = 7.4 Hz, C_6H_5), 7.28 (16H, *m* (br), C_6H_5), 7.19 (8H, *m* (br), C_6H_5), 7.10 (8H, *t*, *J* = 7.6 Hz, C_6H_5), 3.66 (2H, *q*, *J* = 7.1 Hz, OCH_2), 3.36 (1H, *quint*, *J* = 2.56

Hz, =C=CH), 2.88 (8H, *m* (br), C_2H_4), 1.01 (3H, *t*, *J* = 7.2 Hz, CH_3). $^{31}P\{^1H\}$ NMR ($CDCl_3$): δ_P 40.4 (4P, *s*, $Ph_2PCH_2CH_2PPh_2$)

Trans-[RuCl(dppe)$_2$(C=CH(CO_2Et))]OTf (2.039 g, 1.91 mmol) in DCM (20 mL) was stirred until in solution (*ca* 5 min.) before DBU (0.6 mL, 4.01 mmol) was added, and the reaction mixture left to stir for 3 h. Removal of solvent under reduced pressure afforded a brown solid, which was washed with methanol (3 x 15 mL) and dried under reduced pressure to afford a cream-coloured solid. ^1H NMR ($CDCl_3$): δ_H 7.34 (16H, *m*, *J* = 29.7 Hz, C_6H_5), 7.19 (8H, *q, J* = 7.4 Hz, C_6H_5), 7.01 (16H, *q*, *J* = 7.1 Hz, C_6H_5), 3.95 (2H, *q*, *J* = 7.1 Hz, OCH_2), 2.68 (6H, *m* (br), C_2H_4), 1.21 (3H, *t, J* = 7.1 Hz, CH_3). $^{31}P\{^1H\}$ NMR ($CDCl_3$): δ_P 48.2 (4P, *s*, $Ph_2PCH_2CH_2PPh_2$)

***Trans*-[RuCl(C≡CC_6H_4-*p*-CO_2Et)(dppe)$_2$]**

[RuCl(dppe)$_2$]OTf (1.77 g, 1.63 mmol) and ethyl-4-ethylbenzoate (0.55 g, 3.16 mmol) were combined. DCM (20 mL) was added, and the reaction mixture left to stir overnight (*ca* 18 h), resulting in a colour change from red to brown. Solvent was removed under reduced pressure to afford a light brown solid, which was washed with hexane (3 x 15 mL) and dried under reduced pressure to afford *trans*-[RuCl(dppe)$_2$(=C=CH(C_6H_4-*p*-CO_2Et)]OTf. Yield: 1.506 g, 1.36 mmol, 83%. ^1H NMR ($CDCl_3$): δ_H 7.40 (12H, *m* (br), C_6H_5), 7.30 (12H, *m* (br), C_6H_5), 7.10 (16H, *dt*, *J* = 7.13 Hz, C_6H_5), 5.74 (2H, *m (br),* C_6H_4), 4.80 (1H, *m (br),* =C=CH), 4.30 (2H, *q*, *J* = 7.13 Hz, OCH_2), 3.00 (8H, *m (br),* C_2H_4), 1.40 (3H, *t*, *J* = 7.12 Hz, OCH_3). $^{31}P\{^1H\}$ NMR ($CDCl_3$): δ_P 35.7 (4P, *s*, $Ph_2PCH_2CH_2PPh_2$).

Trans-[RuCl(dppe)$_2$(=C=CH(C_6H_4)-*p*-CO_2Et)]OTf (1.506 g, 1.36 mmol) in DCM (15 mL) was stirred until in solution (*ca* 5 min.) before DBU (0.3 mL, 2.0 mmol) was added and the reaction mixture left to stir for 3 h. Removed solvent under reduced pressure, affording a brown solid, which was washed with degassed acetone (3 x 10mL) yielding a yellow solid. Yield: 0.789 g, 0.912 mmol, 52%. ^1H NMR (CD_2Cl_2): δ_H 7.80 (2H, *d, J* = 8.42 Hz, C_6H_4), 7.50 (8H, *m* (br), C_6H_5), 7.40 (8H, *m* (br), C_6H_5), 7.21 (8H, *q, J* = 7.42 Hz, C_6H_5), 7.00 (16H, *dt*, *J* = 7.61 Hz, C_6H_5), 6.60 (2H, *d, J* = 8.42 Hz,

C_6H_4), 4.40 (2H, *q*, *J* = 7.13 Hz, OCH_2), 2.70 (8H, *m (br),* C_2H_4), 1.40 (3H, *t*, *J* = 7.14 Hz, OCH_3). $^{31}P\{^1H\}$ NMR (CD_2Cl_2): δ_P 49.1 (4P, *s*, $Ph_2PCH_2CH_2PPh_2$).

***Trans*-[RuCl(C≡CC_6H_3-3,5-(CF_3)$_2$)(dppe)$_2$]**

[RuCl(dppe)$_2$]OTf (1.024 g, 0.946 mmol) and 1-ethynyl-3,5-bis(trifluoromethyl)benzene (0.33 cm^3, 1.87 mmol) were combined. DCM (20 mL) was added and the reaction mixture left to stir overnight (*ca* 18 h), resulting in a colour change from red to brown. Solvent was removed under reduced pressure to afford a light brown solid, which was washed with hexane (3 x 15 mL) and dried under reduced pressure to afford *trans*-[RuCl(dppe)$_2$(=C=CH(C_6H_3-3,5-(CF_3)$_2$)]OTF. Yield: 0.971 g, 0.928 mmol, 98%.^{1}H NMR (CD_2Cl_2): δ_H 6.56 (4H, *t*, *J* = 7.44 Hz), C_6H_5), 6.45 (20H, *m* (br), C_6H_5), 6.32 (8H, *t*, *J* = 7.67 Hz, C_6H_5), 6.24 (8H, *t*, *J* = 7.16 Hz, C_6H_5), 4.52 (1H, *s,* $C_6H_3F_2$), 4.50 (2H, *m (br),* $C_6H_3F_2$), 4.40 (1H, quint, *J* = 2.9 Hz*,* =C=CH), 2.10 (8H, *m (br),* C_2H_4). $^{31}P\{^1H\}$ NMR (CD_2Cl_2): δ_P 33.9 (4P, *s*, $Ph_2PCH_2CH_2PPh_2$).

Trans-[RuCl(dppe)$_2$(=C=CH(C_6H_3-3,5-(CF_3)$_2$)]OTf (0.971 g, 0.928 mmol) in DCM (10 mL) stirred until in solution (*ca* 5 min.) before DBU (0.2 mL, 1.34 mmol) was added and the reaction mixture left to stir for 2 h. Removed solvent under reduced pressure, affording a brown solid. Washed with degassed acetone (3 x 10mL) yielding a yellow solid. Yield: 0.516 g, 0.44 mmol, 47%. ^{1}H NMR (CD_2Cl_2): δ_H 7.63 (8H, *m(br)*, C_6H_5), 7.39 (1H, *s*, $C_6H_3F_2$), 7.24 (4H, *t*, *J* = 7.40 Hz, C_6H_5), 7.18 (4H, *t*, *J* = 7.42 Hz, C_6H_5), 7.11 (16H, *m* (br), C_6H_5), 6.91 (8H, *t*, *J* = 7.61 Hz, C_6H_5), 6.75 (2H, *s,* $C_6H_3F_2$), 2.67 (8H, *m (br),* C_2H_4). $^{31}P\{^1H\}$ NMR (CD_2Cl_2): δ_P 48.3 (4P, *s*, $Ph_2PCH_2CH_2PPh_2$).

SYNTHESIS OF *trans*-[Ru(P≡CSiMe$_3$)(C≡CR)(dppe)$_2$]$^+$

Trans-[Ru(P≡CSiMe$_3$)(C≡C^{n}Bu)(dppe)$_2$]$^+$ (2.1a$^+$)

Trans-[RuCl(dppe)$_2$(C≡C^{n}Bu)] (0.213 g, 0.161 mmol) and TlOTf (0.0814 g, 0.23 mmol) combined, DCM (*ca* 15 mL) added, left to stir for 10 min. Me$_3$SiCP (2 mL, 0.082 moldm^{-3}, 0.164 mmol) added stirred for 1 h. The reaction mixture was then filtered, and the solvent removed under reduced pressure to afford a yellow/brown solid, which was washed with benzene (2 x 50 mL) and dried under reduced pressure. DCM (*ca* 10 mL) was added then removed under reduced pressure. Yield: 0.184 g, 0.15 mmol, 93%. ^{1}H (CDCl$_3$) NMR: δ_H 7.67 (8H, *m*, C$_6$H$_5$), 7.37 (8H, *t*, *J* = 7.4 Hz, C$_6$H$_5$), 7.14 (16H, *q*, *J* = 7.6 Hz, C$_6$H$_5$), 7.01 (8H, *m*, C$_6$H$_5$), 2.81 (8H, *t*, *J* = 8.4 Hz, C$_2$H$_4$), 2.04 (2H, *m*, CH$_2$), 1.31 (4H, *m*, C$_2$H$_4$), 0.88 (3H, *t* (*J* = 7.1 Hz, CH$_3$), -0.14 (9H, *s*, SiMe$_3$) ^{13}C{^{1}H}-NMR (CDCl$_3$): δ_C 187.0 (*d, J* = 88 Hz, C≡P), 135.0 (*dqnt, J* = 173, 11 Hz, C$_6$H$_5$), 133.0 (*dqnt, J* = 140*,* 3 *Hz,* C$_6$H$_5$), 131.0 (*d, J* = 6 Hz, C$_6$H$_5$), 128.0 (*dqnt, J* = 41, 2 *Hz,* C$_6$H$_5$), 123.0 (*qnt, J* = 321 Hz, Ru–C≡C), 116.0 (*d (br), J* = 22 Hz, Ru–C≡C), 31.5 (*s*, C$_4$H$_9$), 31.0 (*qnt, J* = 12 Hz, C$_2$H$_4$), 23.1 (*s*, C$_4$H$_9$), 23.1 (*s*, C$_4$H$_9$), 14.3 (*s*, C$_4$H$_9$), 0.9 (*s*, Si(CH$_3$)$_3$). ^{31}P{^{1}H} (CDCl$_3$) NMR: δ_P 115.1, (1 P, m, P≡C), 42.4 (4 P, d (J_{PP} = 32.5 Hz), Ph$_2$PCH$_2$CH$_2$PPh$_2$). ^{29}Si{^{1}H} (CD$_2$Cl$_2$) NMR: δ_{Si} −13.7 (*s*, Si(CH$_3$)$_3$). ^{19}F (CD$_2$Cl$_2$) NMR: δ_F −78.9 (*s*, OTf). ν_{max}/cm^{-1} : 1269 (C≡P), 2113 (C≡C). Crystal data for **2.1a$^+$**: Crystals were obtained as the PF_6 salt by slow recrystallization from CH_2Cl_2 and hexanes at ambient temperature. $C_{61}H_{64}P_5SiRu.PF_6$ (M_w = 1226.47 g mol^{-1}), monoclinic, $P2_{1/n}$, a = 18.1155(4) Å, b = 13.7132(2) Å, c = 23.8472(5) Å, α = 90°, β = 90.972(2)°, γ = 90°, V = 5923.3(2) Å^3, Z = 9, T = 100(2) K, μ(Cu $K\alpha$) = 9.232 mm^{-1}, D_c = 1.917 Mg m^{-3}, 32768 independent reflections, full matrix F^2 refinement R_1 = 0.0856 on 11283 independent absorption corrected reflections, [I > 2σ(I); 2ϑ_{max} = 142.322°], 744 parameters, wR_2 = 0.2335 (all data).

***Trans*-[Ru(P≡CSiMe$_3$)(C≡C^{t}Bu)(dppe)$_2$]$^+$ (2.1b$^+$)**

[RuCl(dppe)$_2$(C≡C^{t}Bu)] (0.297 g, 0.29 mmol) and TlOTf (0.1084 g, 0.31 mmol) combined in DCM (*ca* 15 mL) stirred for *ca* 10 min. Me$_3$SiCP (5.0 mL, 0.073 mol dm^{-3}, 0.37 mmol) was added to the solution and stirred for *ca* 1 hour. Filtered and removed solvent under reduced pressure to afford a yellow/brown solid, which was washed with benzene (2 x 50 mL) and dried under reduced pressure. DCM (*ca* 10 mL) was added then removed under reduced pressure to yield a yellow solid. Yield: 0.234 g, 0.22 mmol, 76%. ^{1}H (CD_2Cl_2) NMR: δ_H 8.13 (8H, *m (br),* C_6H_5), 7.46 (4H, *t*, *J* = 7.4 Hz, C_6H_5), 7.35 (4H, *t*, *J* = 7.5 Hz, C_6H_5), 7.26 (9H, *t*, *J* = 7.6 Hz, C_6H_5), 7.09 (9H, *t*, *J* = 7.6 Hz, C_6H_5), 6.75 (9H, *m (br),* C_6H_5), 2.90 (4H, *m (br)*, C_2H_4), 2.34 (4H, *m (br)*, C_2H_4), 1.07 (9H, *s*, CH_3), -0.16 (9H, *s*, $SiMe_3$). ^{31}P{^{1}H} (CD_2Cl_2) NMR: δ_P 114.1 (1P, *qnt*, *J* = 33 Hz, P≡C), 44.6 (4P, *s*, $Ph_2PCH_2CH_2PPh_2$).^{29}Si{^{1}H} (CD_2Cl_2) NMR: δ_{Si} −13.5 (*s*, $Si(CH_3)_3$). ^{19}F (CD_2Cl_2) NMR: δ_F −78.9 (*s*, OTf). ν_{max}/cm^{-1}: 1265 (C≡P), 2163 (C≡C).

***Trans*-[Ru(P≡CSiMe$_3$)(C≡CCO$_2$Me)(dppe)$_2$]$^+$ (1.58g$^+$)**

Trans-[RuCl(dppe)$_2$(C≡CCO$_2$Me)] (1.085 g, 1.31 mmol) and TlOTf (0.485 g, 1.37 mmol) combined, DCM (*ca* 20 mL) added, left to stir for 10 min. Me$_3$SiCP (16 mL, 0.0804 mol dm^{-3}, 1.31 mmol) added stirred for 1 h. The reaction mixture was then filtered, and the solvent removed under reduced pressure to afford a yellow/brown solid, which was washed with benzene (2 x 50 mL) and dried under reduced pressure. DCM (*ca* 10 mL) was added then removed under reduced pressure. Yield: 0.872 g, 0.82 mmol, 60%.^{1}H NMR (CD_2Cl_2): δ_H 7.50 (12H, *m (br)*, C_6H_5), 7.40 (4H, *t*, *J* = 6.5 Hz, C_6H_5), 7.24 (8H, *t*, *J* = 7.62 Hz, C_6H_5), 7.15 (16H, *t*, *J* = 7.49 Hz, C_6H_5) 3.70 (2H, *s,* OCH_3), 2.82 (8H, m (br), PC_2H_4P), -0.10 (9H, *s*, $SiCH_3$). ^{31}P{^{1}H} NMR (CD_2Cl_2): δ_P 108.0 (1P, *quint*, *J* = 35 Hz, P≡C) 41.1 (4P, *d*, *J* = 35 *Hz,* $Ph_2PCH_2CH_2PPh_2$).

***Trans*-[Ru(P≡CSiMe$_3$)(C≡CCO$_2$Et)(dppe)$_2$]$^+$ (1.58f$^+$)**

Trans-[RuCl(dppe)$_2$(C≡CCO$_2$Et)] (0.610 g, 0.592 mmol) and TlOTf (0.219 g, 0.619 mmol) combined, DCM (*ca* 20 mL) added, left to stir for 10 min. Me$_3$SiCP (9.0 mL, 0.0723 mol dm^{-3}, 0.651 mmol) added stirred for 1 h. The reaction mixture was then filtered, and the solvent removed under reduced pressure to afford a yellow/brown solid. Washed with benzene (3 x 15 mL) and dried under reduced pressure. DCM (*ca* 10 mL) was added then removed under reduced pressure. Yield: 0.577 g, 0.46 mmol, 77%. ^{1}H NMR (CD_2Cl_2): δ_H 7.45 (12H, *t*, *J* =7.1 Hz, C_6H_5), 7.38 (4H, *t*, *J* = 7.5 Hz, C_6H_5), 7.23 (8H, *t*, *J* = 7.64 Hz, C_6H_5), 7.15 (16H, *t*, *J* = 7.5 Hz, C_6H_5) 4.12 (2H, *q, J* = 7.1 Hz, OCH_2), 2.82 (8H, *m* (*br*), C_2H_4), 1.30 (3H, *t, J* = 7.1 Hz, CH_3), -0.1 (9H, *s*, $SiCH_3$). ^{13}C{^{1}H}-NMR (CD_2Cl_2): δ_C 193.5 (*d, J* = 86 Hz, C≡P) 153.1 (*s*, C=O), 134.1 (*dqnt, J* = 85, 2.4 Hz, C_6H_5), 131.9 (*d, J* = 32 Hz, C_6H_5), 132.5 (*dqnt*, *J* = 214, 11.6 Hz), ipso-C_6H_5), 129.3 (*dqnt, J* = 22, 2.2 Hz, C_6H_5), 123 (*qnt, J* = 321 Hz, Ru–C≡C), 110 (*d (br), J* = 22 Hz, Ru–C≡C), 61.3 (*s*, OCH_2), 30.2 (*qnt, J* = 11.7 Hz, C_2H_4), 15.2 (*s*, CH_3), −0.1 (*s*, $Si(CH_3)_3$). ^{31}P{^{1}H} NMR (CD_2Cl_2): δ_P 108 (1P, *quint*, *J* = 35 Hz, P≡C) 41.3 (4P, *d*, *J = 35 Hz,* $Ph_2PCH_2CH_2PPh_2$). ν_{max}/cm^{-1}: 1268 (C≡P), 1688 (C≡O), 2094 (C≡C).

***Trans*-[Ru(P≡CSiMe$_3$)(C≡CC$_6$H$_4$-*p*-CO$_2$Et)(dppe)$_2$]$^+$ (2.1c$^+$)**

Trans-[RuCl(dppe)$_2$(C≡C(C_6H_5)-*p*-CO_2Et)] (0.789 g, 0.71 mmol) and TlOTf (0.260 g, 0.74 mmol) combined, DCM (*ca* 20 mL) added, left to stir for 10 min. Me$_3$SiCP (10 mL, 0.073 mol dm^{-3}, 0.73 mmol) added stirred for 1 h. The reaction mixture was then filtered, and the solvent removed under reduced pressure to afford a yellow/brown solid. Washed with benzene (3 x 15 mL) and dried under reduced pressure. DCM (*ca* 10 mL) was added then removed under reduced pressure. Yield: 0.606 g, 0.45 mmol, 63%. ^{1}H NMR ($CDCl_3$): δ_H 7.90 (2H, *d, J* = 8.22 Hz, C_6H_4), 7.60 (8H, *m* (br), C_6H_5), 7.40 (4H, *t, J* = 7.5 Hz, C_6H_5), 7.30 (4H, *t, J* = 7.5 Hz, C_6H_5), 7.20 (8H, *t, J* = 7.8 Hz, C_6H_5), 7.10 (16H, *m (br)*, C_6H_5), 6.80 (2H, *d, J* = 8.3 Hz, C_6H_4), 4.40 (2H, *q*, *J* = 7.1 Hz, OCH_2), 2.90 (8H, *m (br),* C_2H_4), 1.40 (3H, *t*, *J* = 7.1 Hz, OCH_3), -0.16 (9H, *s*, $SiMe_3$). ^{13}C{^{1}H} NMR (CD_2Cl_2): δ_C 191.0 (*d, J* = 88 Hz, C≡P), 167.0 (s, C=O), 134.2 (*dqnt, J* = 110, 2.4 Hz, C_6H_5), 134.1 (*dqnt, J* =

187, 11.4 Hz, C_6H_5), 131.8 (*d*, *J* = 7.57 Hz), 130.0 (*m,* C_6H_5), 129.2 (*dqnt, J* = 17.1, 2.34 Hz, C_6H_5), 61.1 (s, OCH2), 31.2 (*qnt, J* = 11.6 Hz, C_2H_4), 15.0 (s, CH_3), 0.9 (m (br), $Si(CH_3)_3$). $^{31}P\{^1H\}$ NMR (CD_2Cl_2): δ_P 110.8 (1P, *qnt*, *J* = 33 Hz, P≡C), 41.8 (4H, *d*, *J* = 33 Hz, $Ph_2PCH_2CH_2PPh_2$). ν_{max}/cm^{-1}: 1264 (C≡P), 1702 (C≡O), 2094 (C≡C).

***Trans*-[Ru(P≡CSiMe$_3$)(C≡CC$_6$H$_4$-3,5-(CF$_3$)$_2$)(dppe)$_2$]$^+$ (2.1d$^+$)**

Trans-[RuCl(dppe)$_2$(C≡CC$_6$H$_4$-3,5-(CF$_3$)$_2$)] (0.504 g, 0.43 mmol) and $AgPF_6$ (0.112 g, 0.44 mmol) combined, DCM (*ca* 20 mL) added, left to stir for 10 min. Me_3SiCP (10 mL, 0.064 mol dm^{-3}, 0.64 mmol) added stirred for 1 h. The reaction mixture was then filtered, and the solvent removed under reduced pressure to afford a yellow/brown solid, which was washed with benzene (3 x 15 mL) and dried under reduced pressure. DCM (*ca* 10 mL) was added then removed under reduced pressure. Yield: 0.338 g, 0.24 mmol, 56%. ^1H NMR (CD_2Cl_2): δ_H 7.67 (1H, *s, p*-ArF), 7.47 (12H, *m, o/p*-C_6H_5), 7.40 (4H, *t*, J_{HH} = 7.5 Hz, *p*-C_6H_5), 7.25 (8H, *t,* J_{HH} = 7.5 Hz, *m*-C_6H_5), 7.20 (8H, *m (br), o*-C_6H_5), 7.10 (8H, *t,* J_{HH} = 7.5 Hz, *m*-C_6H_5), 6.99 (2H, *s*, *o*-ArF), 2.83 (8H, *m (br),* C_2H_4), −0.05 (9H, *s*, $SiMe_3$). $^{13}C\{^1H\}$-NMR (CD_2Cl_2): δ_C 192.0 (*d, J* = 88 Hz, C≡P), 134.3 (*m (br),* ipso-ArF), 133.6 (*m (br),* o-C_6H_5), 132.5 (*quint,* J_{CP} = 11 Hz, *ipso*-C_6H_5), 131.9 (*s, p*-C_6H_5), 131.8 (*q,* J_{CF} = 32 Hz, *m*-ArF), 131.7 (*s, p*-C_6H_5), 130.8 (*m (br), o*-ArF), 129.2 (*m, m*-C_6H_5), 129.1 (*m, m*-C_6H_5), 124.0 (*q,* J_{CF} = 272 Hz, CF_3), 119.6 (*m (br), p*-ArF), 113.2 (*dm,* J_{CP} = 27 Hz, Ru-C≡C), 30.7 (*quint,* J_{CP} = 11 Hz, C_2H_4), 0.8 (*s*, $SiMe_3$). $^{31}P\{^1H\}$ NMR (CD_2Cl_2): δ_P 108.8 (1P, *qnt*, *J* = 35 Hz, P≡C), 41.6 (4P *d*, *J* = 35 Hz, $Ph_2PCH_2CH_2PPh_2$), −142.3 (1P, *sept*, J_{PF} = 710 Hz, PF_6). ^{19}F NMR (CD_2Cl_2): δ_F −63.3 (*s*, CF_3), −73.4 (*d*, J_{FP} = 710 Hz, PF_6). ν_{max}/cm^{-1}: 1276 (C≡P), 2076 (C≡C).

SYNTHESIS OF *trans*-[Ru(C≡P)(C≡CR)(dppe)$_2$]

Trans-[Ru(C≡P)(C≡C^{n}Bu)(dppe)$_2$] (2.2a)

Trans-[Ru(dppe)$_2$(C≡C^{n}Bu)(η^1-P≡CSiMe$_3$)]OTf (0.987 g, 0.932 mmol) and KO^{t}Bu (0.129 g, 1.15 mmol) combined, THF (*ca* 20 mL) added, giving an orange solution. Left to stir for *ca* 1 hour. Removed solvent under reduced pressure until a white precipitate started to form. Filtered and removed the remaining solvent under reduced pressure. Washed with degassed water (3 x 10 mL). Added benzene (*ca* 10 mL), removed under reduced pressure and dried under vacuum. Yield: 0.439 g, 0.430 mmol, 46%. ^{1}H (CD_2Cl_2) NMR: δ_H 7.60 (8H, *m (br),* C_6H_5), 7.50 (8H, *m (br),* C_6H_5), 7.25 (4H, *t*, *J* = 7.5 Hz, C_6H_5), 7.19 (4H, *t*, *J* = 7.4 Hz, C_6H_5), 7.05 (8H, *t*, *J* = 7.6 Hz, C_6H_5), 6.99 (8H, *t*, *J* = 7.6 Hz, C_6H_5), 2.70 (4H, *m*, C_2H_4), 1.90 (4H, *m*, C_2H_4), 0.90 (3H, *t* (*J* = 6.9 Hz, CH_3). ^{13}C{^{1}H} NMR (CD_2Cl_2): δ_C 284.6 (*m (br),* C≡P), 138.7 (*dqnt, J* = 167, 11.5 Hz, C_6H_5), 139.5 (*m (br),* Ru–C≡C), 135.9 (*qnt*, *J* = 2 Hz, C_6H_5), 129.9 (*d, J = 21 Hz,* C_6H_5), 127.8 (*m (br),* C_6H_5), 118.4 (*s*, Ru–C≡C), 33.2 (*s*, C_4H_9), 32.3 (*qnt, J* = 12 Hz, C_2H_4), 23.1 (*s*, C_4H_9), 23.8 (*s*, C_4H_9), 14.8 (*s*, C_4H_9). ^{31}P{^{1}H} (CD_2Cl_2) NMR: δ_P 155.5 (1P, *m (br)*, C≡P), 50.9 (4P, *d*, *J* = 5.0 Hz, $Ph_2PCH_2CH_2PPh_2$). ν_{max}/cm^{-1}: 1241 (C≡P), 2090 (C≡C).

Trans-[Ru(C≡P)(C≡C^{t}Bu)(dppe)$_2$] (2.2b)

Trans-[Ru(dppe)$_2$(C≡C^{t}Bu)(η^1-P≡CSiMe$_3$)]OTf (0.096 g, 0.091 mmol) and KO^{t}Bu (0.013 g, 0.12 mmol) combined, THF (*ca* 10 mL) added, giving an orange solution. Left to stir for *ca* 1 hour. Removed solvent under reduced pressure until a white precipitate started to form. Filtered and removed the remaining solvent under reduced pressure. Washed with degassed water (3 x 5 mL). Added benzene (*ca* 5 mL), removed under reduced pressure and dried under vacuum. Yield: 0.051 g, 0.049 mmol, 54%. ^{1}H (CD_2Cl_2) NMR: δ_H 8.20 (8H, *m (br),* C_6H_5), 7.30 (4H, *t*, *J* = 7.5 Hz, C_6H_5), 7.10 (12H, *m (br),* C_6H_5), 6.90 (16H, *d*, *J* = 4.2 Hz, C_6H_5), 3.00 (4H, *m*, C_2H_4), 2.50 (4H, *m*, C_2H_4), 1.00 (3H, *s*, CH_3). ^{13}C{^{1}H} NMR (CD_2Cl_2): δ_C 281.1 (*m (br),* C≡P), 137.0 (*dqnt, J* = 331, 9.5 Hz,

C_6H_5), 135.6 (*qnt*, *J* = 2 Hz, C_6H_5), 134.2 (*m (br),* Ru–C≡C), 128.8 (*d, J = 93 Hz,* C_6H_5), 126.0 (*dqnt, J* = 34.9, 2 Hz, C_6H_5), 101.3 (*s*, Ru–C≡C), 31.5 (*qnt, J* = 11 Hz, C_2H_4), 31.4 (*s,* CH_3). $^{31}P\{^1H\}$ (CD_2Cl_2) NMR: δ_P 142.8 (1P, *m (br)*, C≡P), 52.9 (4P, *d*, *J* = 5.1 Hz, $Ph_2PCH_2CH_2PPh_2$). ν_{max}/cm^{-1}: 1251 (C≡P), 2083 (C≡C).

Trans-[Ru(C≡P)(C≡CCO$_2$Me)(dppe)$_2$] (1.59g)

Trans-[Ru(dppe)$_2$(C≡CCO$_2$Me)(η^1-P≡CSiMe$_3$)]OTf (0.872 g, 0.82 mmol) and KO^{t}Bu (0.100 g, 0.89 mmol) combined, THF (*ca* 20 mL) added, giving an orange solution. Left to stir for *ca* 1 hour. Removed solvent under reduced pressure until a white precipitate started to form. Filtered and removed the remaining solvent under reduced pressure. Washed with degassed water (3 x 10 mL). Added benzene (*ca* 10 mL), removed under reduced pressure and dried under vacuum. Yield: 0.309 g, 0.30 mmol, 37%. ^1H NMR (CD_2Cl_2): δ_H 7.60 (8H, *m (br),* C_6H_5), 7.40 (8H, *m (br),* C_6H_5), 7.29 (4H, *t*, *J* = 7.0 Hz, C_6H_5), 7.21 (4H, *t*, *J* = 7.0 Hz, C_6H_5), 7.10 (8H, *t*, *J* = 7.4 Hz, C_6H_5), 7.00 (8H, *t*, *J* = 7.4 Hz, C_6H_5), 3.50 (3H, *s*, OCH_3), 2.80 (8H, *m (br),* PC_2H_4P). $^{31}P\{^1H\}$ (CD_2Cl_2) NMR: δ_P 170.2 (1P, *m (br)*, C≡P), 51.6 (4P, *d*, *J* = 5.5 Hz, $Ph_2PCH_2CH_2PPh_2$).

Trans-[Ru(C≡P)(C≡CCO$_2$Et)(dppe)$_2$] (1.59f)

Trans-[Ru(dppe)$_2$(C≡CCO$_2$Et)(η^1-P≡CSiMe$_3$)]OTf (0.450 g, 0.36 mmol) and KO^{t}Bu (0.049 g, 0.44 mmol) combined, THF (*ca* 20 mL) added, giving an orange solution. Left to stir for *ca* 1 hour. Removed solvent under reduced pressure until a white precipitate started to form. Filtered and removed the remaining solvent under reduced pressure. Washed with degassed water (3 x 10 mL). Added benzene (*ca* 10 mL), removed under educed pressure and dried under vacuum. Yield: 0.251 g, 0.24 mmol, 60%. Anal. Found: C, 66.96%; H, 5.28 %. Calcd for $C_{58}H_{53}O_2P_5Ru$: C, 67.11%; H, 5.15%. ^1H NMR (CD_2Cl_2): δ_H 7.60 (8H, *m (br),* C_6H_5), 7.40 (8H, *m (br),* C_6H_5), 7.29 (4H, *t*, *J* = 7.4 Hz, C_6H_5), 7.21 (4H, *t*, *J* = 7.4 Hz, C_6H_5), 7.10 (8H, *t*, *J* = 7.6 Hz, C_6H_5), 7.0 (8H, *t*, *J* = 7.6 Hz, C_6H_5)

3.97 (2H, *q, J* = 7.1 Hz, OCH_2), 2.70 (8H, m (br), PC_2H_4P), 1.20 (3H, *t, J* = 7.10 Hz, CH_3). $^{13}C\{^1H\}$ NMR (CD_2Cl_2): δ_C 278.7 (*m (br),* C≡P), 152.0 (*s*, C=O), 141.8 (*m (br),* Ru–C≡C), 135.7 (*dqnt, J =* 111, 11 Hz, C_6H_5), 134.9 (*m (br),* C_6H_5), 134.2 (*qnt*, *J* = 2.3 Hz, C_6H_5), 129.0 (*d, J = 40 Hz,* C_6H_5), 127.0 (*dqnt*, *J* = 27, 2 Hz, C_6H_5), 112.1 (*s*, Ru–C≡C), 59.2 (*s*, OCH_2), 30.8 (*qnt, J* = 12 Hz, C_2H_4), 14.6 (*s*, CH_3). $^{31}P\{^1H\}$ (CD_2Cl_2) NMR: δ_P 168.3 (1P, *m (br)*, C≡P), 44.6 (4P, *d*, *J =* 4.7 Hz, $Ph_2PCH_2CH_2PPh_2$). ν_{max}/cm^{-1}: 1238 (C≡P), 1647 (CO), 2063 (C≡C).

***Trans*-[Ru(C≡P)(C≡CC_6H_4-*p*-CO_2Et)(dppe)$_2$] (2.2c)**

Trans-[Ru(dppe)$_2$(C≡C(C_6H_5)-*p*-CO_2Et)(η^1-P≡C$SiMe_3$)]OTf (0.589 g, 0.441mmol) and KO^{t}Bu (0.051 g, 0.45 mmol) combined, THF (*ca* 20 mL) added, giving an orange solution. Left to stir for *ca* 1 hour. Removed solvent under reduced pressure until a white precipitate started to form. Filtered and removed the remaining solvent under reduced pressure. Washed with degassed water (3 x 10 mL). Added benzene (*ca* 10 mL), removed under reduced pressure and dried under vacuum. Yield: 0.324 g, 0.29 mmol, 66%. ^1H NMR ($CDCl_3$): δ_H 7.76 (2H, *d, J* = 8.4 Hz, C_6H_4), 7.60 (8H, *m (br)*, C_6H_5), 7.50 (8H, *m (br)*, C_6H_5), 7.28 (4H, *t, J* = 7.4 Hz, C_6H_5), 7.19 (4H, *t, J* = 7.4 Hz, C_6H_5), 7.10 (8H, *t, J* = 7.6 Hz, C_6H_5), 6.95 (8H, *t, J* = 7.7 Hz, C_6H_5), 6.66 (2H, *d, J* = 8.4 Hz, C_6H_5), 4.33 (2H, *q, J* = 7.1 Hz, OCH_2), 2.80 (8H, *m (br),* C_2H_4), 1.38 (3H, *t*, *J* = 7.1 Hz, OCH_3).$^{13}C\{^1H\}$ NMR (CD_2Cl_2): δ_C 281.0 (*m (br),* C≡P), 168.0 (s, C=O), 142.3 (*m,* Ru–C≡C), 137.8 (*dqnt, J =* 327, 11 Hz, C_6H_5), 136.4 (*qnt, J* = 3 Hz, C_6H_5), 135.0 (*m (br),* C_6H_5), 129.6 (*d*, *J* = 94 Hz), 127.6 (*dqnt, J =* 35, 2 Hz, C_6H_5), 114.3 (*s,* Ru–C≡C), 68.6 (*s*, OCH_2), 32.3 (*qnt, J* = 12 Hz, C_2H_4), 32.2 (*s*, CH_3).$^{31}P\{^1H\}$ NMR (CD_2Cl_2): δ_P 164.9 (1P, *m (br)*, C≡P), 50.3 (4P, *d*, *J =* 4.5 Hz, $Ph_2PCH_2CH_2PPh_2$). ν_{max}/cm^{-1}: 1268 (C≡P), 1706 (C≡O), 2057 (C≡C).

***Trans*-[Ru(C≡P)(C≡CC$_6$H$_3$-3,5-(CF$_3$)$_2$)(dppe)$_2$] (2.2d)**

Trans-[Ru(dppe)$_2$(C≡CC$_6$H$_3$-3,5-(CF$_3$)$_2$)(η^1-P≡CSiMe$_3$)]PF$_6$ (0.338 g, 0.24 mmol) and KO^{t}Bu (0.028 g, 0.25 mmol) combined, THF (*ca* 10 mL) added, giving an orange solution. Left to stir for *ca* 1 hour. Removed solvent under reduced pressure until a white precipitate started to form. Filtered and removed the remaining solvent under reduced pressure. Washed with degassed water (3 x 10 mL). Added benzene (*ca* 10 mL), removed under reduced pressure and dried under vacuum. Yield: 0.110 g, 0.093 mmol, 39%.^{1}H NMR (CD_2Cl_2): δ_H 7.88 (8H, *m (br)*, *o*-C$_6$H$_5$), 7.40 (1H, *s*, *p*-ArF), 7.32 (4H, *t*, J_{HH} = 7.3 Hz, *p*-C$_6$H$_5$), 7.21 (8H, *m (br), o*-C$_6$H$_5$), 7.14 (12 H, *m, m/p*-C$_6$H$_5$), 6.92 (8H, *t*, J_{HH} = 7.1 Hz, *m*-C$_6$H$_5$), 6.84 (2H, *s*, o-ArF), 2.74 (8H, *dm (br),* J_{HP} = 56 Hz, C_2H_4). $^{31}P\{^1H\}$ NMR (CD_2Cl_2): δ_P 172.8 (1P, *m (br)*, C≡P), 50.9 (4P, *d*, *J* = 5.4 Hz, $Ph_2PCH_2CH_2PPh_2$).

SYNTHESIS OF *trans*-[Ru(C≡N)(C≡CPh)(dppe)$_2$] (2.3)

Trans-[RuCl(C≡CPh)(dppe)$_2$] (0.082 g, 0.079 mmol) and TlOTf (0.029 g, 0.082 mmol) in DCM (*ca* 10 mL) stirred for 1 hour, the solution turned cloudy filtration yielded a green/yellow solution. Excess NaCN (0.010 g, 0.20 mmol) added stirred for 18 h. Filtered and removed solvent under reduced pressure yielded a light brown solid. Yield: 0.054 g, 5.3 x 10^{-3} mmol, 67%. ^{1}H NMR (CD_2Cl_2): δ_H 7.65 (7H, *m (br)*, C_6H_5), 7.55 (2H, *m (br)*, C_6H_5), 7.37 (7H, *m (br)*, C_6H_5), 7.29 (4H, *t*, J_{HH} = 7.4 Hz, C_6H_5), 7.22 (4H, *t*, J_{HH} = 7.4 Hz, C_6H_5), 7.14 (10H, *t*, J_{HH} = 7.4 Hz, C_6H_5), 7.03 (10H, *m*, C_6H_5), 6.74 (2H, *t*, J_{HH} = 7.6 Hz, C_6H_5), 2.66 (8H, *dm (br),* J_{HP} = 52.3 Hz, C_2H_4). $^{31}P\{^1H\}$ NMR (CD_2Cl_2): δ_P 55.0 (1P, *m (br)*, $Ph_2PCH_2CH_2PPh_2$), 54.5 (15P, *m (br)*, $Ph_2PCH_2CH_2PPh_2$). ν_{max}/cm^{-1}: 2059 (C≡N), 1261 (C≡C).

Note: In equivalent integrals in the $^{31}P\{^1H\}$ NMR spectrum for dppe ligands due to corresponding to starting material (55.0 ppm) and product (54.5 ppm) respectively.

REACTIVITY STUDIES

Trans-[Ru(C≡P)(C≡C^{n}Bu)(dppe)$_2$] (2.2a) + [Pt$_2$Cl$_4$(PEt$_3$)$_2$] Attempt 1

[$Pt_2Cl_4(PEt_3)_2$] (0.0133 g, 0.017 mmol) was dissolved in DCM (*ca* 10 mL) and added to *trans*-[$Ru(dppe)_2(C{\equiv}C^nBu)(C{\equiv}P)$] (0.0274 g, 0.027 mmol) and stirred for 24 h. Removed solvent under reduced pressure resulting in a light yellow solid. ^{1}H NMR (CD_2Cl_2): Mixed Products. $^{31}P\{^1H\}$ NMR (CD_2Cl_2): δ_P 155.5 (*quint*, C≡P), 50.9 (*s*, *br,* $Ph_2PCH_2CH_2PPh_2$) 8.9 (*s,* $PtCl_2(PEt_3)_2$)

Trans-[Ru(C≡P)(C≡C^{n}Bu)(dppe)$_2$] (2.2a) + [Pt$_2$Cl$_4$(PEt$_3$)$_2$] Attempt 2

[$Pt_2Cl_4(PEt_3)_2$] (0.0038 g, 0.005 mmol) and *trans*-[$Ru(dppe)_2(C{\equiv}C^nBu)(C{\equiv}P)$] (0.005 g, 0.005 mmol) combined in a J-Young NMR tube, CD_2Cl_2 added. ^{1}H NMR (CD_2Cl_2): Mixed Products. $^{31}P\{^1H\}$ NMR (CD_2Cl_2): δ_P 47.9 (*d*, *J* = 20.0 Hz, $Ph_2PCH_2CH_2PPh_2$), 10.6 (*s,* $PtCl_2(PEt_3)_2$), 8.0, 4.5, 4.3 (*s,* unknown)

Trans-[Ru(C≡P)(C≡C^{n}Bu)(dppe)$_2$] (2.2a) + [Pt$_2$Cl$_4$(PEt$_3$)$_2$] Attempt 3

[$Pt_2Cl_4(PEt_3)_2$] (0.002 g, 0.0025 mmol) and *trans*-[$Ru(dppe)_2(C{\equiv}C^nBu)(C{\equiv}P)$] (0.004 g, 0.004 mmol) combined in a J-Young NMR tube, CD_2Cl_2 added. ^{1}H NMR (CD_2Cl_2): Mixed Products. $^{31}P\{^1H\}$ NMR (CD_2Cl_2): δ_P 47.9 (*d*, *br*, $Ph_2PCH_2CH_2PPh_2$), 10.6 (*s,* $PtCl_2(PEt_3)_2$), 14.5 *(s, br,* PPh_3*),* 8.0, 4.5, 4.3 (*s,* unknown).

Trans-[Ru(C≡P)(C≡C^{n}Bu)(dppe)$_2$] (2.2a) + [Pt$_2$Cl$_4$(PEt$_3$)$_2$] Attempt 4

[$Pt_2Cl_4(PEt_3)_2$] (0.030 g, 0.039 mmol) was dissolved in THF (*ca* 10 mL) and added to *trans*-[$Ru(dppe)_2(C{\equiv}C^nBu)(C{\equiv}P)$] (0.040 g, 0.039 mmol) and stirred for 24 h. Removed solvent under reduced pressure resulting in a light yellow solid. ^{1}H NMR (d_8-THF): Mixed Products. $^{31}P\{^1H\}$ NMR (d_8-THF): δ_P 53.9 (*s,* $Ph_2PCH_2CH_2PPh_2$), 50.6 (*d*, *J* = 20.0 Hz, $Ph_2PCH_2CH_2PPh_2$), 7.9 (*s, $PtCl_2(PEt_3)_2$),* 14.5 *(s,* PPh_3*),* 5.9 (*d*, unknown)

***Trans*-[Ru(C≡P)(C≡C^{n}Bu)(dppe)$_2$] (2.2a) + [Pt$_2$Cl$_4$(PEt$_3$)$_2$] Attempt 5**

[Pt$_2$Cl$_4$(PEt$_3$)$_2$] (0.030 g, 0.039 mmol) and *trans*-[Ru(dppe)$_2$(C≡C^{n}Bu)(C≡P)] (0.08 g, 0.078 mmol) combined in a J-Young NMR tube, C_6D_6 added. ^{1}H NMR (C_6D_6): Mixed Products. ^{31}P{^{1}H} NMR (C_6D_6): Intractable mixture of products.

***Trans*-[Ru(C≡P)(C≡CCO$_2$Et)(dppe)$_2$] (1.59f) + [Pt$_2$Cl$_4$(PEt$_3$)$_2$] Attempt 1**

[Pt$_2$Cl$_4$(PEt$_3$)$_2$] (0.014 g, 0.029 mmol) was dissolved in DCM (*ca* 10 mL) and added to *trans*-[Ru(dppe)$_2$(C≡CCO$_2$Et)(C≡P)] (0.030 g, 0.018 mmol) and stirred for 24 h. Removed solvent under reduced pressure resulting in a light yellow solid. ^{1}H NMR (CD_2Cl_2): Mixed Products. ^{31}P{^{1}H} NMR (CD_2Cl_2): δ_P 49.8 (*s*, *br,* $Ph_2PCH_2CH_2PPh_2$), 50.6 (*d*, *J* = 22.3 Hz, $Ph_2PCH_2CH_2PPh_2$), 5.9 (*d*, unknown).

***Trans*-[Ru(dppe)$_2$(C≡C^{n}Bu)(C≡P] (2.2a)+ [RhCl(CO)(PPh$_3$)$_2$] + AgBF$_4$**

[RhCl(CO)(PPh$_3$)$_2$] (0.0034 g, 0.004 mmol) and $AgBF_4$ (0.0014 g, 0.007 mmol) combined in a J-Young's NMR tube, *d*-DCM added and initial ^{31}P{^{1}H} and ^{1}H NMR taken. *Trans*-[Ru(dppe)$_2$(C≡C^{n}Bu)(C≡P] (0.0047 g, 0.004 mmol) was added another ^{31}P{^{1}H} and ^{1}H NMR taken, left mixing for 18 h, second ^{31}P{^{1}H} and ^{1}H NMR were taken.

***Trans*-[Ru(dppe)$_2$(C≡C^{n}Bu)(C≡P] (2.2a)+ AuCl(PPh$_3$)**

Trans-[Ru(dppe)$_2$(C≡C^{n}Bu)(C≡P] (0.005 g, 0.048 mmol) and AuCl(PPh_3) (0.0025 g, 0.050 mmol) combined in a J-Young's NMR tube, *d*-DCM added, initial ^{31}P{^{1}H} and ^{1}H NMR taken, left mixing for 18 h, second ^{31}P{^{1}H} and ^{1}H NMR were taken.

***Trans*-[Ru(C≡P)(C≡CCO$_2$Me)(dppe)$_2$] (1.59g) + AuCl(PPh$_3$)**

Trans-[Ru(dppe)$_2$(C≡CCO$_2$Me)(C≡P] (0.0214 g, 0.021 mmol) and AuCl(PPh$_3$) (0.0103 g, 0.021 mmol) combined in a J-Young's NMR tube, *d*-DCM added, initial $^{31}P\{^1H\}$ and ^1H NMR taken, left mixing for 18 h, second $^{31}P\{^1H\}$ and ^1H NMR were taken. ^1H NMR (CD_2Cl_2): δ_H Intractable mixture. $^{31}P\{^1H\}$ NMR (CD_2Cl_2): δ_P 146.3 (*m*, C≡P), 49.2 (*s*, *br,* $Ph_2PCH_2CH_2PPh_2$), 47.3 (*s*, $Ph_2PCH_2CH_2PPh_2$).

***Trans*-[Ru(C≡P)(C≡CCO$_2$Me)(dppe)$_2$] (1.59g) + AgPF$_6$**

Trans-[Ru(dppe)$_2$(C≡CCO$_2$Me)(C≡P)] (0.020 g, 0.020 mmol) and $AgPF_6$ (0.006 g, 0.024 mmol) combined in a J-Young's NMR tube, CD_2Cl_2 added, initial $^{31}P\{^1H\}$ and ^1H NMR taken, left mixing for 18 h, second $^{31}P\{^1H\}$ and ^1H NMR were taken. ^1H NMR (CD_2Cl_2): δ_H Intractable mixture. $^{31}P\{^1H\}$ NMR (CD_2Cl_2): δ_P 41.6 (*s*, *br,* $Ph_2PCH_2CH_2PPh_2$), −144.2 (*sept*, *J* = 700 Hz, PF_6).

***Trans*-[Ru(C≡P)(C≡CCO$_2$Me)(dppe)$_2$] (1.59g) + AgPF$_6$ + Me$_3$SiCl**

Trans-[Ru(dppe)$_2$(C≡CCO$_2$Me)(C≡P)] (0.022 g, 0.0021 mmol) and $AgPF_6$ (0.005 g, 0.0049 mmol) combined in a J-Young's NMR tube, CD_2Cl_2 added, Me_3SiCl (0.003 mL, 0.0023 mmol) added inverted for 1 hour. ^1H NMR (CD_2Cl_2): δ_H Intractable mixture. $^{31}P\{^1H\}$ NMR (CD_2Cl_2): δ_P 101.0 (*m (br)*, C≡P), 41.4 (*s*, *br,* $Ph_2PCH_2CH_2PPh_2$), −144.2 (*sept*, *J* = 700 Hz, PF_6).

***Trans*-[Ru(C≡P)(C≡CCO$_2$Me)(dppe)$_2$] (1.59g) + AgPF$_6$ + MeI**

Trans-[Ru(dppe)$_2$(C≡CCO$_2$Me)(C≡P)] (0.021 g, 0.020 mmol) and $AgPF_6$ (0.006 g, 0.024 mmol) combined in a J-Young's NMR tube, CD_2Cl_2 added, MeI (0.002 mL, 0.0032 mmol) added and the solution was inverted for 48 hour. ^1H NMR (CD_2Cl_2): δ_H Intractable mixture. $^{31}P\{^1H\}$ NMR (CD_2Cl_2): δ_P 47.0 (*s*, *br,* $Ph_2PCH_2CH_2PPh_2$), 46.0 (*d, J* = 12.4 Hz, $Ph_2PCH_2CH_2PPh_2$), −144.2 (*sept*, *J* = 700 Hz, PF_6).

***Trans*-[Ru(dppe)$_2$(C≡C^{n}Bu)(C≡P] (2.2a) + AgPF$_6$**

Trans-[Ru(dppe)$_2$(C≡C^{n}Bu)(C≡P)] (0.005 g, 0.0048 mmol) and $AgPF_6$ (0.0012 g, 0.0048 mmol) combined in a J-Young's NMR tube, CD_2Cl_2 added, initial $^{31}P\{^1H\}$ and ^1H NMR taken, left mixing for 18 h, second $^{31}P\{^1H\}$ and ^1H NMR were taken. ^1H NMR (CD_2Cl_2): δ_H Intractable mixture. $^{31}P\{^1H\}$ NMR (CD_2Cl_2): δ_P 146.0 (*m*, *br,* C≡P), 82.8 (*s*, *br,* unknown), 55.5 (*s*, *br,* $Ph_2PCH_2CH_2PPh_2$)

***Trans*-[Ru(dppe)$_2$(C≡C^{n}Bu)(C≡P)] (2.2a) + AgPF$_6$ + Me$_3$SiCl**

Trans-[Ru(dppe)$_2$(C≡C^{n}Bu)(C≡P)] (0.005 g, 0.0048 mmol) and $AgPF_6$ (0.0012 g, 0.0047 mmol) combined in a J-Young's NMR tube, d_8-THF added, initial $^{31}P\{^1H\}$ and ^1H NMR taken, Me_3SiCl (0.006 mL, 0.0047 mmol) added another $^{31}P\{^1H\}$ and ^1H NMR taken, left mixing for 18 h, second $^{31}P\{^1H\}$ and ^1H NMR were taken. ^1H NMR (d_8-THF): δ_H Intractable mixture. $^{31}P\{^1H\}$ NMR (d_8-THF): δ_P Intractable mixture.

***Trans*-[Ru(dppe)$_2$(C≡C^{n}Bu)(C≡P)] (2.2a) + AgPF$_6$ + MeI**

Trans-[Ru(dppe)$_2$(C≡C^{n}Bu)(C≡P)] (0.005 g, 0.0048 mmol) and $AgPF_6$ (0.0012 g, 0.0047 mmol) combined in a J-Young's NMR tube, d_8-THF added, initial $^{31}P\{^1H\}$ and ^1H NMR taken, MeI (1 mL, 0.016 mmol) added another $^{31}P\{^1H\}$ and ^1H NMR taken, left mixing for 18 h, second $^{31}P\{^1H\}$ and ^1H NMR were taken. ^1H NMR (d_8-THF): δ_H Intractable mixture. $^{31}P\{^1H\}$ NMR (d_8-THF): δ_P Intractable mixture.

EXPERIMENTAL DETAILS FOR CHAPTER 3

SYNTHESIS OF *trans*-[Ru(dppe)$_2$(Me)$_2$]

A mixture of [RuCl(dppe)$_2$]OTf (2.260 g, 2.09 mmol) and Me_2Mg (0.185 g, 3.41 mmol) was suspended in Et_2O (*ca* 50 mL) at ambient temperature, resulting in an immediate colour change from red to yellow-brown; the resulting solution was stirred for 18 h. Filtration afforded a yellow/brown solid, which was washed with Et_2O (3 × 20 mL) and dried in vacuo. The compound was confirmed by reference to related literature data and then used directly in the subsequent step.[129,130] Yield: 2.00 g, 89%. ^{1}H NMR (CD_2Cl_2): δH 6.55−7.49 (*m (br),* C_6H_5), 2.41 (8H, *m (br)*, C_2H_4), −1.18 (6H, *qnt, J* = 4.4 Hz, CH_3). $^{31}P\{^1H\}$ NMR (CD_2Cl_2): δ_P 59.2 (4H, *s*, $Ph_2PCH_2CH_2PPh_2$). The bulk has a cis/trans ratio of *ca* 5:95 and is used in crude form for the next step.

SYNTHESIS OF *trans*-[Ru(dppe)$_2$(Me)]OTf (3.1.OTf)

Trans-[Ru(dppe)$_2$(Me)$_2$] (1.6889 g, 1.57 mmol), and TlOTf (0.5686 g, 1.61 mmol) combined. DCM (*ca* 30 mL) added. Colour change from yellow-brown to purple observed. Left to stir for *ca* 1 hour. Filtered via canula and volatiles were removed from the filtrate under reduced pressure to afford a red-purple solid that was dried in vacuo. Yield: 0.980 g, 0.92 mmol, 59%. ^{1}H NMR ($CDCl_3$): δ_H 7.38 (8H, *m (br),* C_6H_5), 7.22 (8H, *t*, *J* = 7.6 Hz, C_6H_5), 7.14 (8H, *t*, *J* = 7.6 Hz, C_6H_5), 6.78 (16H, *d*, *J* = 6.5 Hz, C_6H_5), 2.51 (8H, *m (br),* C_2H_4), -0.90 (3H, *m (br),* CH_3). $^{31}P\{^1H\}$ NMR (CD_2Cl_2): δ_P 55.7 (4P, *s,* $Ph_2PCH_2CH_2PPh_2$).

SYNTHESIS OF *trans*-[Ru(Me)(P≡CSiMe$_3$)(dppe)$_2$]OTf (3.2.OTf)

To a stirred suspension of [Ru(dppe)$_2$(Me)]OTf (1.36 g, 12.1 mmol) in 1,4-dioxane (*ca* 20 mL) was added Me_3SiCP (25 mL, 0.05 mol dm^{-3}, 12.5 mmol), and then the mixture left to stir for 1 h. The

resulting precipitate was isolated by canula filtration and dried in vacuo to afford a cream solid. The bulk sample retains an equivalent of dioxane and trace levels of apparently the cis isomer. Yield: 1.068 g, 71%. ^{1}H NMR (CD_2Cl_2): δ_H 7.51 (8H, *m (br), m*-C_6H_5), 7.50 (4H, *t, J* = 7.3 Hz, *p*-C_6H_5), 7.40 (4H, *t, J* = 7.5 Hz, *p*-C_6H_5), 7.30 (8H, *t, J* = 7.3 Hz, o-C_6H_5), 7.10 (8H, *t, J* = 7.3 Hz, *o*-C_6H_5), 6.80 (8H, *m (br), m*-C_6H_5), 2.70 (8H*, m (br)*, C_2H_4), −0.01 (9H, *s*, $SiMe_3$), −0.35 (3H, *m (br),* CH_3).^{13}C{^{1}H} NMR (CD_2Cl_2): δ_C 185.1 (*d, J* = 69 Hz, C≡P), 135.2 (*qnt, J* = 10 Hz, *ipso*-C_6H_5), 134.0 (*qnt, J* = 3 Hz, *m*-C_6H_5), 133.4 (*qnt, J* = 2 Hz, *m*-C_6H_5), 131.6 (*s, p*-C_6H_5), 131.0 (*s, p*-C_6H_5), 129.2 (*qnt, J* = 2 Hz, *o*-C_6H_5), 128.9 (*qnt, J* = 2 Hz, *o*-C_6H_5), 29.4 (*qnt, J* = 12 Hz, CH_2CH_2), 2.7 (*m*, CH_3), 0.9 (*d, J* = 5 Hz, $SiMe_3$). ^{31}P{^{1}H} NMR (CD_2Cl_2): δ_P 121.3 (1P, *qnt, J* = 28 Hz, C≡P), 46.7 (4P, *d, J* = 28 Hz, $Ph_2PCH_2CH_2PPh_2$). ^{19}F NMR (CD_2Cl_2): δ_F −78.9 (*s*, OTF). ^{29}Si NMR (79.37 MHz, CD_2Cl_2): δ_{Si} 15.4 ($RuPCSiMe_3$). ν_{max}/cm^{-1}: 1269 (C≡P). Calcd for $C_{60}H_{60}P_5F_3O_3SSiRu{\cdot}C_4H_8O_2$: C; 59.57, H; 5.31. Found: C; 59.89, H; 5.18

SYNTHESIS OF *trans*-[RuMe(dppe)$_2$(C≡P)] (3.3)

Trans-[Ru(Me)(P≡C$SiMe_3$)(dppe)$_2$]OTf (1.068 g, 0.91 mmol) in THF (*ca* 20 mL) was cooled to −30 °C, prior to the dropwise addition of a solution of NaOPh (0.138 g, 1.2 mmol) in THF (*ca* 5 mL) over the course of 10 min. Upon complete addition, the mixture was stirred for *ca* 2 min, then removed from the cold bath and the volatiles immediately removed under reduced pressure to afford a yellow-brown solid, which was washed with acetonitrile (*ca* 3 × 15 mL) and dried in vacuo, yielding a yellow solid. Yield: 0.543 g, 63%. ^{1}H NMR (399.5 MHz, CD_2Cl_2): δ_H 8.4 (8H, *m (br), m*-C_6H_5), 7.3 (4H, *t, J* = 7.3 Hz, p- C_6H_5), 7.2 (8H, *t, J* = 7.5 Hz, *o*-C_6H_5), 7.1 (4H, *t, J* = 7.4 Hz, *p*-C_6H_5), 6.9 (8H*, t, J* = 7.6 Hz, *o*-C_6H_5), 6.5 (8H, *d, J* = 7.5 Hz, *m*-C_6H_5), 2.6 (8H, *m (br),* C_2H_4), −2.3 (3H, *qnt, J* = 5.6 Hz, CH_3). ^{13}C{^{1}H} NMR (100.46 MHz, CD_2Cl_2): δ_C 294.3 (*m (br),* C≡P), 139.4 (*qnt,* J_{CP} = 9.77 Hz, *ipso*-C_6H_5), 136.1 (*qnt,* J_{CP} = 9.90 Hz*, ipso*-C_6H_5), 136.3 (*m(br), m*-C_6H_5), 133.5 (*qnt,* J_{CP} = 2.02 Hz, *m*-C_6H_5), 130.1 (*s, p*-C_6H_5), 128.8 (*s, p*-C_6H_5), 127.6 (*qnt,* J_{CP} = 1.99 Hz, *o*- C_6H_5), 127.4

(*qnt, J_{CP}* = 2.33 Hz, *o*- C_6H_5), 31.2 (*s,* CH_2CH_2), −9.8 (*m (br),* CH_3). $^{31}P\{^1H\}$ NMR (161.71 MHz, CD_2Cl_2): δ_P 177.9 (1P, *m (br),* C≡P), 58.9 (4P, *d, J_{PP}* = 4.3 Hz, $Ph_2PCH_2CH_2PPh_2$). ν_{max}/cm^{-1}: 1217 (C≡P), 3046 (CH_3). Anal. Calcd for $C_{54}H_{51}P_5Ru$: C; 67.85, H; 5.38. Found: C; 68.13, H; 5.43. Crystal data for **3.3** Crystals were grown by layering of a saturated solution in dichloromethane with hexane at ambient temperature. $C_{54}H_{51}P_5Ru$ (Mw = 955.83 g mol^{-1}), monoclinic, *P*21/*c* (No. 14), *a* = 23.6755(12) Å, *b* = 11.5267(6) Å, *c* = 17.2942(8) Å, *β* = 104.670(5)°, *V* = 4565.7(5) Å, *Z* = 4, *T* = 173(2) K, *μ*(Cu K*α*) = 4.712 mm^{-1}, D_c = 1.391 Mg m^{-3}, 8676 independent reflections, full matrix F^2 refinement R_1 = 0.0614 on 6218 independent absorption corrected reflections [$I > 2\sigma(I)$; $2\vartheta_{max}$ = 142.45°], 543 parameters, wR_2 = 0.1573 (all data).

SYNTHESIS OF *trans*-[RuBr(dppe)$_2$(C≡P)] (3.4)

Anhydrous $ZnBr_2$ (0.305 g, 1.35 mmol), 5 mol % PPh_3 (0.017 g, 0.065 mmol), and *trans*-[RuMe(dppe)$_2$(C≡P)] (1.289 g, 1.35 mmol) were combined in a Schlenk flask prior to the addition of THF (*ca* 20 mL). The resulting solution was stirred for 18 h, leading to the precipitation of a yellow solid, which was isolated by filtration (cannula) and dried in *vacuo*. Yield: 1.027 g, 75%. ^1H NMR (CD_2Cl_2): δ_H 7.60 (8H, *m (br), m*-C_6H_5), 7.32 (4H, *m (br), m*-C_6H_5), 7.26 (8H, *dt, J* = 7.5 and 20.0 Hz, *p*-C_6H_5), 7.10 (16H, *dt, J* = 7.6 and 21.7 Hz, *o*-C_6H_5), 2.90 (8H, *m (br),* C_2H_4). $^{13}C\{^1H\}$ NMR (CD_2Cl_2): δ_C 136.1 (*m (br), ipso*-C_6H_5), 135.6 (*m (br), m*-C_6H_5), 135.3 (*qnt, J_{CP}* = 2 Hz, *m*-C_6H_5), 129.9 (s, *p*-C_6H_5), 129.8 (*s, p*-C_6H_5), 127.5 (*m*, o-C_6H_5), 30.8 (*qnt, JCP* = 12 Hz, CH_2CH_2); the cyaphide carbon could not be resolved. $^{31}P\{^1H\}$ NMR (CD_2Cl_2): δ_P 135.4 (1P, *m (br),* C≡P), 44.8 (4P, *d, J_{PP}* = 4.3 Hz, $Ph_2PCH_2CH_2PPh_2$). ν_{max}/cm^{-1}: 1249 (C≡P). HRMS (ESI). Calcd for $[C_{53}H_{48}P_5BrRu]$+: m/z 1020.0659. Found: m/z 1020.0577 [RMS Err 8 ppm]. Anal. Calcd for $C_{53}H_{48}P_5BrRu$: C; 62.36, H; 4.74. Found: C; 61.6, H; 4.73. Crystal data for 5: Crystals were grown by layering of a saturated solution in dichloromethane with hexane at ambient temperature. $C_{53}H_{48}BrP_5Ru$ (Mw = 1020.73 g mol^{-1}), triclinic, *P*$\bar{1}$ (No. 2), *a* = 10.155(1) Å, *b* = 10.5071(12) Å, *c* = 12.593(1) Å, *α* = 71.169(9)°,

β = 85.317(7)°, γ = 62.172(12)°, V = 1120.8(2) Å3, Z = 1, T = 173(2) K, μ(Cu $K\alpha$) = 5.844 mm^{-1}, D_c = 1.512 Mg m^{-3}, 4334 independent reflections, full matrix F^2 refinement R_1 = 0.0340 on 3412 independent absorption corrected reflections [$I > 2\sigma(I)$; $2\vartheta_{max}$ = 145.78°], 286 parameters, wR_2 = 0.0747 (all data).

SYNTHESIS OF *trans*-[RuCl(dppe)$_2$(C≡P)] (3.5)

Anhydrous $ZnCl_2$ (0.007 g, 0.052 mmol), PPh3 (0.001 g, 0.003 mmol), and *trans*-[RuMe(dppe)$_2$(C≡P)] (0.050 g, 0.052 mmol) were combined in a Schlenk flask prior to the addition of THF (*ca* 5 mL). The resulting solution was stirred for 18 h, leading to the precipitation of a yellow solid, which was isolated by filtration (cannula) and dried in vacuo. Yield: 0.035 g, 80%. ^{1}H NMR (CD_2Cl_2): δ_H 7.8 (8H, *m (br), m*-C_6H_5), 7.3 (8H, *m (br), m*-C_6H_5), 7.26 (8H, *dt, J* = 7.4 and 16.0 Hz, *p*-C_6H_5), 7.06 (16H, *dt, J* = 7.6 and 15.9 Hz, *o*-C_6H_5), 2.9 (8H, *m (br),* C_2H_4). ^{13}C{^{1}H} NMR (CD_2Cl_2): δ_C 265.5 (*m (br),* C≡P), 136.3 (*qnt,* J_{CP} = 10 Hz, *ipso*-C_6H_5), 135.7 (*m (br), m*-C_6H_5), 135.4 (*qnt,* J_{CP} = 3 Hz, *m*-C_6H_5), 135.1 (*qnt,* J_{CP} = 10 Hz, *ipso*-C_6H_5), 129.8 (*s, p*-C_6H_5), 129.7 (*s, p*-C_6H_5), 127.6 (*dqnt,* J_{CP} = 3, 2, and 5 Hz, *o*-C_6H_5), 30.7 (*s*, CH_2CH_2). ^{31}P{^{1}H} NMR (161.71 MHz, CD_2Cl_2): δ_P 132.0 (1P, *m (br),* C≡P), 46.2 (4P, *d,* J_{PP} = 4.2 Hz, $Ph_2PCH_2CH_2PPh_2$). ν_{max}/cm^{-1}: 1250 (C≡P). HRMS (ESI). Calcd for $[C_{53}H_{48}P_5ClRu]^+$: m/z 976.1169. Found: m/z 976.1240 [RMS Err 7 ppm]. Crystal data for **3.5**: Crystals were grown by layering of a saturated solution in dichloromethane with hexane at ambient temperature. $C_{53}H_{48}ClP_5Ru$ (Mw = 976.28 g mol^{-1}), monoclinic, *P21/c* (No. 14), a = 23.6006(6) Å, b = 11.4193(3) Å, c = 17.2737(4) Å, β = 103.781(3)°, V = 4521.3(2) Å, Z = 4, T = 173(2) K, $\mu(Cu\ K\alpha)$ = 5.303 mm^{-1}, D_c = 1.434 Mg m^{-3}, 6901 independent reflections, full matrix F^2 refinement R_1 = 0.0438 on 5275 independent absorption corrected reflections, [$I > 2\sigma(I)$; $2\vartheta max$ = 122.32°], 569 parameters, wR_2 = 0.1123 (all data).

SYNTHESIS OF *trans*-[RuI(dppe)$_2$(C≡P)] (3.6)

Anhydrous ZnI_2 (0.008 g, 0.025 mmol), PPh_3 (0.001 g, 0.003 mmol), and *trans*-[RuMe(dppe)$_2$(C≡P)] (0.023 g, 0.024 mmol) were combined in a Schlenk flask prior to the addition of THF (*ca* 5 mL). The resulting solution was stirred for 18 h, leading to the precipitation of a yellow solid, which was isolated by filtration (cannula) and dried in vacuo. Yield: 0.020 g, 75%. Poor solubility has proven limiting for the acquisition of spectroscopic data, and the material has not been obtained in analytical purity. ^{1}H NMR (CD_2Cl_2): δ_H 7.50 (8H, *m (br),* C_6H_5), 7.40 (8H*, m (br),* C_6H_5), 7.30 (8H, *dt, J* = 7.4 and 15.5 Hz, C_6H_5), 7.10 (16H, *dt, J* = 7.6 and 15.9 Hz, C_6H_5), 2.90 (8H, *m (br),* C_2H_4). ^{13}C{^{1}H} NMR (CD_2Cl_2): δ_C 137.0 (unresolved*, ipso*-C_6H_5), 136.0 (*br, m*-C_6H_5), 135.4 (*br, ipso*-C_6H_5), 135.2 (*br, m*-C_6H_5), 130.2 (*br, p*-C_6H_5), 129.8 (*br, p*-C_6H_5), 127.6 (*br, o*-C_6H_5), 127.5 (*br, o*-C_6H_5), 30.5 (unresolved, CH_2CH_2); the cyaphide carbon was not resolved. ^{31}P{^{1}H} NMR (161.71 MHz, CD_2Cl_2): δ_P 140 (1P, *m (br),* C≡P), 42.1 (4P, *d (br),* $Ph_2PCH_2CH_2PPh_2$).

REACTIVITY STUDIES

Trans-[RuMe(dppe)$_2$(C≡P)] (3.3) + [Pt$_2$Cl$_4$(PEt$_3$)$_2$] Attempt 1

Trans-[RuMe(dppe)$_2$(C≡P)] (0.031 g, 0.032 mmol) and [$Pt_2Cl_4(PEt_3)_2$] (0.015 g, 0.019 mmol) combined, THF (*ca* 15 mL), solution turned dark orange, the resulting solution was stirred for 76 h. Removed volatiles under reduced pressure. ^{1}H NMR (C_6D_6): δ_H Intractable mixture. ^{31}P{^{1}H} NMR (C_6D_6): δ_P 136.8 (*m, (br),* C≡P), 56.5 (*s*, $Ph_2PCH_2CH_2PPh_2$), 46.6 (s, $Ph_2PCH_2CH_2PPh_2$), -20-50 (uncharacterised)

***Trans*-[RuMe(dppe)$_2$(C≡P)] (3.3) + [Pt$_2$Cl$_4$(PEt$_3$)$_2$] Attempt 2**

Trans-[RuMe(dppe)$_2$(C≡P)] (0.032 g, 0.033 mmol) and [Pt$_2$Cl$_4$(PEt$_3$)$_2$] (0.013 g, 0.017 mmol) combined, THF (*ca* 10 mL), solution turned dark orange, the resulting solution was stirred for 76 h. Removed volatiles under reduced pressure. ^{1}H NMR (C_6D_6): δ_H Intractable mixture. $^{31}P\{^1H\}$ NMR (C_6D_6): δ_P 136.8 (*m, (br),* C≡P), 56.5 (s, $Ph_2PCH_2CH_2PPh_2$), 47 (s, $Ph_2PCH_2CH_2PPh_2$), -20-50 (uncharacterised)

***Trans*-[RuMe(dppe)$_2$(C≡P)] (3.3) + [Pt$_2$Cl$_4$(PEt$_3$)$_2$] Attempt 3**

Trans-[RuMe(dppe)$_2$(C≡P)] (0.069 g, 0.072 mmol) and [Pt$_2$Cl$_4$(PEt$_3$)$_2$] (0.031 g, 0.040 mmol) combined in a J-young NMR tube with C_6D_6, solution turned dark orange the resulting solution was inverted for 18 h. ^{1}H NMR (C_6D_6): δ_H Intractable mixture. $^{31}P\{^1H\}$ NMR (C_6D_6): δ_P 136.8 (*m, (br),* C≡P), 56.5 (s, $Ph_2PCH_2CH_2PPh_2$), 47 (s, $Ph_2PCH_2CH_2PPh_2$), -20-50 (uncharacterised)

Trans-[Ru(dppe)$_2$(Me)(C≡P)] + [FeCp(η^6-Tol)]PF$_6$

Trans-[Ru(dppe)$_2$(Me)(C≡P)] (0.058 g, 0.061 mmol) and [FeCp(η^6-Tol)]PF_6 (0.028 g, 0.068 mmol) combined, THF (*ca* 10 mL) added. Left to stir for 18 h. Removed solvent under reduced pressure. Dried under vacuum. ^{1}H NMR (C_6D_6): δ_H Intractable mixture. $^{31}P\{^1H\}$ NMR (C_6D_6): δ_P Intractable mixture.

***Trans*-[Ru(dppe)$_2$(Me)(C≡P)] + [RhCl(CO)(PPh$_3$)$_2$] + AgBF$_4$**

[RhCl(CO)(PPh_3)$_2$] (0.040 g, 0.079 mmol) and $AgBF_4$ (0.016 g, 0.082 mmol) combined, THF (*ca* 10 mL) added left to stir for 10 min. The solution then added to a solution of *trans*-[Ru(dppe)$_2$(Me)(C≡P)] (0.064 g, 0.061 mmol) in THF (*ca* 10 mL), the resulting solution was stirred

for 18 h. Filtered and removed solvent under reduced pressure. Dried under vacuum. ^{1}H NMR (C_6D_6): δ_H Intractable mixture. $^{31}P\{^{1}H\}$ NMR (C_6D_6): δ_P Intractable mixture.

Trans-[Ru(dppe)$_2$(Me)(C≡P)] + AuCl(PPh$_3$) + AgBF$_4$

AuCl(PPh_3) (0.024 g, 0.049 mmol) and $AgBF_4$ (0.009 g, 0.046 mmol) combined, THF (*ca* 5 mL) added, the solution stirred for *ca* 5 min. Solution added to *trans*-[Ru(dppe)$_2$(Me)(C≡P)] (0.043 g, 0.045 mmol) in THF (*ca* 10 mL). Filtered and removed solvent under reduced pressure. Dried under vacuum. ^{1}H NMR (C_6D_6): δ_H Intractable mixture. $^{31}P\{^{1}H\}$ NMR (C_6D_6): δ_P 47 (s, $Ph_2PCH_2CH_2PPh_2$), 29 (*s,* uncharacterised), 25 (*s,* uncharacterised)

Trans-[Ru(dppe)$_2$(Me)(C≡P)] + AuCl(tht)

Trans-[Ru(dppe)$_2$(Me)(C≡P)] (0.041 g, 0.043 mmol) and AuCl(tht) (0.015 g, 0.047 mmol) combined, covered the schlenk in foil to exclude light, THF (*ca* 10 mL) added. Left to stir for 18 h. Removed solvent under reduced pressure. Dried under vacuum. ^{1}H NMR (C_6D_6): δ_H Intractable mixture. $^{31}P\{^{1}H\}$ NMR (C_6D_6): δ_P 135.7 (*m, (br),* C≡P), 56.5 (*s*, $Ph_2PCH_2CH_2PPh_2$), 47 (*s*, $Ph_2PCH_2CH_2PPh_2$), -20-50 (uncharacterised baseline peaks)

Trans-[Ru(dppe)$_2$(Me)(C≡P)] + AgPF$_6$

Trans-[Ru(dppe)$_2$(Me)(C≡P)] (0.038 g, 0.040 mmol) and $AgPF_6$ (0.012 g, 0.047 mmol) combined, covered the schlenk in foil, THF (*ca* 10 mL) added. Left to stir for 18 h. Filtered and removed solvent under reduced pressure. Dried under vacuum. ^{1}H NMR (C_6D_6): δ_H Intractable mixture. $^{31}P\{^{1}H\}$ NMR (C_6D_6): δ_P 136(*m, (br),* C≡P), 46 (*s*, $Ph_2PCH_2CH_2PPh_2$), -20-70 (uncharacterised baseline peaks), −144.2 (*q*, *J* = 700 Hz, PF_6).

Trans-[Ru(dppe)$_2$(Me)(C≡P)] + AgPF$_6$ + Me$_3$SiCl

Trans-[Ru(dppe)$_2$(Me)(C≡P)] (0.040 g, 0.042 mmol) and $AgPF_6$ (0.011 g, 0.042 mmol) combined, covered the schlenk in foil to exclude light, THF (_ca_ 10 mL) added, Me_3SiCl (0.1 mL, 0.79 mmol) added, the resulting solution was stirred for 18 h. Filtered and removed solvent under reduced pressure. Dried under vacuum. ^{1}H NMR (C_6D_6): δ_H Intractable mixture. $^{31}P\{^1H\}$ NMR (C_6D_6): δ_P Intractable mixture.

Trans-[Ru(dppe)$_2$(Me)(C≡P)] + AgPF$_6$ + MeI

Trans-[Ru(dppe)$_2$(Me)(C≡P)] (0.038 g, 0.040 mmol) and $AgPF_6$ (0.010 g, 0.040 mmol) combined, covered the schlenk in foil to exclude light, THF (_ca_ 10 mL) added, MeI (0.14 mL, 0.43 mmol) added. Left to stir for 18 h. Removed solvent under reduced pressure. Dried under vacuum. Unable to characterise due to lack of solubility.

Trans-[Ru(dppe)$_2$(Me)(C≡P)] + HCl

Trans-[Ru(dppe)$_2$(Me)(C≡P)] (0.039 g, 0.041 mmol) in THF (_ca_ 15 mL) stirred, HCl (1 mol dm^{-3}, 0.1 mL, 1 mmol) added. Left to stir for 18 h. Removed solvent under reduced pressure. Dried under vacuum. ^{1}H NMR (C_6D_6): δ_H Intractable mixture. $^{31}P\{^1H\}$ NMR (C_6D_6): δ_P Intractable mixture.

Trans-[Ru(dppe)$_2$(Me)(C≡P)] + Furan Attempt 1

Trans-[Ru(dppe)$_2$(Me)(C≡P)] (0.049 g, 0.051 mmol) in DCM (_ca_ 20 mL) stirred, furan (0.05 mL, 0.69 mmol) added in excess, heated to reflux (_ca_ 38 °C) for _ca_ 3 h. Removed solvent under reduced pressure. Dried under vacuum. ^{1}H NMR (CD_2Cl_2): δ_H Starting materials. $^{31}P\{^1H\}$ NMR (CD_2Cl_2): δ_P Starting materials

***Trans*-[Ru(dppe)$_2$(Me)(C≡P)] + Furan Attempt 2**

Trans-[Ru(dppe)$_2$(Me)(C≡P)] (0.062 g, 0.065 mmol) in THF (*ca* 25 mL) stirred, furan (0.7 mL, 9.62 mmol) added in excess, heated to reflux (*ca* 66 °C) for *ca* 3 h. Removed solvent under reduced pressure. Dried under vacuum. ^{1}H NMR (C_6D_6): δ_H Intractable mixture. ^{31}P{^{1}H} NMR (C_6D_6): δ_P Intractable mixture.

***Trans*-[Ru(dppe)$_2$(Me)(C≡P)] + BPh$_3$**

Trans-[Ru(dppe)$_2$(Me)(C≡P)] (0.034 g, 0.036 mmol) and BPh_3 (0.005 g, 0.044 mmol) combined, THF (*ca* 10 mL) added, the resulting solution was stirred for 18 h. Filtered and removed solvent under reduced pressure. Dried under vacuum. ^{1}H NMR (C_6D_6): δ_H Intractable mixture. ^{31}P{^{1}H} NMR (C_6D_6): δ_P Intractable mixture.

***Trans*-[Ru(dppe)$_2$(Me)(C≡P)] + MeLi**

Trans-[Ru(dppe)$_2$(Me)(C≡P)] (0.037 g, 0.039 mmol) in THF (*ca* 15 mL) cooled to *ca* 0 °C, stirred, MeLi (0.2 mL, 0.044 mmol) added. Left to warm up to room temperature, stirred for *ca* 2 h. Degassed water (0.7 mL) added. Removed solvent under reduced pressure. Dried under vacuum. ^{1}H NMR (C_6D_6): δ_H Intractable mixture. ^{31}P{^{1}H} NMR (C_6D_6): δ_P Intractable mixture.

***Trans*-[Ru(dppe)$_2$(Me)(C≡P)] + MeMgCl**

Trans-[Ru(dppe)$_2$(Me)(C≡P)] (0.055 g, 0.006 mmol) in THF (*ca* 10 mL) cooled to *ca* −78 °C, stirred, MeMgCl (0.7 mL, 2.1 mmol) added. Left to warm up to room temperature, stirred for *ca* 18 h. Degassed water (0.7 mL) added. Removed solvent under reduced pressure. Dried under vacuum. ^{1}H NMR (C_6D_6): δ_H Intractable mixture. ^{31}P{^{1}H} NMR (C_6D_6): δ_P Intractable mixture.

***Trans*-[Ru(dppe)$_2$(Me)(C≡P)] + ZrHCl(C$_5$H$_5$)$_2$**

Trans-[Ru(dppe)$_2$(Me)(C≡P)] (0.048 g, 0.05 mmol) and ZrHCl(C$_5$H$_5$)$_2$ (0.02 g, 0.077 mmol) combined, THF (*ca* 10 mL) added, the resulting solution was stirred for 18 h. Removed solvent under reduced pressure. Dried under vacuum. ^{1}H NMR (C$_6$D$_6$): δ_H Intractable mixture. ^{31}P{^{1}H} NMR (C$_6$D$_6$): δ_P Intractable mixture.

***Trans*-[Ru(dppe)$_2$(Me)(C≡P)] + ZrHCl(C$_5$H$_5$)$_2$ + AgOTf**

ZrHCl(C$_5$H$_5$)$_2$ (0.008 g, 0.031 mmol) and AgOTf (0.008 g, 0.031 mmol) combined, DCM (*ca* 10 mL) added. Left to stir for 5 min. Added to a solution of *trans*-[Ru(dppe)$_2$(Me)(C≡P)] (0.018 g, 0.019 mmol) in DCM (*ca* 15 mL), the resulting solution was stirred for 18 h. Removed solvent under reduced pressure. Dried under vacuum. ^{1}H NMR (C$_6$D$_6$): δ_H Intractable mixture. ^{31}P{^{1}H} NMR (C$_6$D$_6$): δ_P Intractable mixture.

***Trans*-[Ru(dppe)$_2$(Me)(C≡P)] + Me$_3$OBF$_4$**

Trans-[Ru(dppe)$_2$(Me)(C≡P)] (0.045 g, 0.047 mmol) and Me$_3$OBF$_4$ (0.007 g, 0.047 mmol) combined, THF (*ca* 15 mL) added, the resulting solution was stirred for 18 h. Filtered and removed solvent under reduced pressure. Dried under vacuum. Unable to characterise due to lack of solubility.

***Trans*-[Ru(dppe)$_2$(Me)(C≡P)] + MeI**

Trans-[Ru(dppe)$_2$(Me)(C≡P)] (0.021 g, 0.022 mmol) and MeI (0.2 mL, 0.032 mmol) combined in a J-Young NMR tube in C$_6$D$_6$, forming a yellow solution and precipitate. ^{1}H NMR (C$_6$D$_6$): δ_H Intractable mixture. ^{31}P{^{1}H} NMR (C$_6$D$_6$): δ_P Intractable mixture.

***Trans*-[Ru(dppe)$_2$(Me)(C≡P)] + Me$_3$SiCl**

Trans-[Ru(dppe)$_2$(Me)(C≡P)] (0.047 g, 0.049 mmol) and Me_3SiCl (0.3 mL, 2.4 mmol) combined in a J-Young NMR tube in C_6D_6, forming a yellow solution and precipitate. ^{1}H NMR (C_6D_6): δ_H Intractable mixture. $^{31}P\{^1H\}$ NMR (C_6D_6): δ_P Intractable mixture.

ATTEMPTED SYNTHESIS of *trans*-[Ru(dppe)$_2$(Et)(Cl)]

Trans-[Ru(dppe)$_2$(Cl)]OTf (1.00 g, 0.92 mmol) and Et_2Mg (0.039 g, 0.47 mmol) combined, THF (*ca* 20 mL) added, the resulting solution was stirred for 18 h. Filtered and washed with Et_2O (3 x 20 mL). Dried under vacuum. ^{1}H NMR (CD_2Cl_2): δ_H Intractable mixture. $^{31}P\{^1H\}$ NMR (CD_2Cl_2): δ_P Intractable mixture.

ATTEMPTED SYNTHESIS OF *trans*-[Ru(dppe)$_2$(Et)$_2$]

Trans-[Ru(dppe)$_2$(Cl)]OTf (0.53 g, 0.49 mmol) and Et_2Mg (0.041 g, 0.50 mmol) combined, Et_2O (*ca* 20 mL) added the resulting solution was stirred 18 h. Filtered and washed with Et_2O (3 x 20 mL). Dried under vacuum. ^{1}H NMR (CD_2Cl_2): δ_H Intractable mixture. $^{31}P\{^1H\}$ NMR (CD_2Cl_2): δ_P Intractable mixture.

ATTEMPTED SYNTHESIS OF *trans*-[Ru(dppe)$_2$(Bn)(Cl)]

KBn (0.062 g, 0.48 mmol) in toluene (*ca* 20 mL) added to a solution of *trans*-[Ru(dppe)$_2$(Cl)]OTf (0.50 g, 0.46 mmol) in toluene (*ca* 20 mL), the resulting solution was stirred 18 h. Filtered giving a red solid and a yellow solution. Solid dried under vacuum. Solvent removed from solution under reduced pressure. Dried under vacuum. ^{1}H NMR (CD_2Cl_2): δ_H Intractable mixture. $^{31}P\{^1H\}$ NMR (CD_2Cl_2): δ_P Intractable mixture.

EXPERIMENTAL DETAILS FOR CHAPTER 4

REACTIVITY STUDIES OF *trans*-[RuBr(dppe)$_2$(C≡P)]

Trans-[RuBr(dppe)$_2$(C≡P)] + Me$_2$Mg

Trans-[RuBr(dppe)$_2$(C≡P)] (0.031 g, 0.03 mmol) and Me$_2$Mg (0.003 g, 0.04 mmol) were combined in THF (*ca* 10 mL) and stirred overnight. The mixture was filtered, and volatiles were removed under reduced pressure. Key resonances: ^{1}H NMR (CD_2Cl_2): δ_H −2.1 (3H, *qnt*, *J* = 5.6 Hz, CH_3), 2.6 (14H, *m* (*br*), C_2H_4). ^{31}P{1H} NMR (CD_2Cl_2): δ_P 179.8 (1P, *m* (*br*), C≡P), 60.7 (4P, *d*, J_{PP} = 4.3 Hz, $Ph_2PCH_2CH_2PPh_2$).

Note: Solvent shift effects (*cf*. pure *trans*-[RuMe(dppe)$_2$(C≡P)]) result from appreciable residual THF in the solvent mixture.

Trans-[RuBr(dppe)$_2$(C≡P)] + Et$_2$Mg

Trans-[RuBr(dppe)$_2$(C≡P)] (0.050 g, 0.048 mmol) and Et$_2$Mg (0.006 g, 0.18 mmol) were combined in THF (*ca* 5 mL) and stirred overnight. The mixture was filtered, and volatiles were removed under reduced pressure. Key resonances: ^{1}H NMR (CD_2Cl_2): δ_H – 11.2 ppm (*q*, *J* = 20 Hz, Hydride) ^{31}P{1H} NMR (CD_2Cl_2): δ_P 157 (1P, *m* (*br*), C≡P), 65 (4P, *dd*, J_{PP} = 2.0, 5.0 Hz, $Ph_2PCH_2CH_2PPh_2$).

Trans-[RuBr(dppe)$_2$(C≡P)] + PhMgBr

Trans-[RuBr(dppe)$_2$(C≡P)] (0.050 g, 0.049 mmol) in THF (*ca* 5 mL) was stirred and PhMgBr (0.1 mL, 0.3 mmol) was added and the reaction mixture was stirred overnight. The mixture was filtered, and volatiles were removed under reduced pressure. No reaction observed.

Trans-[RuBr(dppe)$_2$(C≡P)] + LiC≡CPh

Trans-[RuBr(dppe)$_2$(C≡P)] (0.050 g, 0.049 mmol) and LiC≡CPh (0.006 g, 0.058 mmol) were combined in THF (*ca* 10 mL) and stirred overnight. The mixture was filtered, and volatiles were removed under reduced pressure. No reaction observed.

Trans-[RuBr(dppe)$_2$(C≡P)] + LiC≡CSiMe$_3$

Trans-[RuBr(dppe)$_2$(C≡P)] (0.050 g, 0.049 mmol) and LiC≡CSiMe$_3$ (0.006 g, 0.058 mmol) were combined in THF (*ca* 10 mL) and stirred overnight. The mixture was filtered, and volatiles were removed under reduced pressure. No reaction observed.

Trans-[RuBr(dppe)$_2$(C≡P)] + NaCN

Trans-[RuBr(dppe)$_2$(C≡P)] (0.050 g, 0.049 mmol) and NaCN (0.005 g, 0.10 mmol) were combined in THF (*ca* 10 mL) and stirred overnight. The mixture was filtered, and volatiles were removed under reduced pressure. No reaction observed.

SYNTHESIS OF *trans*-[Ru(C≡P)(dppe)$_2$]OTf (4.1.OTf)

Trans-Ru(dppe)$_2$(Br)(C≡P) (0.400 g, 0.39 mmol) and TlOTf (0.140 g, 0.39 mmol) combined, and DCM (*ca* 20 ml) was added. The resulting solution was stirred for *ca* 2 h. Filtration and removal of volatiles under reduced pressure yielded a purple solid. Yield = 0.365 g, 0.34 mmol, 87%. ^{1}H NMR (CD_2Cl_2): δ_H 7.7 (8H, *m* (*br*), *m*-C_6H_5), 7.4 (4H, *t*, *J* = 7.5 Hz, *p*-C_6H_5), 7.3 (4H, *t*, *J* = 7.5 Hz, *p*-C_6H_5), 7.1 (16H, *t, J* = 7.6 Hz, *o*-C_6H_5), 6.5 (8H, *m* (*br*), *m*-C_6H_5), 3.0 (4H, *qnt*, *J* = 8.0 Hz, C_2H_4), 2.6 (4H, *qnt*, *J* = 8.0 Hz, C_2H_4). $^{13}C\{^1H\}$ NMR (CD_2Cl_2): δ_C 265 (*m* (*br*), C≡P), 134.1 (*m* (*br*), *m*-C_6H_5), 133.4 (*qnt*, J_{CP} = 2.9 Hz *m*-C_6H_5), 132.3 (*m*, *ipso*-C_6H_5), 131.9 (*s*, *p*-C_6H_5), 131.2 (*s*, *p*-C_6H_5), 129.7 (*qnt*, J_{CP} = 2.1 Hz, o-C_6H_5), 128.7 (*qnt*, J_{CP} = 2.5 Hz, *o*-C_6H_5), 121.5 (*q*, J_{CF} = 320 Hz, CF_3), 29.4 (*qnt,* J_{CP} = 11.7

Hz, CH_2CH_2). $^{31}P\{^1H\}$ NMR (CD_2Cl_2): δ_P 154 (1P, *qnt*, J_{PP} = 7.2 Hz, C≡P), 52.1 (4P, *d*, J_{PP} = 7.2 Hz, $Ph_2PCH_2CH_2PPh_2$). ^{19}F NMR (375.86 MHz, CD_2Cl_2): δ_F −78.9 (s, OTF). ν_{max}/cm^{-1}: 1242 (C≡P). Calcd for $C_{54}H_{48}P_5F_3O_3SRu.0.66C_6H_6$: C, 61.00; H, 4.59. Found: C, 61.70, H, 4.66 (recrystallized sample as the benzene solvate). Crystal data for **4.1$^+$**: Crystals were obtained by slow recrystallization from benzene at ambient temperature. $C_{53}H_{48}P_5Ru.SO_2CF_2.1.5C_6H_6$ (M_w = 1207.07 g mol^{-1}), triclinic, *P*$\bar{1}$ (No. 2), *a* = 10.8285(2) Å, *b* = 13.5818(3) Å, *c* = 19.4936(4) Å, *α* = 99.007(2)°, *β* = 102.147(2)°, *γ* = 91.643(2)°, *V* = 2762.65(10) Å, *Z* =2, *T* = 100(2) K, *μ*(Cu *Kα*) = 4.487 mm^{-1}, D_c = 1.451 Mg m^{-3}, 10477 independent reflections, full matrix F^2 refinement R_1 = 0.0506 on 9214 independent absorption corrected reflections, [I > 2*σ*(*I*); $2\vartheta_{max}$ = 143.20°], 685 parameters, wR_2 = 0.1265 (all data).

SYNTHESIS OF *trans*-[Ru(C≡P)(C≡O)(dppe)$_2$]OTf (4.2.OTf)

CO gas was bubbled through a CH_2Cl_2 solution of 4.1 (0.094 g, 0.086 mmol) for 2 min, resulting in a colour change of the solution from purple to pale yellow. Removal of the volatiles under reduced pressure afforded a pale yellow solid. ^1H NMR (CD_2Cl_2): δ_H 7.57 (8H, *m* (*br*), *m*-C_6H_5), 7.45 (4H, *t*, *J* = 7.3 Hz, *p*'-C_6H_5), 7.42 (4H, *t*, *J* = 7.4 Hz, *p*-C_6H_5), 7.23 (8H, *t*, *J* = 7.5 Hz, *o*'-C_6H_5), 7.19 (8H, *t*, *J* = 7.3 Hz, *o*-C_6H_5), 7.01 (8H, *m* (br), m'-C_6H_5), 3.08 (4H, *qnt*, *J* = 8 Hz C_2H_4), 2.65 (4H, *qnt*, *J* = 8 Hz C_2H_4). $^{13}C\{^1H\}$ NMR (CD_2Cl_2): δ_C 249 (*m* (*br*), C≡P), 200.5 (*qnt*, J_{CP} = 10 Hz, 4 Hz, C≡O), 134.8 (*qnt*, J_{CP} = 2 Hz, *m*-C_6H_5), 133.4 (*qnt*, J_{CP} = 11 Hz, *ipso*'-C_6H_5), 132.9 (*qnt*, J_{CP} = 2.7 Hz, m'- C_6H_5), 131.9 (*s*, *p*'-C_6H_5), 131.7 (*s*, *p*-C_6H_5), 131.0 (*qnt*, J_{CP} = 12 Hz, *ipso*-C_6H_5), 129.5 (*qnt*, J_{CP} = 2 Hz, *o*'-C_6H_5), 128.6 (*qnt*, J_{CP} = 2.5 Hz, *o*-C_6H_5), 121.5 (*q*, J_{CF} = 322 Hz, CF_3), 30.0 (*qnt*, J_{CP} = 11.7 Hz, CH_2CH_2). $^{31}P\{^1H\}$ NMR (CD_2Cl_2): δ_P 181.3 (1P, *qnt*, J_{PP} = 10 Hz, C≡P), 52.1 (4P, *d*, J_{PP} =10 Hz, $Ph_2PCH_2CH_2PPh_2$). ^{19}F NMR (CD_2Cl_2): δ_F −78.9 (s, OTF). ν_{max}/cm^{-1}: 1980 (C≡O), 1261 (C≡P). Anal. Calcd for $C_{55}H_{48}P_5F_3O_4SRu.C_6H_6$: C, 55.91; H, 4.19. Found: C, 55.61; H, 4.08. Crystal data for **4.2$^+$:** Crystals were obtained by slow recrystallization from benzene at ambient temperature.

$C_{55}H_{48}P_5F_3O_4SRu.\cdot C_6H_6$ (M_w = 1196.02 g mol^{-1}), monoclinic, *C*2/*c* (No. 15), *a* = 23.3771(4) Å, *b* = 12.6192(3) Å, *c* = 37.6417(9) Å, *β* = 101.416(2)°, *V* = 10884.6(4) Å, *Z* = 8, T = 100(2) K, *μ*(Cu K*α*) = 4.564 mm^{-1}, D_c = 1.460 Mg m^{-3}, 10225 independent reflections, full matrix F^2 refinement R_1 =0.0546 on 8252 independent absorption corrected reflections, [$I > 2\sigma(I)$; $2\vartheta_{max}$ = 143.40°], 830 parameters, wR_2 = 0.1257 (all data).

SYNTHESIS OF *trans*-[Ru(C≡P)(C≡N)(dppe)$_2$] (4.3)

Trans-[Ru(dppe)$_2$(C≡P)]OTf (0.094 g, 0.086 mmol) and NaCN (0.006 g, 0.12 mmol) were combined and THF (*ca* 5 ml) was added, the resulting solution was stirred for 24 h. Filtration through a filter pipette yielded a pale-yellow solid which was dried under reduced pressure. ^{1}H NMR (CD_2Cl_2): δ_H 7.66 (8H, *m* (*br*), *m*-C_6H_5), 7.31 (8H, *m* (*br*), *m*-C_6H_5), 7.26 (8H, *m*, *p*-C_6H_5), 7.11 (16H, *t*, *J* = 7.6 Hz, *o*-C_6H_5), 7.05 (16H, *t*, *J* = 7.6 Hz, *o'*-C_6H_5), 2.90 (4H, *qnt*, *J* = 7.45 Hz C_2H_4), 2.60 (4H, *qnt*, *J* = 7.45 Hz C_2H_4).^{13}C{^{1}H} NMR (C_6D_6): δ_C 135.3 (*m* (*br*), *ipso*-C_6H_5), 134.8 (*m* (*br*), *m*-C_6H_5), 129.7 (*m* (*br*), *ipso*-C_6H_5), 129.5 (*m* (*br*), *m*-C_6H_5), 127.9 (*qnt*, J_{CP} = 2 Hz, *o*-C_6H_5), 127.3 (*qnt*, J_{CP} = 2 Hz, *o*-C_6H_5), 30.0 (*qnt*, J_{CP} = 12.6 Hz, CH_2CH_2), the cyaphide carbon could not be resolved. ^{31}P{^{1}H} NMR (CD_2Cl_2): δ_P 161.3 (1P, *m (br)*, C≡P), 51.1 (4P, *d*, J_{PP} = 5.1 Hz, $Ph_2PCH_2CH_2PPh_2$). ν_{max}/cm^{-1}: 2075 (C≡N), 1245 (C≡P). Crystal data for **4.3**: Crystals were obtained by slow recrystallization from CH_2Cl_2 and Hexanes at ambient temperature. $C_{54}H_{48}P_5NRu$. (M_w = 967.15 g mol^{-1}), monoclinic, $P2_{1/c}$, *a* = 23.6015(12) Å, *b* = 11.7391(6) Å, *c* = 16.8129(9) Å, *α* = 90.037(4)°, *β* = 103.725(4)°, *γ* = 90.030(4)°, *V* = 4525.2(4) Å^3, *Z* = 4, *T* = 100(2) K, *μ*(Cu *Kα*) = 4.776 mm^{-1}, D_c = 1.419 Mg m^{-3}, 14683 independent reflections, full matrix F^2 refinement R_1 = 0.0773 on 8596 independent absorption corrected reflections, [$I > 2\sigma(I)$; $2\vartheta_{max}$ = 143.938°], 546 parameters, wR_2 = 0.1910 (all data).

SYNTHESIS OF *trans*-[Ru(C≡P)(SC≡N)(dppe)$_2$] (4.4)

Trans-[Ru(dppe)$_2$(C≡P)]OTf (0.020 g, 0.019 mmol) and KSCN (0.005 g, 0.05 mmol) were combined and DCM (*ca* 10 ml) was added, the resulting solution was stirred for 18 h. Filtration yielded a pale-yellow solid which was dried under reduced pressure. ^{1}H NMR (CD_2Cl_2): δ_H 7.75 (8H, *m* (*br*), C_6H_5), 7.34 (4H, *t*, *J* = 7.4 Hz, C_6H_5), 7.26 (4H, *t*, *J* = 7.4 Hz, C_6H_5), 7.15 (8H, *t*, *J* = 7.4 Hz, C_6H_5), 7.05 (8H, *t*, *J* = 7.4 Hz, C_6H_5), 6.91 (8H, *m* (*br*), C_6H_5), 2.90 (4H, *qnt*, *J* = 5.90 Hz C_2H_4), 2.60 (4H, *qnt*, *J* = 5.90 Hz C_2H_4). ^{31}P{^{1}H} NMR (CD_2Cl_2): δ_P 148.0 (1P, *m (br)*, C≡P), 47.0 (4P, *d*, J_{PP} = 4.70 Hz, $Ph_2PCH_2CH_2PPh_2$).

SYNTHESIS OF *trans*-[Ru(C≡P)(OC≡N)(dppe)$_2$] (4.5)

Trans-[Ru(dppe)$_2$(C≡P)]OTf (0.020 g, 0.019 mmol) and KOCN (0.014 g, 0.018 mmol) were combined and DCM (*ca* 5 ml) was added, the resulting solution was stirred for 18 h. Filtration yielded a pale-yellow solid which was dried under reduced pressure. ^{1}H NMR (CD_2Cl_2): Intractable mixture of products including resonance for 4.1. ^{31}P{^{1}H} NMR (CD_2Cl_2): Key Product NMR Resonances δ_P 142.0 (1P, *m (br)*, C≡P), 47.0 (4P, *d*, J_{PP} = 4.70 Hz, $Ph_2PCH_2CH_2PPh_2$).

SYNTHESIS OF *trans*-[Ru(C≡P)F(dppe)$_2$] (4.6)

Trans-[Ru(dppe)$_2$(C≡P)]OTf (0.052 g, 0.048 mmol) and CsF (0.012 g, 0.079 mmol) were combined and DCM (*ca* 5 ml) was added, the resulting solution was stirred for 18 h. Filtration yielded a bright-yellow solid which was dried under reduced pressure. ^{1}H NMR (CD_2Cl_2): 7.60 (6H, *m* (*br*), *m*-C_6H_5), 7.40 (4H, *dt*, *J* = 20.1 Hz and 7.4 Hz, *p*-C_6H_5), 7.26 (2H, *t*, *J* = 7.4 Hz, *m*-C_6H_5), 7.20 (12H, *q*, *J* = 7.0 Hz, *o*-C_6H_5), 7.20 (8H, *m*, *m*-C_6H_5), 6.80 (4H, *m*, *o*-C_6H_5), 2.70 (8H, *dqnt*, *J* = 108 Hz and 5.80 Hz C_2H_4). ^{13}C{^{1}H} NMR (CD_2Cl_2): δ_C 138.0 (*m (br), ipso*-C_6H_5), 135.4 (*m (br), m*-C_6H_5), 135.0(*s, p*-C_6H_5), 134.8 (*m (br)*, *m*-C_6H_5), 132.0 (*d, J*= 10 Hz, *p*-C_6H_5), 132.8 (*qnt*, *J* = 2.4 Hz, *o*-C_6H_5), 130 (*m*, *o*-C_6H_5), 128 (*m*, o-C_6H_5), 31.0 (*qnt, J_{CP}* = 10.8 Hz, CH_2CH_2); the cyaphide carbon could not be

resolved. $^{31}P\{^1H\}$ NMR (CD_2Cl_2): δ_P 125.6 (1P, *qnt*, J_{PP} = 15.5 Hz, C≡P), 45.5 (4P, *d*, J_{PP} = 15.5 Hz J_{PF} = 70 Hz, $Ph_2PCH_2CH_2PPh_2$). ^{19}F NMR (CD_2Cl_2): δ_F 400 (*dm*, J_{PF} = 70 Hz, Ru-F). ν_{max}/cm^{-1}: 1259 (C≡P). Crystal data for **4.6**: Crystals were obtained by slow recrystallization from CH_2Cl_2 and Hexanes at ambient temperature. $C_{53}H_{50}P_5FRu$. CH_2Cl_2 (M_w = 1044.76 g mol^{-1}), triclinic, *P-1* , *a* = 12.5638(5) Å, *b* = 13.2818(5) Å, *c* = 16.7791(7) Å, *α* = 107.843(4)°, *β* = 92.282(3)°, *γ* = 115.409(4)°, *V* = 2359.18(18) Å^3, *Z* = 2, *T* = 100(2) K, *μ*(Cu *Kα*) = 5.660 mm^{-1}, D_c = 1.471 Mg m^{-3}, 13767 independent reflections, full matrix F^2 refinement R_1 = 0.0381 on 8310 independent absorption corrected reflections, [I > 2*σ*(*I*); $2\vartheta_{max}$ = 143.254°], 568 parameters, wR_2 = 0.1176 (all data).

SYNTHESIS OF *trans*-[Ru(C≡P)(P≡CSiMe$_3$)(dppe)$_2$]OTf (4.7.OTf)

To a suspension of *trans*-[Ru(dppe)$_2$(C≡P)]OTf (0.05 g, 0.046 mmol) in 1,4-dioxane (*ca* 5 ml), Me_3SiCP (2 ml, 0.027 moldm^{-3}, 0.054 mmol) was added, the resulting suspension was stirred for *ca* 1 hour. Filtration yielded a cream-yellow solid. ^1H NMR (CD_2Cl_2): 7.62 (8H, *m* (*br*), *m*-C_6H_5), 7.44 (8H, *t*, *J* = 7.4 Hz, *p*-C_6H_5), 7.21 (16H, *t*, *J* = 7.54 Hz, *o*-C_6H_5), 7.13 (8H, , *m* (*br*), *m*-C_6H_5), 3.04 (4H, *m* (*br*), C_2H_4), 2.79 (4H, *m* (*br*), C_2H_4), -0.14 (9H, *s*, $SiMe_3$). $^{13}C\{^1H\}$ NMR (C_6D_6): δ_C 134.9 (*m* (*br*), *ipso*-C_6H_5), 133.6 (*m* (*br*), *m*-C_6H_5), 133.4 (*m* (*br*), *m*-C_6H_5), 132.1 (*m* (*br*), *ipso*-C_6H_5), 131.5 (*m* (*br*), *p*-C_6H_5), 131.1 (*m* (*br*), *m*-C_6H_5), 128.9 (*qnt*, J_{CP} = 2.4 Hz, *o*-C_6H_5), 128.4 (*qnt*, J_{CP} = 2.4 Hz, *o*-C_6H_5), 29.5 (*qnt*, J_{CP} = 10.8 Hz, CH_2CH_2), -0.36 (*s*, $SiMe_3$), the cyaphide carbon could not be resolved. $^{31}P\{^1H\}$ NMR (CD_2Cl_2): δ_P 154 (1P, *qnt,* J_{PP} = 10 Hz, C≡P), 108 (1P, *qnt,* J_{PP} = 32 Hz, C≡P), 39.5 (4P, *d*, J_{PP} = 32 Hz and 10 Hz, $Ph_2PCH_2CH_2PPh_2$). ^{19}F NMR (CD_2Cl_2): δ_F −78.9 (*s*, OTF). ^{29}Si NMR (CD_2Cl_2): δ_{Si} -12.9 ($RuPCSiMe_3$).

SYNTHESIS OF *trans*-[Ru(C≡P)$_2$(dppe)$_2$] (4.8)

A solution of *trans*-[Ru(dppe)$_2$(C≡P)(P≡CSiMe$_3$)]OTf (0.055 g, 0.046 mmol) in THF (*ca* 10 ml) was cooled to -30 ◦C, and a solution of NaOPh (0.008 g, 0.069 mmol) in THF (*ca* 5 ml) was added dropwise. Once the addition was complete the reaction was removed from cold bath. Instant removal of solvent under reduced pressure yielded a yellow solid, which was washed with acetonitrile (*ca* 3 x 5 ml) and dried under reduced pressure. Yield = 0.040 g, mmol, 89 %. ^{1}H NMR (CD_2Cl_2): 7.61 (16H, *m* (*br*), *m*-C_6H_5), 7.27 (8H, *t*, *J* = 7.4 Hz, *p*-C_6H_5), 7.08 (16H, *t*, *J* = 7.50 Hz, *o*-C_6H_5), 2.87 (8H, *m* (*br*), C_2H_4).^{13}C{^{1}H} NMR (C_6D_6): δ_C 246 (*m* (*br*), C≡P),135.7 (*m* (*br*), *m*-C_6H_5), 129.9 (*m* (*br*), *p*-C_6H_5), 127.6 (*m* (*br*), *o*-C_6H_5), 26.3 (*m* (*br*), CH_2CH_2). ^{31}P{^{1}H} NMR (CD_2Cl_2): δ_P 186 (*m* (*br*), C≡P), 49.6 (4P, *d*, J_{PP} = 4.7 Hz, $Ph_2PCH_2CH_2PPh_2$). ν_{max}/cm^{-1}: 1227 (C≡P).

SYNTHESIS OF *trans*-[Ru(C≡P)(N≡CCH$_3$)(dppe)$_2$]OTf (4.9.OTf)

Trans-[Ru(dppe)$_2$(C≡P)]OTf (0.050 g, 0.046 mmol) was stirred in acetonitrile (*ca* 25 mL) for 5 minutes at room temperature. Removal of the solvent under reduced pressure yielded a yellow solid which was dried under vacuum. ^{1}H NMR (CD_2Cl_2): 8.0 (8H, *m* (*br*), *m*-C_6H_5), 7.4 (4H, *t*, *J* = 7.4 Hz, *p*-C_6H_5), 7.3 (4H, *t*, *J* = 7.5 Hz, *p*-C_6H_5), 7.2 (8H, *t*, *J* = 7.6 Hz, *o*-C_6H_5), 7.1 (8H, *t*, *J* = 7.6 Hz, *o*-C_6H_5), 6.7 (8H, *m* (*br*), *m*-C_6H_5), 2.9 (4H, *qnt, J* = 8.0 Hz, C_2H_4), 2.8 (4H, *qnt, J* = 8.0 Hz, C_2H_4), 1.29 (3H, *s*, CH_3). ^{13}C{^{1}H} NMR (C_6D_6): δ_C 258 (*m* (*br*), C≡P), 135.3 (*m* (*br*), *m*-C_6H_5), 133.9 (*qnt, J* = 11.4 Hz, *ipso*-C_6H_5), 133.0 (*qnt, J* = 11.4 Hz, *ipso*-C_6H_5), 132.8 (*m* (*br*), *m*-C_6H_5), 131.2 (*m* (*br*), *p*-C_6H_5), 130.5 (*m* (*br*), *p*-C_6H_5), 128.8 (*m* (*br*), *o*-C_6H_5), 128.2 (*m* (*br*), *o*-C_6H_5), 125.6 (*s*, C≡N), 30.0 (*m* (*br*), CH_2CH_2), 4.1 (*s*, CH_3). ^{31}P{^{1}H} NMR (CD_2Cl_2): δ_P 168 (*m* (*br*), C≡P), 49.6 (4P, *d*, J_{PP} = 5.7 Hz $Ph_2PCH_2CH_2PPh_2$). ^{19}F NMR (CD_2Cl_2): δ_F −78.9 (*s*, OTF). ν_{max}/cm^{-1}: 1255 (C≡P). Crystal data for **4.9$^+$**: Crystals were obtained by slow recrystallization from CH_2Cl_2 and hexanes at ambient temperature. $C_{58}H_{51}P_5NRu.SO_3F_3.CH_4Cl_4$ (M_w = 1310.60 g mol^{-1}), monoclinic, *P2$_{1/n}$* , *a* = 10.51110(10) Å, *b* = 24.5307(2) Å, *c* = 17.4387(2) Å, *α* = 90°, *β* = 97.0930(10)°, *γ* = 90°, *V* =

6027.83(15) Å^3, Z =4, T = 100(2) K, μ(Cu $K\alpha$) = 5.140 mm^{-1}, D_c = 1.444 Mg m^{-3}, 19383 independent reflections, full matrix F^2 refinement R_1 = 0.0734 on 11394 independent absorption corrected reflections, [I > 2σ(I); 2ϑ_{max} = 143.382°], 686 parameters, wR$_2$ = 0.2102 (all data).

SYNTHESIS OF *trans*-[Ru(C≡P)(NC$_6$H$_5$)(dppe)$_2$]OTf (4.10.OTf)

To an NMR sample of *trans*-[Ru(C≡P)(dppe)$_2$]OTf (0.002 g, 0.0018 mmol) in CD_2Cl_2 was added excess pyridine (*ca* 0.01 mL, 0.012 mmol). The sample was sealed, agitated, and then monitored by NMR. A colour change from purple to red was observed over the 1 hour. ^{1}H NMR (CD_2Cl_2): Intractable mixture of products. ^{31}P{^{1}H} NMR (CD_2Cl_2): δ_P 161 (1P, *qnt,* J_{PP} = 5.0 Hz, C≡P), 72.8 (0.14P, *s,* unknown), 50.0 (4P, *d*, J_{PP} = 5.0 Hz $Ph_2PCH_2CH_2PPh_2$), 49.6 (0.77P, *s,* unknown), -9.64 (0.20P, *s,* free $Ph_2PCH_2CH_2PPh_2$).

Note: Due to a mixture of products for the ^{31}P{^{1}H} NMR the relative integrals have been calculated in comparison to the major product resonances at 50.0 ppm (4P) and 161 ppm (1P) hence the fractional integrals values for the other resonances.

Trans-[Ru(C≡P)(dppe)$_2$]OTf (4.1.OTf) and PMe$_3$

1 equivalent PMe$_3$

To an NMR sample of *trans*-[Ru(C≡P)(dppe)$_2$]OTf (0.018 g, 0.017 mmol) in CD_2Cl_2 was added 1 equiv. of PMe_3 (0.002, 0.019 mmol). The sample was sealed, agitated, and then monitored by NMR after 1 hour and after 18 h. ^{1}H NMR (CD_2Cl_2): Intractable mixture of products. ^{31}P{^{1}H} NMR (CD_2Cl_2): δ_P 153.9 (0.68P, *br (m)*, C≡P), 153.7 (0.44P, *br (m)*, C≡P **4.1**$^+$), 144.5 (0.50P, *br (m)*, C≡P), 52.1 (1.60P, *d*, J_{PP} = 7.2 Hz, $Ph_2PCH_2CH_2PPh_2$, **4.1**$^+$), 48.2 (2.12P, *dm*, J_{PP} = 210 Hz, $Ph_2PCH_2CH_2PPh_2$), -12.9 (*s*, free $Ph_2PCH_2CH_2PPh_2$), −20.6 (2.14P, *dm*, J_{PP} = 210 Hz, PMe_3), −28.4 (1.13P, *q*, J_{PP} = 39 Hz, PMe_3), −35.2 (1.05P, *qnt*, J_{PP} = 23 Hz, PMe_3).

3 equivalents PMe_3

To an DCM (*ca* 5 mL) solution of *trans*-[Ru(C≡P)(dppe)$_2$]OTf (0.020 g, 0.018 mmol) 3 equiv. of PMe_3 (0.006, 0.059 mmol) after 18 h, filtration and removal of solvent under vacuum resulted in a cream solid. ^{1}H NMR (CD_2Cl_2): Intractable mixture of products. $^{31}P\{^1H\}$ NMR (CD_2Cl_2): δ_P 153.9 (1.74P, *br (m)*, C≡P), 144.5 (1.00P, *br (m)*, C≡P), 48.4 (3.76P, *dm*, J_{PP} = 210 Hz, $Ph_2PCH_2CH_2PPh_2$), 31.0 (0.61P, *s*, $Ph_2PCH_2CH_2PPh_2$), 30.1 (0.16P, *s*, $Ph_2PCH_2CH_2PPh_2$), −12.34 (0.28P, *d*, J_{PP} = 48.8 Hz, PMe_3), −17.8 (0.58P, *dd*, J_{PP} = 8.7, 27.0 Hz, PMe_3), −12.9 (*s*, free $Ph_2PCH_2CH_2PPh_2$), −20.8 (5.3P, *dm*, J_{PP} = 210 Hz, PMe_3), −28.4 (2.31P, *q*, J_{PP} = 39 Hz, PMe_3), −35.2 (2.11P, *qnt*, J_{PP} = 23 Hz, PMe_3). Crystal data for: Crystals were obtained by slow recrystallization from CD_2Cl_2 and hexanes at ambient temperature. $C_{37}H_{51}P_6Ru.SO_3F_3.CH_2Cl_2$ (M_w = 1004.65 g mol^{-1}), monoclinic, $P2_{1/c}$, a = 10.51110(10) Å, b = 24.5307(2) Å, c = 17.4387(2) Å, α = 90°, β = 97.0930(10)°, γ = 90°, V = 4462.06(8) Å^3, Z =1, T = 100(2) K, μ(Cu $K\alpha$) = 6.821 mm^{-1}, D_c = 1.451 Mg m^{-3}, 40490 independent reflections, full matrix F^2 refinement R_1 = 0.0896 on 8504 independent absorption corrected reflections, [I > 2σ(I); 2ϑ_{max} = 142.376°], 496 parameters, wR$_2$ = 0.2105 (all data).

Excess PMe_3

To an DCM (*ca* 10 mL) solution of *trans*-[Ru(C≡P)(dppe)$_2$]OTf (0.022 g, 0.020 mmol) excess PMe_3 (0.2 mL, 1.97 mmol) after 18 h, filtration and removal of solvent under vacuum resulted in a yellow solid. ^{1}H NMR (CD_2Cl_2): Intractable mixture of products. $^{31}P\{^1H\}$ NMR (CD_2Cl_2): δ_P 112.3 (1.00P, *br (s)*, C≡P), 39.4 (1.83P, *dm*, J_{PP} = 23 Hz and 248 Hz, $Ph_2PCH_2CH_2PPh_2$), 36.8 (0.53P, *s,* $Ph_2PCH_2CH_2PPh_2$), 33.9 (0.77P, *s*, $Ph_2PCH_2CH_2PPh_2$), 24.17 (0.17P, *s*, $Ph_2PCH_2CH_2PPh_2$), −10.2 (2.02P, *dm*, J_{PP} = 17 Hz and 246 Hz, PMe_3), −12.8 (*s*, free $Ph_2PCH_2CH_2PPh_2$).

Neat PMe_3

To *trans*-[Ru(C≡P)(dppe)$_2$]OTf (0.109 g, 0.01 mmol), PMe_3 (*ca* 5.0 mL) was added after 18 h, filtration and washed with benzene (*ca* 3 x 10 mL), dried under vacuum resulted in a cream solid. ^{1}H NMR (399.5 MHz, CD_2Cl_2): Intractable mixture of products. $^{31}P\{^1H\}$ NMR (161.71 MHz, CD_2Cl_2): δ_P 153.7 (1.00P, *br (m)*, C≡P), 144.3 (0.57P, *br (m)*, C≡P), 51.3 (0.7P, *s*, $Ph_2PCH_2CH_2PPh_2$), 48.2 (2.01P, *dm*, J_{PP} = 210 Hz, $Ph_2PCH_2CH_2PPh_2$), 46.1 (0.18, *s*, $Ph_2PCH_2CH_2PPh_2$), 37.8 (0.75P, *s*, $Ph_2PCH_2CH_2PPh_2$), 25.6 (0.33P, *dtd*, J_{PP} = 10 Hz, 30 Hz and 240 Hz, unknown), 20.6 (0.71P, *m*, unknown), −12.9 (*s*, free $Ph_2PCH_2CH_2PPh_2$), −20.7 (2.97P, *dm*, J_{PP} = 210 Hz, PMe_3), −28.4 (1.29P, *q*, J_{PP} = 39 Hz, PMe_3), −35.2 (1.18P, *qnt*, J_{PP} = 23 Hz, PMe_3). ^{19}F NMR (CD_2Cl_2): δ_F −78.9 (*s*, OTF). ν_{max}/cm^{-1}: 1260 (C≡P).

CYCLOPENTADIENYL DERIVATIVES AND REDUCTION CHEMISTRY

Note: Due to a mixture of products for the $^{31}P\{^1H\}$ NMR the relative integrals have been calculated in comparison to the major product resonances hence the fractional integrals values for the other resonances.

Trans*-[Ru(C≡P)(dppe)$_2$]OTf + KCp

A solution of *trans*-[Ru(C≡P)(dppe)$_2$]OTf (0.021g, 0.019 mmol) and KCp* (0.004 g, 0.023 mmol) in THF (*ca* 10 mL), the resulting solution was stirred for 18 h, filtered and volatiles removed under reduced pressure. Dried under vacuum. ^{1}H NMR (CD_2Cl_2): No observed reaction. $^{31}P\{^1H\}$ NMR (CD_2Cl_2): No observed reaction.

***Trans*-[Ru(C≡P)(dppe)$_2$]OTf + LiCp**

To an NMR sample of *trans*-[Ru(C≡P)(dppe)$_2$]OTf (0.013g, 0.011 mmol) in C_6D_6 was added LiCp (0.001g, 0.014 mmol). The sample was sealed, agitated, and then monitored by NMR after 1

hour and after 18 h. ^{1}H NMR (C_6D_6): Intractable mixture of products. $^{31}P\{^{1}H\}$ NMR (C_6D_6): Intractable mixture of products including resonances δ_P 141 (0.7P, *dm* (*br*), C≡P), 140 (1P, *m* (*br*), C≡P), 134 (0.4P, *m* (*br*), C≡P), 50.5 (4P, *s*, $Ph_2PCH_2CH_2PPh_2$) Crystal data for **4.19**: Crystals were obtained by slow recrystallization from C_6D_6 at ambient temperature. $C_{65}H_{60}P_5Ru$ (M_w = 1097.05 g mol^{-1}), triclinic, $P\bar{1}$, a = 13.819052) Å, b = 14.1804(6) Å, c = 15.8661(7) Å, α = 66.223(4)°, β = 78.383(3)°, γ = 72.090(4)°, V = 2696.6(2) Å^3, Z =2, T = 100(2) K, μ(Cu $K\alpha$) = 4.063 mm^{-1}, D_c = 1.451 Mg m^{-3}, 14311 independent reflections, full matrix F^2 refinement R_1 = 0.0630 on 9476 independent absorption corrected reflections, [I > 2σ(I); 2ϑ_{max} = 134.156°], 635 parameters, wR$_2$ = 0.2604 (all data).

Trans-[Ru(C≡P)(dppe)$_2$]OTf + NaNaphthalenide

To a solution of *trans*-[Ru(C≡P)(dppe)$_2$]OTf (0.022g, 0.020 mmol) in THF (*ca* 5 mL), sodium naphthalenide (*ca* 0.5 mL, 0.065 moldm^{-3}, 0.033 mmol) was added, stirred for 18 h, filtered and volatiles removed under reduced pressure. ^{1}H NMR (CD_2Cl_2): Intractable mixture of products. $^{31}P\{^{1}H\}$ NMR (CD_2Cl_2): (Key new resonances) δ_P 147 (1P, *m (br),* C≡P),), 135 (0.64P, *m (br),* C≡P), 118 (1P, *m (br),* C≡P), 49 (2.7P, *s*, $Ph_2PCH_2CH_2PPh_2$), 47 (2.3P, *m* (*br*), $Ph_2PCH_2CH_2PPh_2$), −30 (1P, *dm*, J = 310 Hz, unknown).

X-ray diffraction studies of crystals grown from slow evaporation from benzene gave connectivity data only.

Trans-[Ru(C≡P)(dppe)$_2$]OTf + Na/Hg

A solution of *trans*-[Ru(C≡P)(dppe)$_2$]OTf (0.028g, 0.026 mmol) in THF (*ca* 5 mL), was added to a Na/Hg (0.5919 g. 0.4% Na, 3.3 eq, 0.087 mmol) in THF (*ca* 5 mL). After 2.5 h solution was decanted off from remaining Na/Hg and filtered through a filter pipette and volatiles removed under reduced pressure. ^{1}H NMR (CD_2Cl_2): Intractable mixture of products. $^{31}P\{^{1}H\}$ NMR (CD_2Cl_2):

(Key new resonances) δ_P 166 (1P, *m (br),* C≡P)), 133 (0.34P, *m (br),* C≡P), 65 (4P, *m (br)*, PPh_2), 48 (0.39P, *m (br)*, PPh_2), 47 (1.13P, *m* (*br*), PPh_2).

OTHER REACTIVITY OF *Trans*-[Ru(C≡P)(dppe)$_2$]OTf (4.1.OTf)

Note: Due to a mixture of products for the $^{31}P\{^1H\}$ NMR the relative integrals have been calculated in comparison to the major product resonances hence the fractional integrals values for the other resonances.

Trans-[Ru(C≡P)(dppe)$_2$]OTf + KTp

A solution of *trans*-[Ru(C≡P)(dppe)$_2$]OTf (0.020g, 0.018 mmol) and KTp (0.005 g, 0.020 mmol) in DCM (*ca* 10 mL) was stirred for 18 h, filtered and volatiles removed under reduced pressure. Washed with hexanes (3 x 10 mL). Dried under vacuum. ^1H NMR (CD_2Cl_2): Intractable mixture of products. $^{31}P\{^1H\}$ NMR (CD_2Cl_2): (Key new resonances) δ_P 131 (1P, *m (br),* C≡P), 65 (3P, *m (br)*, unknown), 46 (4P, *m (br)*, unknown), −12.3 (0.2P, *s*, free $Ph_2PCH_2CH_2PPh_2$).

Trans-[Ru(C≡P)(dppe)$_2$]OTf + KTp*

A solution of *trans*-[Ru(C≡P)(dppe)$_2$]OTf (0.020g, 0.018 mmol) and KTp* (0.007 g, 0.018 mmol) in DCM (*ca* 10 mL) was stirred for 18 h, filtered and volatiles removed under reduced pressure. Washed with hexanes (3 x 10 mL). Dried under vacuum. ^1H NMR (CD_2Cl_2): Intractable mixture of products. $^{31}P\{^1H\}$ NMR (CD_2Cl_2): (Key new resonances) δ_P 131 (1P, *m (br),* C≡P), 65 (3P, *m (br)*, unknown), 46 (4P, *m (br)*, unknown), −12.3 (0.2P, *s*, free $Ph_2PCH_2CH_2PPh_2$).

***Trans*-[Ru(C≡P)(dppe)$_2$]OTf + Me$_3$Si-C≡CH**

To a solution of *trans*-[Ru(C≡P)(dppe)$_2$]OTf (0.068 g, 0.062 mmol) in DCM (*ca* 10 mL), Me$_3$Si-C≡CH (0.1 mL, 0.071 mmol) was added stirred for 18 h, volatiles removed under reduced pressure. Dried under vacuum. ^{1}H NMR (CD_2Cl_2): Intractable mixture of products. $^{31}P\{^1H\}$ NMR (CD_2Cl_2): (Key new resonances) δ_P 238 (1P, *qnt,* J_{PP} = 10 Hz, C≡P), 45.6 (1P, *s*, unknown), 45.1 (4P, *d*, J_{PP} = 10 Hz, $Ph_2PCH_2CH_2PPh_2$).

***Trans*-[Ru(C≡P)(dppe)$_2$]OTf + LiC≡CSiMe$_3$**

A solution of *trans*-[Ru(C≡P)(dppe)$_2$]OTf (0.051g, 0.047 mmol) and LiC≡CSiMe$_3$ (0.010 g, 0.09 mmol) in THF (*ca* 10 mL) was stirred for 18 h, filtered and volatiles removed under reduced pressure. Dried under vacuum. No observed reaction.

***Trans*-[Ru(C≡P)(dppe)$_2$]OTf + NaC≡CH**

A solution of *trans*-[Ru(C≡P)(dppe)$_2$]OTf (0.048 g, 0.044 mmol) and NaC≡CH (5.0 mL, 0.021 moldm^{-3}, 0.11 mmol) in DCM (*ca* 10 mL) was stirred for 18 h solution turned brown, filtered and volatiles removed under reduced pressure. Dried under vacuum. ^{1}H NMR (CD_2Cl_2): Intractable mixture of products. Key Resonances: $^{31}P\{^1H\}$ NMR (CD_2Cl_2): 153.7 (1P, *m (br),* C≡P), 132.3 (0.4P, *m (br),* C≡P), 51.6 (4P, *d*, J_{PP} = 6 Hz, $Ph_2PCH_2CH_2PPh_2$), 50.6 (0.5P, *s,* $Ph_2PCH_2CH_2PPh_2$), 46.2 (1.6P, *s,* $Ph_2PCH_2CH_2PPh_2$).

***Trans*-[Ru(C≡P)(dppe)$_2$]OTf + (HC≡C)$_3$C$_6$H$_3$**

A solution of *trans*-[Ru(C≡P)(dppe)$_2$]OTf (0.025g, 0.03 mmol) and 1,3,5-(HC≡C)$_3$C$_6$H$_3$ (0.0012 g, 0.008 mmol) in DCM (*ca* 10 mL) was stirred for 1 hour, DBU (0.01 mL, 0.07 mmol) and stirred for 18 h, filtered and volatiles removed under reduced pressure. Washed with hexanes (3 x 10 mL).

Dried under vacuum. ^{1}H NMR (CD_2Cl_2): Intractable mixture of products. $^{31}P\{^{1}H\}$ NMR (CD_2Cl_2): (Key new resonances) δ_P 132 (1P, *m (br),* C≡P), 46 (4P, *d*, J_{PP} = 2 Hz, $Ph_2PCH_2CH_2PPh_2$).

***Trans*-[Ru(C≡P)(dppe)$_2$]OTf + 2,5-(SiMe$_3$C≡C)$_2$-C$_4$H$_2$S**

A solution of *trans*-[Ru(C≡P)(dppe)$_2$]OTf (0.056g, 0.051 mmol) and 2,5-(C≡CSiMe$_3$)$_2$-C$_4$H$_2$S (0.0075 g, 0.027mmol) in DCM (*ca* 15 mL), the resulting solution was stirred for 18 h, DBU (0.1 mL, 0.7 mmol) and stirred for a further 2 h, filtered and volatiles removed under reduced pressure. Washed with hexanes (3 x 10 mL). Dried under vacuum. ^{1}H NMR (CD_2Cl_2): Intractable mixture of products. Key new resonances $^{31}P\{^{1}H\}$ NMR (CD_2Cl_2): δ_P 167 (1P, *m (br),* C≡P), 132 (5P, *m (br),* C≡P), 50 (5P, *s,* $Ph_2PCH_2CH_2PPh_2$), 46 (18P, *d*, J_{PP} = 4 Hz, $Ph_2PCH_2CH_2PPh_2$), 27 (0.5P, *s,* $Ph_2PCH_2CH_2PPh_2$).

***Trans*-[Ru(C≡P)(dppe)$_2$]OTf + 2,5-(LiC≡C)$_2$-C$_4$H$_2$S**

A solution of *trans*-[Ru(C≡P)(dppe)$_2$]OTf (0.025g, 0.030 mmol) and 2,5-(C≡CLi)$_2$-C$_4$H$_2$S (0.002 g, 0.014 mmol) in THF (*ca* 5 mL), the resulting solution was stirred for 18 h, filtered and volatiles removed under reduced pressure. Dried under vacuum. ^{1}H NMR (CD_2Cl_2): Intractable mixture of products. Key new resonances $^{31}P\{^{1}H\}$ NMR (CD_2Cl_2): δ_P 154 (1P, *m (br),* C≡P), 132 (0.1P, *m (br),* C≡P), 52 (4P *d*, J_{PP} = 7 Hz, $Ph_2PCH_2CH_2PPh_2$), 46 (0.4P, *s* $Ph_2PCH_2CH_2PPh_2$).

***Trans*-[Ru(C≡P)(dppe)$_2$]OTf + 4-cyanoisophthalic acid**

To an NMR sample of *trans*-[Ru(C≡P)(dppe)$_2$]OTf (0.010g, 0.009 mmol) in CD_2Cl_2 was added 4-cyanoisophthalic acid (0.002g, 0.010 mmol). The sample was sealed, agitated, and then monitored by NMR after 1 hour and after 18 h. ^{1}H NMR (CD_2Cl_2): Intractable mixture of products.

$^{31}P\{^{1}H\}$ NMR (CD_2Cl_2): (Key new resonances) δ_P 164 (1P, *m (br)*, C≡P), 46 (4P, *m* (*br*), $Ph_2PCH_2CH_2PPh_2$).

***Trans*-[Ru(C≡P)(dppe)$_2$]OTf + P(SiMe$_3$)$_3$**

To an THF (*ca* 5 mL) solution of *trans*-[Ru(C≡P)(dppe)$_2$]OTf (0.049 g, 0.045 mmol) in an ampule, was added $P(SiMe_3)_3$ (0.02 mL, 0.069 mmol), after 18 h, volatiles were removed under reduced pressure. ^{1}H NMR (C_6D_6): Intractable mixture of products. $^{31}P\{^{1}H\}$ NMR (C_6D_6): (Key new resonances) δ_P 180.5 (1P, *m (br)*, C≡P), 47.4 (4P, *dd*, , *J* = 8 Hz and 25 Hz, $Ph_2PCH_2CH_2PPh_2$), 46.1 (4P, *m*, $Ph_2PCH_2CH_2PPh_2$), 44.9 (2P, *m*, $Ph_2PCH_2CH_2PPh_2$), −104.4 (1P, *qnt*, *J* = 25 Hz, PH_3), −174.5 (0.63P,d, , *J* = 25 Hz, unknown), −236.7 (0.18P, *s*, unknown), −250 (17.24P, *m*, unknown).

***Trans*-[Ru(C≡P)(dppe)$_2$]OTf + P(SiMe$_3$)$_2$H**

To an NMR sample of *trans*-[Ru(C≡P)(dppe)$_2$]OTf (0.010 g, 0.009 mmol) in C_6D_6 was added $P(SiMe_3)_2H$ (0.02 mL, 0.010 mmol). The sample was sealed, agitated, and then monitored by NMR after 1 hour and after 18 h. ^{1}H NMR (C_6D_6): Intractable mixture of products. . $^{31}P\{^{1}H\}$ NMR (C_6D_6): (Key new resonances) δ_P 180.5 (1P, *m (br)*, C≡P), 114.5 (0.09P, s, unknown), 48.7 (4P, *d, J* = 25 Hz, $Ph_2PCH_2CH_2PPh_2$), −104.4 (1.2P, qnt, *J* = 25 Hz, PH_3), −236.1 (1.3P, *s*, unknown), −236.7 (12.2P, *m*, unknown), −252.1 (1.8P, *s*, unknown).

***Trans*-[Ru(C≡P)(dppe)$_2$]OTf + [C$_6$H$_4$-1,2-P$_2$BPh][Li$_2$(TMEDA)$_2$]**

To an NMR sample of *trans*-[Ru(C≡P)(dppe)$_2$]OTf (0.030 g, 0.028 mmol) in C_6D_6 was added [C_6H_4-1,2-P_2BPh][Li_2(TMEDA)$_2$] (0.007g, 0.015 mmol). The sample was sealed, agitated, and then monitored by NMR after 1 hour and after 18 h. ^{1}H NMR (C_6D_6): Intractable mixture of products.

$^{31}P\{^{1}H\}$ NMR (C_6D_6): (Key new resonances) δ_P 135 (1P, *dm*, *J* = 6.1 Hz and 2.8 Hz, C≡P), 47 (4P, *m* (*br*), $Ph_2PCH_2CH_2PPh_2$).

OTHER REACTIONS

Trans-[RuMe(dppe)$_2$(C≡P)] + TlOTf

To an NMR sample of **3.3** (0.025 g, 0.026 mmol) in CD_2Cl_2 was added 1 equiv. of TlOTf (0.010 g, 0.028 mmol). The sample was sealed, agitated, and then monitored by NMR after 5 min and after 18 h. No reaction was observed.

Trans-[RuH(dppe)$_2$(C≡P)] + Ph_3CBF_4

To an NMR sample of *trans*-[RuH(dppe)$_2$(C≡P)] (*ca* 0.020 g) in CD_2Cl_2 was added excess of Ph_3CBF_4. The sample was sealed, agitated, and then monitored by NMR after 5 min and after 18 h. Key resonances $^{31}P\{^{1}H\}$ NMR (399.5 MHz, CD_2Cl_2): 247 (1P, *m*, uncharacterised), 63 (1.4P, *s*, uncharacterised), 52.5 (4P *d*, J_{PP} = 27 Hz, $Ph_2PCH_2CH_2PPh_2$), 49.9 (0.6P, *s*, uncharacterised).

Trans-[RuMe(dppe)$_2$(C≡P)] + H[OEt$_2$][BAr$^F_4$]

To an NMR sample of **3.3** in CD_2Cl_2 was added 1 equiv. of Brookhart's acid. The sample was sealed, agitated, and then monitored by NMR after 5 min and upon completion. Key NMR Data: ^{1}H NMR (399.5 MHz, CD_2Cl_2): δ_H 0.21. $^{31}P\{^{1}H\}$ NMR (399.5 MHz, CD_2Cl_2): 460 (1P, *m*, uncharacterised), 178 (0.6P, *m*, C≡P), 131 (0.4P, *m*, C≡P), 59 (2.7P, *s*, $Ph_2PCH_2CH_2PPh_2$), 57.5 (1.4P *d*, J_{PP} = 27 Hz, $Ph_2PCH_2CH_2PPh_2$), 56 (9P, *s*, $Ph_2PCH_2CH_2PPh_2$), 47 (8P *d*, J_{PP} = 27 Hz, $Ph_2PCH_2CH_2PPh_2$), 57.5 (5.5P, *m,* uncharacterised),

REFERENCES

1 N. N. Greenwood and A. Earnshaw, *Chemistry of the Elements*, Butterworth-Heineann, London, 2nd Edition., 1997.

2 J. I. Bates, J. Dugal-Tessier and D. P. Gates, *Dalton Trans.*, 2010, **39**, 3151–3159.

3 K. B. Dillon, F. F. Mathey and J. F. Nixon, *Phosphorus: The Carbon Copy*, Chichester, 1998.

4 R. Hoffmann, *Angew. Chem. Int. Ed.*, 1982, **27**, 1009–1112.

5 K. S. Pitzer, *J. Am. Chem. Soc.*, 1948, **70**, 2140–2145.

6 R. S. Mulliken, *J. Am. Chem. Soc.*, 1950, **72**, 4493–4503.

7 D. C. Frost, S. T. Lee and C. A. McDowell, *Chem. Phys. Lett.*, 1973, **23**, 472–475.

8 W. Ensslin, H. Bock and G. Becker, *J . Am. Chem. Soc.*, 1974, **96**, 2757–2762.

9 J. C. T. R. Burckett-St Laurent, M. A. King, H. W. Kroto, J. F. Nixon and R. J. Suffolk, *J. Chem. Soc. Dalt. Trans.*, 1983, 755–759.

10 K. K. Laali, B. Geissler, M. Regitz and J. J. Houser, *J. Org. Chem.*, 1995, 6362–6367.

11 F. Mathey, *Angew. Chem. Int. Ed.*, 2003, **42**, 1578–1604.

12 R. H. Staley, J. E. Kleckner and J. L. Beuchamp, *J . Am. Chem. Soc.*, 1976, **98**, 2081–2085.

13 T. E. Gier, *J. Am. Chem. Soc.*, 1961, **83**, 1769–1770.

14 J. K Tyler, *J. Chem. Phys.*, 1964, **40**, 1170.

15 M. J. Hopkinson, H. W. Kroto, J. F. Nixon and N. P. C. Simmons, *J. Chem. Soc. Chem. Commun.*, 1976, 513–515.

16 H. W. Kroto, J. F. Nixon and N. P. C. Simmons, *J. Mol. Spectrosc.*, 1979, **77**, 270–285.

17 H. W. Kroto, J. F. Nixon, N. P. C. Simmons and N. P. C. Westwood, *J. Am. Chem. Soc.*, 1978, **100**, 446–448.

18 H. W. Kroto, J. F. Nixon and N. P. C. Simmons, *J. Mol. Spectrosc.*, 1980, **82**, 185–192.

19 M. J. Hopkinson, H. W. Kroto, J. F. Nixon and N. P. C. Simmons, *Chem. Phys. Lett.*, 1976, **42**, 460–461.

20 N. P. C. Westwood, H. W. Kroto, J. F. Nixon and N. P. C. Simmons, *J. Chem. Soc. Dalt. Trans.*, 1979, 6–9.

21 R. Appel, G. Maier, H. P. Reisenauer and A. Westerhaus, *Angew. Chem. Int. Ed.*, 1981, **20**, 197.

22 G. Becker, G. Gresser and W. Uhl, *Z. Naturforsch*, 1981, **36**, 16–19.

23 J. C. Guillemin, T. Janati, J. M. Denis, P. Guenot and P. Savignac, *Angew. Chem. Int. Ed.*, 1991, **30**, 196–198.

24 J. C. Guillemin, T. Janati and J. M. Denis, *J. Chem. Soc., Chem. Commun.*, 1992, 415–416.

25 J. C. Guillemin, T. Janati and J. M. Denis, *J. Org. Chem.*, 2001, **66**, 7864–7868.

26 C. E. Averre, M. P. Coles, I. R. Crossley and I. J. Day, *J. Chem. Soc. Dalt. Trans.*, 2012, **41**, 278–284.

27 J. G. Cordaro, D. Stein, H. Rüegger and H. Grützmacher, *Angew. Chem. Int. Ed.*, 2006, **45**, 6159–6162.

28 W. Rosch, T. Allspach, U. Bergstrasser and M. Regitz, *Multiple Bonds and Low Coordination in Phosphorus Chemistry*, Thieme, 1990.

29 M. Regitz, *Chem. Rev.*, 1990, **90**, 191–213.

30 S. M. Mansell, M. Green, R. J. Kilby, M. Murray and C. A. Russell, *C. R. Chem.*, 2010, **13**, 1073–1081.

31 N. Trathen, V. K. Greenacre, I. R. Crossley and S. M. Roe, *Organometallics*, 2013, **32**, 2501–2504.

32 V. K. Greenacre and I. R. Crossley, *Inorg. Chem.*, 2016, **4**, 30.

33 G. Becker, W. Becker, R. Knebl, H. Schmidt, U. Hildenbrand and M. Westerhausen, *Phosphorus, Sulfur and Silicon*, 1987, **30**, 349–352.

34 M. Schmitz, R. Goller, U. Bergstraber, S. Leininger and M. Regitz, *Eur. J. Inorg. Chem.*, 1998, 227–223.

35 M. Schmitz, R. Göller, U. Bergsträßer, S. Leininger and M. Regitz, *Eur. J. Inorg. Chem.*, 1998, 227–235.

36 A. M. Hibbs, C. Jones and A. F. Richards, *J. Chem. Soc., Dalt. Trans.*, 1999, 3531–3532.

37 A. M. Arif, A. R. Barron, A. H. Cowley and S. W. Hall, *J. Chem. Soc. Chem. Commun.*, 1988, **171**, 171–172.

38 O. Wagner, M. Ehle and M. Regitz, *Angew. Chem. Int. Ed.*, 1989, **28**, 225–226.

39 S. Annemarie, M. Weidenbruch, W. Saak and P. Siegfried, *Angew. Chem. Int. Ed.*, 1987, **26**, 776–777.

40 A. H. Cowley, S. W. Hall, C. M. Nunn and J. M. Power, *J. Chem. Soc. Chem. Commun.*, 1988, **753**, 753–754.

41 B. E. Niecke, R. Streubel, M. Nieger and D. Stalke, *Angew. Chem. Int. Ed.*, 1989, **28**, 1673–1674.

42 F. Mercier, L. Ricard, F. Mathey and M. Regitz, *J. Chem. Soc., Chem. Commun.*, 1991, 1305–1307.

43 A. H. Cowley, S. W. Hall, C. M. Nunn and J. M. Power, *Angew. Chem. Int. Ed.*, 1988, **27**, 838–839.

44 G. M. Jamison, R. S. Saunders, D. R. Wheeler, M. D. McClain, D. A. Loy and J. W. Ziller, *Organometallics*, 1996, **15**, 16–18.

45 J. Grobe, D. Le Van, T. Pohlmeyer, B. Krebs, O. Conrad, E. Dobbert and L. Weber, *Organometallics*, 1998, **17**, 3383–3386.

46 F. Tabellion, C. Peters, U. Fischbeck, M. Regitz and F. Preuss, *Chem. Eur. J.*, 2000, **6**, 4558–4566.

47 F. Geoffrey, N. Cloke, P. B. Hitchcock, J. F. Nixon and D. J. Wilson, *Chem. Commun.*,

2000, 2387–2388.

48 R. Armbrust, M. Sanchez, R. Réau, U. Bergstrasser, M. Regitz and G. Bertrand, *J. Am. Chem. Soc.*, 1995, **117**, 10785–10786.

49 T. Allspach, M. Regitz, G. Becker and W. Becker, *Synthesis (Stuttg).*, 1986, 31–36.

50 W. Rosch and M. Regitz, *Synthesis (Stuttg).*, 1987, 689–693.

51 M. Regitz, W. Rösch, T. Allspach, U. Annen, K. Blatter, J. Fink, M. Hermesdorf, H. Heydt, U. Vogelbacher and O. Wagner, *Phosphorous, Sulfur and Silicon*, 1987, **30**, 479–482.

52 Y. Y. C. Ko Yeung Lam, R. Carrie, A. Muench and G. Becker, *J. Chem. Soc. Chem. Commun.*, 1984, 1634–1635.

53 W. Rösch, T. Facklam and M. Regitz, *Tetrahedron*, 1987, **43**, 3247–3256.

54 M. Regitz and S. Krill, *Phosphorus, Sulfur Silicon Relat. Elem.*, 1996, **115**, 99–103.

55 B. Burkhart, S. Krill, Y. Okano, W. Ando and M. Regitz, *Synlett*, 1991, 356–358.

56 B. Breit, U. Bergsträsser, G. Maas and M. Regitz, *Angew. Chem. Int. Ed.*, 1992, **31**, 1055–1058.

57 J. Nixon, *Coord. Chem. Rev.*, 1995, **145**, 201–258.

58 I. R. Crossley, *Pers. Comun.*

59 B. T. Wettling, J. Schneider, O. Wagner, C. G. Kreiter and M. Regitz, *Angew. Chem. Int. Ed.*, 1989, **28**, 1013.

60 M. Birkel, J. Schulz, U. Bergstrasser and M. Regitz, *Angew. Chem. Int. Ed.*, 1992, **31**, 879–882.

61 V. Caliman, P. B. Hitchcock, C. Jones and J. F. Nixon, *Phosphorus, Sulfur Silicon Relat. Elem.*, 1996, 15–37.

62 J. C. T. R. Burckett-St. Laurent, P. B. Hitchcock, H. W. Kroto and J. F. Nixon, *J. Chem. Soc., Chem. Commun.*, 1981, 1141–1143.

63 S. I. Al-Resayes, S. I. Klein, H. W. Kroto, M. F. Meidine and J. F. Nixon, *J. Chem. Soc., Chem. Commun.*, 1983, 930–932.

64 S. I. Al-Resayes, P. B. Hitchcock, M. F. Meidine and J. F. Nixon, *J. Chem. Soc. Chem. Commun.*, 1984, **4**, 1080–1082.

65 P. Binger, B. Biedenbach, A. T. Herrmann, F. Langhauser, P. Betz, R. Goddard and C. Krüger, *Chem. Ber.*, 1990, **123**, 1617–1623.

66 G. Brauers, M. Green, C. Jones and J. F. Nixon, *J. Chem. Soc., Chem. Commun.*, 1995, 1125–1126.

67 R. A. Sanguramath, N. S. Townsend, J. M. Lynam and C. A. Russell, *Chem. Eur. J.*, 2014, 1783–1787.

68 B. P. B. Hitchcock, M. J. Maah, J. F. Nixon, J. A. Zora, G. J. Leigh and M. A. Bakar, *Angew. Chem. Int. Ed.*, 1987, **26**, 474.

69 P. B. Hitchcock, M. Amélia, N. D. A. Lemos, M. F. Meidine, J. F. Nixon and A. J. L. Pombeiro, *J. Organomet. Chem.*, 1991, **402**, 23–26.

70 M. F. Meidine, M. A. N. D. A. Lemos, A. J. L. Pombeiro, J. F. Nixon and P. B. Hitchcock, *J. Chem. Soc. Dalt. Trans.*, 1998, 3319–3323.

71 P. B. Hitchcock, M. F. Meidine, J. F. Nixon, H. Wang, D. Gudat and E. Niecke, *J. Organomet. Chem.*, 1989, **368**, 29–32.

72 J. F. Nixon, *Chem. Rev.*, 1988, **88**, 1327–1362.

73 J. M. Goicoechea and H. Grützmacher, *Angew. Chem. Int. Ed.*, 2018, **57**, 16968–16994.

74 Z.-J. Quan and X. Wang, *Org. Chem. Front.*, 2014, **1**, 1128–1131.

75 G. Becker, W. Schwarz, N. Seidler and M. Westerhausen, *Z. Anorg. Allg. Chem.*, 1992, **612**, 72–82.

76 M. Westerhausen, S. Schneiderbauer, H. Piotrowski and M. Suter, *J. Organomet. Chem.*, 2002, **644**, 189–193.

77 F. F. Puschmann, D. Stein, D. Heift, C. Hendriksen, Z. A. Gal, H. Grützmacher and H. Grützmacher, *Angew. Chem. Int. Ed.*, 2011, 8420–8423.

78 R. Suter, Z. Benkő, M. Bispinghoff and H. Grützmacher, *Angew. Chem. Int. Ed.*, 2017, **56**, 11226–11231.

79 I. Krummenacher and C. C. Cummins, *Polyhedron*, 2012, **32**, 10–13.

80 A. R. Jupp and J. M. Goicoechea, *Angew. Chem. Int. Ed.*, 2013, **52**, 10064–10067.

81 M. Jost, L. H. Finger, J. Sundermeyer and C. Von Hänisch, *Chem. Commun.*, 2016, **52**, 11646–11648.

82 G. Becker, G. Heckmann, K. Hubler and W. Schwarz, *Z. Anorg. Allg. Chem.*, 1995, **621**, 34–46.

83 S. Alidori, D. Heift, G. Santiso-Quinones, Z. Benko, H. Grützmacher, M. Caporali, L. Gonsalvi and M. Peruzzini, *Chem. Eur. J.*, 2012, **18**, 14805–14811.

84 L. N. Grant, B. Pinter, B. C. Manor, H. Gr and D. J. Mindiola, *Angew. Chem. Int. Ed.*, 2018, **57**, 1049–1052.

85 L. N. Grant, J. Krzystek, B. Pinter, J. Tesler, H. Grützmacher and D. J. Mindiola, *Chem. Commun.*, 2019, **55**, 5966–5969.

86 C. J. Hoerger, F. W. Heinemann, E. Louyriac, L. Maron, H. Grützmacher and K. Meyer, *Organometallics*, 2017, **36**, 4351–4354.

87 C. Camp, N. Settineri, J. Lefèvre, A. R. Jupp, J. M. Goicoechea, L. Maron and J. Arnold, *Chem. Sci.*, 2015, **6**, 6379–6384.

88 L. Liu, D. A. Ruiz, D. Munz and G. Bertrand, *Chem. Cell Press*, 2016, **1**, 147–153.

89 D. W. N. Wilson, A. Hinz and J. M. Goicoechea, *Angew. Chem. Int. Ed.*, 2018, 2188–2193.

90 L. Liu, D. A. Ruiz, F. Dahcheh, G. Bertrand, R. Suter, A. M. Tondreau and H. Grützmacher, *Chem. Sci.*, 2016, **7**, 2335–2341.

91 M. M. D. Roy, M. J. Ferguson, R. McDonald and E. Rivard, *Chem. Commun.*, 2018, **54**, 483–486.

92 G. Hierlmeier, A. Hinz, R. Wolf and J. M. Goicoechea, *Angew. Chem. Int. Ed.*, 2018, **57**, 431–436.

93 W. Lü, C. Wang, Q. Luo, Q. S. Li, Y. Xie, R. B. King and H. F. Schaefer, *New J. Chem.*, 2015, **39**, 1390–1403.

94 L. N. Grant, B. Pinter, B. C. Manor, R. Suter, H. Grützmacher and D. J. Mindiola, *Chem. Eur. J.*, 2017, **23**, 6272–6276.

95 T. P. Robinson, M. J. Cowley, D. Scheschkewitz and J. M. Goicoechea, *Angew. Chem. Int. Ed.*, 2015, **54**, 683–686.

96 C. J. Hoerger, F. W. Heinemann, E. Louyriac, M. Rigo, L. Maron, H. Grützmacher, M. Driess and K. Meyer, *Angew. Chem. Int. Ed.*, 2019, **58**, 1679–1683.

97 O. Mo, M. Ya, J.-C. Guillemin, E. Hassan Riague, J. Gal, P. Maria and C. Dubin Poliart, *Chem. Eur. J.*, 2002, **8**, 4919–4924.

98 G. Pascoli and H. Lavendy, *J. Phys. Chem. A.*, 1999, **103**, 3518–3524.

99 H. Jun, V. G. Young and R. J. Angelici, *J. Am. Chem. Soc.*, 1992, **114**, 10064–10065.

100 H. Jun and R. J. Angelici, *Organometallics*, 1994, **13**, 2454–2460.

101 J. G. Cordaro, D. Stein, H. Rüegger and H. Grützmacher, *Angew. Chem. Int. Ed.*, 2006, **45**, 6159–6162.

102 S. M. Mansell, M. Green and C. A. Russell, *Dalton Trans.*, 2012, **41**, 14360–14368.

103 N. Trathen, M. C. Leech, I. R. Crossley, V. K. Greenacre and S. M. Roe, *Dalton Trans.*, 2014, **43**, 9004–9007.

104 S. K. Furfari, M. C. Leech, N. Trathen, M. C. Levis and I. R. Crossley, *Dalton Trans.*, 2019, **48**, 8131–8143.

105 M. C. Leech and I. R. Crossley, *Dalton Trans.*, 2018, **47**, 4428–4432.

106 P. Aguirre-Etcheverry and D. O'Hare, *Chem. Rev.*, 2010, **110**, 4839–4864.

107 L. Paul and C. Lapinte, *Coord. Chem. Rev.*, 1998, **178**–**180**, 431–509.

108 M. I. Bruce, *Chem. Rev.*, 1998, **98**, 2797–2858.

109 C. Olivier, B. S. Kim, D. Touchard and S. Rigaut, *Organometallics*, 2008, **27**, 509–518.

110 P. J. Low and M. I. Bruce, *Transition metal chemistry of 1,3-diynes, poly-ynes, and related compounds*, Elsevier Masson SAS, 2001, vol. 48.

111 M. I. Bruce and P. J. Low, *Adv. Organomet. Chem.*, 2004, **50**, 179–444.

112 P. J. Low, R. L. Roberts, R. L. Cordiner and F. Hartl, *J. Solid State Electrochem.*, 2005, **9**, 717–731.

113 X. He and T. Baumgartner, *RSC. Adv.*, 2013, **3**, 11334–11350.

114 V. A. Wright, B. O. Patrick, C. Schneider and D. P. Gates, *J. Am. Chem. Soc.*, 2006, **128**, 8836–8844.

115 M. A. Shameem and A. Orthaber, *Chem. Eur. J.*, 2016, **22**, 10718–10735.

116 E. Deschamps and L. Ricard, *Angew. Chem. Int. Ed.*, 1994, **33**, 1158–1161.

117 V. A. Wright and D. P. Gates, *Angew. Chem. Int. Ed.*, 2002, **41**, 2389–2392.

118 N. Trathen, PhD Thesis, University of Sussex, 2014.

119 M. C. Leech, PhD Thesis, University of Sussex, 2018.

120 M. C. B. Colbert, J. Lewis, N. J. Long, P. R. Raithby, A. J. P. White and D. J. Williams, *J. Chem. Soc. - Dalt. Trans.*, 1997, 99–104.

121 N. D. Jones, M. O. Wolf and D. M. Giaquinta, *Organometallics*, 1997, **16**, 1352–1354.

122 C. Y. Wong, C. M. Che, M. C. W. Chan, J. Han, K. H. Leung, D. L. Phillips, K. Y. Wong and N. Zhu, *J. Am. Chem. Soc.*, 2005, **127**, 13997–14007.

123 A. Vacher, F. Barriere, T. Roisnel, L. Piekara-Sady and D. Lorcy, *Organometallics*, 2011, **30**, 3570–3578.

124 M. C. Levis, K. G. Pearce and I. R. Crossley, *Inorg. Chem.*, 2019, **58**, 14800–14807.

125 M. A. Fox, J. E. Harris, S. Heider, V. Pérez-Gregorio, M. E. Zakrzewska, J. D. Farmer, D. S. Yufit, J. A. K. Howard and P. J. Low, *J. Organomet. Chem.*, 2009, **694**, 2350–2358.

126 J. Conradie, *Electrochim. Acta*, 2020, **337**, 135801.

127 R. B. Bedford, A. F. Hill, C. Jones, A. J. P. White, D. J. Williams and J. D. E. T. Wilton-Ely, *Chem. Commun.*, 1997, **2**, 179–180.

128 S. B. Clendenning, P. B. Hitchcock, G. A. Lawless, J. F. Nixon and C. W. Tate, *J. Organomet. Chem.*, 2010, **695**, 717–720.

129 L. D. Field, A. M. Magill, T. K. Shearer, S. J. Dalgarno and P. Turner, *Organometallics*, 2007, **26**, 4776–4780.

130 L. D. Field, A. M. Magill, M. M. Bhadbhade and S. J. Dalgarno, *Organometallics*, 2009, **28**, 5514–5521.

131 R. Kumar, S. Ramakrishnan, E. D. Jemmis and B. R. Jagirdar, *Organometallics*, 2015, **34**, 1245–1254.

132 R. C. Groom, I. Bruno, M. P. Lightfoot and S. C. Ward, *Cambridge Structual Database. Acta Crystalogr., Sect. B Struct. Sci., Cryst. Eng. Mater.*, 2016, **72**, 171–179.

133 H. S. Kim, J. Y. Bae, J. S. Lee, O. S. Kwon, P. Jelliarko, S. D. Lee and S. H. Lee, *J. Catal.*, 2005, **232**, 80–84.

134 F. A. Cotton and G. Schmid, *Polyhedron*, 1996, **15**, 4053–4059.

135 J. E. Fergusson and P. F. Heveldt, *Inorg. Chim. Acta*, 1978, **31**, 145–154.

136 P. O. Dunstan, *Thermochim. Acta*, 2005, **437**, 100–105.

137 E. E. Wilson, A. G. Oliver, R. P. Hughes and B. L. Ashfeld, *Organometallics*, 2011, **30**, 5214–5221.

138 W. A. Herrmann, A. M. J. Rost, J. K. M. Mitterpleininger, N. Szesni, S. Sturm, R. W. Fischer and F. E. Kühn, *Angew. Chem. Int. Ed.*, 2007, **46**, 7301–7303.

139 S. Schulz, M. Münch and U. Flörke, *Z. Anorg. Allg. Chem.*, 2008, **634**, 2221–2225.

140 J. Lewiński, W. Marciniak, Z. Ochal, J. Lipkowski and I. Justyniak, *Eur. J. Inorg. Chem.*, 2003, **043**, 2753–2755.

141 G. R. Fulmer, A. J. M. Miller, N. H. Sherden, H. E. Gottlieb, A. Nudelman, B. M. Stoltz, J. E. Bercaw and K. I. Goldberg, *Organometallics*, 2010, **29**, 2176–2179.

142 E. C. Ashby and A. B. Goel, *J. Chem. Soc. Chem. Commun.*, 1977, 169.

143 T. N. Dymova, S. S. Grazhulene, N. I. Kuchinskii and V. A. Kuznetsov, *Bull. Acad. Sci. USSR Div. Chem. Sci.*, 1971, **20**, 1532–1535.

144 R. P. Hsung and A. I. Gerasyuto, *Encyl. Reagents Org. Synth.*, 2003, 1–9.

145 D. Mukherjee and J. Okuda, *Angew. Chem. Int. Ed.*, 2018, **57**, 1458–1473.

146 G. R. Fulmer, A. J. M. Miller, N. H. Sherden, H. E. Gottlieb, A. Nudelman, B. M. Stoltz, J. E. Bercaw and K. I. Goldberg, *Organometallics*, 2010, **29**, 2176–2179.

147 M. G. Tay, C. Y. Ying, S. H. Chin and P. T. Pei, *Transtion Met. Chem.*, 2018, **44**, 293–301.

148 S. E. Trentowsky, A. J. Lough and R. H. Morris, *Polyhedron*, 2018, **156**, 342.

149 P. N. Liu, J. Li, F. H. Su, K. D. Ju, L. Zhang, C. Shi, H. H. Y. Sung, I. D. Williams, V. V. Fokin, Z. Lin and G. Jia, *Organometallics*, 2012, **31**, 4904–4915.

150 N. L. Wieder, P. J. Carroll and D. H. Berry, *Organometallics*, 2011, **30**, 2125–2136.

151 S. L. Chatwin, M. F. Mahon, T. J. Prior and M. K. Whittlesey, *Inorg. Chim. Acta*, 2010, **363**, 625–632.

152 Q. Zhang, C. Lai, W. Wong and W. Leung, *Organometallics*, 2002, 4017–4020.

153 T. Tsuda and M. O. Shiro, *Organometallics*, 1999, **18**, 2741–2743.

154 D. Huang, R. H. Heyn, J. C. Bollinger and K. G. Caulton, *Organometallics*, 1997, **16**, 292–293.

155 A. Pedersen, M. Tilset, K. Folting and K. G. Caulton, *Organometallics*, 1995, **14**, 875–888.

156 G. J. Kruger, T. V. Ashworth and E. Singleton, *Acta Crystallogr. Sect. A Found. Adv.*, 1981, **37**, C220.

157 A. Reinholdt, T. Vosch and J. Bendix, *Angew. Chem. Int. Ed.*, 2016, **55**, 12484–12487.

158 T. J. Morsing, A. Reinholdt, S. P. A. Sauer and J. Bendix, *Organometallics*, 2016, **35**, 100–105.

159 W. Stuer, B. Weberndorfer, J. Wolf and H. Werner, *Dalton Trans.*, 2005, 1796–1803.

160 M. Liu, J. Hu and Y. Wang, *Polyhedron*, 2018, **149**, 79–83.

161 V. K. Greenacre, N. Trathen and I. R. Crossley, *Organometallics*, 2015, **34**, 2533–2542.

162 D. A. J. Harding, E. G. Hope, G. A. Solan and J. Fawcett, *Acta Crystallogr. Sect. C Cryst. Struct. Commun.*, 2007, **63**, 383–384.

163 T. Brackemeyer, G. Erker, R. Frohlich, J. Prigge and U. Peuchert, *Chem. Ber.*, 1997, 899–902.

164 R. F. Winter and T. Scheiring, *Z. Anorg. Allg. Chem.*, 2000, **626**, 1196.

165 V. Sivakumar, M. Nethaji, B. R. Jagirdar and N. Mathew, *Synth. React. Inorganic, Met. Nano-Metal Chem.*, 2007, **37**, 677.

166 A. A. Adeniyi and P. A. Ajibade, *J. Chem.*, 2016, **2016**, 3672062.

167 A. Ceccon, S. Santi, L. Orian, A. Bisello, C. Fisica, A. Miolati and V. Loredan, *Coord. Chem. Rev.*, 2004, **248**, 683–724.

168 J. B. G. Gluyas, N. J. Brown, J. D. Farmer and P. J. Low, *Aust. J. Chem.*, 2016, **70**, 113–119.

169 W. E. Geiger, *Coord. Chem. Rev.*, 2013, **257**, 1459–1471.

170 M. I. Bruce, M. L. Cole, C. R. Parker, B. W. Skelton and A. H. White, *Organometallics*, 2008, **27**, 3352–3367.

171 N. L. Narvor, L. Toupet and C. Lapinte, *J . Am. Chem. Soc.*, 1995, **117**, 7129–7138.

172 F. De Montigny, G. Argouarch, T. Roisnel, L. Toupet, C. Lapinte, S. C. F. Lam, C. H. Tao and V. W. W. Yam, *Organometallics*, 2008, **27**, 1912–1923.

173 J. G. Planas, T. Marumo, Y. Ichikawa, M. Hirano and S. Komiya, *J. Mol. Catal. A Chem.*, 1999, **147**, 137–154.

174 M. Hirano, R. Fujimoto, K. Hatagami, N. Komine and S. Komiya, *Chem Cat Chem*, 2013, **5**, 1101–1115.

175 L. Weber, S. Kleinebekel, A. Rühlicke and H. Stammler, *Eur. J. Inorg. Chem.*, 2000, **1**, 1185–1191.

176 L. Weber, *Eur. J. Inorg. Chem.*, 2000, 2425.

177 D. Gudat, E. Niecke, A. M. Arif, A. H. Cowley and S. Quashie, *Organometallics*, 1986, **5**, 593–595.

178 Y. Wang, Y. Xie, P. Wei, R. B. King, H. F. Schaefer, P. R. Schleyer and G. H. Robinson, *J . Am. Chem. Soc.*, 2008, 14970–14971.

179 F. A. Cotton, G. Wilkinson, C. Murello and M. Bochmann, *Advanced Inorganic Chemistry*, Wiley, New York, 6th edn., 1999.

180 S. Torker, A. Müller, R. Sigrist and P. Chen, *Organometallics*, 2010, **29**, 2735–2751.

181 H. Katayama, M. Nagao and F. Ozawa, *Organometallics*, 2003, **22**, 586–593.

182 D. E. Bublitz, W. E. McEwen and J. Kleinberg, *Org. Synth.*, 1961, **41**, 96.

183 E. O. Fisciier and W. Hafner, *Z. Naturforsch. Tiel B.*, 1954, **9**, 503–504.

184 E. O. Fisciier and W. Hafner, *Z. Anorg. Allg. Chem.*, 1955, **282**, 47–62.

185 G. Wilkinson, F. A. Cotton and J. M. Birmingham, *J. Inorg. Nucl. Chem.*, 1956, **2**, 95–113.

186 E. O. Fischer and H. Grubert, *Chem. Ber.*, 1959, **92**, 2302–2309.

187 T. D. Tilley, R. A. Andersen, B. Spencer, H. Ruben, D. H. Templeton and A. Zalkin, *Inorg. Chem.*, 1980, **19**, 2999–3003.

188 M. S. Dutkiewicz, C. Apostolidis, O. Walter and P. L. Arnold, *Chem. Sci.*, 2017, **8**, 2553–2561.

189 J. S. Figueroa and C. C. Cummins, *Angew. Chem. Int. Ed.*, 2004, **43**, 984–988.

190 K. G. Pearce, E. Canham, I. R. Crossley and J. F. Nixon, *Prep.*

191 S. D. Bohle, G. R. Clark, C. E. F. Rickard, W. R. Roper and M. J. Taylor, *J. Organomet. Chem.*, 1988, **348**, 385–409.

192 M. Al-Noaimi, I. Warad, O. S. Abdel-Rahman, F. F. Awwadi, S. F. Haddad and T. B.

Hadda, *Polyhedron*, 2013, **62**, 110–119.

193 X. He, J. Borau-Garcia, A. Y. Y. Woo, S. Trudel and T. Baumgartner, *J. Am. Chem. Soc.*, 2013, **135**, 1137–1147.

194 P. A. Bouit, A. Escande, R. Szücs, D. Szieberth, C. Lescop, L. Nyulászi, M. Hissler and R. Réau, *J. Am. Chem. Soc.*, 2012, **134**, 6524–6527.

195 A. Bruch, A. Fukazawa, E. Yamaguchi, S. Yamaguchi and A. Studer, *Angew. Chem. Int. Ed.*, 2011, **50**, 12094–12098.

196 Y. Takeda, K. Hatanaka, T. Nishida and S. Minakata, *Chem. - A Eur. J.*, 2016, **22**, 10360–10364.

197 Y. Takeda, T. Nishida, K. Hatanaka and S. Minakata, *Chem. - A Eur. J.*, 2015, **21**, 1666–1672.

198 Y. Takeda, T. Nishida and S. Minakata, *Chem. - A Eur. J.*, 2014, **20**, 10266–10270.

199 G. Jia, H. P. Xia, W. F. Wu and W. S. Ng, *Organometallics*, 1996, **15**, 3634–3636.

200 J. Li and P. Huang, *Beilstein J. Org. Chem.*, 2011, **7**, 426–431.

201 C. Stuhl and R. Anwander, *Dalton Trans.*, 2018, 12546–12552.

202 A. Seidler, J. Svoboda, V. Dekoj, J. V. Chocholoušová, J. Vacek, I. G. Stará and I. Starý, *Tetrahedron Lett.*, 2013, **54**, 2795–2798.

203 L. Jing, F. Hongwei, H. Pan, Z. Zilong, X. Li and C. Yanxiang, *Chem. Eur. J.*, 2012, **18**, 13941–13944.

204 N. C. Baenziger, W. E. Bennett, D. M. Soboroff, P. S. O'Donnell and J. R. Doyle, *Polyhedron*, 1998, **17**, 2379–2410.

205 G. M. Sheldrick, *Acta Crystallogr., Sect. A Found. Crystallogr.*, 2015, **71**, 3−8.

206 G. M. Sheldrick, *Acta Crystallogr., Sect. C Struct. Chem.*, 2015, **71**, 3−8.

207 O. V. Dolomanov, L. J. Bourhis, R. J. Gildea, J. A. K. Howard and H. Puschmann, *J. Appl. Crystallogr.*, 2009, **42**, 339.

208 M. J. Frisch, G. W. Trucks, H. B. Schlegel, G. E. Scuseria, M. A. Robb, J. R. Cheeseman, G. Scalmani, V. Barone, B. Mennucci, G. A. Petersson, H. Nakatsuji, M. Caricato, H. P. Hratchian, X. Li, A. F. Izmaylov, J. Bloino, G. Zheng, J. L. Sonnenberg, M. Had, J. Cioslowski, A. Marenich, B. G. Janesko, R. Gomperts, J. V. Ortiz, D. Willams-Young, F. Ding, F. Lipparini, F. Egidi, J. Goings, B. Peng, A. Petrone, T. Hendeson, D. Ranasinghe, V. G. Zakrzewski, J. Gao, N. Rega, W. Liang, M. Hada, M. Ehara, K. Toyata, R. Fukuda, J. Hasegawa, M. Ishida, T. Nakajima, Y. Honda, O. Kitao, H. Nakai, T. Vreven, K. Throssell, J. A. Montgomery, J. A. Peralta, F. Ogliaro, M. Bearpark, J. J. Heyd, E. Brothers, K. N. Kudin, V. N. Staroverov, T. Keith, R. Kobayashi, J. Normand, K. Raghavachari, A. Rendell, J. C. Burant, S. S. Iyrngar, J. Tomasi, M. Cossi, O. Farkas, J. B. Foresman and D. J. Fox, *Gaussian 09, Revis. D.01, Inc., Wallingford CT*, 2013.

209 N. M. O'Boyle, A. L. Tenderhold and K. M. Langner, *J. Comput. Chem.*, 2008, 839–845.

APPENDICIES

PUBLICATION LIST

1. M. C. Levis, K. G. Pearce, and I. R. Crossley, *Inorg. Chem*. 2019, **58**, 21, 14800-14807 'Controlled reactivity of terminal cyaphide complexes: Isolation of the 5-coordinate $[Ru(dppe)_2(CP)]^+$.'
2. S. K. Furfari, M. C. Leech, N. Tranthen, M. C. Levis, and I. R. Crossley, *Dalton Trans.,* 2019, **48**, 8131-8143 'Cyaphide-alkynyl complexes: metal-ligand conjugation and the influence of remote substituents.'

CONFERENCES AND SYMPOSIA ATTENDED

Dalton Younger Members Event (5th to 6th September 2019)

- Speaker: Synthesis and reactivity of the first *trans*-alkyl and halide cyaphide complexes

16th European Workshop on Phosphorus Chemistry (24th to 26th April 2019)

- Poster Presenter: Synthesis and reactivity of the first *trans*-alkyl and halide cyaphide complexes

RSC Sir Geoffrey Wilkinson Dalton Poster Symposium (30th April 2019)

- Poster Presenter: Synthesis and reactivity of the first *trans*-alkyl and halide cyaphide complex leading to novel cyaphide complexes

2018 RSC Dalton Division Southern Regional Meeting (19th September 2018)

- Poster Presenter: Synthesis and reactivity of the first *trans*-alkyl cyaphide complex

International Conference Organometallic Chemistry (15th to 20th July 2018)

- Poster Presenter: Synthesis and reactivity of the first *trans*-alkyl cyaphide complex

RSC Dalton Meeting (3rd to 5th April 2018)

- Poster Presenter: Synthesis of the first *trans*-alkyl cyaphide complex